NATIONAL AERONAUTICS AND SPACE ADMINISTRATION

Technical Report No. 32-800

Ranger VIII and IX
Part I. Mission Description and Performance

H. M. Schurmeier
Ranger Project Manager

JET PROPULSION LABORATORY
CALIFORNIA INSTITUTE OF TECHNOLOGY
PASADENA, CALIFORNIA

January 31, 1966

Prepared Under Contract No. NAS 7-100
National Aeronautics & Space Administration

CONTENTS

CONTENTS (Cont'd)

TABLES

FIGURES

FIGURES (Cont'd)

FIGURES (Cont'd)

ABSTRACT

The *Ranger VIII* and *IX* missions successfully concluded the *Ranger* unmanned lunar-investigation project. The Block III *Ranger* spacecraft, launched by the *Atlas/Agena* vehicle and tracked by the Deep Space Network, contained a six-camera television package and had the objective of obtaining high-resolution photographs of the lunar surface prior to impact. *Ranger VIII*, launched February 17, 1965, returned 7137 pictures before its impact in southwestern Mare Tranquillitatis on February 20. *Ranger IX* was launched on March 21, 1965, and impacted in the crater Alphonsus on March 24. A successful terminal maneuver performed on *Ranger IX* brought the resolution of the final pictures to 0.4 m; a total of 5814 pictures was obtained from this mission. A brief loss of telemetry during *Ranger VIII's* midcourse maneuver, apparently caused by a conducting particle forming a temporary short circuit in the spacecraft radio, was the only significant anomaly observed in the two flights. The initial accuracy of the *Ranger IX* launch made it possible to defer the midcourse maneuver 22 hr; the actual impact was within 5 km of the selected aiming point.

I. INTRODUCTION

The *Ranger VIII* and *IX* missions were the last two flights of *Ranger* Block III and of the *Ranger* series. They were conducted February 17–20 and March 21–24, 1965, respectively. Each spacecraft was launched from Complex 12 at the Air Force Eastern Test Range (AFETR), Cape Kennedy, Florida, and boosted to injection by the *Atlas/Agena* launch vehicle. The AFETR downrange tracking and telemetry stations and other facilities supported the early portions of the flights. Space-flight operations were supported by the Deep Space Network (DSN), including Deep Space Stations 51 (Africa), 41 (Australia), and 11 and 12 (Goldstone, Calif.) and the Space Flight Operations Facility (SFOF) at JPL.

The mission objective, to obtain close-up television pictures of the lunar surface, was met in each case. *Ranger VIII* impacted in Mare Tranquillitatis after a long sweep across the south-central lunar highlands; *Ranger IX* came within 2.76 mi of its selected aiming point in the crater Alphonsus, achieving, in the final pictures, a photographic resolution of approximately 12 in.

A. Ranger VIII Mission Summary

Liftoff occurred at 17:05:00.795 GMT*, February 17, 1965, after a smooth countdown with no spacecraft holds. Launch-vehicle performance was satisfactory, and injection of the spacecraft into a nominal trajectory occurred at 17:27:36.8 GMT.

Earth and Sun acquisition were accomplished within the nominal times. Pre-midcourse orbit data indicated that the *Ranger VIII* spacecraft would fly by the trailing edge of the Moon at a closest-approach distance of 1136 mi; therefore, a midcourse maneuver was performed at approximately launch (L) + 17 hr. The spacecraft performed the maneuver as commanded. Sun and Earth reacquisition occurred within the nominal times.

It was determined that no terminal maneuver would be required. At 09:33:09, February 20, 1965, the F and P (full-scan and partial-scan) television channels indicated warmup; at 09:34:30, both channels indicated full power, and the Echo and Pioneer Sites at Goldstone began receiving TV pictures of the surface of the Moon. Goldstone received pictures from all cameras on both channels continuously to lunar impact. In all, 7137 pictures were received and recorded. At 09:57:38, the spacecraft impacted the Moon at selenographic 2.7°N latitude and 24.8°E longitude.

*Times used in this Report will be GMT; for comparison, *Ranger VIII* liftoff occurred at 12:05 p.m., EST, or 9:05 a.m. PST.

B. Ranger IX Mission Summary

Ranger IX liftoff occurred at 21:37:02.456 GMT, March 21, 1965, after a normal countdown. The launch period had been reduced, first to obtain the desired lunar target, and then to accommodate the scheduling of Gemini Mission GT-3. Launch-vehicle performance was excellent, and the spacecraft was injected into a nominal lunar-transfer trajectory at 21:49:48.3.

Pre-midcourse orbit data indicated that *Ranger IX* would impact the Moon approximately 400 mi due North of the target, the crater Alphonsus; therefore, a midcourse maneuver was performed. The spacecraft performed the maneuver as commanded at approximately launch plus 38½ hr. Sun and Earth reacquisition occurred within the nominal times.

The terminal maneuver required to align the camera axis with the spacecraft velocity vector was performed as commanded, starting 65 min before impact (I−65 min). At 13:48:14 GMT, March 24, 1965, the full- and partial-scan television channels indicated warmup; at 13:49:34, both channels indicated full power, and the Echo and Pioneer Sites at Goldstone began receiving television pictures of the surface of the Moon. Goldstone received 5814 television pictures from all cameras, which operated continuously to lunar impact at 14:08:20. Impact occurred in the crater Alphonsus at a selenographic latitude of 13.1° S and a longitude of 2.4° W.

C. Project Background

Rangers VIII and *IX* were the third and fourth missions of the four-flight Block III of the *Ranger* Project. The Project was initiated in 1959, with the following basic mission elements:

1. *Atlas D/Agena B* launch, from the Cape, with a parking-orbit ascent trajectory.
2. Attitude-stabilized spacecraft employing solar power and capable of a midcourse maneuver and high-gain directional communications.

3. World-wide tracking, telemetry, and command facilities.

4. Integrated space-flight operational control, computation, and data handling.

Block I of the Project consisted of two test missions in 1961, designed as non-lunar-oriented engineering development flights for verification of the parking-orbit launch concept and soundness of the spacecraft design. Both flights experienced launch-vehicle failures. The spacecraft remained in their parking orbits as low-altitude Earth satellites, which permitted the testing of some spacecraft design elements, and the acquisition of some scientific data, but the test objectives were not met.

In Block II, a lunar rough-landing capsule (incorporating a seismometer experiment), with its retro-propulsion system, and lunar-approach television and gamma-ray experiments were used in conjunction with the basic spacecraft bus. The Block II spacecraft were sterilized. The three missions were flown in 1962.

Both spacecraft design adequacy and launch-vehicle performance were successfully demonstrated, but, unfortunately, in separate attempts. The *Ranger III* mission demonstrated spacecraft midcourse maneuver, attitude control, and communications capabilities, but was unable to impact the Moon. Missions *IV* and *V* had satisfactory vehicle performance: *Ranger IV* impacted the Moon, but the spacecraft had failed early in the flight; the *Ranger V* spacecraft also malfunctioned early in the flight.

Ranger Block III consisted of four missions, with a new payload comprising a six-camera television subsystem designed to operate during the last 10 to 15 min before impact on the Moon. The first mission, *Ranger VI*, launched January 30, 1964, performed satisfactorily throughout the flight up to the terminal phase, when the television system failed to operate. A number of minor spacecraft-bus and major TV-subsystem modifications were made.

The second mission, *Ranger VII*, launched July 28, 1964, was successful, and returned more than 4300 close-up lunar photographs before its impact on July 31, 1964, in a region since named Mare Cognitum.

The balance of *Ranger* Block III consisted of the two successful missions described in this Report.

D. Project Description

The effort in support of the *Ranger VIII* and *IX* missions was organized in four Systems: Launch Vehicle (including launch facilities), Spacecraft, Space Flight Operations, and Deep Space Network.

1. Launch Vehicle System

The function of the Launch Vehicle System was to place the *Ranger* spacecraft on a prescribed lunar-transfer trajectory. Launches were conducted from the Air Force Eastern Test Range, Cape Kennedy, Florida, including downrange facilities of AFETR, by Goddard Space Flight Center Launch Operations (GLO). The *Atlas D* first stages were manufactured by General Dynamics/Astronautics (GD/A) and procured by the USAF Space Systems Division for the Lewis Research Center (LeRC), the Launch Vehicle System Manager. The *Agena B* stages were manufactured by Lockheed Missiles and Space Company (LMSC), under contract to LeRC.

2. *Ranger* Spacecraft System

The requirement placed upon the spacecraft was to deliver the cameras to the proper lunar encounter geometry, with the necessary operating environment, and to transmit the required video. These spacecraft functions included the complex activities associated with launch, cruise, midcourse maneuver, and terminal maneuver. The TV subsystem was designed and manufactured under JPL contract by RCA's Astro-Electronics Division.

3. Space Flight Operations

The function of the Space Flight Operations System was to conduct and control the missions from Earth: to use the tracking and telemetry data in determining flight path and spacecraft performance, and to prepare the necessary commands for transmission to the spacecraft.

4. Deep Space Network

Consisting of a group of large tracking stations at Goldstone, California; Woomera, Australia; and Johannesburg, South Africa; the Space Flight Operations Facility at JPL; and the communication links binding these elements together, the Deep Space Network had the function of tracking and providing communication with the spacecraft throughout the missions, and making original data recordings for analysis.

The relationships of the various project elements supporting the *Ranger* missions are sketched in Fig. 1.

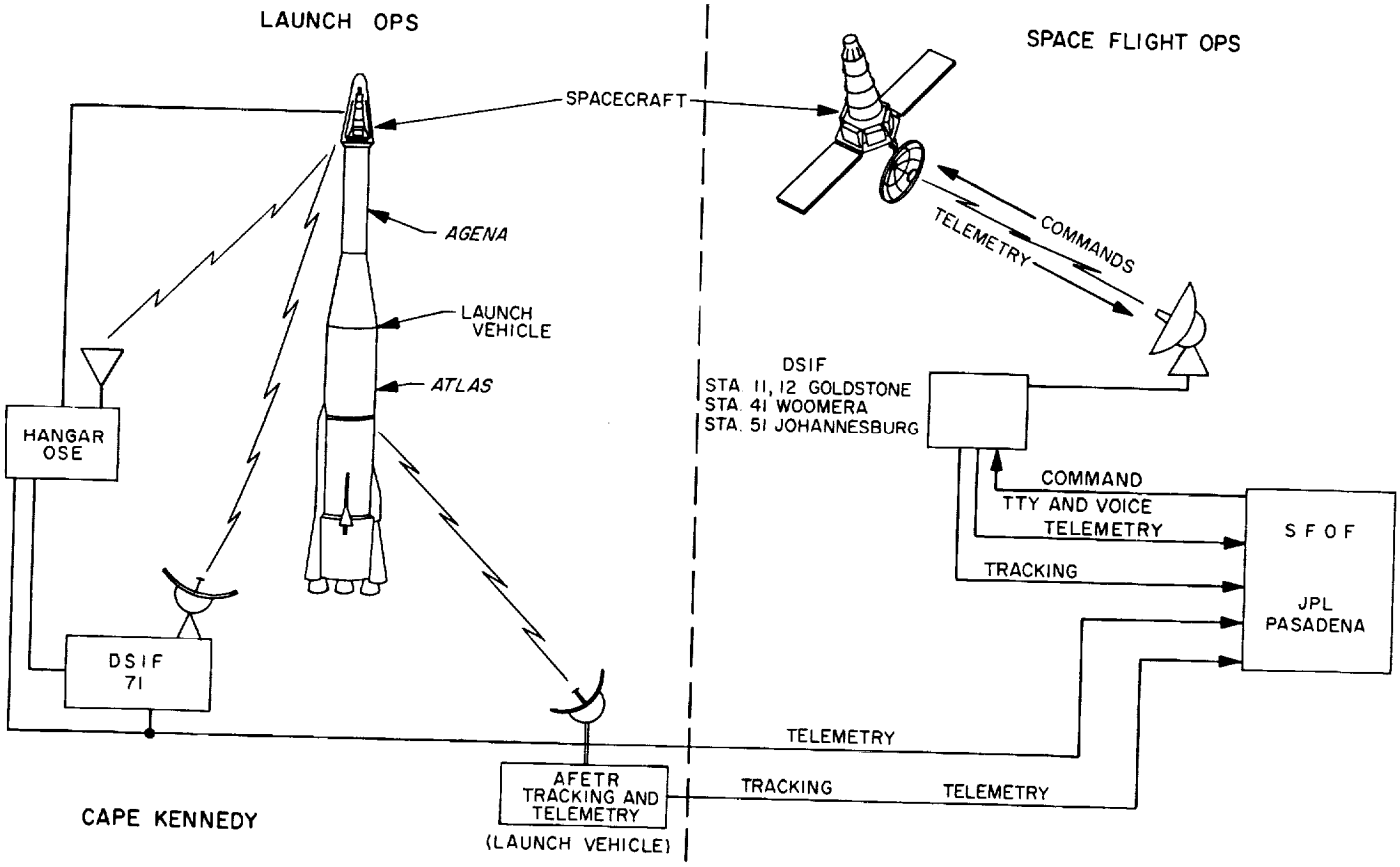

Fig. 1. *Ranger* system elements

II. PRE-LAUNCH AND LAUNCH OPERATIONS

The *Ranger VIII* and *IX* spacecraft were assembled, tested, and inspected at JPL and shipped to AFETR on January 5 and February 18, 1965, respectively. There they were unpacked and put together, tested, mated to the launch vehicles for compatibility checkout, retested, and launched. *Ranger VIII* was launched February 17, and *Ranger IX* on March 21, 1965, each from Launch Complex 12; the Range supported not only pre-launch and liftoff but also, through the downrange tracking and telemetry stations, launch-to-injection flight operations.

A. Spacecraft Assembly and System Tests

Ranger spacecraft operations leading from initial assembly to the final launch commitment follow a coherent pattern of testing, calibration, assembly and disassembly, verification, and checkout covering, nominally, 6 months of elapsed time and several hundred hours of actual spacecraft operation. *Ranger VIII* and *IX* operations were interrupted, as were those of *Ranger VII*, by the failure in the *Ranger VI* mission and the resulting investigation, rework, and modifications. The *Ranger VIII* spacecraft had completed three system tests and was preparing for vibration and mission tests prior to the rework and recycle; it resumed operations near the beginning after a 6-months' delay. *Ranger IX* had been in initial assembly at the time of the recycling.

Ranger spacecraft operations are conducted in six phases: initial assembly, subsystem test and calibration, system testing and pre-vibration operations, vibration and post-vibration testing, mission testing and pre-shipment operations, and AFETR operations culminating in launch. A summary of these operations for the *Ranger VIII* and *IX* missions is given in Table 1.

Table 1. *Ranger VIII* and *IX* spacecraft testing and operations

Activity	*Ranger VIII*		*Ranger IX*	
	Date completed	Operating hours	Date completed	Operating hours
Initial assembly	1/6/64[a]	–	3/10/64[a] 11/17/64	– –
Subsystem test and calibration	1/24/64[a] 10/15/64	74 58	12/4/64	55
System test phase[b]	2/6/64[a] 10/27/64	45.7 31	12/18/64	45
Vibration preparation and dummy runs[c]	2/15/64[a] 11/16/64	8 34	1/8/65	42
Vibration and system test No. 4	11/20/64	37	1/14/65	24
Mission tests[d]	12/8/64	195	1/29/65	175
Pre-shipment operations[e]	1/5/65	23	2/18/65	11
Cape operations[f]	2/17/65	70.5	3/21/65	49.5
Total operating hours		576.2		401.5

[a]Conducted prior to recycle; repeated or completed in second period as indicated.

[b]Includes System Tests No. 1–3 and Backup Functions Test No. 1.

[c]Includes nose fairing and adapter match-mate, secondary Sun-sensor checks, explosive-safe tests, pre-countdown and countdown dummy runs.

[d]Includes premission verification, high- and low-temperature mission tests, no-cables RF-link test.

[e]Includes TV RFI test, System Test No. 5, inspection, packing.

[f]Includes System Test No. 6 (final) Backup Functions Test No. 2, inspections and assembly operations, Explosive Safe Area tests, joint flight-acceptance compatibility test (waived on *Ranger IX*), pre-countdown, simulated launch, countdown, and launch.

1. *Ranger VIII* at JPL

The *Ranger VIII* spacecraft bus was reassembled following the rework effort in August and September 1964. The reworked and modified television subsystem was completed by October 18, permitting System Test No. 2 to be performed with this subsystem installed. The first backup functions test and a system test with electromagnetic interference concluded the system-testing phase.

The phase immediately preceding vibration testing included a number of tests, as well as the match-mate compatibility check, with nose fairing and *Agena*/spacecraft adapter, weight and center-of-gravity measurement, and countdown dummy run. The vibration test series consisted of x-, y-, and z-axis and torsional runs. Following the vibration test (November 16–20), a fourth system test verified post-vibration operation. The two full-duration mission-verification tests, at high and low temperatures (110 and 60°F at the spacecraft bus), were conducted in the 25-ft space simulator during December 1–4 and 4–7. The TV backup clock was found out of tolerance and was replaced, and camera P_4 was found to have been defocussed by temperature degradation. A series of special tests followed, designed to examine the problem of RF interference between the television subsystem and spacecraft telecommunications. No TV interference was detected on the spacecraft re-

ceiver frequency. Finally, environmental testing successfully passed, the spacecraft was checked for compatibility with the SFOF, system-tested, accepted, and shipped to AFETR on January 4, 1965. The flight-spares van was involved in a traffic accident en route, but the equipment sustained no damage.

2. *Ranger IX* at JPL

Initial assembly of the *Ranger IX* spacecraft bus was begun on January 20, 1964. Following the *Ranger VI* mission, work was stopped on February 28, pending rework; operations resumed on October 7. System Test No. 1 was conducted on December 4, the same day the television subsystem was delivered. The first complete flight-hardware system test, therefore, was No. 2, performed 6 days later. Except for minor variations, the same sequence of system test, match-mate, dummy run, environmental testing, and pre-shipment checks was pursued as with *Ranger VIII*. Environmental testing began on January 8, 1965, with the vibration test series, consisting of a modal survey before and after x-, y-, and z-axis and torsional vibration runs, and terminating in System Test No. 4. The z-axis run was made with the attitude-control gas system pressurized to flight levels as previously.

Preparation for and conduct of two simulated spacecraft missions in the 25-ft space simulator occupied the January 15–28 period. The first mission test was conducted at 110°F, the second at 55°F. Operations were essentially normal throughout both tests. An RF-link test in the chamber was also carried out, followed by an RF-interference test with deployment of the spacecraft high-gain antenna.

Following disassembly and microscopic inspection, the spacecraft was reassembled, system-tested (No. 5, on February 11), accepted, packed, and shipped to AFETR on February 18. One of the vans of this shipment was involved in a traffic accident, but, as in the case of *Ranger VIII*, the equipment was found to be undamaged.

B. AFETR Pre-launch Operations

The normal sequence of operations after spacecraft and operational support equipment (OSE) arrival at AFETR involves unpacking, inspection, reassembly, and testing at Hangar AO; testing and assembly to the bus of propulsion and pyrotechnic elements at the Explosive Safe Facility; space-vehicle assembly and composite testing on the pad; and the final complete repetition from system test to countdown, culminating in launch.

The *Ranger VIII* spacecraft arrived at AFETR on January 8, 1965, *Ranger IX* on February 22. Operational support equipment and flight spares for the two missions were shipped with *Ranger VIII*.

1. *Ranger VIII* at AFETR

Following inspection, and independent checking of some subsystem functions such as the television backup clock, the second backup-functions test was conducted at Hangar AO on January 15; the first system test at AFETR (No. 6) was completed 3 days later, with no spacecraft problems. An operational test employing the RF link (cable connections were broken at simulated launch) was also run.

During preparations for the joint flight-acceptance compatibility test (J-FACT) with the launch vehicle, the solar-panel outputs were plotted under sunlight exposure, antenna deflection was measured, and other independent operations were carried out. The spacecraft was moved to the Explosive Safe Facility, where leak and other checks of the attitude-control gas system, a TV high-power check, and an operational checkout were conducted; propulsion and pyrotechnics were assembled; and the nose fairing was mated to the spacecraft. The encapsulated spacecraft was removed to the launch pad and mated to the vehicle on January 29; pre-countdown and countdown were conducted the same day. The *Agena* umbilical cable and connector were checked out in three release tests.

Spacecraft/launch-vehicle J-FACT was successfully carried out on February 1; at the conclusion of the test, the spacecraft was returned to Hangar AO, where preparations for the final system test occupied the next 3 days.

Atlas missile No. 196D and *Agena* 6006 had arrived at AFETR on December 29, 1964; the *Atlas* was installed at the launch complex on January 6, and the *Agena* was mated to it on January 21. The initial booster flight-acceptance test was accomplished the next day. After J-FACT with the spacecraft, *Atlas* tanking tests were run, and the final booster flight-acceptance test was conducted on February 9. The simulated launch (February 14) was cancelled to accommodate correction of minor problems encountered in the *Atlas* propellant-utilization system, and final functional checks were made on the launch vehicle on February 15.

No problems occurred during the final spacecraft system test, held on February 5, and the spacecraft was

committed for the *Ranger VIII* mission. Following final Explosive Safe Facility operations and tests, similar to those performed prior to J-FACT and including final weight and center-of-gravity determinations, the spacecraft was transported to the launch complex, mated, and put through pre-countdown on February 13. The final flight weight of the spacecraft was 812.07 lb. Simulated countdown (spacecraft only) was run on February 15.

Launch countdown began at T−395 min at 09:20 GMT, February 17, 1965; spacecraft countdown commenced 3 hr later. At T−100 min, a hold was called to permit removal of a signal flag left on an *Atlas* LOX prevalve. The only other countdown holds were those built into the procedure.

Liftoff occurred at 17:05:00.795. The 118-min launch window had opened at 17:05:00. Launch weather was generally good: 78°F, 65% relative humidity, 14-knot surface winds at 150 deg, with maximum wind shear 12 knots per 1000 ft between 37,000 and 38,000 ft, scattered clouds high and at 3000 ft.

2. *Ranger IX* at AFETR

Ranger IX pre-launch AFETR operations were similar to those conducted for *Ranger VIII*, with the exception that only one system test was run, and the J-FACT and pre-J-FACT sequences were omitted. This omission was justified on the basis of the immediacy of *Ranger VIII* operations the previous month and the necessity of meeting the launch schedule. The launch-vehicle system conducted a J-FACT without the spacecraft on March 3.

The TV clock test was concluded with normal operation on February 26, and the backup-function test was conducted March 1. The RF-link operational test was run March 3. Following pre-flight calibration of the television cameras and the Earth sensor, and other preparations, the single pre-flight system test was conducted on March 8.

Agena 6007 had arrived at AFETR on January 29; *Atlas* 204D arrived on February 9. The *Atlas* booster was installed on Pad 12 on February 19, 2 days after the *Ranger VIII* launch. The *Agena* stage was mated to the *Atlas* on February 24.

The initial booster flight-acceptance test was run on March 1, followed by the *Atlas/Agena* J-FACT without the spacecraft on March 3. Problems encountered in J-FACT included electrolyte discharge from the *Atlas* telemetry battery, necessitating post-test cleanup; failure of an *Atlas* umbilical connector to eject electrically, requiring readjustment of the lock; and low and varying automatic gain control (AGC) on the *Atlas* command receiver. These problems were corrected and rechecked. The *Atlas* tanking test was conducted March 5, and the final *Atlas* flight-acceptance test occurred on March 11.

The spacecraft and television subsystem were removed to the Explosive Safe Facility on March 11, and the propulsion and television subsystems were installed. Weight and center-of-gravity measurements were made on the completed spacecraft, whose flight weight was determined to be 811.31 lb. On completion of operations and following an electrical test (March 16), the spacecraft was transferred to Launch Complex 12 and mated to the launch vehicle. Pre-countdown and simulated launch were conducted March 17 and 19. In the process, small RF fluctuations were observed during *Agena* fuel and oxidizer tanking, a phenomenon previously associated with this operation and not considered indicative of spacecraft performance anomaly. In addition, two *Atlas* telemetry transducer anomalies were noted, and the transducers were subsequently replaced. The *Agena* velocity meter and yaw-gyro temperature telemetry exhibited anomalies, which were traced to ground-equipment defects.

The launch countdown was begun on March 21 at 12:51 GMT at T−395 min. Difficulties were observed in the *Agena* velocity meter at T−355, T−255 (hold: 8 min), and T−230 (hold: 22 min), and the *Atlas* telemetry system at T−101 (telemetry can replaced during built-in hold at T−60). Because of high winds, the service tower was not removed until almost the end of the T−60 hold. The spacecraft joined the count at T−215 min (16:16 GMT) and introduced no anomalies or holds.

Liftoff occurred at 21:37:02.456. The weather was moderately good: 68°F, 18- to 22-knot northerly winds with 30-knot gusts; wind shears were 15 knots per 1000 ft at 35,000 to 40,000 ft. Cloud cover was 0.3 at 2000 ft, increasing with altitude.

C. *Range Flight Support*

From liftoff at the pad through spacecraft/*Agena* separation*, AFETR tracking, telemetry, photography, and data-handling elements supported the *Ranger VIII* and *IX* operations, providing, in addition to range-safety

*DSIF 71, the spacecraft checkout station of the DSN, maintained contact with the spacecraft from well before liftoff until the vehicle was over the horizon. AFETR and/or MSFN C-band elements maintained contact with the *Agena* vehicles after separation.

tracking and launch-vehicle performance telemetry, DSIF acquisition information and spacecraft telemetry. Tracking coverage was maintained by a number of land-based (and ship-based) radars (nine stations supported *Ranger VIII*, eleven supported *Ranger IX*). *Atlas*, *Agena*, and spacecraft telemetry data were received and recorded by stations stretching downrange from the Cape as far as Australia. In addition to the normal downrange AFETR stations, the Manned Space Flight Net (MSFN) including stations at Bermuda, Tananarive, and Carnarvon, supported the two *Ranger* missions. Figure 2 shows the extent of the downrange tracking and telemetry stations, including some Deep Space Network elements.

Spacecraft telemetry was provided during the launch phase both directly (at 960 Mc) via a parasitic antenna prior to nose-fairing jettison and via the spacecraft omni-antenna after jettison, and via the *Agena* telemetry system at 244 Mc. The DSIF spacecraft checkout station at the Cape (DSIF 71) maintained two-way lock from long before liftoff through loss of signal at the horizon, providing spacecraft telemetry at L-band and an emergency command capability. A number of the Range's telemetry-reception stations had L-band equipment also.

Tracking and telemetary coverage by AFETR were generally satisfactory (tracking coverage is summarized in Table 2). The *Ranger VIII* parking orbit was computed by the Range's real-time computing facility from Grand Turk data; DSIF initial look angles were based on this orbit. Tracking data from other stations served to refine the parking orbit and calculate the transfer orbit and post-*Agena*-retro orbit. In the *Ranger IX* mission, the real-time computing facility was out of service for approximately 4 min from L + 15 to L + 19 min, delaying

Table 2. AFETR tracking coverage

Station	Location	*Ranger VIII* coverage, sec from launch	*Ranger IX* coverage, sec from launch
DSIF 71	Cape Kennedy	0–468[a]	0–465[a]
DSIF 51	Johannesburg	1710–[a]	1498–[a]
AFETR 1	Cape Kennedy	10–310	11–200
AFETR 19	Merritt I.	12–477	9–374
AFETR 0	Patrick AFB	14–463	13–315
AFETR 3	Grand Bahama I.	56–487	142–490
AFETR 7	Grand Turk I.	208–598	204–592
AFETR 9	Antigua I.	—[b]	385–715
AFETR RIS 1886	(Twin Falls)	970–1340	690–1210
AFETR 12	Ascension I.	—[c]	1184–3330
AFETR 13	Pretoria	1730–7928	1376–2448

[a]DSIF coverage cited for reference; see Section V.
[b]Failures in angle-tracking system precluded service.
[c]Space-vehicle trajectory remained below acquisition elevation angle.

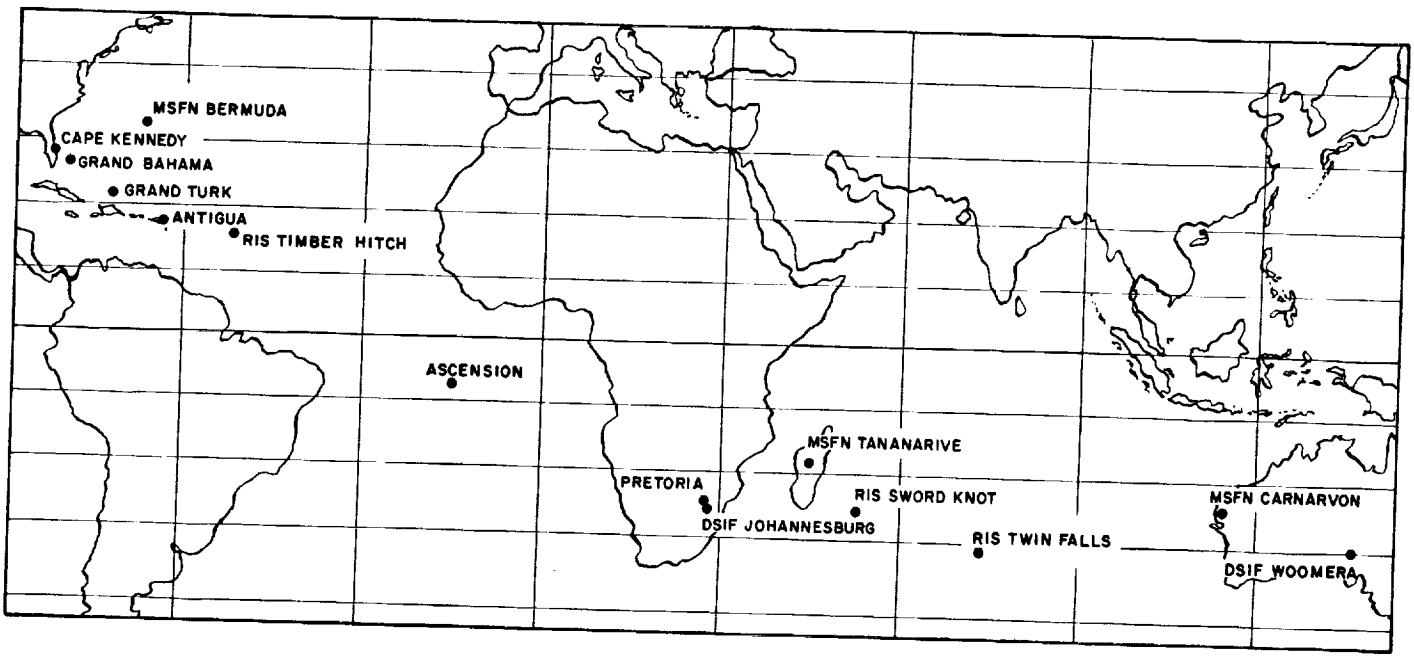

Fig. 2. Downrange tracking and telemetry coverage

transmission of DSIF look angles based on the parking orbit, which was calculated from Antigua tracking points. Transfer-orbit calculations based on post-*Agena*-retro Ascension Island tracking served to refine the look angles, but were also delayed somewhat.

Telemetry coverage of the launch phase is given in Fig. 3. Differences in ascent trajectory account for the varying spread of discrete events and the consequent difference in the shape of the coverage. All *Atlas* events were confirmed in real time from the Cape stations.

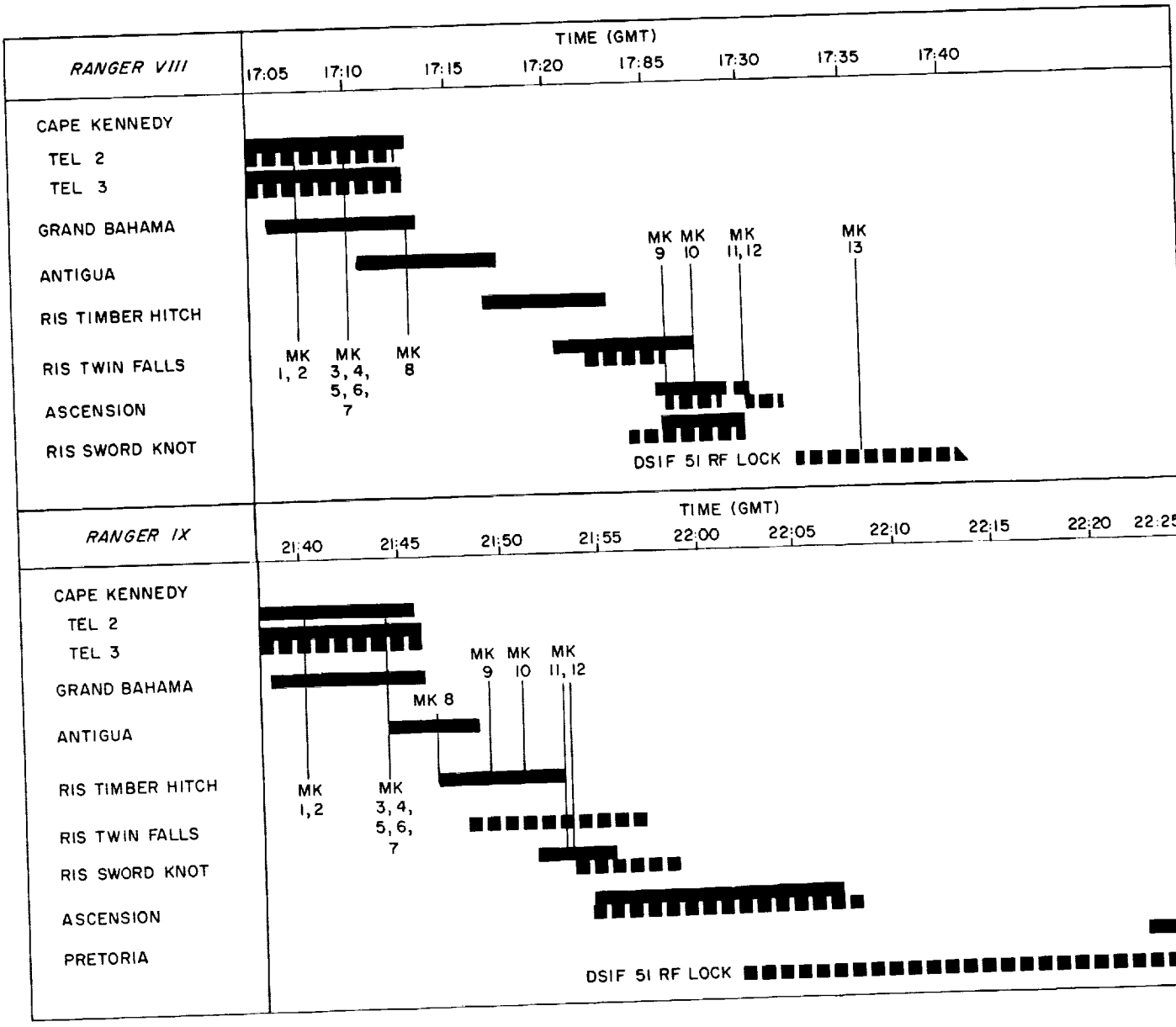

Fig. 3. *Ranger VIII* and *IX* AFETR telemetry coverage

III. LAUNCH-VEHICLE SYSTEM

The *Atlas D/Agena B* vehicle system was used to launch the *Ranger VIII* and *Ranger IX* flight missions from Complex 12 at Cape Kennedy, Florida.

The *Ranger VIII/Atlas* 196*D/Agena B* 6006 space vehicle was launched as scheduled on the first day of the launch period. Liftoff was at 17:05 GMT on February 17, 1965, less than 1 sec into the window.

The *Ranger IX/Atlas* 204*D/Agena B* 6007 space vehicle was launched as scheduled on the third day of the possible launch period. Liftoff was at 21:37 GMT on March 21, 1965, 26 min after opening of the window.

The *Atlas D/Agena B* is a 2½-stage vehicle in which all engines of the *Atlas* are ignited and stabilized prior to launch commitment. The single *Agena* engine is ignited twice in flight, first to accelerate the *Agena*/spacecraft combination to the velocity required to maintain a circular orbit about the Earth, and then, after a suitable coasting period in this "parking orbit," to accelerate the *Agena*/spacecraft to the injection velocity necessary to escape the Earth's gravitational field and coast to the lunar vicinity.

A. Atlas Booster

The *Atlas D* is a 1½-stage boost vehicle (Fig. 4) modified from the U.S. Air Force (USAF) *Atlas* missile. It contains five rocket engines that utilize a kerosene-like hydrocarbon and liquid oxygen as propellants, and at launch has a thrust-to-weight ratio of approximately 1.25.

All five engines (two boosters, one sustainer, and two vernier engines) are ignited on the ground prior to liftoff to ensure maximum reliability of this stage. After the major portion of the *Atlas* propellants has been consumed in flight, and before the vehicle has attained an acceleration of 7 *g*, the two outboard booster engines are shut down and jettisoned, and power is supplied primarily by the sustainer engine. When the approximate required velocity for the *Atlas* portion of the flight has been achieved, the sustainer engine is shut down, and for a few seconds, only the vernier engines provide thrust to stabilize the vehicle and to achieve the precise velocity desired. When this has been accomplished, the verniers are shut down, the *Agena*/spacecraft combination is separated from the *Atlas*, and the *Atlas* is backed away from the *Agena* by two small solid-propellant retrorockets.

The *Atlas* is guided during its flight first by an on-board programmer and autopilot and later by a radio guidance system. Correction signals are sent to the autopilot based on information obtained from a ground-based radar tracking station. The on-board programmer and autopilot guide the vehicle from liftoff through the jettisoning of the booster engines, except for a 10-sec period when the radio guidance (booster steering) system is enabled to receive, and steer in accordance with, the radio signals from the ground. After the booster engines are jettisoned, the radio guidance loop is enabled, and the vehicle is guided by the ground-based guidance and computer system for the rest of the *Atlas* portion of the powered flight.

1. *Atlas* 196D Operation, *Ranger VIII* Mission

All *Atlas* 196D discrete events were close to nominal. The residual quantity of propellants corresponded to a 4.97-sec burning period. Downward booster steering was employed during the flight. The indicated booster lofting was 1.6 σ. The General Electric (GE) guidance canisters were soft-mounted on this vehicle for the first time.

Heat-protective paint had been applied to certain regions of the booster skin. The temperature-reduction effects of the paint were noted and tabulated. At booster cutoff, a shock of 60 *g* peak-to-peak was perceived by the rate beacon. Two telemetry measurements were lost in flight.

2. *Atlas* 204D Operation, *Ranger IX* Mission

The *Atlas* 204D flight was nominal. Residual propellants represented 6.0 sec of remaining burning time. The *Atlas* trajectory was lofted 2.4 σ at 100 sec, and booster steering was employed at 100.2 sec.

The only configuration change from the *Ranger VIII* launch was the use of a small wedge to lock the *Atlas* LOX prevalve open, after the attribution of the AC-5 failure to inadvertent prevalve closing.

B. Agena Stage

The *Agena B* (Fig. 5) is a single-engine, dual-start, upper-stage vehicle utilizing unsymmetrical dimethyl hydrazine as fuel and inhibited red fuming nitric acid as oxidizer. At first ignition, it has a thrust-to-weight ratio of approximately unity. Its flight-control system

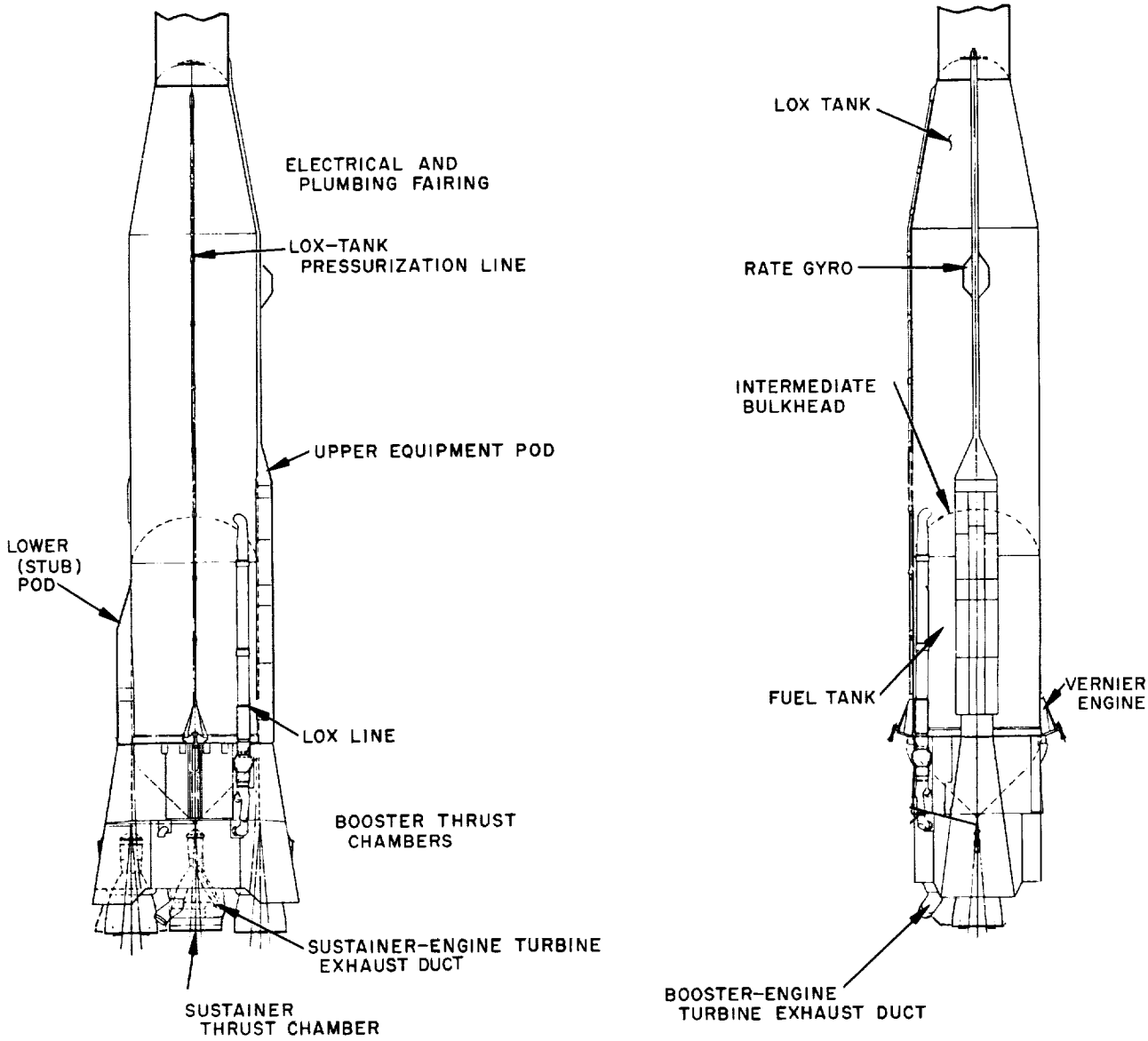

Fig. 4. *Atlas* launch vehicle

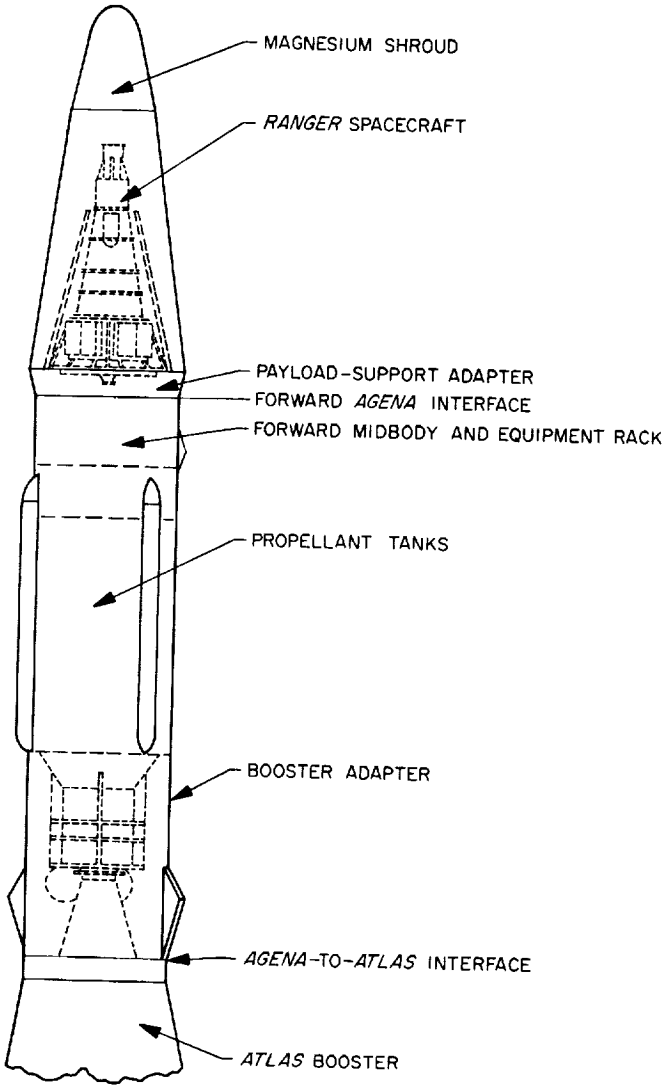

Fig. 5. *Agena* injection vehicle

consists of a programmer, a reference gyro system, two horizon sensors, and a velocity meter. Elements of the flight-control system are preset on the ground prior to launch. Via the *Atlas* radio guidance system, a ground-calculated discrete command initiates the timing function for *Agena* second burn; the *Agena* receives no further guidance or control signals from the ground subsequent to separation from the *Atlas*. The programmer and the gyro references provide the discrete events and the basic vehicle attitude information during coasting and powered flight phases. The horizon sensors view the Earth and update the gyro information during the flight to compensate for gyro drift. The velocity meter is preset for the required velocity-to-be-gained by the *Agena* stage, and determines when the engine will be shut down. The *Agena* engine ignites twice in order to accelerate the spacecraft to the required injection conditions. After the desired velocity is attained, the engine is shut down, the spacecraft separates from the *Agena*, and the *Agena* is decelerated by a small solid-propellant retrorocket to prevent it from impacting the Moon.

1. *Agena B* 6006 Operation, *Ranger VIII* Mission

A refurbished engine was incorporated in the final flight configuration after a long delay in storage. A series of tests and a study of the refurbished engine performance indicated a need for additional fuel.

There was evidence that a failure occurred in the helium pressure regulator at L + 6 sec. Helium leaked through the regulator and was dumped through the oxidizer spill valve. This was believed to be a random failure, but the possibility of vibration occurring just after the transonic period was considered.

Several minor anomalies were recorded during the flight. The umbilical door closure on the *Agena*/spacecraft adapter was monitored by motion pictures; the door appeared to bounce before it finally closed and latched. Two temperature measurements were lost at launch. The fuel-tank pressure transducer read low, possibly because of an obstruction in its vent port. However, data from the transducer were usable.

2. *Agena B* 6007 Operation, *Ranger IX* Mission

All primary and secondary *Agena* objectives were met on the *Ranger IX* flight, and its performance was satisfactory in nearly all respects. A refurbished engine was used on this flight (as on the *Ranger VIII* flight) to retain high flight reliability in spite of long storage.

Several minor anomalies occurred during the launch phase. The spacecraft-adapter umbilical door did not latch in the closed position during flight. PL 33, a tangential accelerometer, and PL 34, an axial accelerometer, exhibited erratic behavior during the *Atlas* powered flight (L + 40 to L + 60 sec). PL 35, another tangential accelerometer, became erratic during the *Agena* burns, but useful data were obtained. A better low-frequency accelerometer system is recommended for possible future flights.

IV. SPACECRAFT SYSTEM

The *Ranger VIII* and *IX* spacecraft performed successfully and well within design tolerances throughout their missions, with the exception of a temporary failure in the *Ranger VIII* radio subsystem which caused the loss of telemetry for more than 25 min during the midcourse maneuver. This anomaly occurred in addition to the expected loss associated with omnidirectional antenna pattern nulls, and was believed to be related to an RF short in the transponder or RF amplifier, possibly caused by a conducting particle. The anomalous behavior terminated at midcourse motor burn and did not recur. Repetition in the *Ranger IX* mission was judged extremely unlikely, and no modification was undertaken. The *Ranger IX* mission was without anomaly. A tabulation of spacecraft events for the two flight missions is given in Appendix A.

The spacecraft system employed in the *Ranger VIII* and *IX* missions was made up of twelve basic subsystems, whose general relationships are presented in Fig. 6. The configuration, coordinate system, and functional diagram are given in Appendix B.

The function, mechanization, and performance in the *Ranger VIII* and *IX* missions of each subsystem are discussed below. Changes to spacecraft mechanization implemented since *Ranger VII*, particularly in attitude control and television, are described under the appropriate subsystems.

A. Radio Subsystem

The spacecraft L-band radio subsystem is composed of five major elements: omnidirectional antenna, high-gain antenna, receiver, transmitter, and auxiliary oscillator (Fig. 7). The subsystem is designed to receive signals and commands via the omnidirectional antenna. The omniantenna is also used to transmit signals when the spacecraft is solar-oriented or nonoriented. The high-gain antenna transmits signals when the spacecraft is Earth-oriented. The transmitter–receiver combination is designed to transmit a phase-modulated signal which is phase-coherent with the received signal. When no signal is received by the spacecraft, a noncoherent signal is provided to the transmitter by an auxiliary oscillator.

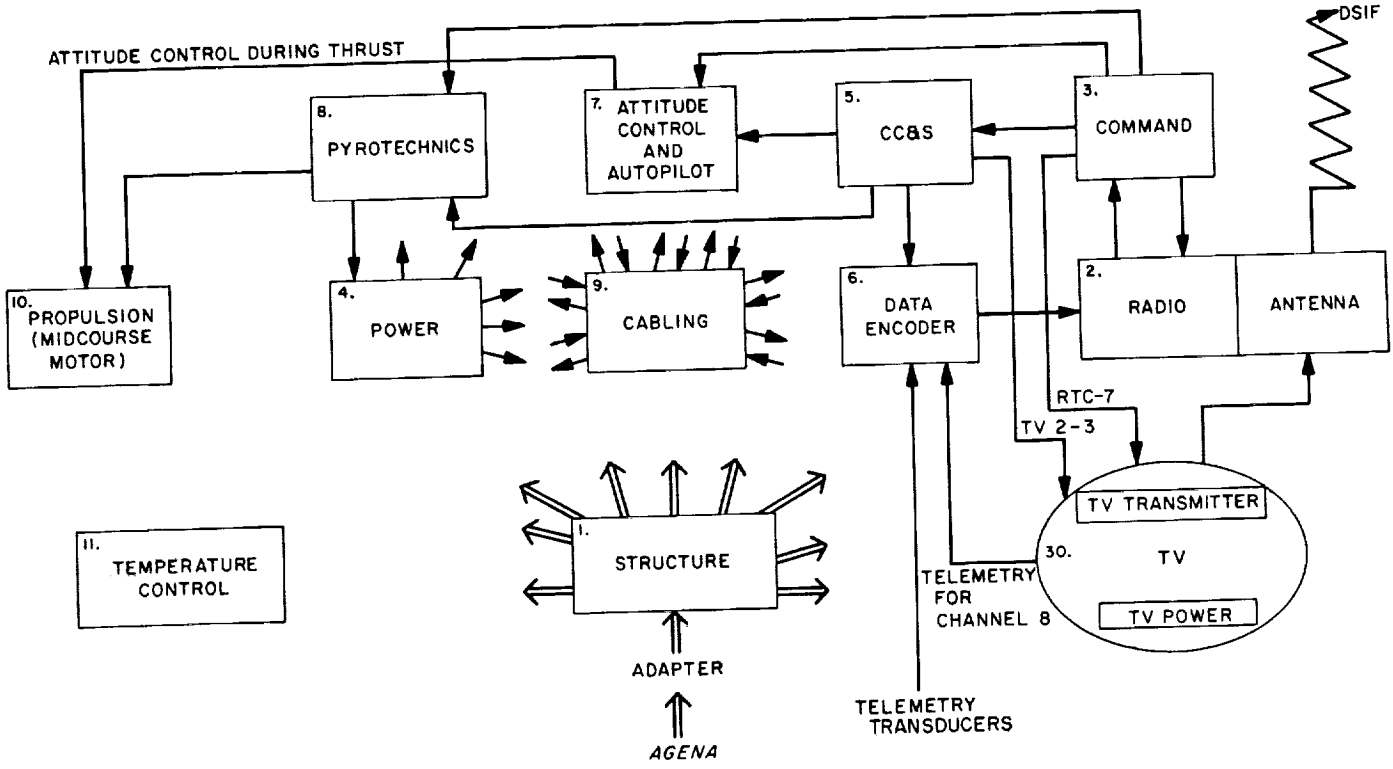

Fig. 6. *Ranger* Block III spacecraft subsystems

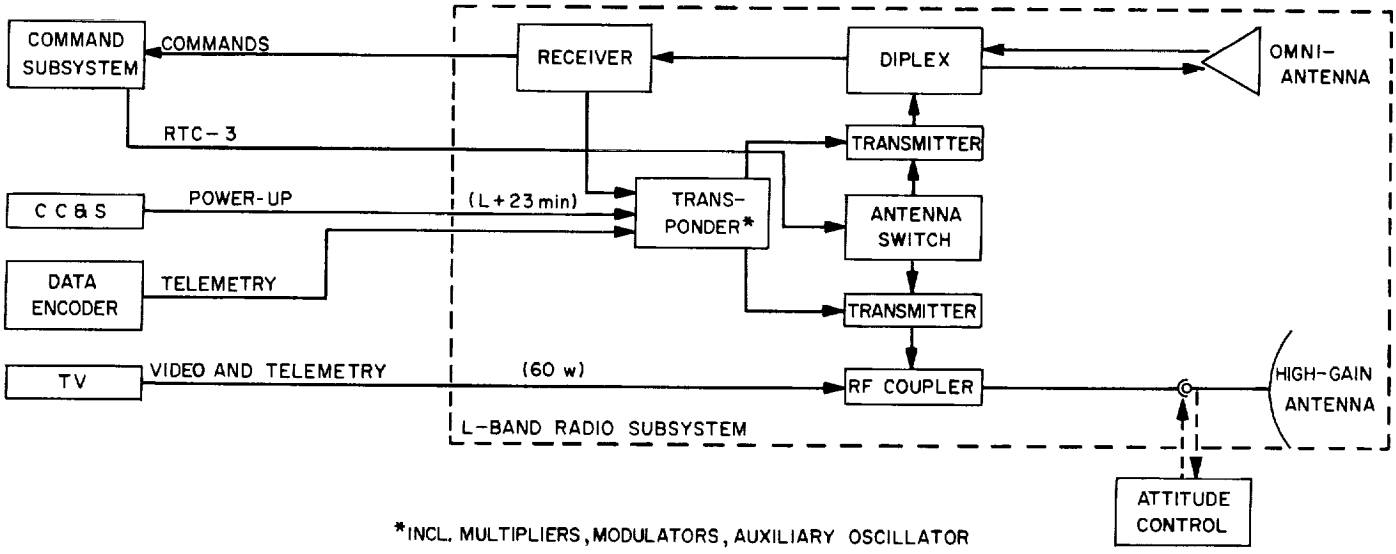

Fig. 7. L-band radio subsystem

Operation of the transmitter is monitored by three telemetered measurements. Two antenna-drive measurements indicate the amount of power supplied to each antenna, and a 250-v monitor shows the amount of plate voltage on the RF power amplifiers.

The receiver operation is monitored by means of five telemetered measurements. Two measurements of receiver AGC voltage with coarse and fine resolution indicate the spacecraft-received signal strength, and a local-oscillator-drive measurement registers the amount of power supplied by the receiver local oscillator. Two other measurements, coarse and fine static phase error, indicate the dc correction voltage resulting from the frequency difference between the up-link signal and the receiver voltage-controlled oscillator (VCO). These measurements are generally zeroed for the transmission of a command and thus become operational aids for ground stations.

1. Performance

For both the *Ranger VIII* and *IX* missions, Cape station DSIF 71 maintained two-way lock with the spacecraft during launch. Two-way lock was necessary in case a command had to be sent. Although the station momentarily lost lock at liftoff for *Ranger IX*, telemetry indicated that the receiver on the spacecraft maintained lock with the DSIF 71 transmitted signal until the spacecraft went over the horizon. Thus, a command could have been sent if necessary.

Power-up is normally scheduled to occur at L + 23 min, and the proper central computer and sequencer (CC&S) event was telemetered and received by AFETR for each of the spacecraft at that time. Normal power-up operation was not confirmed by spacecraft data, however, until DSIF 51 acquired the spacecraft — *Ranger VIII* at L + 29 min and *Ranger IX* at L + 24 min. The 250-v monitor measurement for *Ranger VIII* indicated 256 v at that time, and the omnidirectional antenna drive 34.4 dbm. For *Ranger IX*, the voltage was 259 v and the antenna drive 34.4 dbm. All values corresponded to normal power-up operation.

During the initial rise of *Ranger VIII* over DSIF 51, the station utilized a new procedure in which two-way lock was attempted immediately. Normally, the station first acquires in one-way and then transfers to two-way lock. Since two-way lock was obtained immediately with *Ranger VIII*, the same procedure was followed for *Ranger IX*, also with success.

At the same time, during the first pass over DSIF 51, each of the spacecraft appeared to be tumbling. The tumbling motion was reflected by the fine and coarse AGC measurements, which showed the variation in received signal levels. All signal-strength values, however, appeared to fall within predicted tolerances.

Solar acquisition was completed at L + 69 min for *Ranger VIII* and at L + 70 min for *Ranger IX*. As indicated by the telemetered AGC measurements, the solar orientation reduced the variations of received signal levels for each spacecraft below those of pre-acquisition levels. Since the spacecraft were rolling at that time, the small variations in signal level were due to the variations in omniantenna gain for different clock angles. All signal-level values fell within predicted tolerances.

Earth acquisition was completed at L + 215 min for *Ranger VIII* and at L + 214 min for *Ranger IX*. After Sun and Earth stabilization, the spacecraft-received signal levels stabilized. Signal levels for *Ranger VIII* generally fell within 2 db for the remainder of the mission and within 3 db for *Ranger IX*.

A real-time command RTC-3 was sent to *Ranger VIII* at L + 260 min to switch to the high-gain antenna. After the switchover, the high-gain antenna drive measurement indicated 24.6 dbm, corresponding to normal operation. In the case of *Ranger IX*, it was decided to postpone the antenna switchover because of intermittent transmitter problems at DSIF 51, the station tracking at the time. At L + 713 min, DSIF 12 sent RTC-3 to switch antennas. After the switchover, the high-gain antenna drive measurement indicated 24.1 dbm, again corresponding to normal operation.

Both spacecraft performed normally during the cruise phase, and all of the measurements fell within predicted tolerances.

Prior to the midcourse maneuver for each mission, the effects of the various proposed maneuvers on signal level were analyzed. Since the omniantenna pattern contains numerous nulls in the direction of the roll axis, the DSIF-received signal levels can fall below threshold for some maneuvers. Analysis of the *Ranger VIII* maneuver indicated that only a brief loss of data might occur during the last portion of the pitch turn. During the actual maneuver, however, a radio subsystem failure caused much of the spacecraft data to be lost. The maneuver began at L + 16 hr, 55 min, and approximately 3½ sec after the end of the roll turn a large drop in DSIF-received signal level occurred as indicated in Fig. 8. Simultaneously with the start of motor burn, however, the signal strength returned to the proper level. The radio subsystem then functioned normally for the remainder of the mission.

It was decided to postpone the midcourse maneuver for *Ranger IX* until the second pass over DSIF 12 because of the small trajectory correction needed and the desirability of obtaining additional tracking before making the maneuver. The maneuver was initiated at L + 38 hr, 26 min, and all events were executed normally. Because of its small magnitude, very little degradation in DSIF-received signal levels occurred.

Throughout the post-midcourse phase until impact, both spacecraft radio subsystems appeared to function normally in all respects.

2. Anomalies

The only anomaly which occurred in either mission was the radio subsystem failure of the *Ranger VIII* spacecraft during the midcourse maneuver.

As mentioned previously, the failure occurred approximately 3½ sec after the end of the roll turn and lasted until the start of motor burn. After this period, the radio subsystem appeared to function normally for the remainder of the mission.

The failure took the form of a large decline in ground-received signal strength. Although the drop in signal

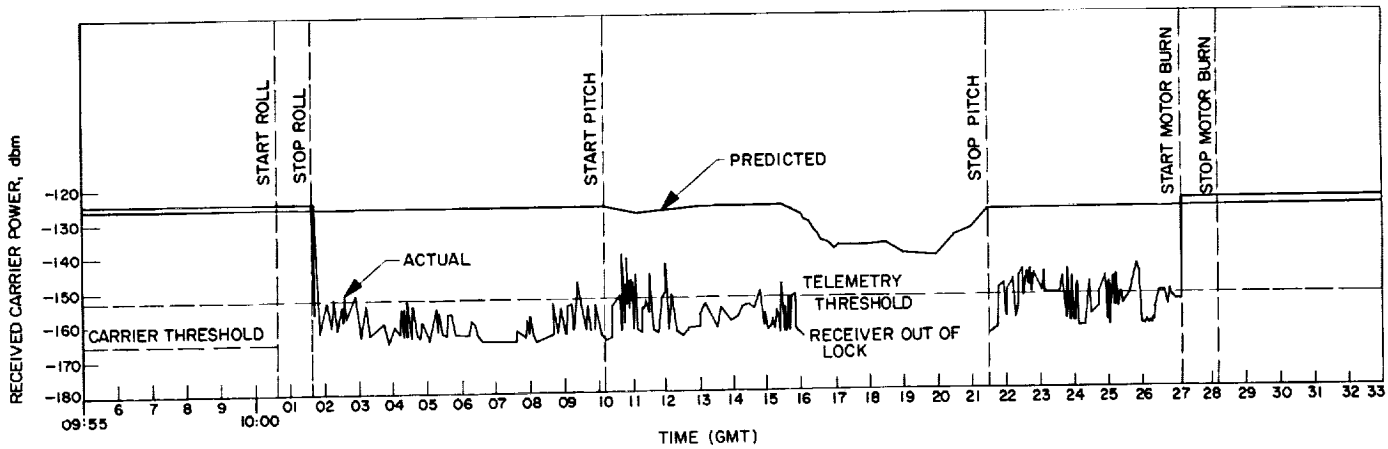

Fig. 8. *Ranger VIII* radio subsystem failure

power caused much of the telmetry data to be lost, some spacecraft telemetry was successfully recovered, as shown in Fig. 8. Analysis of these data indicated that all spacecraft measurements appeared normal except for the omnidirectional antenna drive power, which was definitely low. Analysis of the data indicated that all ground station measurements were also normal, except for the measurement of ground-received signal power. In addition, a test program was conducted on representative radio systems. Based on the magnitude of the drop in signal power which was observed, the test program indicated the three most likely sources of the failure:

1. An RF short in the ×4 multiplier cavity of the transponder.
2. An RF short in the input to the ×4 multiplier of the transponder.
3. An RF short, internal to the cavity, of the 3-w cavity amplifier.

Although it is difficult to postulate the cause of an RF short of the type that would induce the failure, it was considered possible that a conductive particle might have been responsible. Consequently, a number of spare transponders were disassembled and examined for loose conductive particles. No such particles were found, and because of the intensive quality-assurance procedures carried out during the manufacture of the radio subsystem, it was felt that the possibility of a recurrence of the failure was very low. Therefore, the *Ranger IX* transponder was flown without modification.

B. Command Subsystem

The command subsystem consists of a command detector and a command decoder. Commands are sent to the spacecraft over the radio link by means of a frequency-shift-keyed (FSK) subcarrier signal that is recovered in the spacecraft radio receiver. Since the command subsystem operates asynchronously, one of the functions of the command detector is to detect the spacecraft radio-receiver FSK signal to determine when a command is being sent. When a command is sent, the detector converts the FSK signal to a serial sequence of binary ones and zeros which comprise the command code. The first bit detected is always a binary one, called a start bit. The start bit opens a gate allowing the command to be serially transferred to the decoder (Fig. 9). The start bit also enables a counter, which performs two functions. First, the counter receives a 25-pps signal from the CC&S and divides it by 25, thus providing a 1-pps output; this signal is sent to the decoder to be used as its sync pulse. Secondly, the counter also counts at a 1-pps rate until count 57 is reached (one command cycle). Count 57 resets the detector to its original condition, thus readying it for the next command. The detector has an auxiliary 25-pps clock, so that should the CC&S 25-pps clock fail, it would still be possible for the command system to operate. The detector receives two signals from the decoder — an alert pulse and a real-time command indication — and sends these to the proper subsystem. The alert pulse (count 16 of the command cycle) is sent to the CC&S to tell it that a command is in process. The RTC indication is generated by the closing of an RTC relay, and is sent to the telemetry.

With nominal input signal, the probability of a command subsystem bit error is $\leq 10^{-5}$. However, since noise inherent in transmitting and receiving commands could alter the command, considerable attention is given to the strength of the signal provided to the command system by the radio receiver. As the receiver power decreases

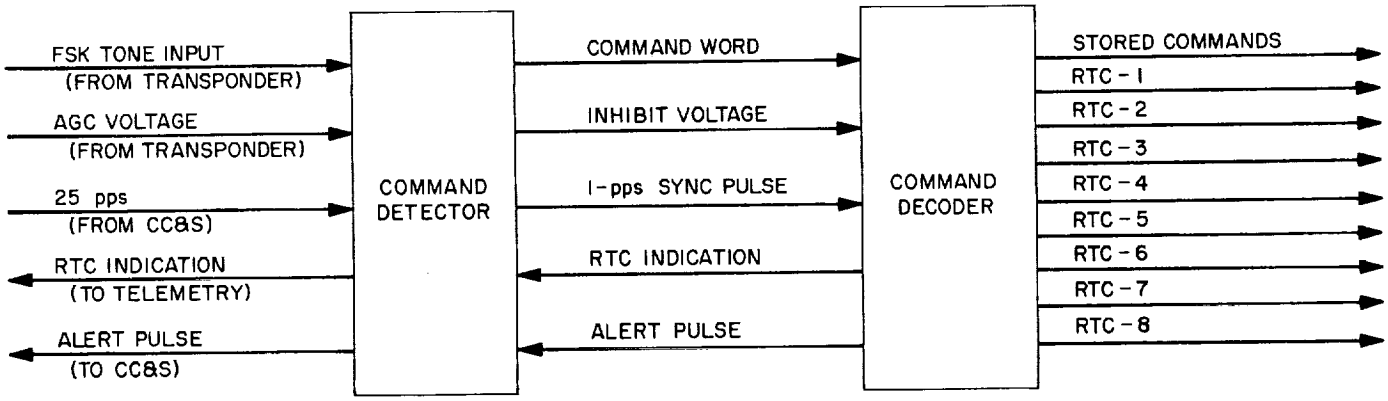

Fig. 9. *Ranger* command subsystem

to about −130 dbm, the probability of a bit error increases but remains below 10^{-5}; should the receiver drop lock, an inhibit signal is developed within the command system derived from the receiver AGC. (The power levels quoted above vary slightly for different systems.) Typical signal strengths are from approximately −90 dbm at launch to approximately −120 dbm at lunar distance, thus normally being well within command threshold.

The command decoder receives the serial, binary command from the command detector and shifts it into a storage register. The command is then checked to see if it is recognizable. For recognizable commands, the decoder differentiates between stored commands (SC) and real-time commands. All of the SC's are transferred to the CC&S for further processing. If an RTC has been detected, the decoder determines which one it is and closes the appropriate relay to inform the corresponding addressee (CC&S, attitude control, etc.).

Verification that the decoder has received and correctly acted on a command is obtained in two ways. When a command is acted on, it is telemetered in the form of frequency-modulated pulses on a subcarrier (B-20), which, in turn, phase-modulates the RF carrier transmitted from the spacecraft. This can be viewed on the record of the telemetry signals. If an RTC has been received, a single pulse will occur indicating that some RTC relay closed. If an SC was received, each bit of the command transferred to the CC&S will be recorded, thus enabling a check to be made of the entire contents of the command. The second method of verification is to observe, by telemetry, the behavior of the other subsystems. If the affected subsystems respond as they should, it can be assumed that the command was correctly received and acted upon.

A complete list of the commands received during the *Ranger VIII* and *IX* flights is shown in Tables 3 and 4, respectively. The sole purpose of RTC-0 is to cycle the logic of the command subsystem to ensure that it is in the correct state to receive a command; however, there are no telemetry data to confirm that the command was in fact received. Telemetry data for all other commands, using the above methods of verification, indicate that the command subsystem functioned perfectly in all respects throughout both missions. It should be noted that the *Ranger IX* mission was the first in which a terminal maneuver was performed. The commands necessary for this maneuver were correctly detected, decoded, and acted upon by the command subsystem. Similarly, *Ranger IX* was the first mission in which antenna hinge-angle updating was accomplished, and on which the TV backup clock was inhibited.

Table 3. *Ranger VIII* command history

	Command initiated (Date/GMT)	DSIF sending station	Associated event blips
RTC-0	17:21:21:38	51	–
RTC-0	17:21:23:38	51	–
RTC-3	17:21:25:39	51	Ch. B-20 at 21:25:41
RTC-0	18:08:50:38	12	–
RTC-0	18:08:52:38	12	–
SC-1	18:08:54:38	12	Ch. B-20 at 08:54:41
SC-2	18:08:56:38	12	Ch. B-20 at 08:56:41
SC-3	18:08:58:38	12	Ch. B-20 at 08:58:41
RTC-0	18:09:36:38	12	–
RTC-0	18:09:38:38	12	–
RTC-3	18:09:40:38	12	Ch. B-20 at 09:40:40
RTC-4	18:10:00:38	12	Ch. B-20 at 10:00:41
RTC-0	18:11:30:38	12	–
RTC-0	18:11:32:38	12	–
RTC-3	18:11:34:38	12	Ch. B-20 at 11:34:40
RTC-0	20:07:37:00	12	–
RTC-0	20:07:39:00	12	–
SC-4	20:07:41:00	12	Ch. B-20 at 07:41:41
SC-5	20:07:43:00	12	Ch. B-20 at 07:43:41
SC-6	20:07:45:00	12	Ch. B-20 at 07:45:41
RTC-0	20:08:23:00	12	–
RTC-0	20:08:25:00	12	–
RTC-8	20:08:27:00	12	Ch. B-20 at 08:27:40
RTC-6	20:08:47:30	12	Ch. B-20 at 08:48:11

The commands used and their definitions are as follows:

RTC-0 — Clear command

RTC-2 — Antenna hinge-angle override and preset-angle preselect

RTC-3 — Antenna transfer

RTC-4 — Start midcourse maneuver

RTC-5 — Telemetry mode change, inhibit TV backup clock, and turn off TV

RTC-6 — Start terminal maneuver

RTC-8 — Maneuver inhibit and emergency Sun reacquisition

SC-1 — Midcourse roll duration

SC-2 — Midcourse pitch duration

Table 4. *Ranger IX* command history

	Command initiated (Date/GMT)	DSIF sending station	Associated event blips
RTC-0	22:09:26:00	12	–
RTC-0	22:09:28:00	12	–
RTC-3	22:09:30:00	12	Ch. B-20 at 09:30:41
RTC-0	22:26:00:00	41	–
RTC-0	22:28:00:00	41	–
RTC-2	22:30:00:00	41	Ch. B-20 at 30:00:39
RTC-0	23:10:50:00	12	–
RTC-0	23:10:52:00	12	–
SC-1	23:10:54:00	12	Ch. B-20 at 10:54:40
SC-2	23:10:56:00	12	Ch. B-20 at 10:56:41
SC-3	23:10:58:00	12	Ch. B-20 at 10:58:40
RTC-0	23:11:31:00	12	–
RTC-0	23:11:33:00	12	–
RTC-3	23:11:35:00	12	Ch. B-20 at 11:35:42
RTC-4	23:12:03:00	12	Ch. B-20 at 12:03:40
RTC-0	23:13:26:00	12	–
RTC-0	23:13:28:00	12	–
RTC-3	23:13:30:00	12	Ch. B-20 at 13:30:41
RTC-0	24:11:54:00	12	–
RTC-0	24:11:56:00	12	–
SC-4	24:11:58:00	12	Ch. B-20 at 11:58:42
SC-5	24:12:00:00	12	Ch. B-20 at 12:00:41
SC-6	24:12:02:00	12	Ch. B-20 at 12:02:42
RTC-6	24:13:02:34	12	Ch. B-20 at 13:03:13
RTC-5	24:13:17:00	12	Ch. B-20 at 13:17:41

SC-3 — Midcourse velocity increment

SC-4 — Terminal first pitch duration

SC-5 — Terminal yaw duration

SC-6 — Terminal second pitch duration

Other commands available but not used during the two *Ranger* flights are:

RTC-1 — Roll override and Earth-acquisition command backup

RTC-7 — TV warmup

C. *Data Encoder*

The data-encoder subsystem accepts, encodes, and prepares spacecraft engineering information for radio transmission. This information, consisting of voltages, temperatures, pressures, and verification of specific events, is vital to the evaluation of spacecraft performance. A total of 85 such measurements is made; a listing of these measurements, together with the processing elements, is presented in Fig. 10.

The encoder is fully transistorized and consists of 16 modules mounted in a standard *Ranger* case. The unit occupies 0.9 ft^3, weighs 27 lb, and consumes 10 w of power. The exterior of the case is gold-plated and is painted with a special pattern to control the data-encoder temperature in space.

The unit may be functionally described as a PAM/FM/PM encoder. Both time-division and frequency-multiplexing techniques are used because of the limited transmitter power available from the spacecraft's 3-w transmitter. Time-division multiplexing is performed by four commutators comprising a total of ten measurement decks. Frequency multiplexing employs ten subcarrier channels which form a subcarrier composite signal ranging in frequency from 350 to 3024 cps. The data encoder generates six wideband channels for telemetering analog information and three narrow-band channels employing frequency-shift keying for telemetering digital information. One subcarrier channel is used to telemeter a CC&S timing signal which is used to evaluate the performance of the spacecraft master timing source and to provide commutator-rate information to the ground telemetry equipment.

The major elements of the data encoder are:

1. Signal-conditioning circuits
2. Commutators
3. Rate-limiting amplifiers
4. Voltage-controlled oscillators
5. Binary oscillators
6. Programmer
7. Event coder
8. Auxiliary clock

1. Element Description

The signal-conditioning circuits, consisting of voltage dividers, dc amplifiers, and temperature (Wheatstone)

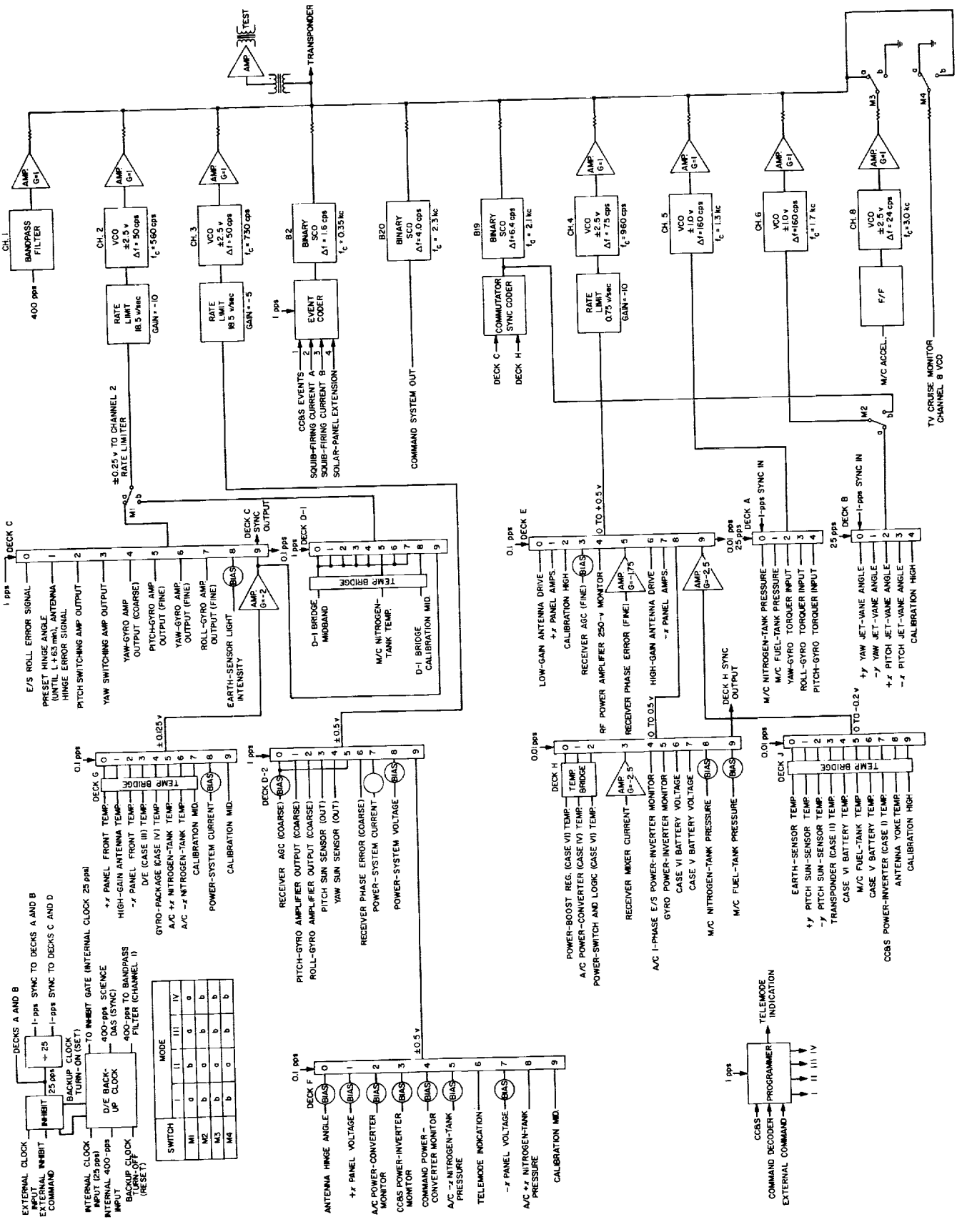

Fig. 10. Data encoder

bridges, are used to tailor the measurement ranges of the many transducer outputs to voltages which are easily processed by the other encoder elements. After the necessary signal conditioning is performed, the measurement is applied to a position on one of the ten commutator decks (see Fig. 10).

The commutators allow several measurements to be carried on a single subcarrier channel. The rate at which the information changes and the rate at which it is required by the data users determine which of the encoder's four commutators is used to sample the measurement. Four rates of commutation are employed: 25 samples per second (or 25 pps), 1 sample per second (1 pps), 1 sample per 10 seconds (0.1 pps), and 1 sample per 100 seconds (0.01 pps).

Framing pulses supplied by the 1.0- and 0.01-pps commutators are telemetered on Channels B-19 and 6 to synchronize the ground telemetry equipment with the commutator system. Commutator-rate information is also supplied by transmitting the 400-cps signal, from which the commutator drive signals are derived, on Channel 1.

The voltages on the output of the commutator decks produce frequency changes of the voltage-controlled oscillators, which, in turn, phase-modulate the spacecraft transmitter. The output signals of the commutators appear as a series of pulses, which change amplitude rapidly as the commutators step from one measurement to the next. To limit the rate at which these voltages change the VCO frequency, rate-limiting amplifiers are used between the relay commutators and the VCO's for Channels 2, 3, and 4. The maximum allowable rate of change of frequency for Channels 2 and 3 is 185 cps/sec and for Channel 4, 11.2 cps/sec. Channels 5 and 6 do not contain rate-limiting amplifiers. These channels require wide bandwidths (160 cps), and consequently, to conserve transmitter power, they are assigned measurements which are not required after the midcourse maneuver.

The data encoder uses voltage-controlled oscillators to generate six of the ten subcarrier frequencies. These oscillators contain multivibrator circuits whose frequencies are proportional to voltages applied to their inputs. The squarewave output of the multivibrator is converted to a sine wave by a bandpass filter contained in the VCO. Required properties of the VCO's include high linearity, constant sensitivity, good frequency stability, and low distortion.

Channels B-2, B-19, and B-20 are generated by binary (two-state) oscillators. The information telemetered on these channels is in the form of pulses corresponding to spacecraft events (B-2), commutator framing pulses (B-19), and radio commands received by the spacecraft (B-20).

During different phases of the flight, different information is required by the subsystem analysts to evaluate spacecraft performance. The programmer changes the measurement inputs to the rate limiters and VCO's to meet these information requirements. Although the programmer has the capability of four data-selection modes, in the Block III *Rangers* only two different data formats are used. During the midcourse maneuver, the Channel 6 information was changed from the redundant commutator framing pulses to jet-vane actuator positions, Channel 8 transmitted acceleration data in place of TV 15-point telemetry, and Channel 2 carried temperature information in place of some attitude-control measurements. The telemetry mode is changed by CC&S commands or by a command sent from the ground.

The CC&S subsystem issues commands to various other subsystems to initiate certain operations. To report the CC&S commands and the resulting occurrences, the data encoder's event coder has four flip-flop circuits, associated with CC&S commands, squib-firing events A, squib-firing events B, and solar-panel extension, respectively. The event coder samples the state of each flip-flop every second and generates a coded output for any event that has occurred.

The operations of the data encoder rely heavily on the presence of timing pulses. The timing pulses supplied to the commutators, programmer, and event coder are all derived from the 25-pps signal supplied by the CC&S subsystem. The loss of this signal would result in the stoppage of data sampling, event encoding, and data format changing. As a safeguard against such stoppages, a separate 25- and 400-pps generator—the auxiliary clock—is contained in the data encoder.

2. Performance

The *Ranger VIII* and *IX* flight data encoders met all of the design requirements. The spacecraft engineering data processed by the encoders was, as expected, of sufficient accuracy and fidelity to permit real-time evaluation of all spacecraft subsystems. The commutators, synchronization signals on Channel B-19, and the basic encoder timing information on Channel 1 all functioned perfectly, permitting continuous automatic reduction of the telemetry signal.

The event coders properly coded all events on both flights, giving accurate indications of the occurrence and duration of both programmed and commanded sequences. The programmer responded to all mode-change commands, providing the required data modes for each phase of the flights, and Channel B-20 indicated all ground commands received by the spacecraft.

D. Ground Telemetry Equipment

Ranger's primary ground telemetry subsystem, located at each DSIF station, performs the function of demodulating and decommutating the *Ranger* spacecraft signal. The subsystem consists of the following functional elements:

1. Discriminators to detect and demodulate the individual telemetry subcarrier channels from the composite spacecraft signal.

2. Decommutator to digitize and identify the commutated engineering data samples.

3. Teletype (TTY) encoder to encode and format the output of the decommutator for teletype transmission to JPL in Pasadena.

The output signal from the station's RF (L-band) receiver is routed to the phase-lock-loop discriminators, which separate the spacecraft composite signal into the ten bandwidths or "channels" assigned to the *Ranger* Block III telemetry subsystem. The discriminators recover a "cleaned-up" facsimile of the input waveform as one output, and an analog output proportional to the input frequency as the other. The reconstructed output of discriminator Channels 2–6 is fed to the counter circuits of the digital decommutator, where the spacecraft time-shared engineering measurements are counted and identified with a two-digit number or "address." The identification is made by utilizing the synchronization information contained in Channels 1 (spacecraft 400-cps drive) and B-19 (sync pulse) to determine which segment the airborne commutator is sampling at a given time. The address used to identify a particular spacecraft measurement corresponds to a specific position on the airborne commutator.

After an engineering measurement has been identified, the decommutator formats the data for input to the TTY encoder, which adds time, station identification, and parity information to the data. The TTY encoder also converts the 8-bit parallel signal received from the decommutator to a serial format suitable for transmission over teletype lines. The encoder output drives a teletype punch unit which records the encoded data on punched paper tape. The punched tape is then fed into teletype distribution units for transmission over teletype lines to the SFOF.

An alternate system transmits the spacecraft composite telemetry signal over analog phone lines to JPL, where the channels are separated using discriminators and displayed on an analog recorder for the Spacecraft Data and Telecommunications Analysis Teams (SDAT and TCAT). Either the primary or the secondary signal as received at JPL may be given to the programmed data-processor (PDP) computer in the SFOF. During the major portions of the *Ranger VIII* and *IX* missions, both real-time telemetry-recovery systems were effectively utilized.

The only real-time data-recovery link from Hangar AO at AFETR for both *Rangers VIII* and *IX* was the analog transmission line. This proved to be adequate. After launch coverage was completed, the line was "turned around," and JPL, Pasadena, fed the spacecraft analog signals to Hangar AO, allowing the AFETR launch team to assist in evaluating the data.

In the primary telemetry system at all DSIF stations, the teletype paper punch is physically separated from its associated teletype reader. This produces a slight delay in the real-time transmission of data from a particular DSIF station to the SFOF. This delay amounted to less than 40 sec for both *Ranger VIII* and *IX* missions. Signals from the secondary system were received with little or no delay by the chart recorder at JPL, but the repeaters along the transmission path caused positive frequency shifts of from 3 to 6 cps.

There were no ground telemetry equipment failures during either mission. All equipment operation was at near-optimum design levels.

With the exception of the *Ranger VIII* RF-dropout anomaly, the quantity and quality of the spacecraft telemetry data for both the *VIII* and *IX* missions exceeded those received from any other *Ranger* mission. The increased level of performance can be attributed to a greater familiarity with the ground telemetry equipment by the DSIF crews and to improved circuit links in the DSN.

E. Central Computer and Sequencer

The CC&S provides the spacecraft frequency reference; issues launch-, midcourse-, and terminal-phase sequence commands; receives and stores (in flight) midcourse- and terminal-maneuver parameter information; controls the roll, pitch, and yaw turns in accordance with the maneuver parameters received; and integrates the velocity increments received from the accelerometer during the midcourse-motor burn and commands motor shutoff when the proper velocity is achieved.

The CC&S subsystems performed nominally during the entirety of the *Ranger VIII* and *IX* missions. Telemetry data indicated no malfunctions or abnormal conditions during either mission; data from other subsystems using CC&S functions confirmed this. All CC&S fixed-time events occurred within less than 1½ sec of their nominal times in all three phases of both missions. All spacecraft pre-flight tests were completed without encountering any problems that could be construed as subsequent mission problems.

The launch-phase commands from the CC&S were received and acted upon by the other subsystems well within the tolerances of the predicted times. The midcourse-maneuver functions of the CC&S were exercised and confirmed to be in agreement with the stored commands transmitted to the spacecraft. The terminal maneuvers (for *Ranger VIII*, a truncated maneuver whose only function was the initiation of a TV-warmup clock) were performed without incident and resulted in the establishment of the declared terminal conditions.

The CC&S central clocks' timing accuracy was much better than specified by the functional requirements. For the 64-hr, 52-min *Ranger VIII* mission, the clock error, as indicated by the analog record, was 0.001% or less; the *Ranger IX* 64-hr, 31-min mission had a clock error, as indicated by the analog record, no greater than 0.002%. The requirement for clock accuracy is ±0.01%.

1. Pre-launch and Launch-Phase Performance

The *Ranger VIII* and *IX* CC&S subsystems were shipped to Cape Kennedy on board the spacecraft and were never removed. During pre-flight testing, the only anomaly detected was the *Ranger IX* CC&S response to transients from its operational support equipment to give an "acquire Earth" command; this anomaly was documented and corrected procedurally. Immediately prior to each launch, central-clock accuracy was verified from the 1000-sec sync pulses.

Launch-phase operations of the CC&S were nominal: B-2-1 telemetry indications showed that transmitter power increase, solar-panel deployment, start of Sun acquisition, and start of Earth acquisition occurred within 0.5 sec of predicted times for both missions, except for the *Ranger IX* Earth-acquisition command, which was 1.2 sec late. The CC&S power-inverter temperature rose sharply just after launch in the *Ranger VIII* mission, when Case I was exposed to sunlight; a maximum temperature of 113°F was attained, after which the temperature fell sharply and stabilized at 106°. In *Ranger IX*, the spacecraft was in the Earth's shadow for 33 min, 45 sec; the CC&S inverter dropped to 86.3°F, then rose again to a value within the nominal range.

The cruise period from Earth acquisition to midcourse maneuver was, in each mission, uneventful.

2. Midcourse and Second Cruise

The *Ranger VIII* and *IX* midcourse maneuvers were controlled by CC&S functions, based on quantities generated on Earth. Pitch and roll turns were specified as to polarity and magnitude, the angular quantity being translated into a time duration at a known turn rate. The velocity-change quantity was translated into a number of accelerometer pulses to be counted, and a motor burn time was also calculated for reference.

The transmission of stored commands to the spacecraft, to load the CC&S shift registers with the proper roll, pitch, and velocity information, began 1 hr, 6 min before initiation of the start of the midcourse maneuver for *Ranger VIII*. *Ranger IX*'s stored commands were transmitted 1 hr, 9 min before the start of the maneuver. The command subsystem on the spacecraft receives, decodes, and routes the stored commands to the input decoder subassembly of the CC&S, which, in turn, decodes the addresses and routes the command quantities to the proper register.

The receipt of the stored commands by the command decoder was verified by telemetry data on analog Channel B-20. The CC&S issues a capacitor cycling pulse (AC-1) to the attitude-control subsystem on the third bit of the roll (SC-1) address. The presence of this pulse was verified by a B-2-1 event coincident with the third address bit of SC-1 on *Rangers VIII* and *IX*.

The *Ranger VIII* midcourse maneuver was initiated 16 hr, 55 min after launch; a +11.60-deg (53-sec) roll turn, a +151.75-deg (681-sec) pitch, and a 36.4409-m/sec (1192-pulse or 59-sec) velocity change from the motor were commanded.

The *Ranger IX* maneuver was initiated 38½ hr after launch, in order to further refine the tracking of a near-perfect trajectory. The roll turn commanded was −27.41 deg (126 sec), the pitch +127.96 deg (587 sec), and the motor burn was to change the velocity by 18.15 m/sec, corresponding to 591 pulses or, nominally, 30 sec of thrust duration. These commands were executed flawlessly.

Midcourse events were verified by B-2-1 event indications. On *Ranger IX*, the motor-burn time was 2 sec longer than predicted; this is of small concern for the CC&S because the predicted burn time is based on nominal motor performance, which can change with temperature and fuel-tank pressure changes. The number of accelerometer pulses is a true measure of motor performance in terms of agreeing with the stored velocity increment. The midcourse turn durations were also timed, by the use of a stopwatch, and were found to be in agreement with the previously stored information, with the exception of the *Ranger VIII* pitch turn, which could not be confirmed. About 3 sec after the end of the roll turn, the *Ranger VIII* spacecraft transmitter power dropped to a degree that caused loss of lock on all telemetry channels. This condition continued through pitch turn until suddenly, coincident with the firing of the midcourse motor, the power level returned to normal. Some telemetry channels came in and out of lock during this time, and enough data were received to verify that a pitch turn had been started. A mode change was also indicated, confirming the assumption that the pitch turn had been completed, since the CC&S gives a mode change pulse at the end of the pitch turn. Trajectory information subsequently gave no reason to believe that the pitch-turn duration was other than specified.

After the midcourse motor burn, the CC&S issued the reacquire Sun and Earth commands, at nominal times for both missions, which were executed by the attitude-control subsystem. The reacquire commands are the last in the midcourse sequence for the CC&S; therefore, during the second cruise phase of the missions, only the sync times and CC&S power-inverter temperature required monitoring.

3. Terminal Maneuver

Ranger VIII, like *Ranger VII*, did not perform a terminal maneuver, though it was deemed desirable to take advantage of the two CC&S fixed-time commands in the terminal-maneuver sequence—the TV warmup command and the TV full-power backup command. The decision was made, as in *Ranger VII*, to disconnect the attitude-control subsystem from the CC&S by an RTC-8 command after sending the stored commands. Even though the CC&S, on receipt of the RTC-6 command, issued commands to break solar lock, start and stop first pitch turn, start and stop yaw turn, and start and stop second pitch turn, the attitude-control subsystem did not react accordingly. The two TV commands from the CC&S, TV-2 and TV-3, were not disconnected by the RTC-8 and occurred at their nominal times after the start of the terminal maneuver. As a backup in the event the attitude-control subsystem was not disconnected by the RTC-8 command from the CC&S, it was decided to store the minimum turn durations of 1 sec in the CC&S registers, which would result in an insignificant change in camera pointing angle.

Command and attitude-control telemetry verified receipt of the three stored and two real-time commands and non-execution of the turns, as desired. The TV warmup and full-power commands were given by the CC&S as scheduled, 45 and 50 min after start of the terminal maneuver. The full-power command was not needed, as the TV subsystem had automatically gone into full power after 80 sec of warmup.

Ranger IX was unique in the Block III series in that it was the only one to exercise its full capabilities by performing a terminal maneuver. The terminal-maneuver computer program was issued, and the maneuver magnitudes were confirmed to be in agreement with the stored turn durations, as well as the coded words to be transmitted. Transmission of the stored commands was started 1 hr, 4 min prior to initiation of the terminal maneuver.

The stored commands were verified by the CC&S analysts as having been correctly received by the spacecraft and being in agreement with the computer program. The capacitor cycling pulse occurred at the nominal time, as evidenced by the B-2-1 event.

The *Ranger IX* terminal maneuver was initiated by an RTC-6 command from the Goldstone station and was verified by a B-20 event.

The performance of the *Ranger IX* CC&S in the terminal-maneuver sequence was entirely satisfactory. All fixed-time events occurred at their predicted times, and the three turn durations were as stored prior to the maneuver. The TV warmup command was given 45 min after start of the maneuver and was followed by both F and P TV systems going to full power 80 sec later. The CC&S full-power TV backup command was given at the nominal time but was not needed or acted upon.

The thermal behavior of the CC&S power inverter on *Ranger IX* was unlike that of its Block III predecessors

during the last hour before impact. *Rangers VI, VII,* and *VIII* exhibited an increase in temperature just prior to impact, explained as being the result of solar infrared reflection from the lunar surface. The *Ranger IX* inverter temperature dropped sharply beginning with the start of the terminal maneuver and continued to decrease until impact. The total decrease in temperature was 7°F. The sharp decrease in temperature is attributed to the attitude of the spacecraft in response to the terminal maneuver; it was oriented in a position which reduced direct solar radiations as well as lunar reflection.

The total mission performance of the *Ranger VIII* and *IX* CC&S subsystems equalled all expectations. At no time during either mission were the telemetry data indicative of any cause for concern about the CC&S.

F. Attitude-Control Subsystem

The *Ranger* attitude-control subsystem is designed to maintain spacecraft orientation with respect to Sun and Earth and to control high-gain antenna pointing. Spacecraft turn maneuvers are carried out by control elements. In flight, position error signals are received from the Sun sensors and the Earth sensor, and, during acquisition, rate information is obtained from three single-axis gyros. During the cruise phase, rate feedback is obtained for the derived-rate networks. Control torques about the spacecraft are produced by a cold-gas-expulsion system. During the midcourse motor firing, an autopilot and jet-vane thrust-direction control provide vehicle stability. The sensor and control elements are shown in Fig. 11; spacecraft coordinate axes are presented in Fig. 12.

The flight-performance analyses presented below are, in general, based on hand-plotted unprocessed data, which at times required resynchronization and calibration.

1. System Changes for *Rangers VIII* and *IX*

The *Ranger VIII* and *IX* attitude-control subsystem incorporated several changes from the *Ranger VII* system that significantly affected its mechanization and performance.

Cruise attitude control was modified from a gyro-control, hysteresis system to a derived-rate, minimum-on-time system. The change was implemented by replacing the switching amplifier with a derived-rate switching amplifier, as indicated in Fig. 13. The significant difference between these two systems is the replacement of the gyro-rate signals by a derived-rate feedback signal

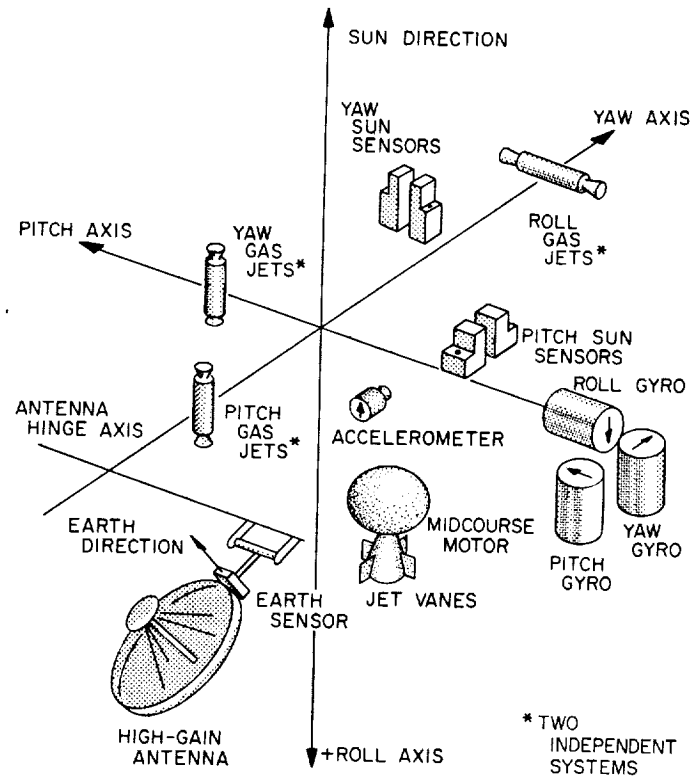

Fig. 11. Attitude-control elements

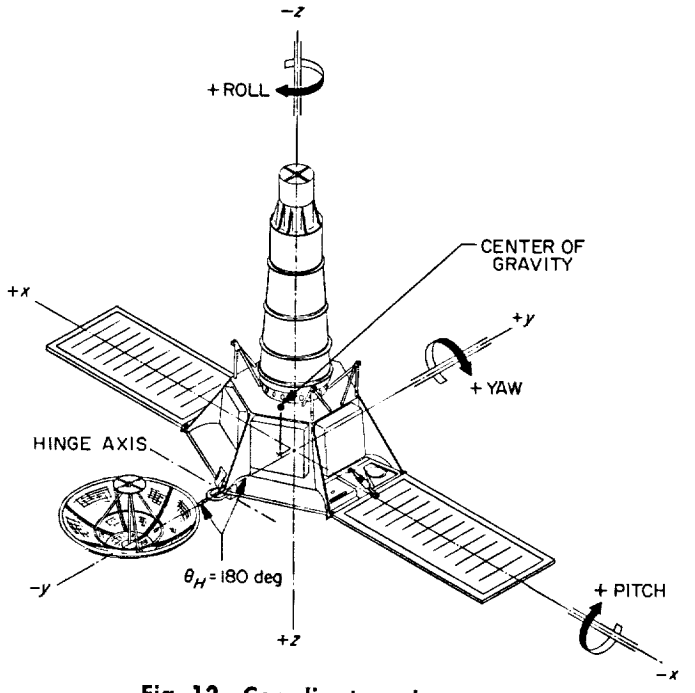

Fig. 12. Coordinate-axis system

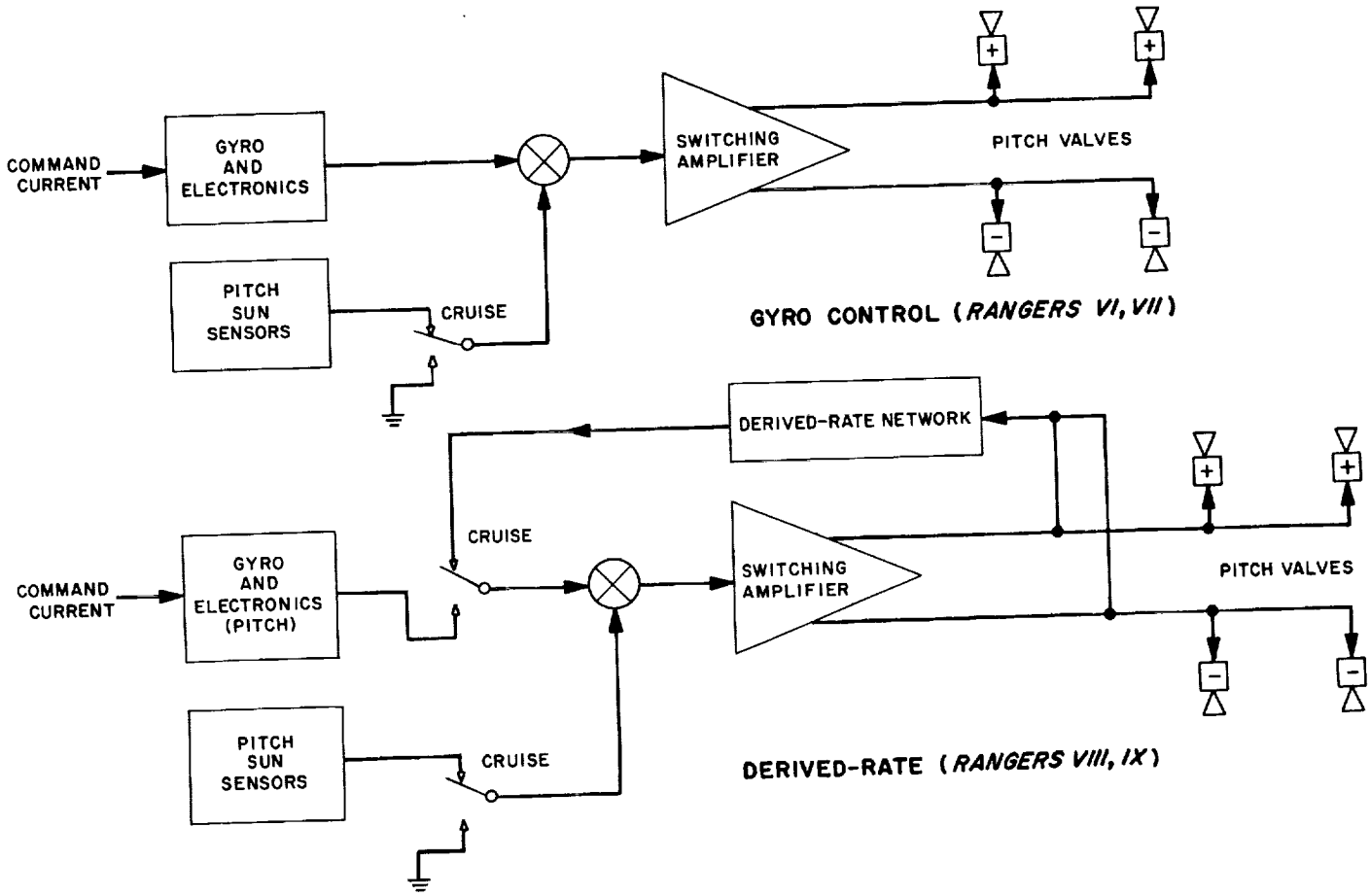

Fig. 13. Single-axis control networks, gyro control and derived-rate systems

after Earth acquisition. The derived-rate system also has a lower velocity increment — 20 ±2 instead of 60 ±30 μrad/sec.

In a detailed post-flight study of the gas-system acceleration constants for *Rangers VI* and *VII*, it was noted that the pitch accelerations during the commanded turns were the only accelerations that fell within the specification limits. In order to correct for the low accelerations, and to provide a greater tolerance for error, the acceleration constant was changed from 0.60 ±0.06 to 0.72 ±0.18 μrad/sec² for *Rangers VIII* and *IX*.

Partly because of a low roll-position scale factor (which would result in a large roll deadband of 8.8 mrad instead of the specification value of 5 mrad at midcourse) and partly in an effort to increase the midcourse-maneuver accuracy, the roll limit-cycle position was calibrated and plotted in real time prior to the midcourse maneuver. This made it possible to time the maneuver-execute command with an optimum roll position. (A proposed change which would have reduced the roll deadband within the derived-rate switching amplifier was rejected in favor of "timing" the maneuver.) Calibration of the roll position required special calibration of the Earth sensor with a globe Earth simulator at AFETR prior to the final spacecraft systems test.

In addition to these modifications, a change in the Earth-sensor temperature-control paint pattern was made on *Ranger IX* in order to maintain the Earth-sensor temperature within an acceptable range after the terminal maneuver orientation.

2. *Ranger VIII* Mission Performance

a. Pre-launch conditions. High-accuracy (10-sec count) telemetry data indicated a stored gas weight of 2.12 lb in the $+x$ system and 2.09 pounds in the $-x$ system. The pitch- and yaw-gyro output voltages measured in the blockhouse were within 2 mv of the expected values computed from gyro laboratory readings, and the roll gyro

was within 4 mv. One RTC-2 command was transmitted to select the 135-deg antenna preset angle required for the particular launch day, February 17, 1965 (liftoff at 17:05:00 GMT).

b. Separation. Spacecraft separation occurred at 17:30:14. The earliest data available indicated that the pitch, yaw, and roll rates were −3.0, −6.0, and +1.5 mrad/sec, respectively, at 17:33:30. The separation rates are estimated to have been −1.5, −6.6, and +1.5 mrad/sec in pitch, yaw, and roll, respectively.

When the solar panels extended at 18:05:01, the pitch rate was beyond the telemetry band limit of −7.3 mrad/sec and the yaw and roll rates were +0.60 and +1.20 mrad/sec, respectively. Solar-panel extension caused no observable rate change.

c. Sun acquisition and reacquisition. The CC&S commanded Sun acquisition at 18:08:00. The yaw axis acquired the Sun at 18:14:06 and the pitch axis at 18:14:18. A detailed analysis of the acquisitions follows.

Yaw axis. At 18:07:52, the yaw position was +1562 mrad, and the yaw rate was +0.7 mrad/sec (Fig. 14). The spacecraft yaw axis was moving away from the Sun line. At 18:08:00, the attitude-control system was energized and the spacecraft accelerated up to the acquisition rate of −4.14 mrad/sec in 9 sec. The acceleration constant for the start transient was −0.506 mrad/sec².

The antenna system was also energized at the Sun-acquisition command so that the antenna actuator began moving the high-gain antenna out from its nested (0-deg) position. The high-gain antenna and yoke combination was turning about the pitch axis at the (−) yaw axis (Fig. 12). The antenna motion therefore increased the spacecraft yaw moment of inertia for antenna hinge angles of 0 to 90 deg and decreased (from the inertia

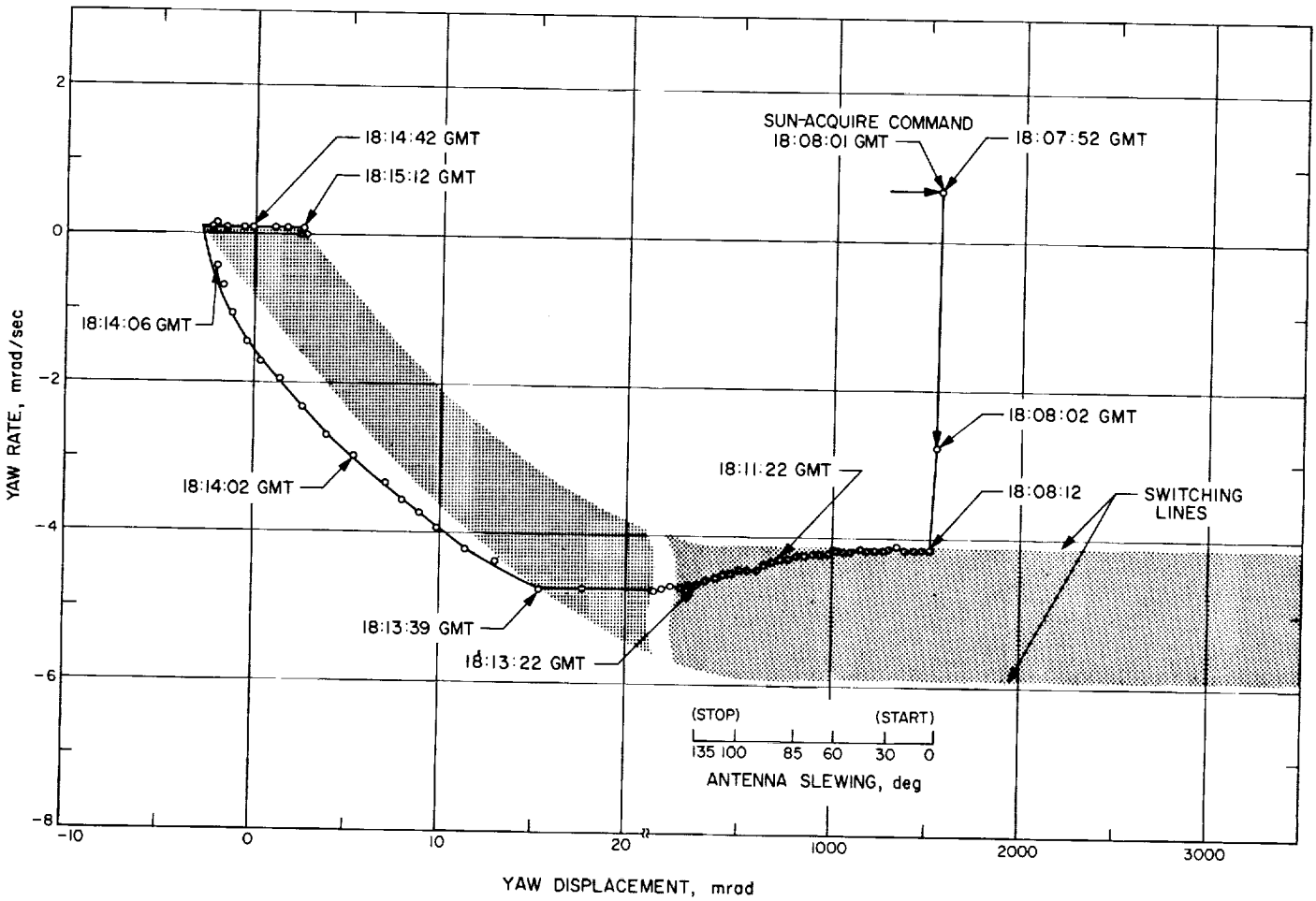

Fig. 14. *Ranger VIII* Sun acquisition, yaw axis

value for a hinge angle of 90 deg) for antenna hinge angles of 90 to 180 deg.

This effect can be seen on the phase-plane plot (Fig. 14), where the increase of inertia is reflected by a decrease in rate (due to the conservation of momentum) about the yaw axis and the subsequent effect of having the yaw rate held by the upper switching line*. At 18:11:22, the antenna reached 90 deg, and the decrease in the yaw inertia was reflected by an increase in yaw rate until 18:13:22. At that time, the antenna reached the preset angle, and the yaw-acquisition rate remained constant until the switching line was crossed at 18:13:59. The yaw-stop-transient acceleration constant was +0.657 mrad/sec.[2]

*Switching lines are the two loci of the limits of the combined position and rate deadband mechanized in the switching amplifiers, position sensors, and rate gyros.

The Sun was in the yaw-roll plane at the reacquire command after midcourse, so that the yaw limit cycle was immediately re-established.

Pitch axis. At 18:07:52 GMT, the pitch position was −1546 mrad, and the pitch rate was −8.08 mrad/sec (Fig. 15). The spacecraft pitch axis was moving away from the Sun line. When the Sun-acquire command was issued, the pitch-axis control system reacted, changing

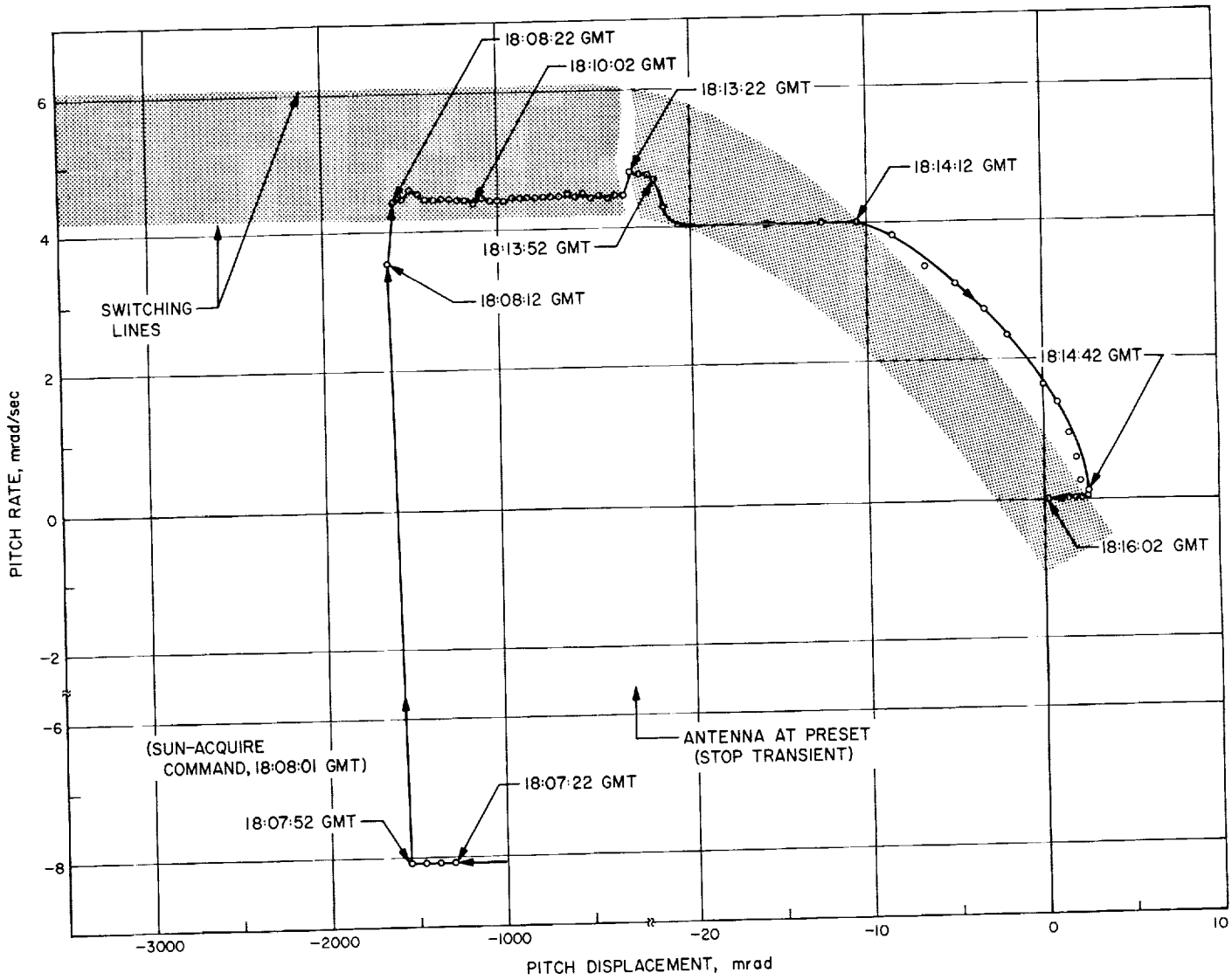

Fig. 15. *Ranger VIII* Sun acquisition, pitch axis

the pitch rate to +4.47 mrad/sec. The start transient had an acceleration constant of +0.848 mrad/sec^2.

Since the antenna hinge axis is parallel to the pitch axis, the effect of the antenna slewing from 0 to 135 deg on the spacecraft moment of inertia is one of increasing the inertia; the spacecraft reaction to the antenna slewing out is also one of slowing the pitch rate down; therefore, the overall effect is to maintain the pitch rate at the lower switching line. At 18:13:22, the antenna reached its preset angle; the stop transient can be seen on the pitch rate in Fig. 15.

The stop transient of the yaw-axis acquisition started at 18:13:59, and the cross-axis acceleration from yaw to pitch is noticeable in Fig. 14. The cross-axis acceleration observed on the pitch-gyro torquer data corresponds to 20% of the yaw acceleration, or about −0.135 mrad/sec^2. This acceleration, attributed to the vertical component (pitch) of the gas jets, resulted in decreasing the pitch-acquisition rate to +4.0 mrad/sec.

Thereafter, the pitch rate remained constant until the upper switching line was crossed at 18:14:12. The pitch-stop-transient acceleration constant was −0.705 mrad/sec^2.

Pitch reacquisition after midcourse was initiated at 10:30:40. The start- and stop-transient acceleration constants were −0.465 and +0.560, respectively. The acquisition is shown in Fig. 16. The effect of the antenna motion in slewing from 180 to 122 deg was similar to that observed in the first acquisition. The combination of the decreasing inertia and the spacecraft reaction to the antenna slewing in about the pitch axis resulted in the pitch rate being held at the upper switching line. The stop transient of the antenna can be seen at approximately 10:32:53 in Fig. 16. The pitch axis was acquired at 10:40:13.

d. Earth acquisition and reacquisition. At 20:36:01, the attitude-control subsystem received the Earth-acquire

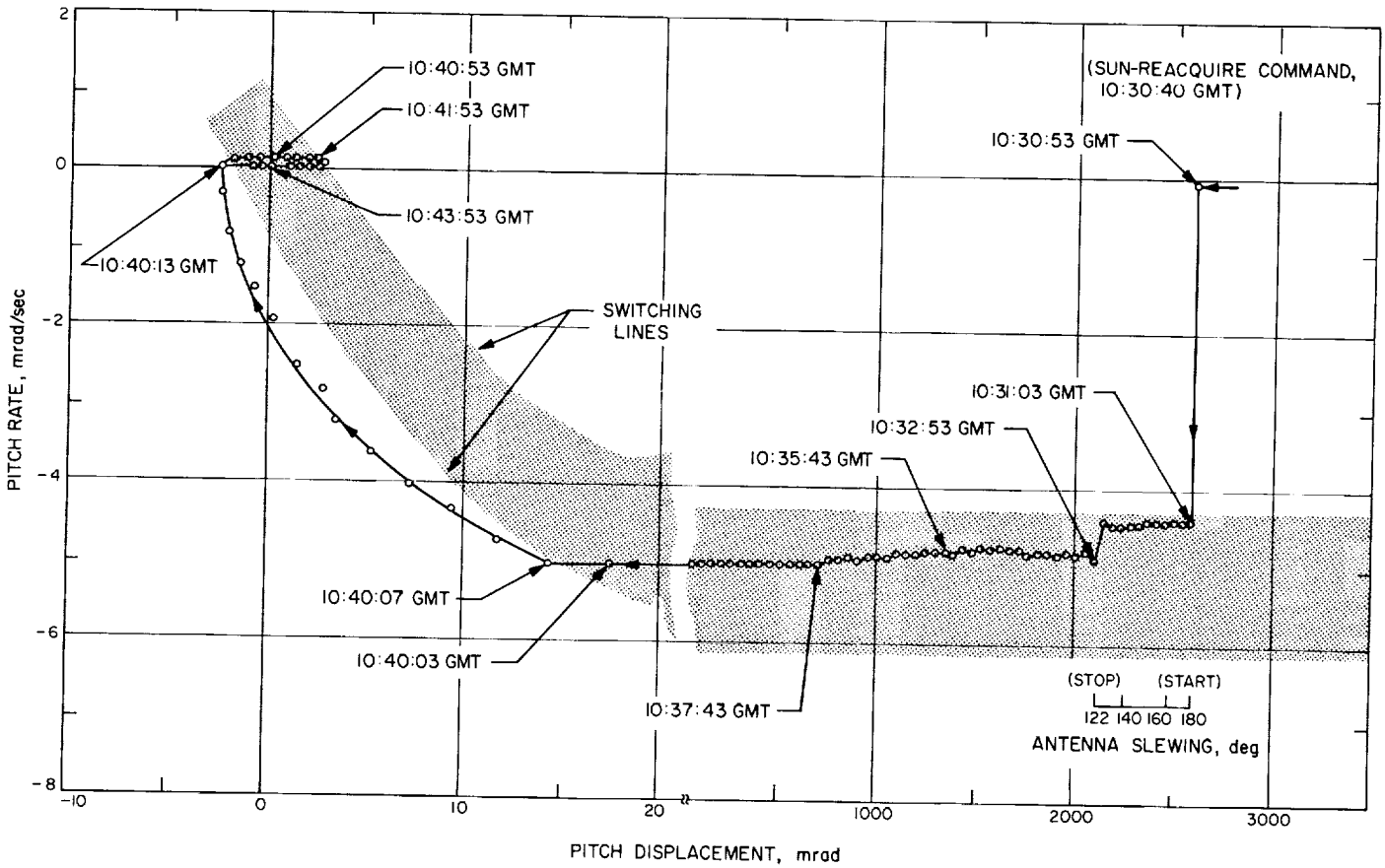

Fig. 16. *Ranger VIII* Sun reacquisition, pitch axis

command, and the Earth sensor was energized. Conditions were as follows:

1. Earth–probe–Sun angle, 43.74 deg.
2. Earth–probe–Moon angle, 147.43 deg.
3. Earth angular diameter, 13.81 deg.
4. Earth phase angle, 136.24 deg.
5. Expected light intensity of the Earth, 2.73 ft-cd.

As a result of the above conditions, Earth acquisition occurred with the Earth presenting a thin, lighted crescent of approximately 1.5 deg to the Earth-sensor field of view, and with approximately 1.9 deg of the crescent ends extending beyond the roll field of view after acquisition. Since the Earth sensor seeks the center of light, the center of the Earth-sensor field of view was approximately 8 deg from the center of light in the hinge angle. This condition then required the hinge to drive out to approximately 143 deg as the roll search brought the Earth within the field of view.

As can be seen from Fig. 17, the roll scale factor is significantly affected by the large angular diameter of the Earth. The scale factor, as determined from calibrations made at AFETR with the painted-globe Earth simulator, should have been 1.8 v/deg. The scale factor as determined from the acquisition data using the following equation was found to be 1.77 v/deg (averaged over two points).

$$\text{Roll scale factor} = \frac{E_2 - E_1}{\int \dot{\theta}_r\, dt \sin H + (Y_2 - Y_1 \cos H)}$$

where

E = Earth-sensor roll-error voltage
Y = yaw angle
$\dot{\theta}_r$ = roll rate
H = hinge angle
t = time

This scale factor results in a position deadband of +27 and −23 mrad. The shape of the scale-factor curve determines the form of the switching lines in Fig. 18.

Roll axis. After Sun acquisition, the roll rate stabilized at +0.798 mrad/sec until the Earth-acquisition command was issued (Fig. 18). It is estimated that the spacecraft rolled a total angle of 29.6 deg.

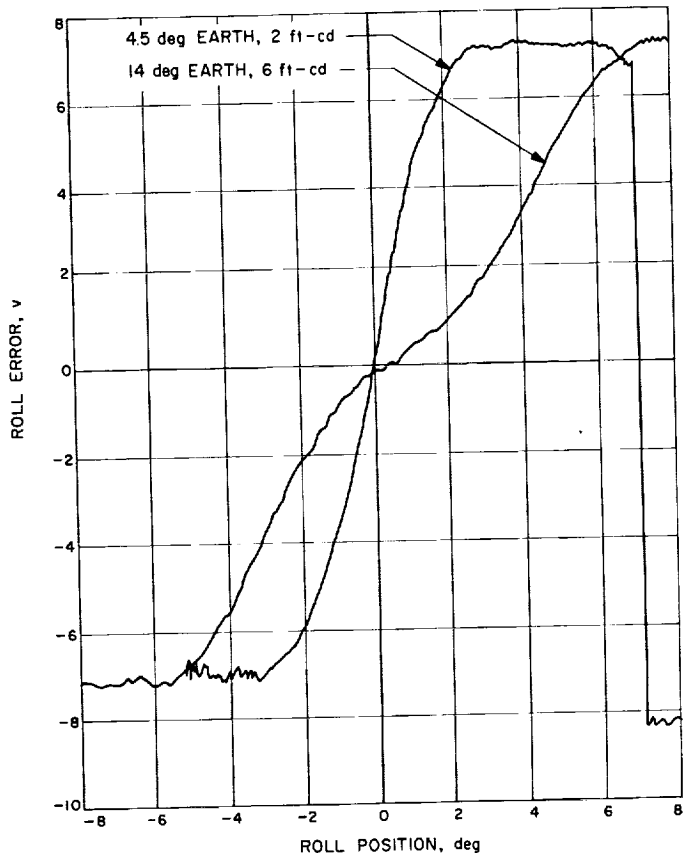

Fig. 17. *Ranger VIII* roll scale factor

At 20:35:52, the spacecraft roll position was +517 mrad, with a roll rate of +0.798 mrad/sec. At 20:36:01, the attitude-control subsystem received the Earth-acquire command, and the roll rate increased to −2.30 mrad/sec over a 4-sec period, with a roll-start-transient acceleration constant of −0.778 mrad/sec². The roll rate remained constant until 20:33:06, when the lower switching line was crossed. Since the control system was overdamped at this time, it followed the lower switching line until 20:41:12, when the gyro signals were switched out and the system went into a derived-rate mode of operation. The effect of the derived-rate feedback is evident in Fig. 18, where the system is shown to leave the switching line and establish a limit-cycle mode of operation.

At 10:58:38 GMT, on February 18, the Earth-reacquisition command was issued, and the following conditions prevailed:

1. Earth–probe–Sun angle, 53.97 deg.
2. Earth–probe–Moon angle, 140.04 deg.
3. Earth angular diameter, 4.32 deg.

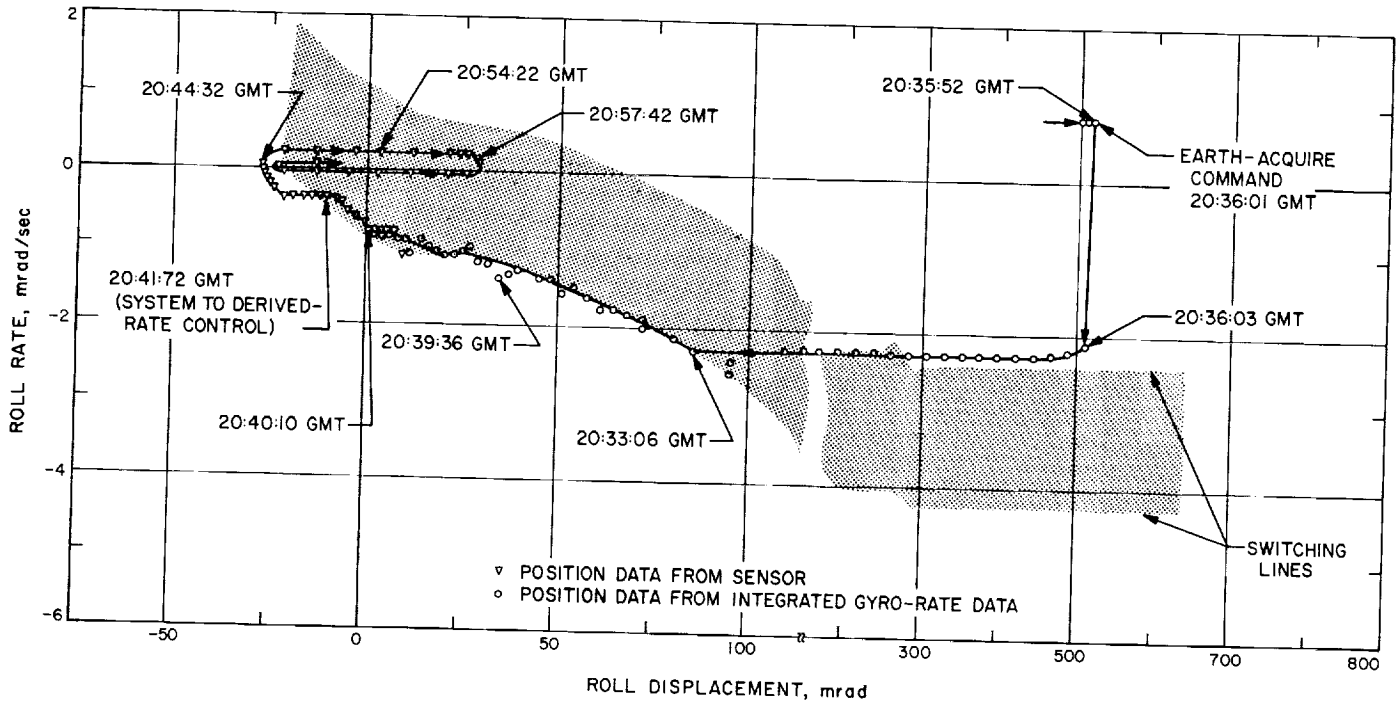

Fig. 18. *Ranger VIII* Earth acquisition, roll axis

4. Earth phase angle, 125.98 deg.
5. Expected light intensity of the Earth, 0.41 ft-cd.

As a result of the midcourse maneuver and residual roll rate after motor burn (−0.082 mrad/sec from motor burn to the Sun-acquire command and +0.16 mrad/sec from Sun acquisition to the Earth-acquire command), the roll position and rate at 10:58:33 were +279 mrad and +0.16 mrad/sec, respectively. Upon receiving the Earth-reacquire command, the spacecraft increased the roll rate to −2.33 mrad/sec and acquired the Earth in 123 sec. A phase-plane plot of the acquisition is shown in Fig. 19.

e. Midcourse maneuver. The midcourse-maneuver parameters were as follows:

1. Roll turn, +11.6 deg (53-sec duration).
2. Pitch turn, + 151.75 deg (681-sec duration).
3. Velocity magnitude, 36.44 m/sec.

At 10:00:44 on February 18, the CC&S commanded the start of the roll turn. The pitch, yaw, and roll positions at that time were −2.54, −0.279, and −3.5 mrad, respectively. The roll-turn-start and -stop acceleration constants were +0.642 and −0.646 mrad/sec^2, respectively. Prior to sending the execute command, the roll limit cycle was observed and plotted; it was decided to send the command at the predetermined time, since the maneuver-execute time was more significant than the roll position for the particular trajectory and target area.

At the end of the roll turn, the spacecraft–to–Earth communications link was lost and telemetry was interrupted until the start of motor burn. No detailed evaluation of the pitch turn can be made; however, evaluation of the pitch reacquisition indicates that the pitch turn was normal. The midcourse autopilot performance appears to have been normal, although a thorough analysis has not been undertaken.

f. Antenna hinge control. Prior to launch, one RTC-2 was stored in the antenna control electronics to select the 135-deg antenna preset angle required for the first launch day. At the Sun-acquire command, the antenna slewed out to the first preset angle at a rate of 0.42 deg/sec. At the start of the midcourse maneuver, the antenna was moved to the 180-deg exit angle at a rate of 0.61 deg/sec, and the preset counter in the antenna control electronics was stepped to the second preset angle. At the Sun-reacquire command, the antenna slewed to the second preset angle of 122 deg at a rate of 0.403 deg/sec. These values are well above the 0.30-deg/sec minimum requirement.

g. Earth-sensor brightness. The telemetered earthlight intensity from the Earth sensor was approximately twice

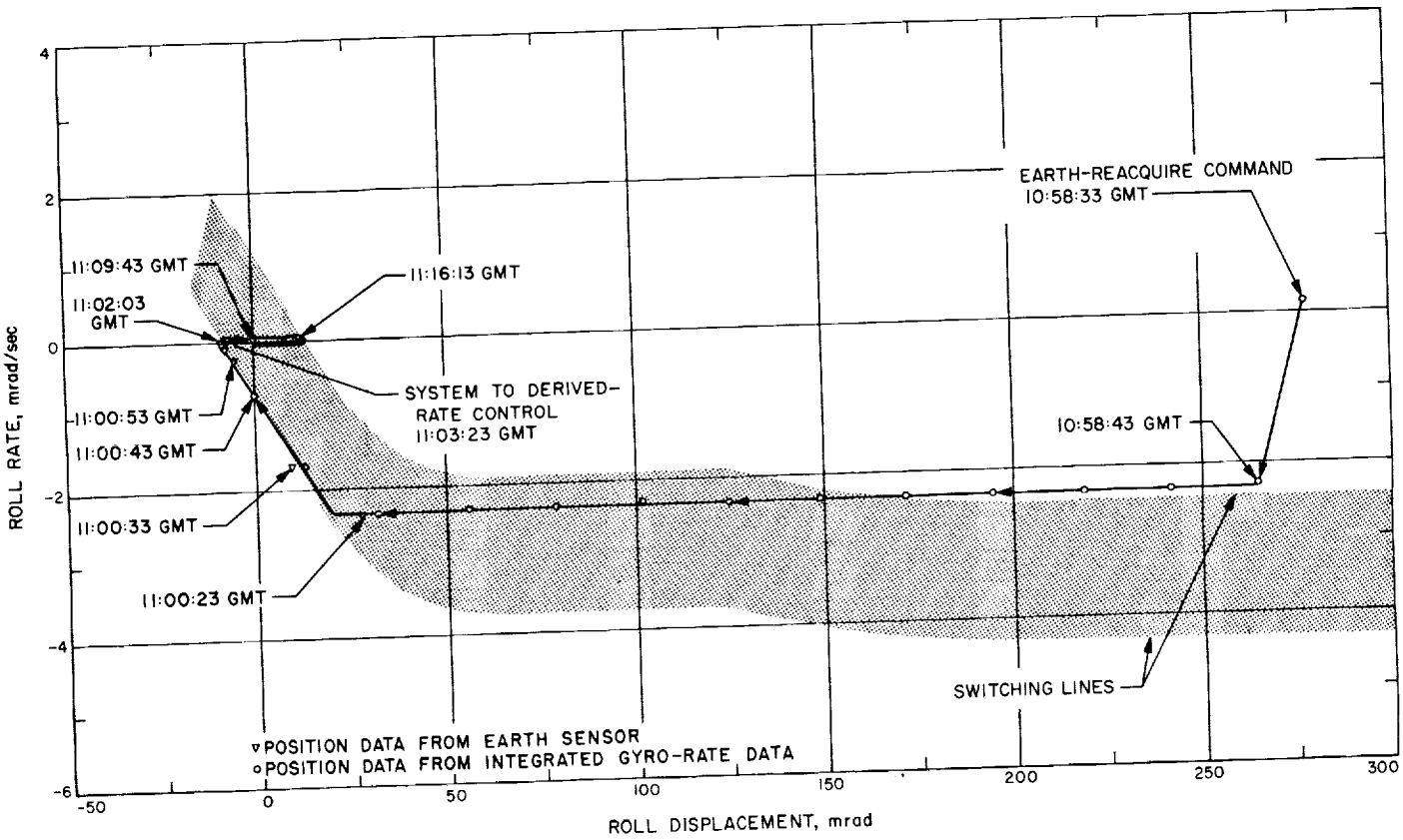

Fig. 19. *Ranger VIII* Earth reacquisition, roll axis

the predicted value. The predicted and the actual light intensity are shown in Fig. 20.

h. Cruise mode. During cruise, the attitude-control subsystem operates in a limit-cycle mode as shown in Fig. 21. Operating parameters which characterize the limit-cycle mode of operation are position deadbands, limit-cycle velocity increments, and external torques. The cruise mode of operation is of special interest, since the system is automatically switched over to derived-rate control 180 sec after the Earth sensor has detected light. Since a decoupling network had been added to the roll channel, the interaxis coupling which had been observed on previous missions was eliminated.

Yaw axis. As can be seen in Fig. 21, the control system maintained the spacecraft yaw position between +2.2 and −3.0 mrad. The external torque about the yaw axis varied between −8 and −28 dyne-cm. This torque can be seen in Fig. 21 by observing the rate of change of the yaw-rate signal. The torque is quite small and is reflected in the number of yaw-valve actuations. It is estimated that there were 175 actuations of the (+) yaw valves and 90 actuations of the (−) yaw valves, which required 6.25×10^{-3} and 2.47×10^{-3} lb of gas, respectively, for the cruise modes of operation. The average limit-cycle velocity increment was 17 μrad/sec.

Pitch axis. The external torque about the pitch axis (Fig. 22) varied from −60 to −300 dyne-cm and resulted in holding the pitch position between −2.0 and −3.4 mrad. It is estimated that 978 actuations of the (+) valves and none of the (−) valves were required, resulting in the use of 18.4×10^{-3} lb of gas. The average limit-cycle velocity increment was 17 μrad/sec. As can be seen in Figs. 22 and 23, the external torque was increased rapidly by the gravitational gradient torques of the Moon. This resulted in the spacecraft pitch position being held against the negative deadband limit.

Roll axis. The roll position was contained within the normal limits, which varied from −10.16 and +8.6 mrad at the midcourse range to −7.4 and +5.4 mrad at the terminal-sequence range. The external torque was approximately −8 dyne-cm. The roll axis required 51 actuations of the (+) valves and 106 actuations of the (−) valves, using 0.79×10^{-3} and 1.56×10^{-3} lb of gas, respectively.

The two points in Fig. 21 labeled A and B indicate where valve firings in the yaw axis affected the Earth-sensor roll-error signal. Since the roll rate did not change at the point of inflection of the position signal, it is believed that the spacecraft position did not change but that the Earth-sensor roll-error output was not independent of the yaw axis at this hinge angle.

The roll rate during this time period is interesting because the limit-cycle operation is asymmetrical and the velocity increment from a single valve opening does not add a sufficient velocity magnitude to the spacecraft roll rate to enable the spacecraft roll axis to leave the deadband edge before the derived-rate feedback decays and the system is pulsed again. This is a perfectly normal operation and should not be confused with multiple pulsing.

As can be seen in Fig. 22, the roll-axis external torque was increased by the gravitational-gradient torque on the Moon. The roll-axis torque increased in a positive direction, while the pitch-axis torque increased in a negative direction.

The average roll limit-cycle velocity increment was 20 μrad/sec.

i. Terminal maneuver. Since the spacecraft was on a trajectory which would permit taking good pictures in solar orientation, it was decided that no terminal maneuver would be required. However, in order to use the terminal maneuver's backup function of turning on the television system, nominal 1-sec pitch and yaw turns were stored in the CC&S and an RTC-8 was transmitted to inhibit the attitude control against acting upon the CC&S commands. The commanded turns were observed with no indication of a response from the attitude-control subsystem. The limit-cycle operation is shown in Fig. 23.

j. Gas system. The observed acceleration constants (in mrad/sec²) were as follows:

Pitch	
Initial Sun acquisition	+0.848
	−0.705
Sun reacquisition	−0.465
	+0.560
Yaw	
Initial Sun acquisition	−0.506
	+0.657
Roll	
Initial Earth acquisition	−0.778
Midcourse roll turn	+0.642
	−0.646

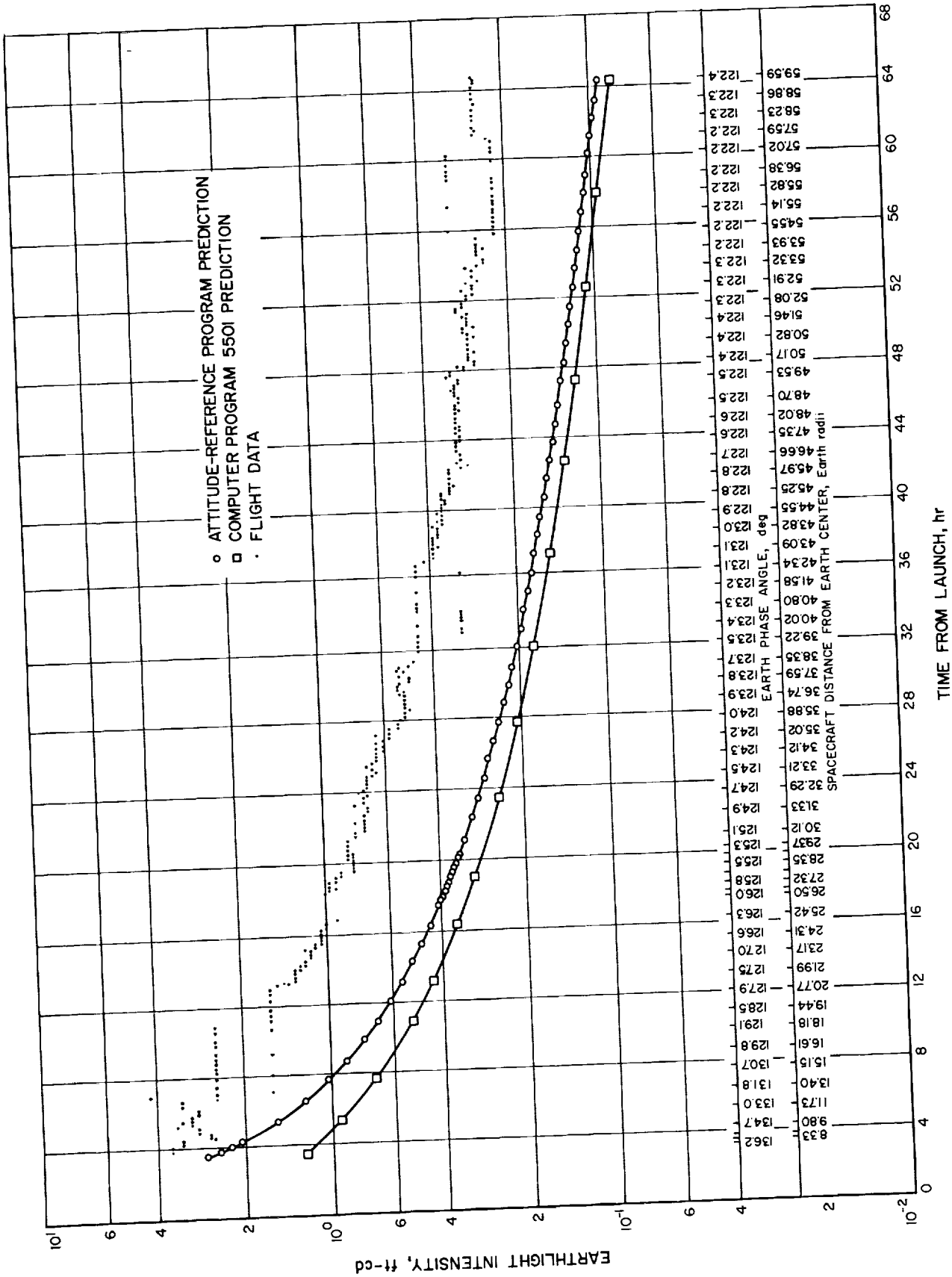

Fig. 20. *Ranger VIII* Sun-sensor light intensity

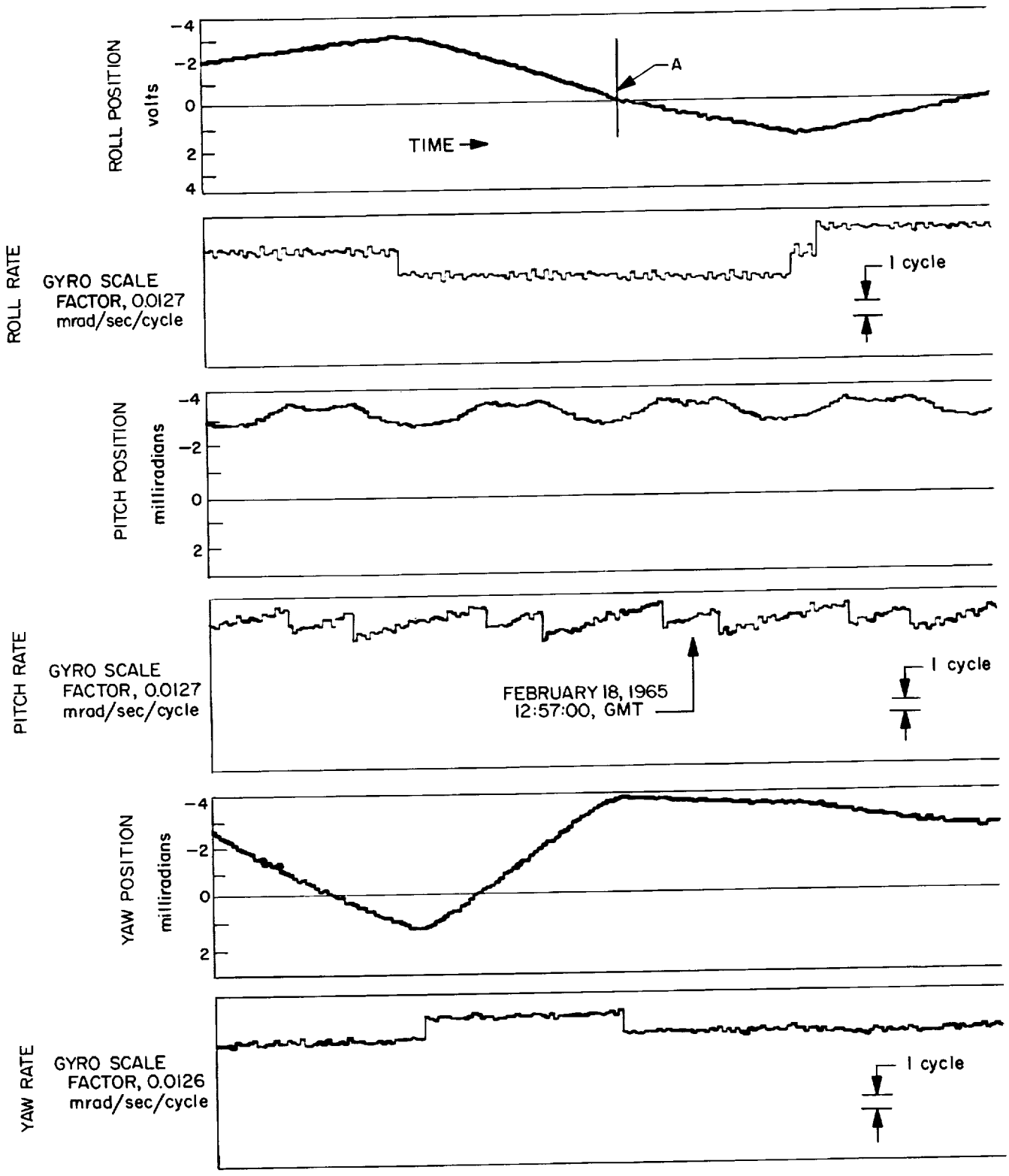
ROLL POSITION
volts
-4
-2
0
2
4
A
TIME
ROLL RATE
GYRO SCALE
FACTOR, 0.0127
mrad/sec/cycle
1 cycle
PITCH POSITION
milliradians
-4
-2
0
2
PITCH RATE
GYRO SCALE
FACTOR, 0.0127
mrad/sec/cycle
FEBRUARY 18, 1965
12:57:00, GMT
1 cycle
YAW POSITION
milliradians
-4
-2
0
2
YAW RATE
GYRO SCALE
FACTOR, 0.0126
mrad/sec/cycle
1 cycle

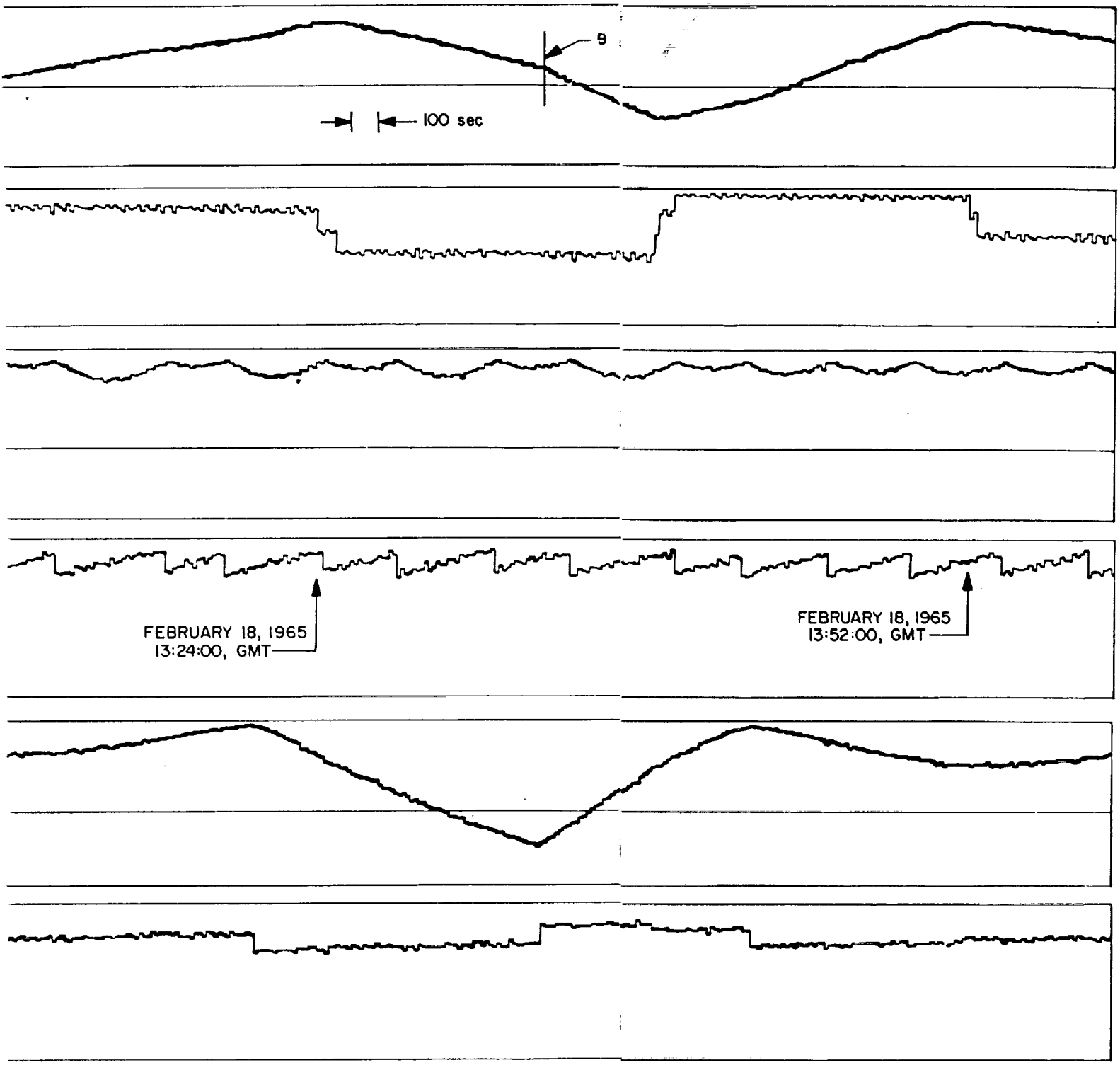

Fig. 21. *Ranger VIII* limit-cycle operation, post-midcourse cruise

2# 33# 3#

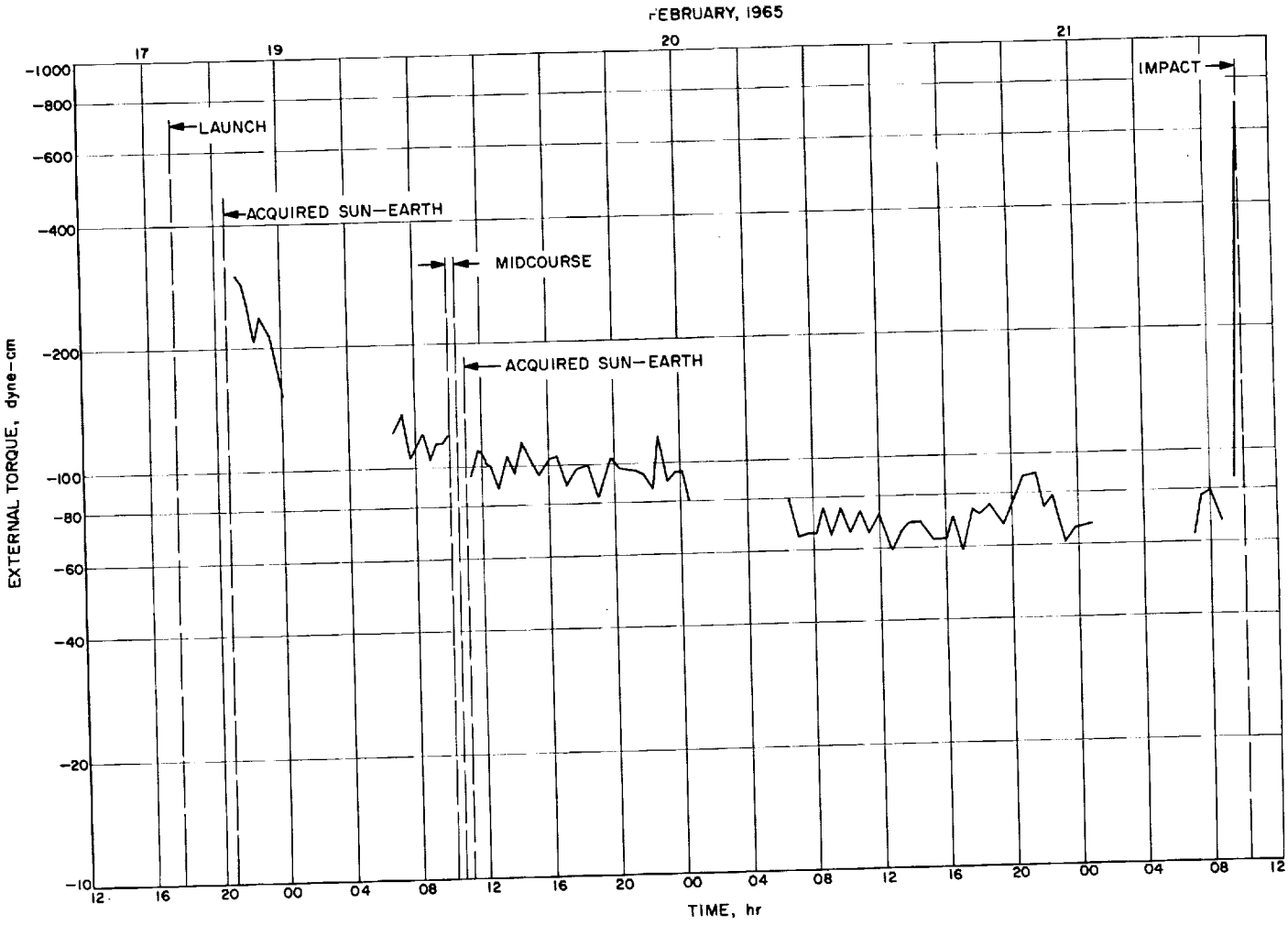

Fig. 22. *Ranger VIII* pitch torque

Table 5. *Ranger VIII* calculated gas consumption

	Pitch ($\times 10^{-3}$ lb)	Yaw ($\times 10^{-3}$ lb)	Roll ($\times 10^{-3}$ lb)
Sun acquisition	19.61	25.53	0.36
Earth acquisition	0	0	6.34
Cruise periods	18.4	8.72	2.30
Sun reacquisition	11.10	0	0
Earth reacquisition	0	0	5.58
Roll turn	0	0	8.37
Pitch turn (estimated)	9.00	0	0
Total (per axis)	58.11	34.25	22.95
Total gas consumption = 0.115 lb.			

The gas consumption as calculated from the spacecraft performance is shown in Table 5. As may be expected, the telemetry data do not indicate any gas usage, and the derived-rate system reduced the gas consumption from that calculated on *Ranger VII* (0.248 lb).

3. *Ranger IX* Mission Performance

The mission requirements for the *Ranger IX* attitude-control subsystem were identical to those for the *Ranger VI, VII,* and *VIII* missions, with the following exceptions:

1. The midcourse maneuver was executed at L+38 hr instead of the normal L+16 hr. This late maneuver required that an Earth reacquisition be accomplished at L+39 hr, 24 min.

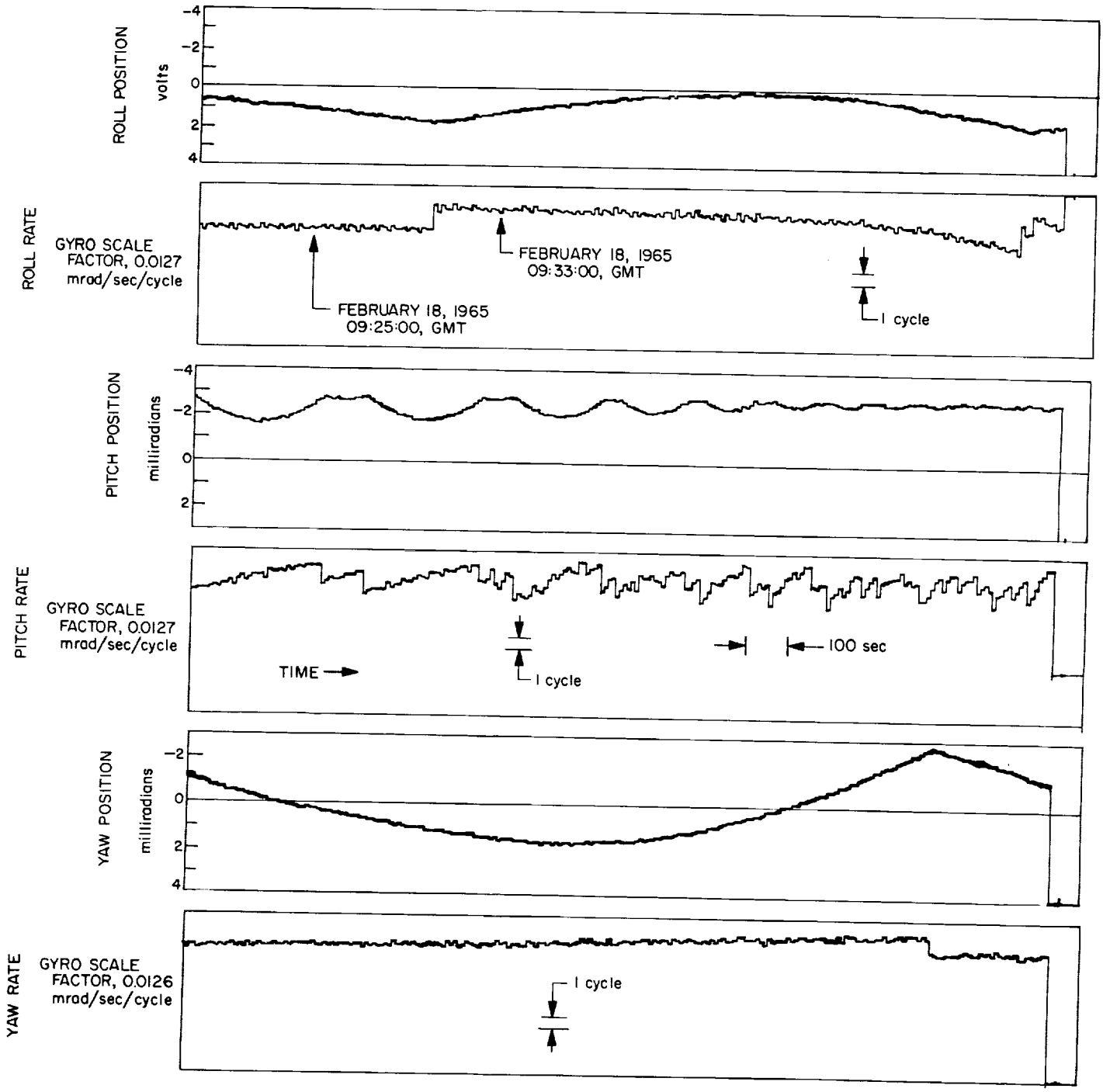

Fig. 23. *Ranger VIII* limit-cycle operation, terminal sequence

2. A timed midcourse maneuver.

3. A terminal maneuver.

a. Pre-launch conditions. High-accuracy (10-sec count) telemetry data indicated a stored gas weight of 2.10 lb in each half of the gas system for a total stored gas weight of 4.20 lb. The pitch-, yaw-, and roll-gyro output voltages measured in the blockhouse were within 10 mv of the expected values computed from gyro laboratory readings. Two RTC-2 commands (one sent at 17:48:50 and the second at 17:49:50 GMT) were transmitted to select the 122-deg antenna preset angle required for the particular launch day, March 21, 1965 (liftoff occurred at 21:37:02).

b. Separation. Spacecraft separation took place at 21:52:26. The earliest reliable data available indicate the pitch, yaw, and roll rates to have been −8.1, −8.5, and −2.1 mrad/sec, respectively, at 22:08:00. The separation rates are estimated to have been <-9, −4.5, −0.6 mrad/sec in pitch, yaw, and roll, respectively.

When the command to extend the solar panels was given at 22:37:01, the yaw rate was beyond the telemetry band limit of −10.0 mrad/sec. The pitch and roll rates were +0.6 and +2.7 mrad/sec, respectively. After the solar panels were extended, the rates in pitch, yaw, and roll were reduced to −0.6, −8.2, and +1.2 mrad/sec.

c. Sun acquisition and reacquisition. When Sun acquisition was commanded by the CC&S at 22:40:01, the attitude-control subsystem deployed the antenna to the first preset angle of 122 deg and acquired the Sun in pitch at 22:46:50 and in yaw at 22:47:30.

Pitch axis. When the attitude-control subsystem received the Sun-acquire command, the pitch-axis position and rate were −1738 mrad and −1.05 mrad/sec, respectively (Fig. 24). The spacecraft pitch axis was moving away from the Sun. By 22:40:13, the spacecraft had accelerated up to the acquisition rate of 4.43 mrad/sec and remained there until the stop transient of the high-gain antenna indicated at 22:45:13. The acquisition was

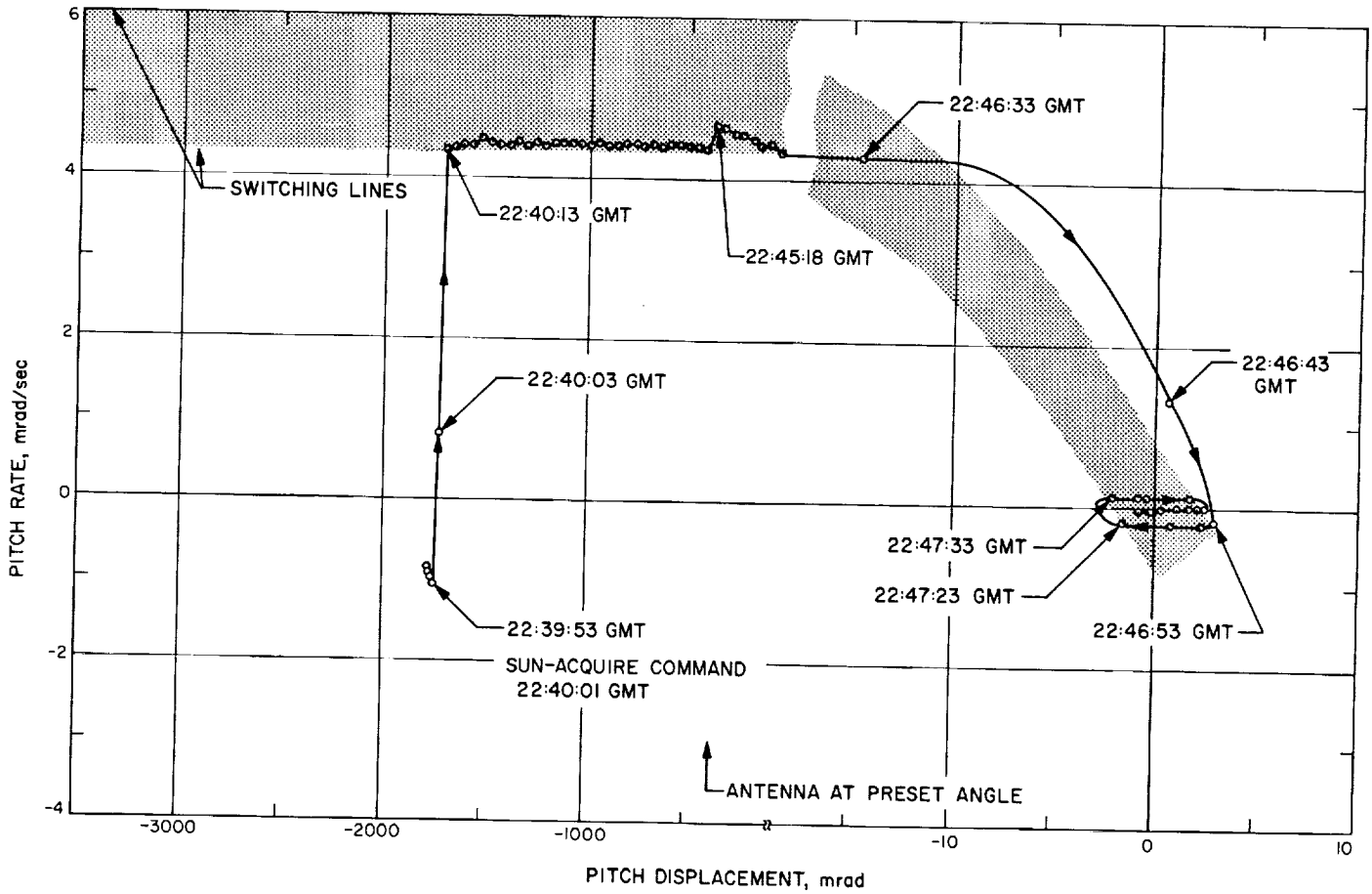

Fig. 24. *Ranger IX* Sun acquisition, pitch axis

normal, with one data point being sampled after the switching line was crossed at 22:46:43.

Sun reacquisition was initiated at 12:33:38 GMT, March 23. The pitch-axis position was +2280 mrad, and the rate was near zero, as shown in Fig. 25. The spacecraft accelerated up to −4.34 mrad/sec in 7 sec, with a start-transient acceleration constant of −0.593 mrad/sec². The stop transient of the antenna can be seen at 12:36:55 in Fig. 25. At 12:42:01, the system crossed the switching line and acquired the Sun with a stop-transient acceleration constant of +0.513 mrad/sec² at 12:42:10.

Yaw axis. At 22:34:53 GMT, the spacecraft yaw position and rate were +2478 mrad and −7.85 mrad/sec, respectively (Fig. 26). At the Sun-acquire command, the spacecraft yaw rate was decreased to the acquisition rate of −5.25 mrad/sec. The effect of the high-gain antenna on the yaw rate was noticeable until 22:44:42, when the antenna reached its preset angle. The acquisition rate then remained constant until 22:46:43, when the pitch axis had crossed its switching line; the effect of the pitch-stop transient can be observed on the yaw axis in Fig. 26. The yaw axis then crossed the switching line and acquired the Sun in a normal manner.

When the Sun-reacquire command was received, the spacecraft yaw axis had already acquired the Sun, and a limit-cycle mode of operation was established without an acquisition phase.

d. Earth acquisition and reacquisition. At 01:08:02 GMT on March 22, the CC&S commanded the start of the Earth-acquisition phase; conditions were as follows:

1. Earth–probe–Sun angle, 61.17 deg.
2. Earth–probe–Moon angle, 167.58 deg.

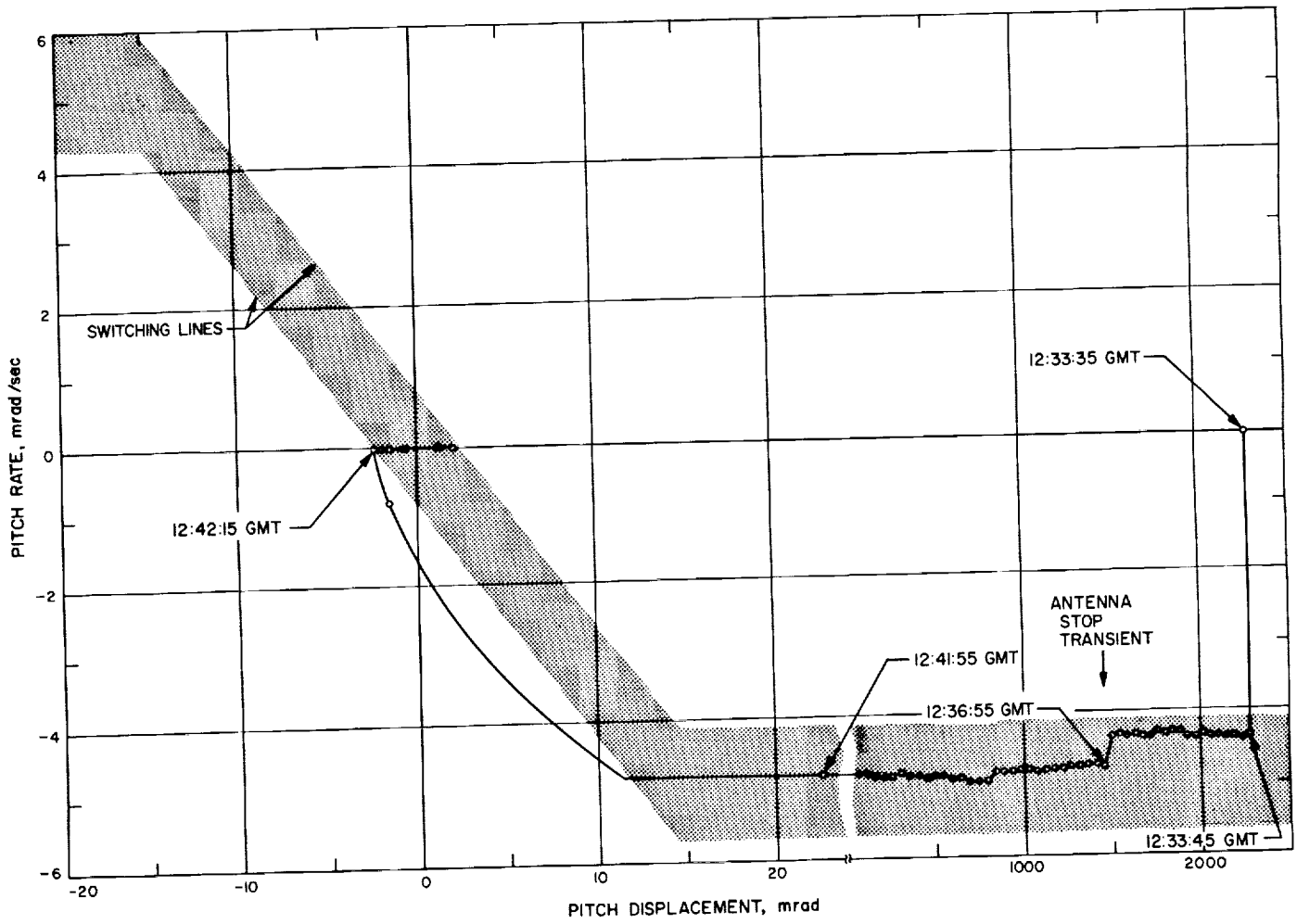

Fig. 25. *Ranger IX* Sun reacquisition, pitch axis

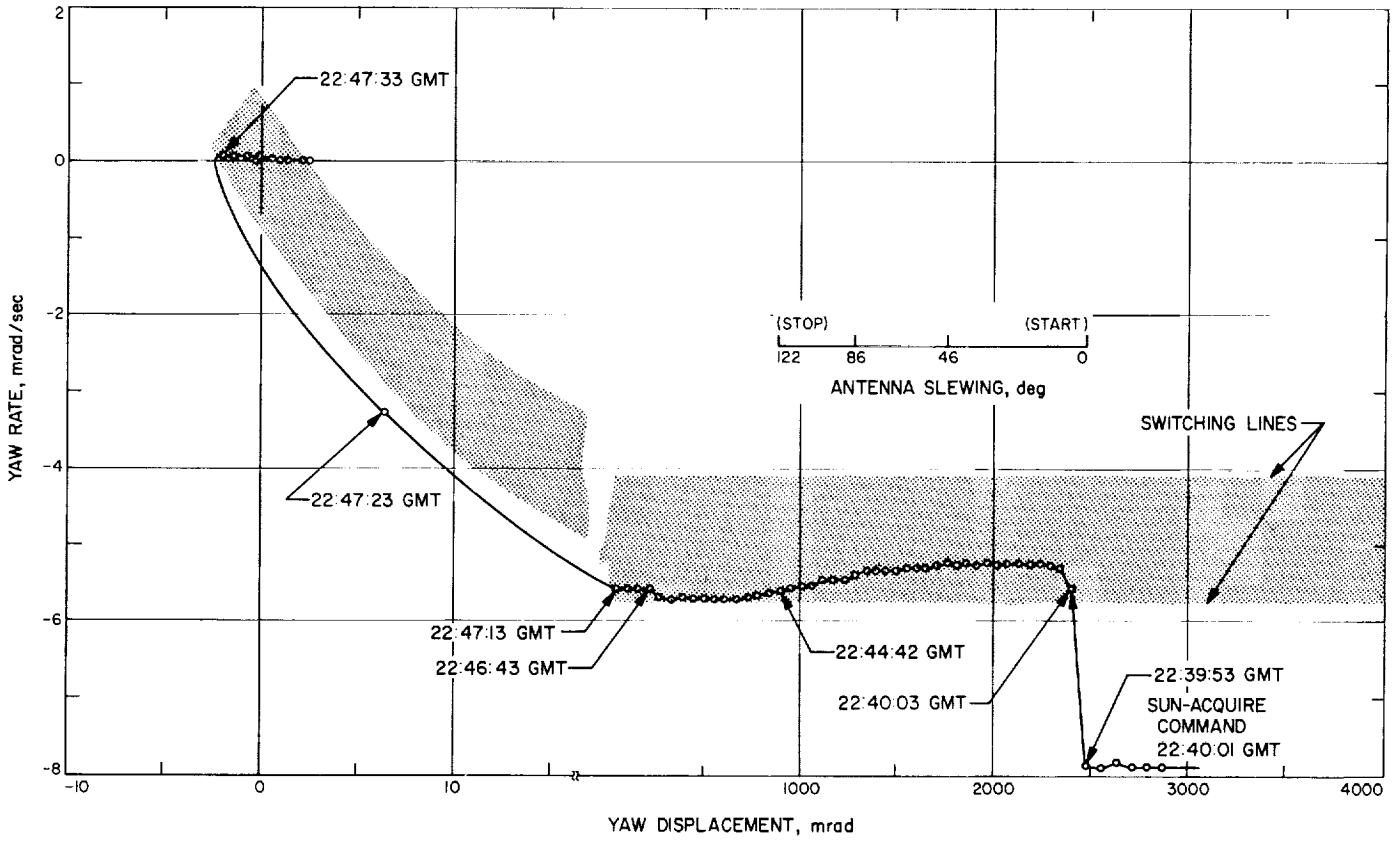

Fig. 26. *Ranger IX* Sun acquisition, yaw axis

3. Earth angular diameter, 12.91 deg.
4. Earth phase angle, 118.81 deg.
5. Earth light intensity, 6.13 ft-cd.

Under the above conditions, the Earth presented a lighted crescent to the Earth sensor approximately 3 deg wide in hinge angle, the center of light being within 1 deg of the center of view of the sensor. As was the case with *Ranger VIII*, the Earth was larger than the field of view in roll, so that the lighted portions of the crescent extended beyond the roll field of view.

Immediately prior to Sun acquisition, the roll rate was +1.14 mrad/sec. During the Sun-acquisition phase, the rate was reduced to +0.80 mrad/sec, and after the pitch and yaw axes had acquired the Sun, the rate was again reduced to +0.44 mrad/sec. At the time of the Earth-acquisition command, the roll rate and position were 0.53 mrad/sec and +584 mrad, respectively.

Upon receipt of the Earth-acquire command, the spacecraft roll axis accelerated up to the acquisition rate of −2.69 mrad/sec and remained there until the switching line was encountered (Fig. 27). The acquisition was normal; the system went into derived-rate control at 01:13:03 and established a limit-cycle mode of operation.

The roll scale factor was −2.0 v/deg as determined from calibration data and −2.06 v/deg as determined from the flight data.

The Earth-reacquisition command was issued at 13:01:40. The conditions for the acquisition were as follows:

1. Earth–probe–Sun angle, 83.49 deg.
2. Earth–probe–Moon angle, 143.92 deg.
3. Earth angular diameter, 2.48 deg.
4. Earth phase angle, 96.40 deg.

Since the spacecraft had performed a −27.41-deg roll turn for the midcourse maneuver (and the angular contribution of the sensor field and Earth diameter was 6.2 deg), a −326.4-deg roll search could have been expected.

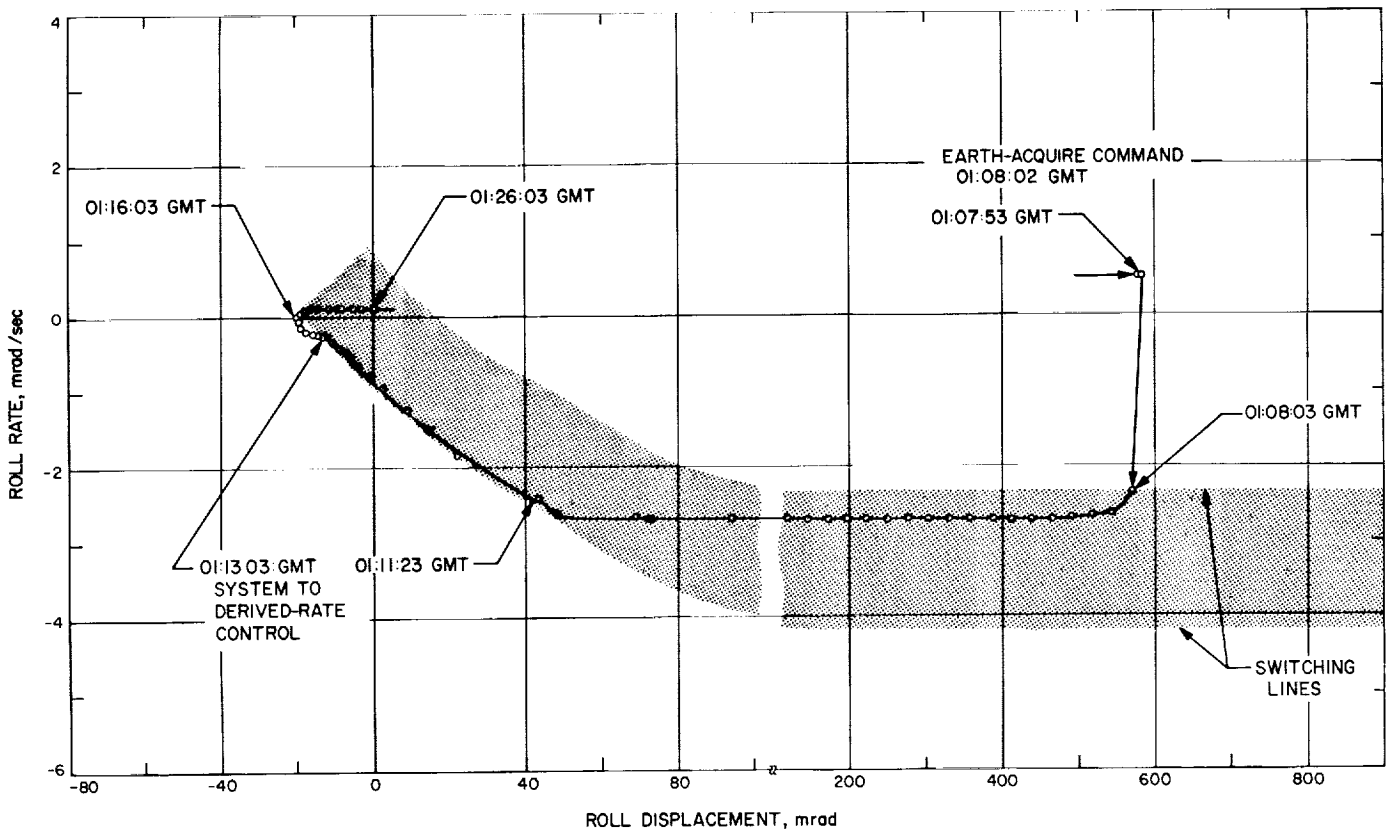

Fig. 27. *Ranger IX* Earth acquisition, roll axis

However, a residual roll rate within the rate deadband of the system left the spacecraft in a roll position that required only −5.7-deg search. The roll scale factor for the reacquisition was −7.4 v/deg.

When the Earth-reacquire command was received, the spacecraft roll-axis rate and position were +0.48 mrad/sec and +109 mrad, respectively (Fig. 28). The spacecraft then accelerated up to the search rate of −2.72 mrad/sec in 3 sec, with a start-transient acceleration constant of −0.91 mrad/sec². The Earth was reacquired in a normal manner by 13:02:32.

e. Midcourse maneuver. The midcourse maneuver was performed at L + 38 hr instead of the usual L + 16 hr in order to obtain a better orbit determination and to increase the accuracy of the midcourse maneuver in general. The maneuver parameters were as follows:

1. Roll turn, −27.41 deg (126.1-sec duration).
2. Pitch turn, +127.96 deg (587-sec duration).
3. Velocity magnitude, 18.15 m/sec.

These midcourse-maneuver parameters were calculated for an execution time (RTC-4) of 12:00:00. The roll position was plotted (Fig. 29) prior to the maneuver, and the RTC-4 was transmitted at 12:03:00.

The spacecraft responded to the command at 12:03:44, and the roll axis accelerated to the commanded turn rate in 4 sec, with a start-transient acceleration constant of −0.925 mrad/sec². The spacecraft pitch, yaw, and roll positions at the start of the maneuver were −1.50, +0.82, and +1.30 mrad, respectively. At 12:05:50, the spacecraft roll axis decelerated from the commanded rate, with a stop-transient acceleration constant of +0.77 mrad/sec².

At 12:13:08, the pitch turn was initiated, and the spacecraft accelerated to the commanded turn rate in 5 sec, with an acceleration constant of +0.85 mrad/sec². The pitch and yaw positions at the start of the maneuver were −1.89 and +0.21 mrad, respectively. At 12:22:55, the pitch axis decelerated from the commanded rate, with a stop-transient acceleration constant of −0.75 mrad/sec².

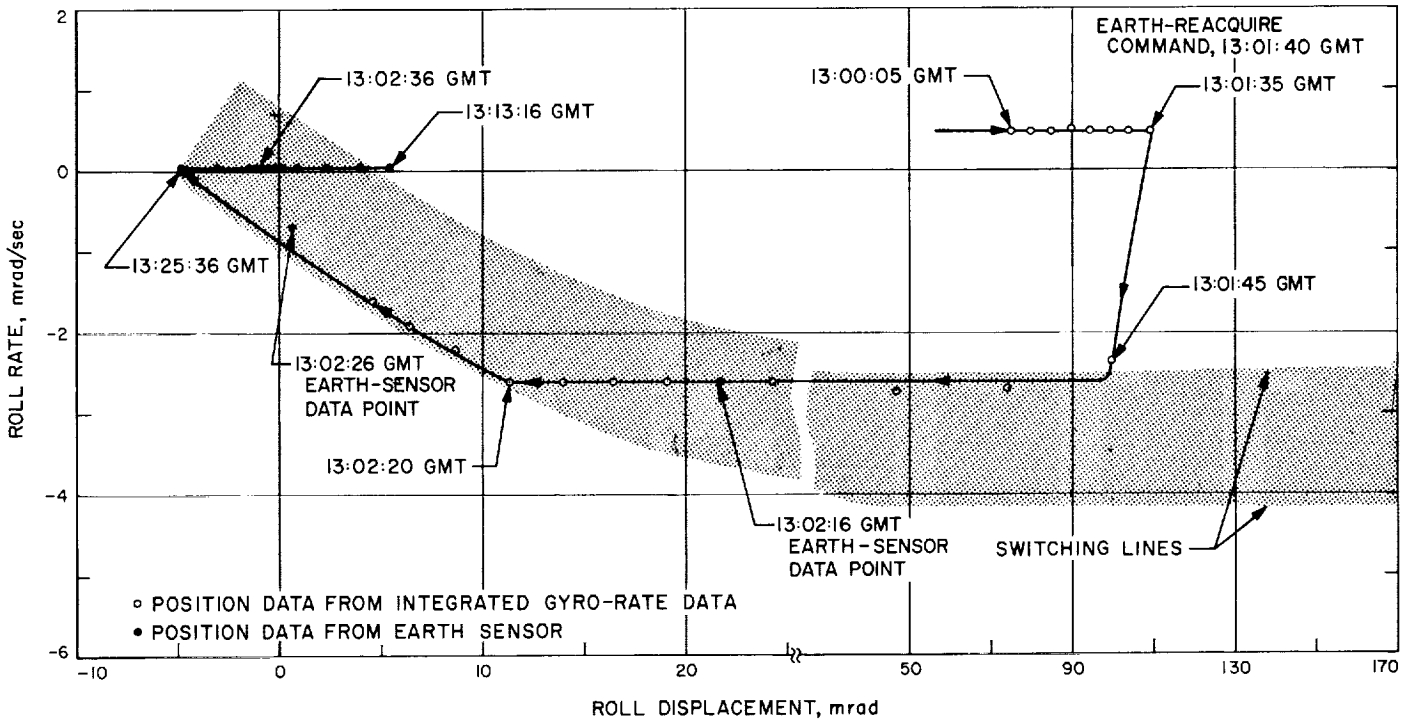

Fig. 28. *Ranger IX* Earth reacquisition, roll axis

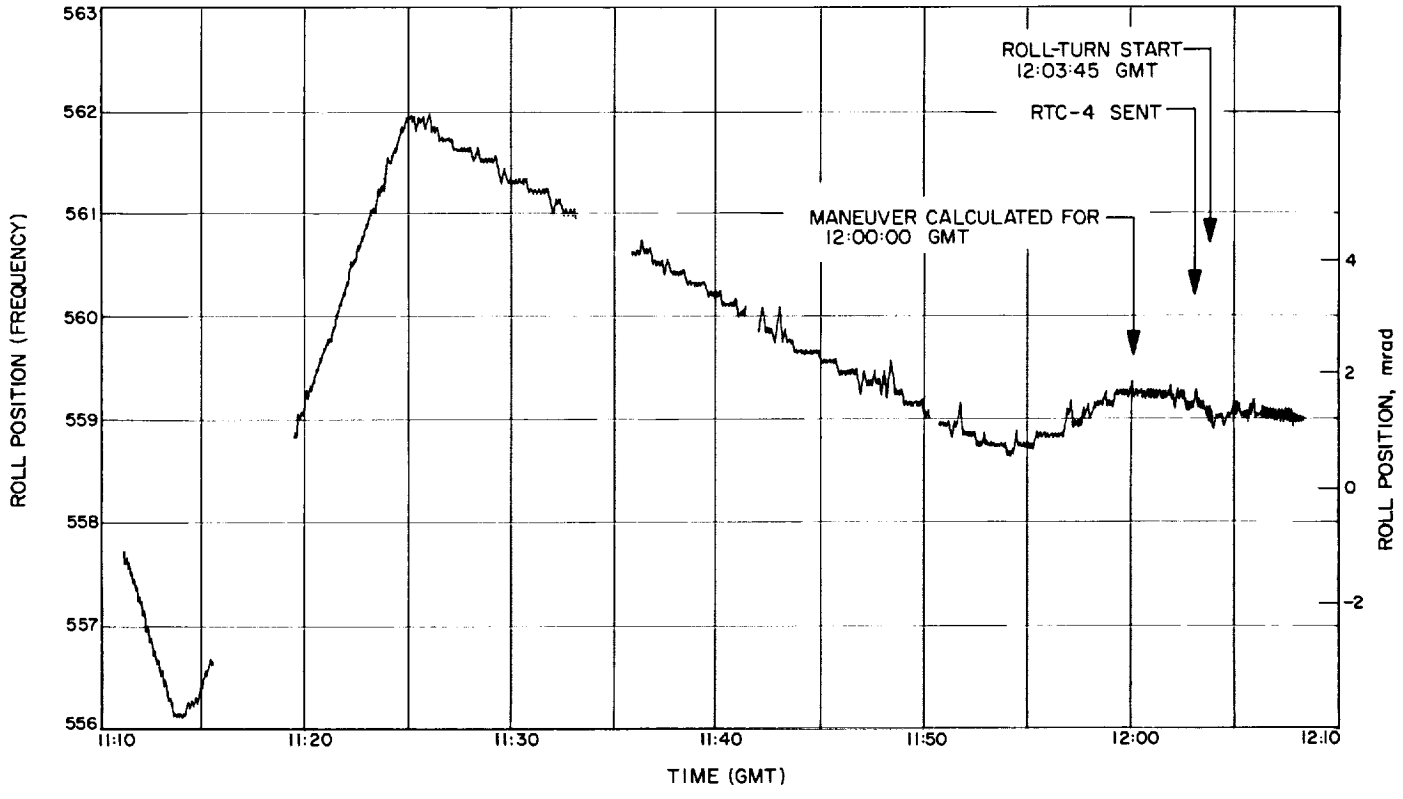

Fig. 29. *Ranger IX* roll position prior to midcourse maneuver

The autopilot performed normally during the motor-burn period, and all jet vanes were within 1 deg of null.

f. Antenna hinge control. Prior to launch, two RTC-2's were stored in the antenna control electronics to select the 122-deg hinge angle required for the Earth acquisition. Since the late midcourse maneuver was utilized, another RTC-2 was sent at 22:30:00 on March 22, in order to change the preset angle counter from 109 to 96.5 deg. The slewing rates for the antenna actuator, listed below, were well above specification requirements:

0 to 122 deg (first preset)	0.44 deg/sec
98 to 180 deg (exit)	0.41 deg/sec
180 to 97 deg (second preset)	0.46 deg/sec

Earth-sensor brightness was approximately 1.3 to 1.5 times predicted values during the flight, as shown in Fig. 30.

g. Cruise. The cruise mode of operation is shown in Fig. 31. The attitude-control subsystem was in a limit-cycle mode of operation and is shown in a period just prior to the terminal-maneuver sequence. The performance was very similar to that of *Ranger VIII*.

Yaw axis. The yaw-control system maintained the yaw position between −2.9 and +2.1 mrad. The external torque about the yaw axis varied from −5 dyne-cm to some value near −2.25 dyne-cm, the latter number being the resolution of the measurement. The average limit-cycle velocity increment in pitch and yaw was 18 μrad/sec.

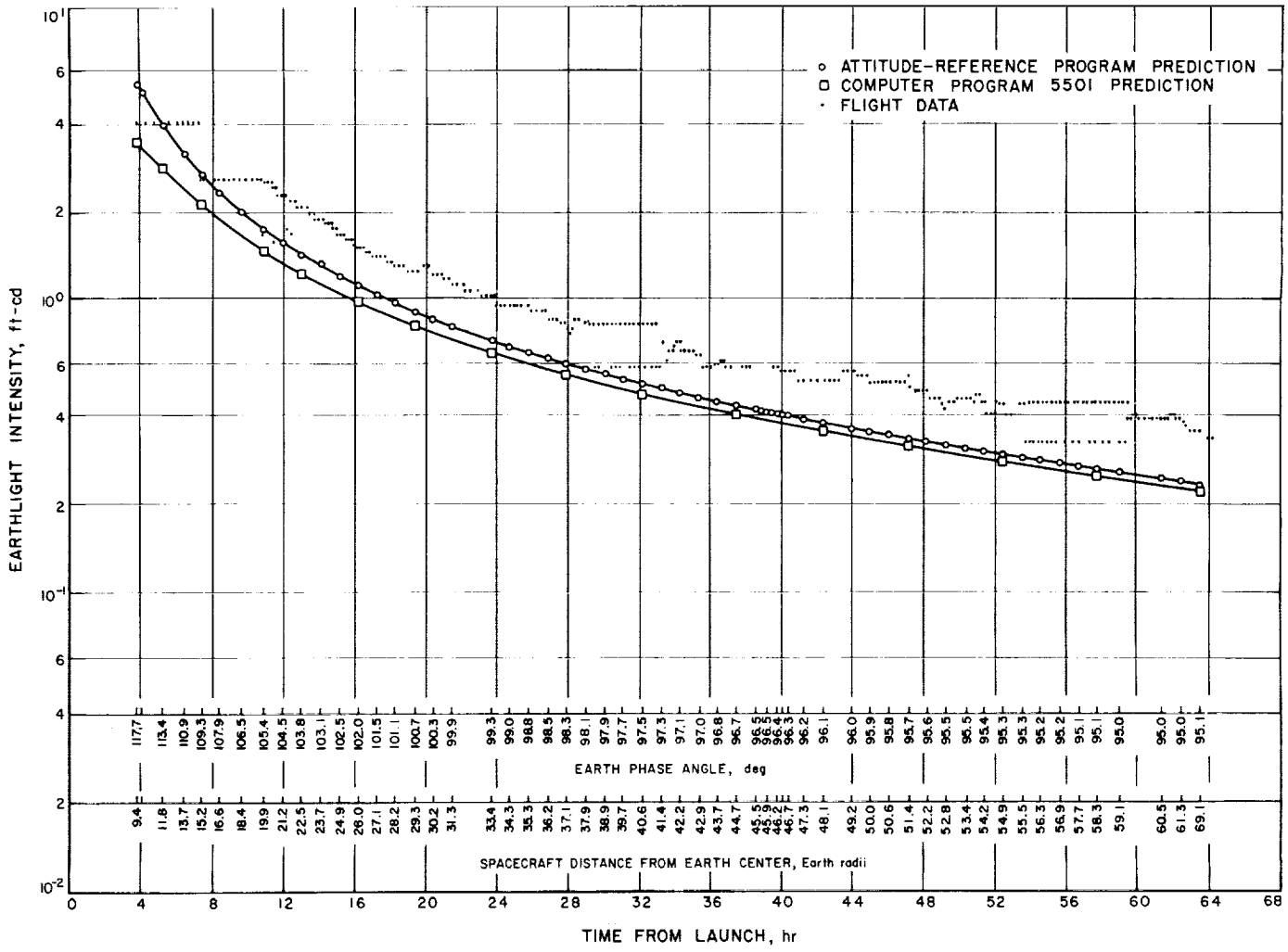

Fig. 30. *Ranger IX* Earth-sensor light intensity

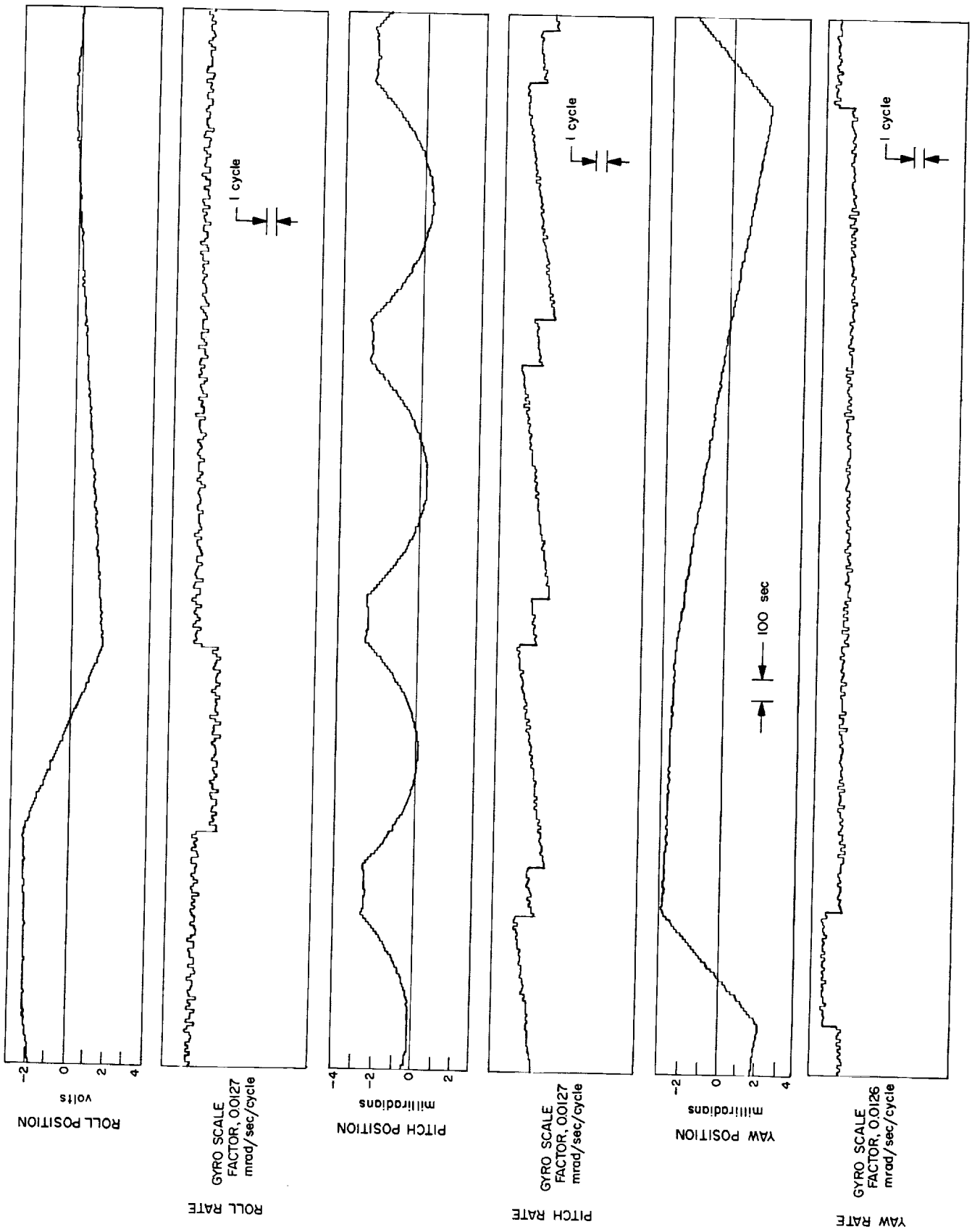

Fig. 31. *Ranger IX* limit-cycle operation prior to terminal sequence

It is estimated that 123 actuations and 3.92×10^{-3} lb of gas were required by the (+) valves, and 99 actuations and 3.57×10^{-3} lb of gas by the (−) valves.

Pitch axis. The external torque about the pitch axis is shown in Fig. 32. The torque varied from −130 dyne-cm at L + 12 hr to −48 dyne-cm just prior to the terminal sequence.

The (+) valves required 768 actuations and 14.12×10^{-3} lb of gas; the (−) valves were not actuated. The high torque in pitch was caused by the solar pressure on the high-gain antenna and varied as the antenna was extended or retracted. The pitch position was maintained between −2.5 and +0.5 mrad.

Roll axis. The external torque about the roll axis was extremely small, varying between +3 and +1.5 dyne-cm (the latter number being the resolution of the measurement). The (+) valves required 70 actuations and 1.22×10^{-3} lb of gas, the (−) valves 81 actuations and 1.83×10^{-3} lb of gas. There appeared to be a small amount of cross-coupling from the (−) roll valves into the yaw axis. Normally, no cross-coupling is expected, since the roll valves are a pure couple. However, the amount of cross-coupling was quite small (7%) and approached the resolution of the telemetered signal. The few instances that were observed required two firings of the (−) roll valves within a short period of time.

The average limit-cycle velocity increment was 19 μrad/sec.

h. Terminal maneuver. The terminal-maneuver parameters were as follows:

1. First pitch turn, +5.20 deg (24-sec duration).
2. Yaw turn, −16.30 deg (75-sec duration).
3. Second pitch turn, −20.50 deg (94-sec duration).

The first pitch turn was commanded to start at 13:03:20. The pitch and yaw positions at the start of the turn were −1.37 and −2.39 mrad, respectively. The yaw turn was commanded to start at 13:12:44; the yaw position was −1.23 mrad at the start of the turn. The turns were performed normally; the acceleration constants are listed below.

i. Gas system. The observed acceleration constants (in mrad/sec²) were as follows:

Pitch	
Midcourse turn	+0.85
	−0.75
Sun reacquisition	+0.593
	−0.513

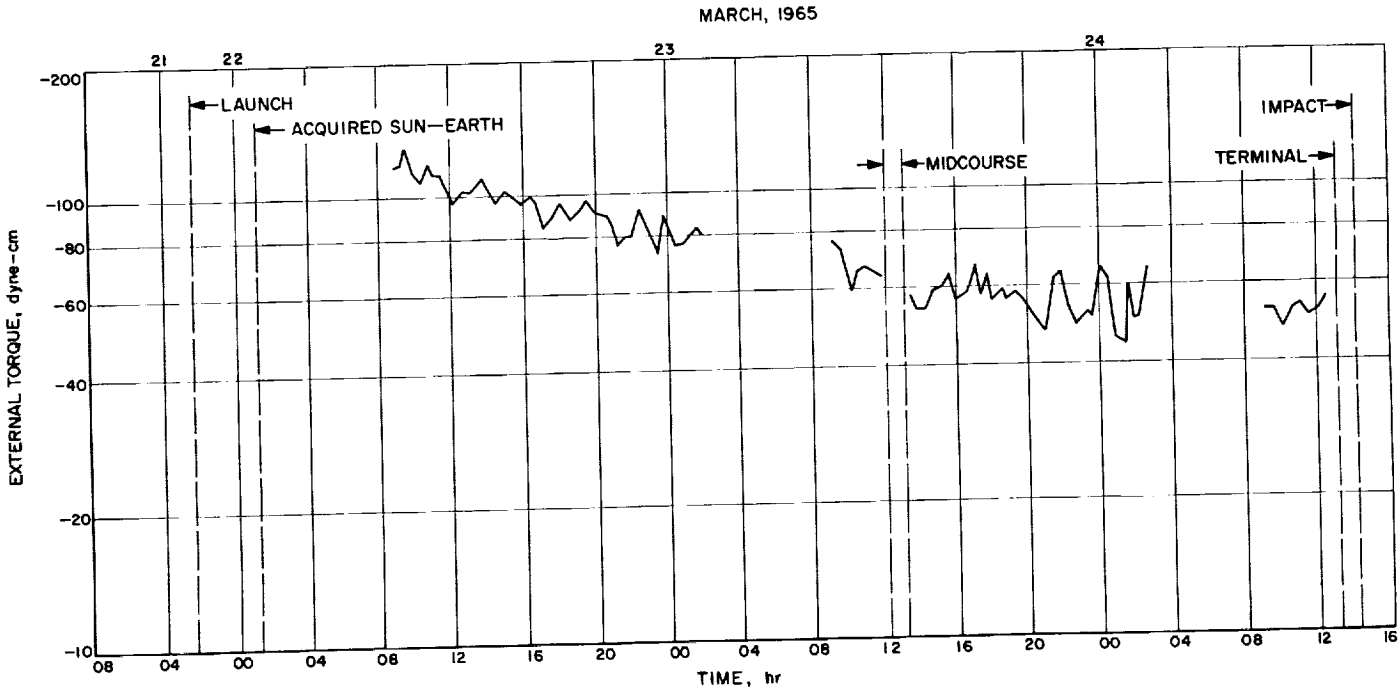

Fig. 32. *Ranger IX* pitch torque

Terminal maneuver (first turn)	+0.75
	−0.70
Terminal maneuver (second turn)	−0.70
	+0.84
Yaw	
Terminal maneuver	−0.66
	+0.58
Roll	
Midcourse turn	−0.925
	+0.77
Earth reacquisition	−0.91

The gas consumption as calculated from the spacecraft performance is shown in Table 6.

In summary, the *Ranger VIII* and *IX* missions afforded an excellent demonstration of the *Ranger* Block III derived-rate attitude-control subsystem, which fulfilled its mission functions admirably in each case.

Table 6. *Ranger IX* calculated gas consumption

	Pitch ($\times 10^{-3}$ lb)	Yaw ($\times 10^{-3}$ lb)	Roll ($\times 10^{-3}$ lb)
Sun acquisition	11.79	21.56	–
Earth acquisition	0	0	6.25
Cruise periods	14.12	7.49	2.60
Sun reacquisition	10.66	0	0
Earth reacquisition	0	0	6.54
Roll turn	0	0	7.75
Pitch turn	9.23	0	0
Pitch turn (first terminal)	8.56	0	0
Yaw turn (terminal)	0	18.39	0
Pitch turn (second terminal)	8.35	0	0
Total (per axis)	62.71	47.44	23.14
Total gas consumption = 0.133 lb.			

G. Power Subsystem

Generating, storing, and converting electrical power required for the operation of the various power-using spacecraft subsystems is the function of the power subsystem. The user subsystems include the radio, command, data encoder, attitude control, CC&S, and pyrotechnics subsystems; the television subsystem incorporates an independent power source and distribution equipment.

The power subsystem consists of raw-power sources; connections for external OSE power for ground use; two each photovoltaic-cell solar panels and on-board batteries for flight operations; switching and control equipment; and local subsystem conversion equipment to provide power tailored to individual subsystem needs. A simplified diagram of the subsystem is shown in Fig. 33.

External power is supplied at 25.5 v until 5 min before liftoff, when the two spacecraft batteries assume the load at 20.5 v. The total initial battery capacity is 84 amp-hr. A normal *Ranger* mission uses less than 20% of this capability, and no provision is made for recharging the batteries during solar-panel operations, which cover the entire mission after Sun acquisition except, in most cases, the midcourse-maneuver phase and, possibly, operation after a terminal maneuver. The two panels have 4896 *p*-on-*n* silicon solar cells each. The batteries supply the pyrotechnic subsystem directly; the power-conversion system selects the appropriate raw-power source, provides a regulated bus voltage, and converts this to the individual voltage and current requirements of the other user subsystems.

Power-subsystem operations throughout the *Ranger VIII* and *IX* missions were devoid of failure or any evidence of degraded performance. System current, voltage, and power during the two missions are illustrated in Figs. 34 and 35. The two batteries on each spacecraft operated normally during the missions; approximately 16% of available capacity was required during each flight, which was not sufficient to permit a determination of actual maximum capacity. The solar panels operated within their predicted limits throughout both flights. Panel temperatures during cruise mode were some 8°F higher than on *Ranger VII*, corresponding to the expected increase in solar intensity of 7 mw/cm^2. Shroud ejection was noted in each flight from the small solar-panel voltage increase resulting from exposure of the panels to space (an insufficient voltage to provide significant power). On Sun acquisition, the panels assumed the entire cruise-mode raw-power load of 138 w. In each mission, telemetry indicated a slight imbalance (0.3 amp on *Ranger VIII*, 0.2 amp on *IX*) in solar-panel current, conforming in both calibration pre-flight cases with measurements. During the midcourse maneuvers, the spacecraft were turned sufficiently from solar orientation so that first the panels and batteries shared the power load, then the batteries carried it alone; on Sun reacquisition, the panels resumed the load. During the *Ranger IX* pitch turn, it

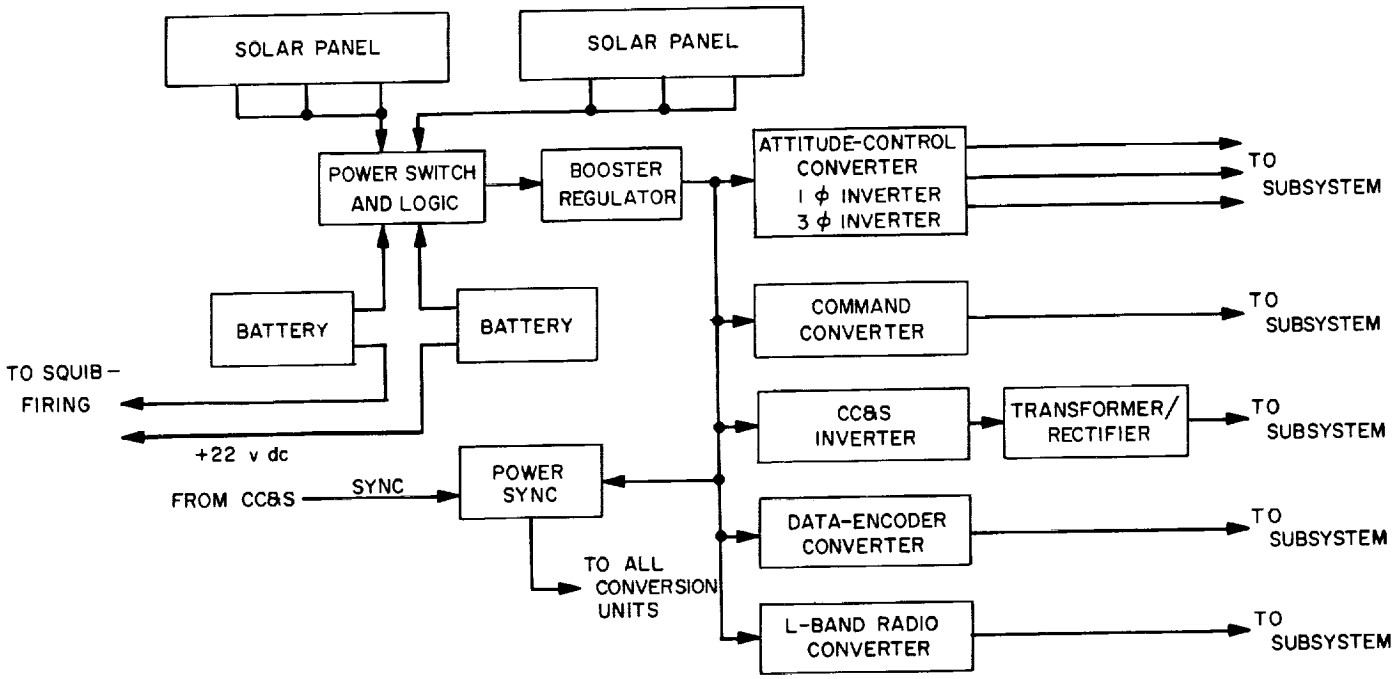

Fig. 33. Power subsystem

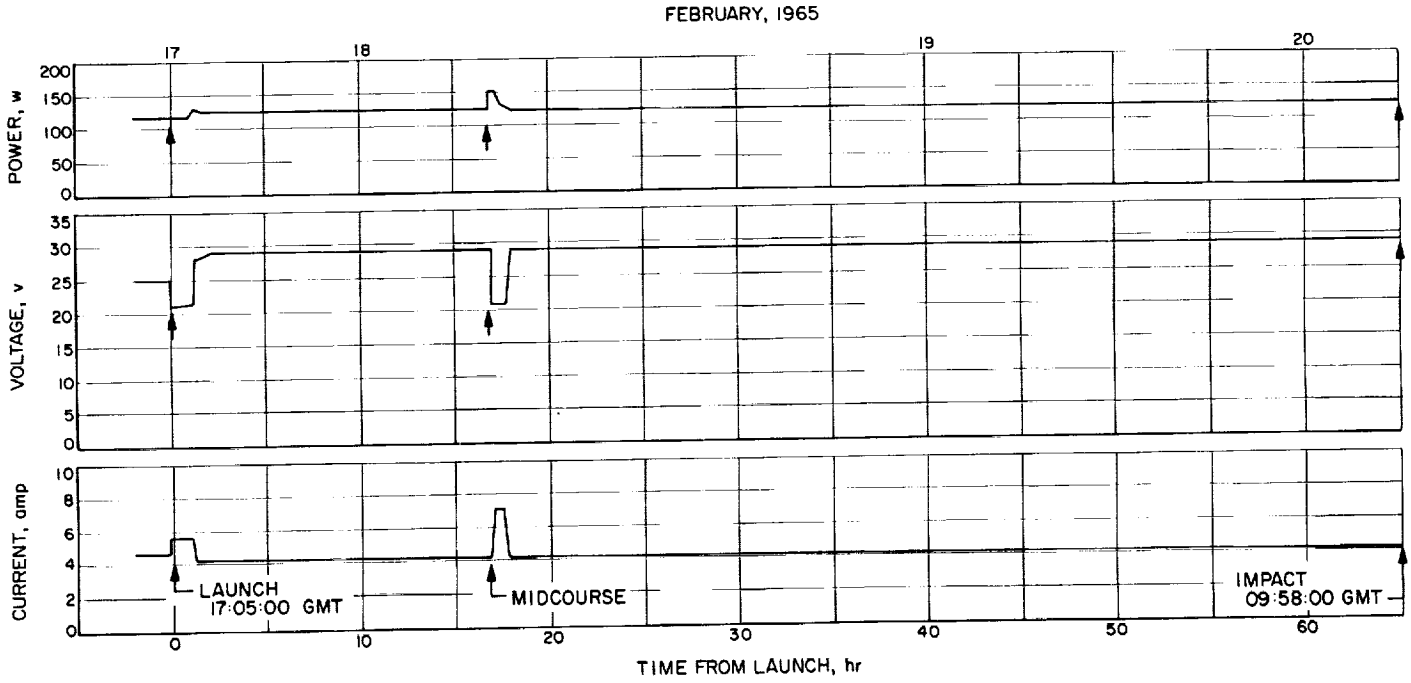

Fig. 34. *Ranger VIII* system power parameters

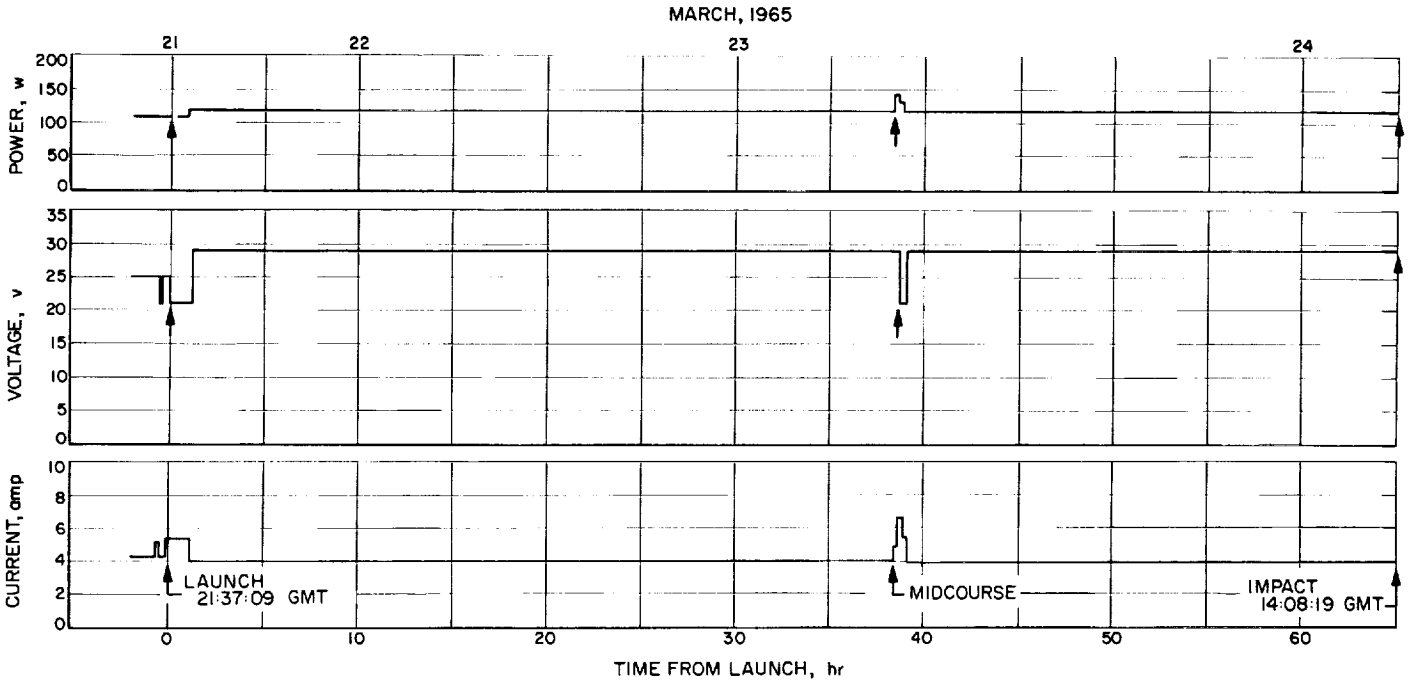

Fig. 35. *Ranger IX* system power parameters

was found that the $+x$ solar panel briefly received solar energy reflected by the Moon.

The *Ranger IX* terminal maneuver resulted in a partial shading of the $+x$ solar panel from the completion of the yaw turn to impact, as seen in a slight reduction in panel current. The loss was small compared to the available power.

Performance parameters throughout the missions are summarized in Table 7.

H. Spacecraft Structure

Structural and mechanical elements of the *Ranger* spacecraft include the bus structure; the high-gain antenna dish and its hinge and drive; the solar-panel substrates with their hinge, latch, and deploy mechanisms; and the electronic packages and cables.

1. Spacecraft Frame

The spacecraft bus structure is a redundant truss-type design of aluminum and magnesium alloys. In configuration, it appears as a series of concentric hexagons, the lower and larger of which comprises the attachment and separation plane from the *Agena* adapter. This plane or base is surmounted by a smaller, double-walled hexagonal structure which houses and supports the electronics cases around its outer periphery, and the midcourse propulsion system within its inner periphery. Appendix C includes drawings that show structural details. The structure provides stable reference for the Sun-sensor units, the TV subsystem, the directional-antenna–Earth-sensor system, the midcourse-propulsion system, and the attitude-control system.

During the *Ranger VIII* and *IX* missions, the structure performed its required functions satisfactorily and with no known anomalies.

2. High-Gain Antenna

The high-gain antenna is a circular, dish-shaped structure constructed of fabricated sheet aluminum-alloy ribs emanating radially from the center and supported at midpoint and the outer diameter by sheet-metal rings. The dish surface is covered by a black anodized-aluminum mesh, held in conformation by the radial ribs and the mid and outer rings. The antenna feed is mounted at the center of the concave side of the dish, supported by four tubular fiberglass struts. The antenna is driven and maintained at the required attitude by the antenna gearbox through a yoke and arm attached to the convex side of the antenna. In its retracted position, the antenna

Table 7. *Ranger VIII* and *IX* representative power parameters

Mission phase	Power source[c]	*Ranger VIII*			*Ranger IX*		
		System voltage, v	Current, amp	Power, w	System voltage, v	Current, amp	Power, w
Pre-launch	E	25.0	4.72	118	25.0	4.39	110
Launch	B	20.9	5.69	119	20.7	5.23	108
Pre-acquisition	B	21	6.3	135	21.2	5.6	119
Post-acquisition	SP	28.1	4.76	135	28.9	4.11	119
Pre-midcourse	SP	29.2	4.24	124	29.3	3.97	116
Midcourse[a]	B	20.7	7.0	145	20.8	6.7	139
Post-midcourse	SP	28.4	4.52	128	28.9	4.11	119
Terminal[b]	SP	28.4	4.52	128	29.3	4.11	120

[a] For *VIII*, motor burn; for *IX*, mid-pitch turn.

[b] For *IX*, following maneuver.

[c] E = external, B = batteries, SP = solar panels.

nests in the rearward end of the spacecraft, just above the separation plane. During ascent, the antenna is protected from vibration effects by snubbing elements provided in the *Agena* adapter.

From a structural and mechanical standpoint, the high-gain antenna performed satisfactorily during the two missions. There were no known anomalies.

3. Solar-Panel Substrates and Mechanisms

The solar-panel substrates are fabricated of spot- and seam-welded aluminum-alloy sheets, providing structural support and protection for the solar cells. The cells are mounted on a flat, rectangular aluminum-alloy sheet, whose flatness and rigidity are maintained by corrugated aluminum-alloy sheets in the longitudinal direction and by cross-bracing in the transverse direction. The cross braces also provide the mounting and the heat sink for the zener diodes of the power system.

During the *Ranger VIII* and *IX* missions, the solar-panel substrates performed satisfactorily. There were no known anomalies.

The solar-panel hinge, latch-support structure, pyrotechnic pinpuller, point damper, and actuator support the solar panels in a manner to avoid high dynamic loads during the launch and deploy the panels in approximately 1 min after the squib-firing current is applied.

The solar-panel actuators for *Ranger VIII* were predicted to open the panels in 60 sec nominal after the B-2-1 indication of solar-panel-extension command. The B-2-1 blip occurred at 18:05:01. The B-2-4 blip indicated that the solar panels deployed at 18:05:40, 39 sec after the CC&S command. It was later found that the *Ranger VIII* solar panels would trip the switches that send the B-2-4 command when they still had 23 deg to open. A test was run which showed that the actuators reach this point in 40 sec at room temperature (the time decreases with increasing temperature). This indicates that the temperature prediction for the actuators was off by less than 1°F.

The solar-panel actuators for *Ranger IX* were predicted to open the panels in 46 sec after the B-2-1 indication of solar-panel-extension command. The B-2-1 blip occurred at 22:37:01. The B-2-4 blip indicated solar-panel deployment at 22:37:51, 50 sec after the CC&S command. The error was 4 sec, equivalent to an error of about 3°F in the estimated actuator temperature.

The deployment time and solar-panel performance throughout the *Ranger VIII* and *IX* flights indicated normal performance of the support and extension equipment.

4. Electronic Packages and Cabling

The electronic assemblies for *Rangers VIII* and *IX* provided conservative mechanical support for electronic

components in order to ensure proper operation throughout the various environmental exposures. The assemblies consist of structural units integrated into the spacecraft by bolting to the six bays of the structure. Each electronic assembly is made up of one or more functional subsystems consisting of subassemblies of various widths and standard cross section, bolted into a metal chassis and interconnected by pigtailed cable harnesses which are connected into the system "ring" harness. The subassemblies were designed to perform as an integral part of the spacecraft structure and to provide a high conductive thermal path from the components to the primary thermal-control surfaces.

By means of electronic packaging specifications, the following system goals were achieved:

a. Materials were restricted to a few whose space-environment behavior had been evaluated and was understood.

b. Hard-mounted circuit boards were employed for added structural strength and to minimize temperature gradients from components to temperature-control surfaces. This technique provided an operating margin in the dynamic and temperature environments without weight penalty. Further, the circuit-board design permitted optimum maintainability and modification without reducing subassembly integrity, and provided for simple and unlimited replacement.

c. Since a standard subassembly cross section and a defined chassis mounting were used, the requirements for the thermal and dynamic environments could be evaluated and understood prior to subassembly layout and design, resulting in improved end reliability.

d. Conformal coating was employed to obtain an assured complete insulation of all electrical conductors, which reduced the hazards from peripatetic space trash.

e. Hidden solder joints and trapped air voids were eliminated.

f. Connector-pin-retention tests were used to obtain interconnection integrity.

g. Test-equipment connections were provided on the assemblies to permit electrical testing without hardware degradation.

The function of the cabling system is to interconnect the various assemblies. The cables were built in accordance with a JPL specification and properly fitted; samples of wire were tested environmentally prior to final assembly. The spacecraft cabling is divided into three groups: (1) the subsystem interconnection harness, usually referred to as the "ring harness," (2) the squib harness, and (3) the assembly or case harness. The ring harness separates the wires into two bundles for "clean" and "dirty" signal characteristics to eliminate or minimize noise pickup. The squib harnesses are physically separated from the other harnesses to prevent impulse signals from affecting squibs. The assembly harnesses permit environmental and functional testing as well as checkout of the assemblies prior to incorporation into the total spacecraft system.

During the *Ranger VIII* and *IX* missions, the spacecraft electronic packaging and cabling areas performed within their design expectations, and no anomalies were recorded.

I. Temperature-Control Subsystem

The temperature-control subsystem was designed to provide an acceptable temperature environment within the operating limits of all spacecraft components throughout all spacecraft operating periods. This includes the time from pre-flight testing to lunar impact, regardless of spacecraft attitude, with the exception that the temperature environment cannot be guaranteed on all components during an Earth-shadow or non-Sun-oriented attitude of a duration longer than 60 min. (Violation of these constraints on the trajectory will, in general, result in an overcooling of some components and, perhaps, an overheating of others.)

The thermal-control subsystem on *Ranger* Block III is a passive system with no moving parts. Through precise regulation of the radiating characteristics of the external surfaces, the relationship between the input energy and the energy lost to space is regulated to yield the proper spacecraft temperatures.

One of the major problem areas encountered has been the effects of reflected solar energy. The *Ranger* Block III design is aimed at eliminating or minimizing solar reflections as much as possible. Black paint or black cloth is used on surfaces which might reflect to the spacecraft; polished surfaces are used where practical to direct the reflected energy away from the spacecraft.

There are uncertainties and unaccountable variations both in directly absorbed solar energy and in internal power dissipation. Since these are the only sources of input energy, an attempt was made to have each source

account for approximately half of the total. In this way, uncertainties and variations in either source produce minimum variations in spacecraft temperatures.

A side effect of the use of significant amounts of solar energy is that a relatively larger amount of energy must be radiated to space, which, in turn, dictates higher average emittance on the radiating surface. Since uncertainties in emittance measurements seem to be a fixed increment regardless of the absolute magnitude of the emittance, these uncertainties are reflected in smaller temperature uncertainties with increasing average emittance.

The higher average emittance also makes it possible to use a low-absorptance–high-emittance surface on the large radiating area to minimize the change in solar load when the spacecraft is in a non-Sun-oriented maneuver.

1. Thermal-Control Elements

The temperature-control subsystem on the *Ranger* Block III vehicles was tested and verified insofar as was practicable in the JPL space simulator, using the temperature-control model and the proof-test model. A space simulator is at best a rather inexact duplication of the space environment. One area of difference is the spectrum of the solar simulator, which, in general, is very different from the actual spectrum of the Sun. However, by use of surfaces which exhibit similar properties regardless of spectrum, the validity of solar-simulator tests is greatly enhanced. Such surfaces are called thermally grey, and black paint is one of them. In addition, black absorbs almost all of the incident energy, leading to very little reflected solar energy. For these reasons, *Ranger* used black paint on most of the sunlit areas where energy input and/or solar reflections were important.

Thermal shields (good insulators) are used over large areas of the spacecraft to control the amount of solar energy absorbed and to close off openings in order to help raise the remaining average emittance.

The forward thermal shield covers the top of the bus, including the area between the bus and the television subsystem. The portion of the shield extending outward beyond the television subsystem is sloped down to reflect the solar energy away from the spacecraft. The outboard edges of the thermal shield are carefully anchored to the tops of the electronic assemblies with thermal insulators. These insulators were designed to isolate the electronic cases from the outer layers of the shield which experience large temperature extremes. The location of the shield edge on each electronic assembly was determined by the desired solar heat input as derived from the heat-balance calculations.

The aft thermal shield is a two-piece shield which covers the aft side of the spacecraft, extending to the outboard edge of the shear panels. A hole in the center of the shield allows the midcourse-motor gases to escape.

There are thermal shields on the attitude-control gas bottles, the battery cases, the hydraulic backup command timer, and the antenna yoke. These shields, with the exception of the antenna-yoke shield, were designed to reduce to a minimum any energy gain or loss of these components by absorption or radiation. The antenna-yoke shield was designed to modify the absorption and radiation of the yoke, resulting in a lower temperature excursion as the high-gain-antenna hinge angle varied.

The intercostal tubes, diagonal braces, and the legs are made of polished aluminum. The intercostal tubes and diagonal braces are painted black on the inboard forward quadrant where they are exposed to the solar radiation. The purpose of the black paint is to minimize the unpredictable reflections to the spacecraft from these components. The tubes are covered with white paint on the aft side, so that a temperature of approximately 75°F is maintained.

The Earth sensor and antenna-drive gear box are surfaced with rough gold and polished aluminum, respectively. Black paint and black velveteen cloth are applied to the top of the gear box to eliminate reflections to the vehicle and into the Earth sensor via the Earth-sensor Sun shield. The desired temperature is maintained by the addition of white paint on areas not exposed to solar radiation.

Other components in the vicinity of the Earth sensor are covered with nonreflective coatings. The rotary coax joint and portions of the yoke are painted black. Black velveteen cloth covers the rotary-joint (high-gain-antenna cable and portions of the Earth-sensor cable and the rotary joint) case II cable. The high-gain antenna is also painted black. The purpose of these finishes is to eliminate reflections into the Earth sensor and has no thermal basis.

All cables outside the spacecraft are wrapped with strips of aluminized mylar. Cables 0.25 in. or more in diameter exposed to solar radiation have a strip of glass-cloth tape on the sunlit side approximately half the cable diameter in width. Cables covered with black velveteen cloth have no tape applied to them. The purpose of the

tape is to lower the equilibrium temperature of the cables and to protect the mylar from solar deterioration.

There were a few minor changes on *Ranger VIII* as compared to *Ranger VI* and *VII*. More white paint was added to case II and less sunlit black paint on case VIA, lowering their temperatures and the temperatures of the surrounding components in an effort to compensate for the unusually high power dissipation in the boost regulator. Two transducers were relocated to obtain data on the yoke and antenna temperatures; this permitted additional analysis to be made of thermal effects on the Earth sensor and coax cable and the adjacent region.

The only change on *Ranger IX* relative to *VIII* was the addition of 1.97 in^2 of white paint to the Earth sensor. The additional paint was applied so that the Earth sensor would run some 15° cooler than it had on *Ranger VIII*. The yoke and antenna temperature transducers were used again on *IX*.

2. Flight Performance

Table 8 shows the temperatures of the various components as derived from telemetry tabulated for the critical phases of the flight. A loss of *Ranger VIII* temperature data was observed when the midcourse maneuver was started, and data transmission was not resumed until the motor was fired. *Ranger VIII* was not in the Earth's shadow after launch, so no shadow data were obtained. For *Ranger IX*, good data were obtained during Earth shadow, midcourse maneuver, and terminal maneuver. The thermal reactions during these periods were as expected.

The solar panels indicated temperatures that were within the predicted bands at all times. The cruise equilibrium temperatures of the front faces were 135–140°F. Since the transducers on the fronts of the solar panels had a polished stainless-steel finish on *Ranger VIII* and gray paint on *Ranger IX*, the temperatures indicated

Table 8. *Ranger VIII* and *IX* flight-temperature summary

Location	Temperatures, °F								Predicted limits, °F (cruise)	Operating limits, °F
	Launch		Pre-midcourse		Post-midcourse		Terminal			
	VIII	*IX*	*VIII*	*IX*	*VIII*	*IX*	*VIII*	*IX*		
+*x* solar panel (front)	78	86	121	119	119	122	122	116	105–131	112–131
High-gain antenna	67	64	57	−63	46	−61	89	−23	−60–100	−260–200
−*x* solar panel (front)	80	87	123	119	121	122	144	116	105–131	112–131
Data encoder	95	89	98	88	96	89	99	88	70–110	32–121
Gyro package	96	96	102	97	102	100	104	104	75–115	40–131
+*x* N_2 bottle	73	76	80	78	78	80	88	72	65–105	32–148
−*x* N_2 bottle	78	75	85	76	81	80	87	83	65–105	32–148
Booster regulator	102	98	108	101	111	102	114	101	80–125	32–131
Attitude-control inverter	95	94	97	92	98	93	97	100	75–115	32–131
Power switch and logic	98	96	103	96	108	99	108	59	75–120	32–131
Earth sensor	77	71	80	63	80	61	85	70	20–90	14–94
+*y* pitch sensor	76	73	75	74	76	75	84	92	65–110	40–140
−*y* pitch sensor	77	75	88	81	88	80	93	94	65–110	40–140
Transponder	91	91	95	92	96	93	96	90	70–110	32–148
Case VI battery	84	81	88	83	88	86	89	85	65–105	50–130
Propulsion fuel tank	85	81	90	86	96	89	93	88	70–105	32–148
Case V battery	81	79	85	79	86	81	85	82	65–105	50–130
CC&S inverter	100	98	106	100	107	100	108	94	80–110	32–131
Antenna yoke	71	67	93	37	88	34	95	42	20–90	−200–200

Solar-panel temperatures include corrections of 16°F for *Ranger VIII* and 21°F for *Ranger IX*.

were higher than the true panel temperatures. Corrected values are given in the Table.

During *Ranger IX*'s 33.7 min in the Earth's shadow, the most marked changes occurred in the solar panels and high-gain antenna, as evidenced in Table 9. Both panels exhibited the expected temperature drop. The $+x$-panel temperature dropped to $-83°$F and that of the $-x$ panel to $-64°$. The difference could possibly be explained by a greater absorption of Earth radiation by one panel than the other. The high-gain antenna temperature dropped to $-74°$F during Earth shadow and then came back up to 49° when the spacecraft was again in the Sun. Thereafter, it dropped steadily as the hinge angle decreased until it was in the middle -60's. The Earth-sensor temperature dropped 17°F, the $-y$ Sun sensor 13°, and the yoke 40° during the shadow period. The rest of the vehicle experienced smaller changes, ranging from no change to a 10° drop. All of the data looked very reasonable and were well within the minimum predictions for the shadow phase of the flight.

During the midcourse maneuver, spacecraft attitude is shifted from the designed Sun orientation for 1 to 1½ hr. Each maneuver situation will have an individual thermal effect, which is estimated prior to maneuver execution.

For *Ranger VIII*, the attitude during the maneuver was such that the electronics temperature in case II should have dropped about 10°F. The motor burn during this period provided enough heat to raise the temperature of case II about 15°F, which should have resulted in a 5° net rise. Since data were lost during the initial phase of the maneuver, the only effect noticeable after good data started coming in was one data point with a 4° drop and then a gain of 6° above the cruise temperature for a period of 5 hr. The rest of the data after the maneuver looked nominal. The single point indicating a 4° drop could be attributed to a 1-cycle shift in the raw data and not an actual temperature change.

After the maneuver, an examination was made of the possible effects of dumping the 3 w of RF power in

Table 9. *Ranger IX* Earth-shadow temperatures

Location	Measured temperature, °F					
	Launch	Prior to entering shadow	10 min after entering shadow	20 min after entering shadow	34 min after entering shadow (exit shadow)	16 hr after entering shadow
$+x$ solar panel (front)	86	77	−20	−45	−76	116
High-gain antenna	64	61	−4	−40	−70	−62
$-x$ solar panel (front)	87	76	−25	−56	−69	119
Data encoder	89	89	76	76	76	87
Gyro package	96	94	94	94	95	95
$+x$ N_2 bottle	76	75	68	68	68	76
$-x$ N_2 bottle	75	75	73	70	68	75
Booster regulator	98	98	92	92	92	100
Attitude-control inverter	94	95	95	93	90	92
Power switch and logic	96	96	96	95	93	95
Earth sensor	71	72	71	60	53	66
$+y$ pitch sensor	73	74	64	51	46	74
$-y$ pitch sensor	75	75	63	58	54	82
Transponder	91	92	87	82	97	92
Case VI battery	81	82	81	80	80	82
Propulsion fuel tank	81	82	79	78	78	84
Case V battery	79	78	77	77	77	78
CC&S inverter	98	98	95	93	89	100
Antenna yoke	67	64	54	38	25	53

Solar-panel temperatures include a correction of −21°F.

case II instead of radiating it through the antenna; in addition, case I, where the electrical power equipment was located, was studied. The power dumping would have been expected to change the case II temperature by about 4°. The rest of the vehicle showed normal post-maneuver temperature changes due to the midcourse-motor heat being distributed to the internal components. All the temperatures were back to pre-maneuver cruise temperatures within a period of 4 to 6 hours.

The *Ranger IX* maneuver was not expected to produce significant temperature changes over the main part of the bus. The orientation resulted in about the same Sun input to the cases as during normal Sun-acquired attitude. The maneuver was also of such short duration (39 min from Sun orientation to reacquisition) that there was little effect on the electronics. The only components that were noticeably affected were the solar-dependent antenna, the solar panels, the Earth sensor, the yoke, the Sun sensors, and the attitude-control pans. The solar-panel temperatures dropped some 60°F because of the lower effective sunlit area of the panels, while the antenna, having more sunlit area, experienced a temperature increase of some 75°. The Earth sensor also rose in temperature (17°F) because it, too, had more Sun input. The yoke showed the same characteristics, its temperature rising 21°. The attitude-control-pan temperatures increased from 6 to 11° as a result of the midcourse orientation. The midcourse burn was of such short duration (31 sec) that it did not affect the spacecraft temperature to a very great degree. The midcourse tank temperature rose only 17°. All of the case temperatures rose some 6° within 7 to 17 hr. The data transmitted during the maneuver looked normal and were as expected.

During the terminal phase of the *Ranger* missions, solar energy reflected from the lunar surface impinged on the spacecraft and increased their temperatures. The change in the spacecraft solar orientation during a terminal maneuver can also affect spacecraft temperature.

Ranger VIII did not undergo a terminal maneuver. From the thermal standpoint as well as that of the mission in general, this was the desired choice, since the Earth sensor was running warmer than predicted and a terminal maneuver would have exposed it to additional solar radiation, bringing its temperature above the upper operating limit.

During the last 1¼ hr of the *Ranger VIII* flight, the solar panels warmed up about 16°, and the high-gain antenna temperature rose 38°. The rest of the spacecraft experienced smaller increases because of the greater mass per unit area and smaller dependence on solar energy (vs internal power) for heating.

The *Ranger IX* spacecraft showed little effect of lunar-reflected sunlight except in the solar panels and high-gain antenna; but the terminal maneuver had widespread and varying effects. The panel temperature dropped 8° after the terminal maneuver before the lunar reflection again increased it by about 6°. The antenna temperature rose 42°, the Earth sensor about 10°. Some sections of the spacecraft, such as case I and the $+x$ gas bottle, received less solar input in the new orientation and cooled off; others received more and warmed up.

The thermal-control subsystem maintained critical temperatures within the maximum limits at all times. The yoke and Earth sensor ran above the predicted ranges during both missions but did not go over maximum limits. The telemetry indicated that the majority of the measured temperatures were within the predicted nominal ranges based on average solar intensity for the time of the mission. Most of the measurements were near the top of the band for *Ranger VIII*, near the center for *IX*. On *Ranger VIII*, the Earth sensor was near its upper operating limit throughout the flight. This condition was moderated but not entirely corrected for *Ranger IX*.

In general, the thermal-control performance was entirely satisfactory.

J. Miscellaneous Timing and Arming Functions

1. Backup Command Timer

The backup command timer (BUCT) is a hydraulic device which, through mechanical linkage, actuates a switch assembly to complete a common circuit. It provides spacecraft on-board command-signal redundancy for four crucial commands. The BUCT is installed between the spacecraft and the *Agena* adapter and is set into operation by the removal, at spacecraft separation, of the restraint provided by the adapter.

The command sequencing and nominal times with respect to spacecraft/*Agena* separation were as follows:

1. Arm squib-firing assembly (SFA) at 2.5 min (backup).
2. Release inhibit of TV subsystem at 30 min (backup).
3. Deploy-solar-panels command at 45 min (backup).
4. Initiate-Sun-acquisition command at 60 min (backup).

These functions were successfully accomplished, presumably by primary command.

2. TV-Subsystem Arming Switch

The primary function of releasing inhibit of the TV subsystem is accomplished by a solar-panel-actuated microswitch located at foot E of the spacecraft. The indications are that this function was satisfactorily performed during the *Ranger VIII* and *IX* missions.

3. TV Backup-Clock Turn-On Switch

A microswitch located at the base of the spacecraft and actuated by spacecraft/*Agena* separation causes turn-on of the TV backup clock. This function was satisfactorily performed during both missions.

K. Pyrotechnics Subsystem

The pyrotechnics subsystem (Fig. 36) consists of four squib-actuated pinpullers, three squib-actuated valves, and a squib-firing assembly. The SFA is a redundant unit employing separate battery sources, armed by separate *g*-switches during the boost phase, and fires redundant squibs upon command from the CC&S. The arming of the unit is backed up by the BUCT; in the event of a CC&S failure, the BUCT will command the SFA to fire the solar-panel squibs.

The arming of the SFA was accomplished as attested by the fact that the squib-firing events did occur. Whether the *g*-switches or the BUCT armed the SFA is not known, since telemetry does not provide this information.

The predicted time for command of solar-panel extension (62 min after CC&S inhibit release) is given in Table 10. B-2-1, B-2-2, and B-2-3 event blips observed at the time indicated that the CC&S sent the command to the SFA, which, in turn, sent the current to the A and B redundant squib circuits.

Nominally, the nitrogen, fuel, and oxidizer valves on the midcourse motor are opened by the firing of dual-bridge squibs on command from the CC&S at 26.5 min after maneuver initiation. The nitrogen and fuel shutoff valves are closed by the firing of dual-bridge squibs on command from the CC&S when the accelerometer pulse count reaches the stored value. The B-2-1, B-2-2, and B-2-3 blips occurring at the times shown in Table 10 indicated that both A and B redundant firing curcuits operated for motor ignition and cutoff. The start and stop of accelerometer pulses at these times verify that the pyrotechnic subsystem performed its design task.

One design change, effective on *Ranger VIII*, was made in the pyrotechnics subsystem. The midcourse-motor squib harness was redesigned to make the cable shielding continuous to the squib connectors. This modification was made on the basis of a recommendation by Franklin Institute Laboratories, which performed a study of the RF hazards associated with the *Ranger* Block III pyrotechnics subsystem. Accomplishment of the Franklin study was a requirement imposed by AFETR Range Safety before release would be granted to launch the spacecraft.

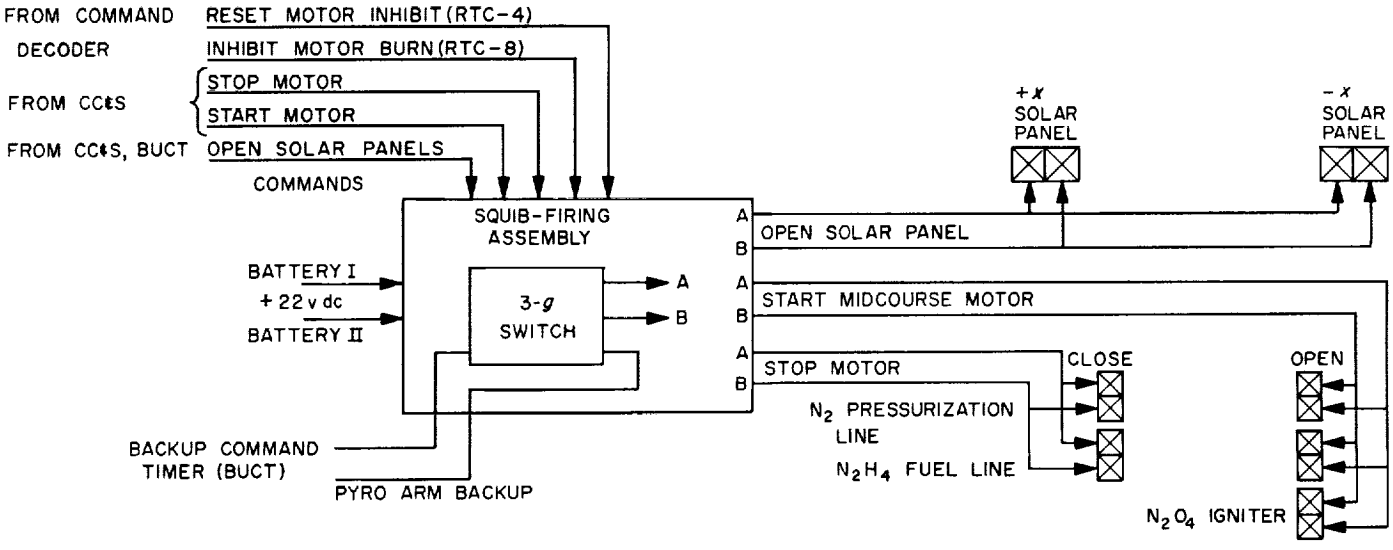

Fig. 36. Pyrotechnics subsystem

Table 10. *Ranger VIII* and *IX* pyrotechnics and associated events

Event	*Ranger VIII*		*Ranger IX*	
	Predicted times (GMT)	Actual times (GMT)	Predicted times (GMT)	Actual times (GMT)
SFA arming	17:05:10	—[a]	21:37:11	—[a]
Solar-panel deployment CC&S command (B-2-1)	18:05:00.5	18:05:00.5	22:37:00.8	22:37:01
SFA Ch. A current (B-2-2)	:04.5	:04.5	:04.8	:06
SFA Ch. B current (B-2-3)	:08.5	:08.5	:08.8	:10
Panel-extension microswitch (B-2-4)	18:05:40	18:05:39.5	22:37:47	22:37:51
Midcourse-motor ignition[b] CC&S command (B-2-1)	10:27:08.5	10:27:08.5	12:30:08.5	12:30:08.6
SFA Ch. A current (B-2-2)	:12.5	:12.5	:12.5	:12.6
SFA Ch. B current (B-2-3)	:16.5	:16.5	:16.5	:16.6
Midcourse-motor shutoff[b] CC&S command (B-2-1)	10:28:09.5	10:28:09.5	12:30:38.5	12:30:38.6
SFA Ch. A current (B-2-2)	:13.5	:13.5	:42.5	:42.6
SFA Ch. B current (B-2-3)	:17.5	:17.5	:46.5	:46.6

[a]No telemetry indication associated with SFA arming.

[b]Results of maneuver correction indicate successful actuation of end items.

L. Midcourse Propulsion Subsystem

Successful accomplishment of the *Ranger* mission required the spacecraft to be capable of undergoing a single midcourse maneuver to remove or reduce launch-vehicle injection-dispersion errors. The on-board propulsion system designed to accomplish this trajectory correction (Fig. 37) employs a small radiation-cooled thrust chamber developing 50 lb of thrust and utilizing hydrazine as a monopropellant. The choice of this type of propulsion system for a midcourse-correction maneuver was based upon its simplicity and inherent reliability, its high degree of flexibility with regard to required impulse, and its advanced state of development.

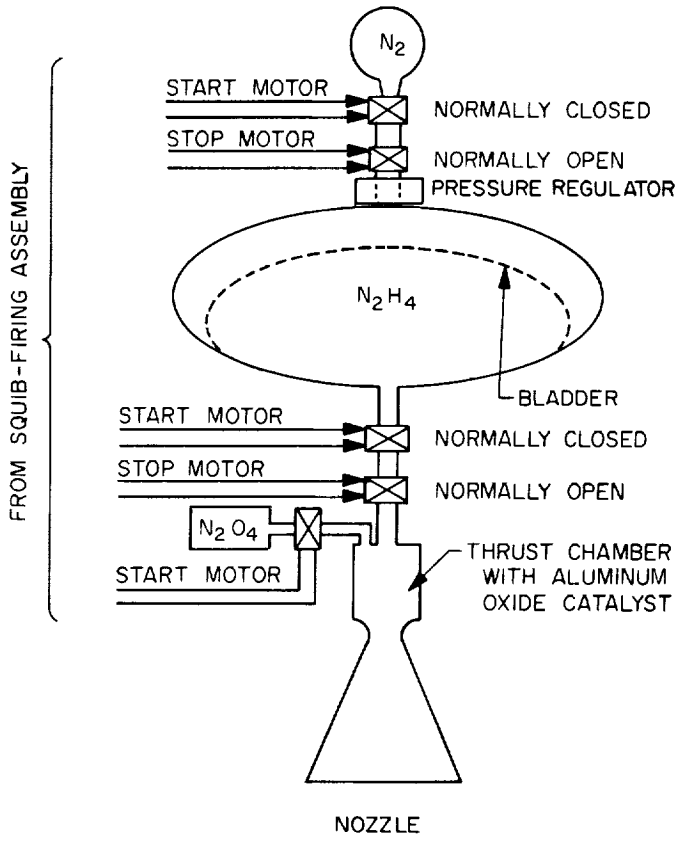

Fig. 37. Propulsion subsystem

The rocket is a constant-thrust device, with the injection pressure derived from compressed nitrogen gas which passes through a pressure regulator and forces the fuel from a bladdered propellant tank into the rocket engine. The engine contains a quantity of catalyst to accelerate the decomposition of anhydrous hydrazine, and ignition is accomplished through the injection of a small quantity of nitrogen tetroxide. Three simultaneously operating explosively actuated valves initiate operation of the system, and two simultaneously operating explosive valves terminate system operation. The amount of total impulse delivered to the spacecraft is controlled by an integrating accelerometer system capable of providing a velocity increment of about 60 m/sec to an 800-lb-mass spacecraft.

1. *Ranger VIII* Mission

During pre-flight checkout and testing, leaks at the oxidizer-cartridge explosive valve, nitrogen fill valve, and oxidizer fill needle valve were detected, repaired, and rechecked. On assembly into the spacecraft, the system was found to be flight-ready, and flight telemetry indicated its ready condition during the pre-midcourse portion of the mission.

The propulsion system operated normally during the midcourse-maneuver sequence. A velocity increment of 36.44 m/sec was required, corresponding to a desired motor-burn time of 59 sec. This represented only 59.7% of its capability. Pre-midcourse normalized pressures (converted to values corresponding to 70°F temperature) were approximately 3300 psia in the high-pressure nitrogen reservoir and 275 psia in the fuel tank. These pressures remained constant until the motor-burn period, indicating no leakage from either tank. A normal motor burn was accomplished at 10:27:08 GMT on February 18, followed by positive shutoff of the system. System pressures remained stable until lunar impact.

2. *Ranger IX* Operations

Pre-flight checkout revealed an apparent fuel-tank leak, which was concluded to be in the ground-support-equipment tank-pressurizing fixture, and a slight oxidizer-cartridge explosive-valve leak, which was repaired and rechecked. Initial power turn-on after the motor was installed in the spacecraft indicated that the propulsion system was flight-ready. All subsequent data received prior to launch, during launch, and during pre-midcourse cruise verified the integrity of the propulsion system and its readiness to operate.

The propulsion system operated normally during the midcourse-maneuver sequence, with motor burn occurring at 12:30:09 on March 23. A velocity increment of 18.15 m/sec was required, corresponding to a desired motor-burn time of 30.59 sec. Since the system was capable of imparting to the spacecraft a velocity increment of 60.09 m/sec, only 30.3% of its capability was used.

Predicted propellant-tank regulated pressure was 305 psia, while the actual pressure was slightly less, as shown in Fig. 38. The fuel-tank pressure undergoes an abrupt change at ignition as a result of high-pressure nitrogen gas being released to the pressure regulator at this time. The nitrogen-reservoir pressure decayed from approximately 3300 to 2200 psia. Superimposed on the nitrogen-tank pressure data shown in Fig. 39 is the curve of "predicted" pressure decay. The nitrogen-tank pressure-decay curve is typical of such a process, with limited heat transfer occurring between the gas and its surroundings during the blowdown process. The scatter of data points is caused by instrumentation noise, which is typical of the high sampling-rate parameters. A positive shutoff of the system was obtained at the end of motor burn, and the pressures remained stable until lunar impact.

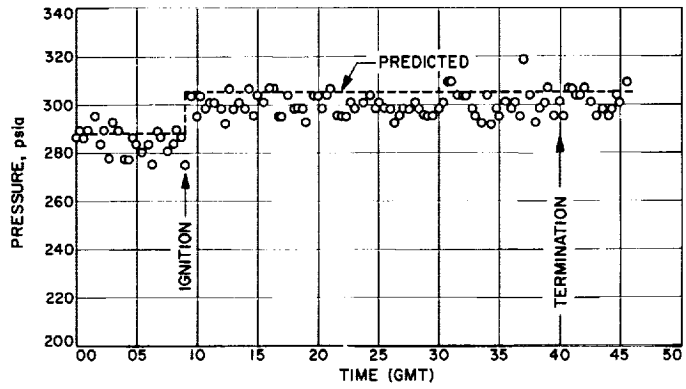

Fig. 38. *Ranger IX* midcourse fuel-tank pressure during motor firing

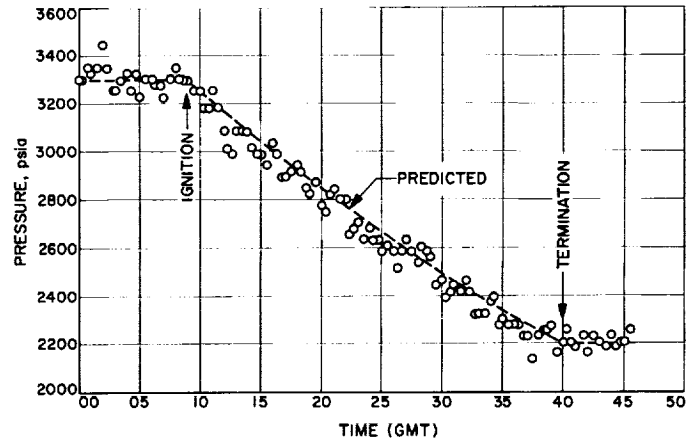

Fig. 39. *Ranger IX* midcourse nitrogen-tank pressure during motor firing

M. Television Subsystem

The TV subsystem consists of two separate chains of equipment designed to give a high reliability and probability of receiving video pictures to meet the mission objectives. Each chain contains slow-scan video cameras, camera electronics, sequencing circuits, transmitters, power supplies, and control circuitry.

The two chains are essentially similar, with the exception of the camera configurations. One chain, whose output is the F-channel, contains two fully scanned 1-in. vidicons, while the other, whose output is the P-channel, contains four partially scanned 1-in. vidicons. The cameras are sequentially exposed and read out, with both channels operating simultaneously. Fig. 40 shows the TV subsystem.

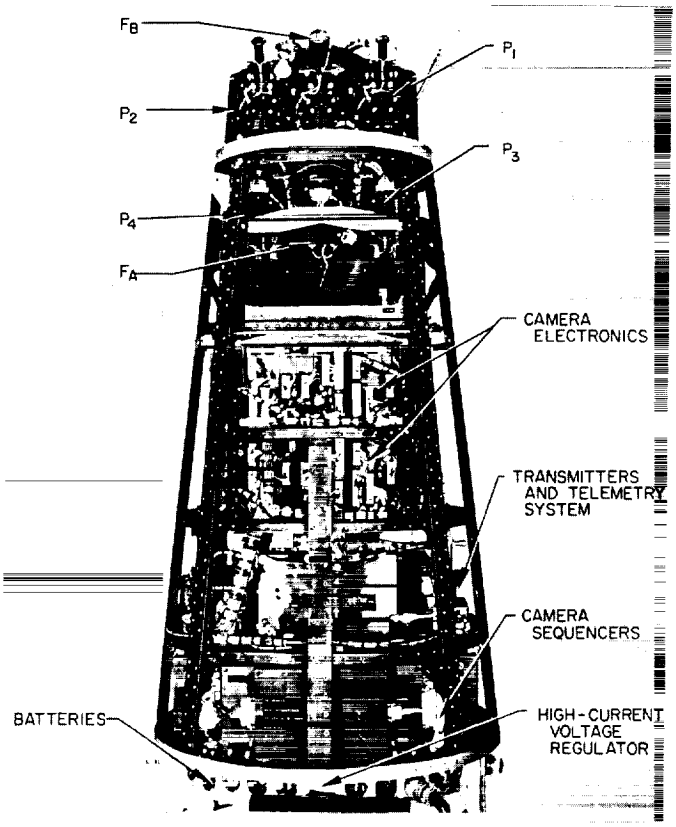

Fig. 40. TV subsystem configuration

The TV subsystem is electrically complete and independent of the spacecraft, except that commands may be received either from the spacecraft command receiver or the on-board CC&S, the spacecraft data encoder is used for cruise telemetry transmission, and the high-gain antenna for transmission of terminal video.

The subsystem operates in two basic modes — cruise and terminal. Cruise-mode TV subsystem operation furnishes commutated 15-point TV subsystem telemetry data to the spacecraft Channel 8 carrier. The cruise telemetry data consist of 15 points of engineering measurements. The telemetry is initiated prior to launch and remains in operation throughout the mission, with the exception of spacecraft telemetry mode II operation during the midcourse maneuver. Also operating during the cruise mode is the TV backup clock, initiated at *Agena/* spacecraft separation. The clock is preset to start the F-channel terminal-phase video operation at a predetermined turn-on interval before a nominal predicted impact time.

At the initiation of TV warmup during the terminal video phase, the 15-point data are switched from Channel 8 to the TV subsystem F-channel carrier, and 90-point data are transmitted over the Channel 8 carrier. The 90-point data contain engineering measurements of the operating parameters during the TV warmup and video transmission periods. Terminal-mode TV operation furnishes a dual-channel (F and P) FM signal in the 960-Mc band for transmission of video and telemetry to the Earth-based data-recovery stations.

The terminal mode is normally initiated via the CC&S warmup command (TV-2) 15 min before lunar impact. The CC&S may be backed up by an RTC-7 turn-on command. After an 80-sec warmup cycle (for the high-power transmitter tubes), each channel is switched to the full-power mode, thereby allowing the video signal to be transmitted via the high-gain antenna to the ground equipment. A backup for the full-power mode is provided by a CC&S full-power command (TV-3), given 5 min after the initial CC&S warmup command to switch the transmitter power-supply relays if the 80-sec warmup command from the internal sequencer fails. The TV backup clock initiates F-channel operation at a predetermined time (nominally 45 min) before impact, independent of the spacecraft commands.

1. Description

The major assemblies of the subsystem are: cameras, camera and control sequencer, telecommunications, electrical power, command and control, backup clock, and structure with associated passive thermal control. A block diagram of the electrical elements is shown in Fig. 41.

a. Cameras. The camera system is composed of six vidicons which operate in a slow-scan mode. The F-chain has two fully scanned cameras, F_A and F_B, and the P-chain has four partially scanned cameras, P_1, P_2, P_3, and P_4. The camera tube is an electromagnetically focused and deflected 1-in.-diameter vidicon with an antimony sulfide/oxygen sulfide (ASOS) photoconductor target.

Each camera consists of a camera head assembly (vidicon, shutter, lens, preamplifier, and housing) and its individual camera electronics assembly. The received image is focused on the vidicon photoconductor target by the lens and exposed by the shutter, an electromagnetically driven, linearly actuated slit, located in front of the vidicon focal plane. The image formed on the photoconductor causes target resistance variations equivalent to the image brightness. After exposure, an electron-beam signal scans the target, and then restores the charges

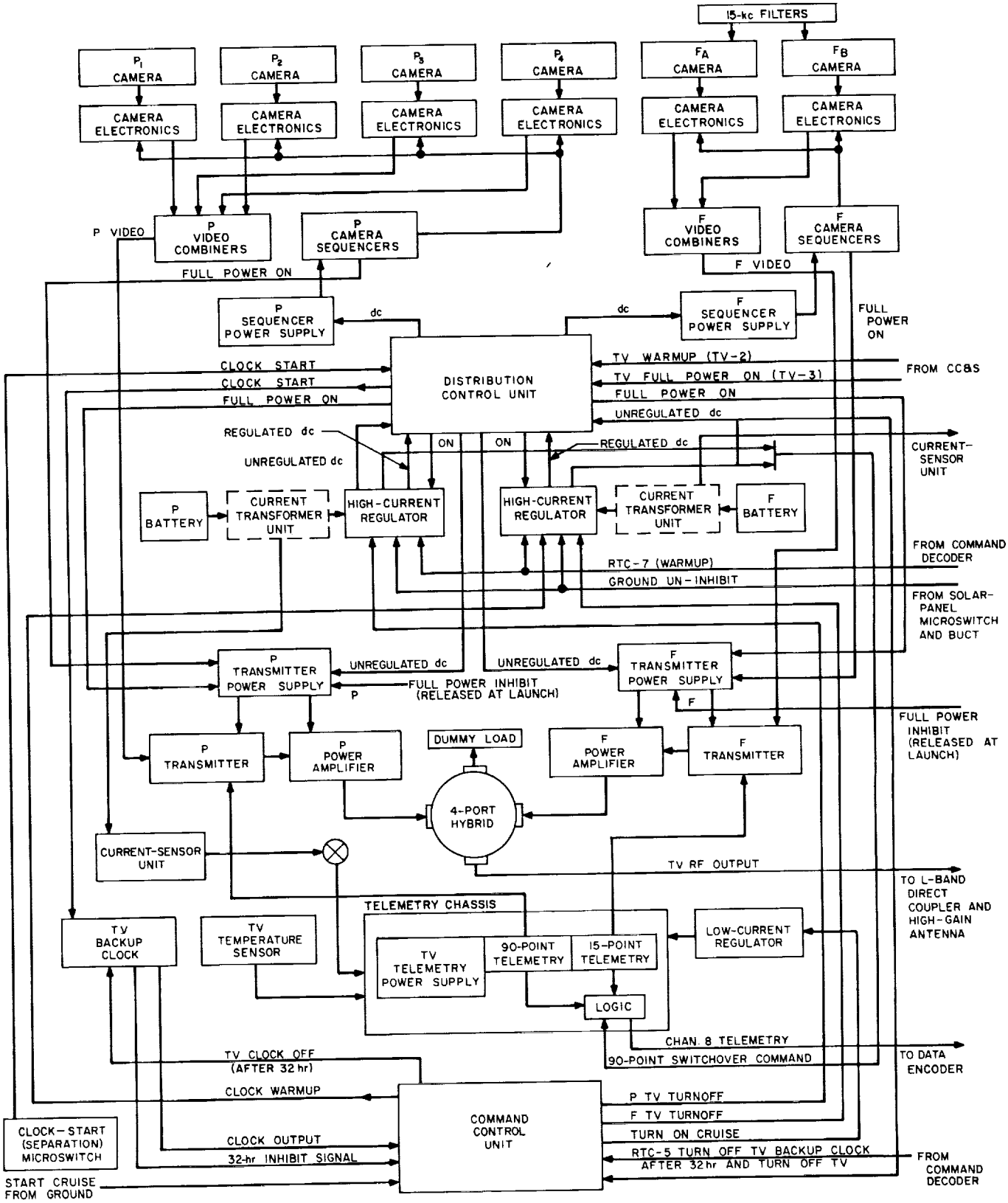

Fig. 41. TV subsystem elements

conducted off as video signal during the beam scan and coupled to a preamplifier. The signal is passed through the preamplifier and a video amplifier, gated in a video combiner, and sent to the respective transmitter. The associated camera electronics supplies the necessary operating voltage, sweep signals, focus signals, and shutter pulses for the camera head assembly. The nominal camera fields of view are indicated in Fig. 42.

The dynamic ranges of the cameras are set to cover a possible lunar-luminance range from 20 to 1500 ft-L. Cameras F_A, P_3, and P_4 cover 20 to 650 ft-L, and cameras F_B, P_1, and P_2 range from 80 to 1500 ft-L. The F-cameras have 4-msec shutter-exposure times; F_A has a 25-mm focal-length lens and F_B a 75-mm lens. The P-cameras have 2-msec shutter-exposure times; P_1 and P_2 have 75-mm lenses and P_3 and P_4 25-mm lenses.

The F-cameras utilize 1130 active horizontal scan lines over a vidicon faceplate area of 0.44 × 0.44 in. The horizontal scan rate is 450 cps, with 0.22 msec apportioned to horizontal blanking. The active scan lines, plus 46.6 msec for vertical blanking, add up to a 2.56-sec frame rate. At the end of the active scan, the camera enters an erase cycle to prepare the target for the next exposure. The two F-cameras are alternately scanned and erased, so that while one is being scanned and read out, the other is erased and prepared for the next exposure.

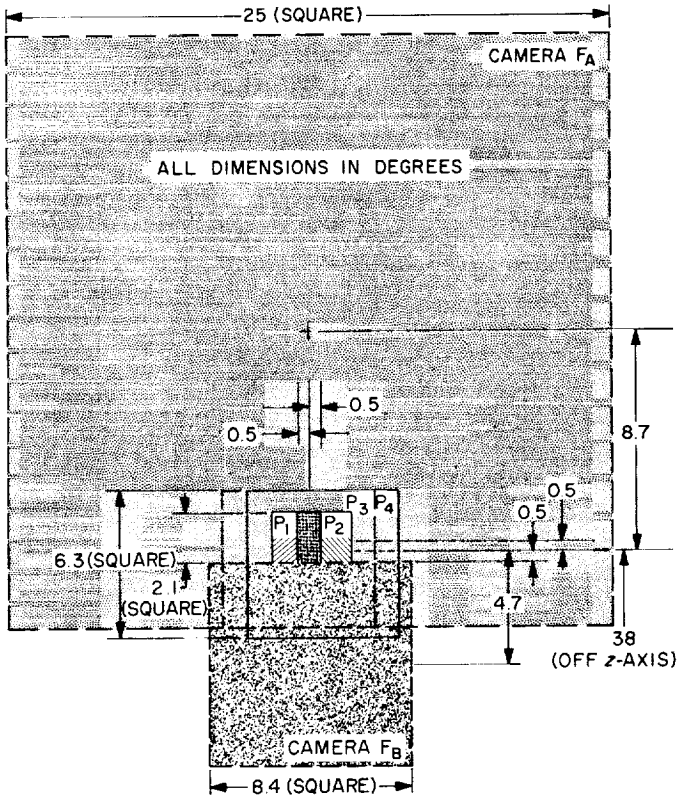

Fig. 42. Camera fields of view (nominal)

The P-cameras utilize 290 horizontal scan lines over a vidicon faceplate area of 0.11 × 0.11 in. The horizontal line rate is 1500 cps, with 0.1111 msec allocated to horizontal blanking. The vertical scan and a 6.6-msec blanking period occupy 0.2 sec. At the end of the active vertical scan, the cameras enter an erase cycle of 0.64 sec to prepare the target for the next exposure. The four P-cameras are sequentially scanned and erased, so that while one is being scanned, the remaining three are in various portions of the erase cycle. A 40-msec pulse is used to separate each sequence of the four P-cameras. Therefore, the total time period per sequence is 0.84 sec. The camera parameters are summarized in Table 11.

b. Camera and control sequencer. The sequencer consists of separate links for the two channels. Each link contains a video combiner, control programmer, camera sequencer, and sequencer power supply. The group generates synchronizing signals for the individual cameras, controls camera exposure and readout, combines the video from the individual cameras with sync and tone code signals (e.g., camera F_B video is identified by a 144-kc tone burst), and applies the composite video signal to the respective RF-transmitter channel modulator.

c. Telecommunications and telemetry. The telecommunications equipment is designed to convert the composite video signal into an RF signal for subsequent transmission through the spacecraft-to-ground antenna system. An FM transmission system utilizing an FM modulation index of 0.95 was chosen based upon the frequency and bandwidth constraints. Thus, the 177-kc base video bandwidth signal is converted to an L-band RF signal with a 900-kc bandwidth and the communications equipment provides a minimum of 30-db signal-to-noise gain, so that there is no degradation to the input video signal. Each channel has a complete transmitter chain, whose respective outputs are combined and fed to the spacecraft high-gain antenna. Each chain consists of an L-band FM transmitter, an intermediate power amplifier, a 60-w power amplifier, and an associated power supply. The L-band transmitter modulator generates a 20-Mc RF signal, modulated by the 177-kc composite video signal. The 20-Mc RF carrier is then frequency-multiplied by ×4 and ×12 multipliers to the transmitted frequency of 960 Mc. The power amplifiers apply gain to the RF carrier, so that a final 60-w power

Table 11. Summary of camera characteristics

Characteristic	Camera F_A	Camera F_B	Cameras P_1 and P_2	Cameras P_3 and P_4
Aspect ratio	1 to 1	1 to 1	1 to 1	1 to 1
Active scan area, in.	0.44 × 0.44	0.44 × 0.44	0.11 × 0.11	0.11 × 0.11
Line rate, cps	450	450	1500	1500
Horizontal line time, msec	2.22	2.22	0.6666	0.6666
Horizontal blanking time, msec	0.22	0.22	0.1111	0.1111
Frame rate, cps	0.39	0.39	5	5
Frame time, sec	2.56	2.56	0.2	0.2
Vertical blanking time, msec	46.6	46.6	6.6	6.6
Group vertical blanking time, msec	—	—	40	40
Video bandwidth, kc	177	177	144	144
Lens optics	25 mm, f/1	75 mm, f/2	25 mm, f/1	75 mm, f/2
Shutter speed, msec	4	4	2	2
Horizontal erase rate, cps	25	25	3000	3000
Number of TV lines scanning	1130	1130	280	280

output is attained for each channel. A strip-line four-port hybrid ring is used to combine the two channels with an associated dummy load to dissipate the combining loss. The actual RF carriers for the F- and P-channels are centered at 959.52 and 960.58 Mc, respectively. A 160-kc bandwidth between the transmitter output frequencies is reserved for the spacecraft transponder.

Channel P is tuned for a maximum operating time of 30 min; thus, peak power is immediately available, and the supply remains approximately constant for the 30-min period. The F-channel must be capable of a 60-min operational period; therefore, the longer constant profile is accomplished by a slower rise to peak operating power. The parameters associated with the TV communications link are catalogued in Table 12.

The telemetry assembly consists of the telemetry chassis, temperature-sensor unit, current-sensor unit, and current-transformer unit.

The telemetry equipment must be capable of sampling the key subsystem operating parameters, signal conditioning, commutation, and analog-to-FM conversion. During cruise-mode operation, a commutator samples 15 measurements at the rate of one sample per second; the commutator output drives a 3-kc center-frequency VCO, coupled into the spacecraft data encoder, for subsequent transmission of the measurements with other spacecraft telemetry as the Channel 8 data. The 15-point sampling includes voltages, temperatures, currents, and backup-clock accumulated count. Terminal-mode operation telemetry (activated at initiation of TV warmup) drives a 90-point sampling commutator operating at the rate of three samples per second to provide detailed diagnostic measurements of critical operating parameters. The output of the 90-point commutator is fed continuously into the P-channel 225-kc VCO, whose output is multiplexed with the P-channel video at the input to the transmitter modulator. The 90-point data are also applied to the 3-kc Channel 8 VCO for transmission through the spacecraft data encoder. The 15-point cruise data are switched from Channel 8 to the F-channel 225-kc VCO for mixing with the F-channel video and subsequent transmission.

Table 12. Nominal TV communications parameters

Losses, db	145.6	
RCA circuit		3.5
JPL circuit		1.3
Spacecraft high-gain antenna		−19.9
Antenna pointing		0.3
Path		204.0
Receiving antenna		−44.1
Receiver circuit		0.5
Transmitter power (60 w), dbw	17.8	
Total power received (maser input), dbw	127.8	
System noise temperature, °K	141.2	
Noise bandwidth, kc	900	
Receiver noise power, dbw	147.6	
Received carrier-to-noise ratio	19.8	

The switching is accomplished via two redundant relays for greater reliability. The transmission of the 90-point data over the spacecraft communications system is based on the assumption that in the event of a TV subsystem transmission failure, diagnostic telemetry will be received.

The 15-point cruise data derives power from the P-channel via the low-current voltage regulator. In terminal mode, telemetry power is derived from either the P-channel, through the low-current regulator and the 25-v regulator, or the F-channel, through the 25-v regulator. The power is diode-gated at warmup so that the telemetry can be powered by either channel in the event one of them should fail.

A temperature-sensor assembly incorporating 15 associated thermistors is used for temperature measurements at critical heat-dissipating locations. Using zener diodes located in the unit and the output of the low-current voltage regulator for power, temperatures are translated into representative voltages and sent to the telemetry chassis to be encoded by the 15- and 90-point commutators.

The main battery harness passes through the center of the current-transformer units so that the transformers are able to sense changes in dc current in the F- and P-batteries without actually being in the battery circuit. The information is sent to the current-sensor unit, which, by means of a magnetic amplifier, transforms it into a dc voltage proportional to the dc current. The transformation curve is nonlinear but continuous, with a slope of 0.10 v/50 ma up to 500 ma, and 0.10 v/amp between 14 and 17 amp. The current sensor draws its power from the low-current voltage regulator through a current-limiting circuit in order to prevent the loss of the total cruise-mode telemetry in case of a failure in the sensor unit.

The sensor-unit output is sent to the telemetry chassis to be encoded by the 15- and 90-point commutators.

d. Electrical power. The subsystem power assembly comprises battery power sources, high- and low-current voltage regulators, and appropriate control circuitry. The power supplies are capable of supplying regulated and unregulated voltage to the electronic assemblies for the cruise-mode and terminal-mode operation as well as in support of pre-launch test phases. The subsystem power is independent of the spacecraft power sources, and each of the TV channels (F and P) has independent, isolated supplies, so that a failure in one channel will not affect the operation of the other. The power source must support a mission profile of a maximum of 70 hr of cruise-mode operation, 1 hr of terminal-mode F-channel operation, and ½ hr of terminal-mode P-channel operation, as well as the pre-launch reduced-power testing. The current drains for the various modes are indicated in Table 13.

Table 13. Current drains for various modes

	Channel P, amp	Channel F, amp
Cruise mode	0.165	0.04
Terminal warmup	10	8.1
Terminal reduced power	11	9
Terminal full power	15	13

The batteries are silver–zinc, with potassium hydroxide as the electrolyte, and consist of 22 series-connected cells. The batteries are hermetically sealed and are rechargeable for a maximum of 3 cycles; they incorporate a temperature transducer for telemetry indication. The unregulated battery output voltage is −30.5 to −38 v dc with a capacity of 1600 w-hr, or 45 amp-hr, per battery, which provides an adequate margin over the subsystem requirements.

The transistorized high-current regulator for each channel supplies unregulated voltage to the transmitter power supplies, the camera-electronics shutter drive, and lamp erase circuits. Regulated voltage at −27.5 ±0.5 v dc is supplied to the other assemblies from an unregulated input battery voltage of −30.5 to −38 v dc. The input of the regulator incorporates a silicon-controlled rectifier (SCR) acting as a power switch controlled by the gate circuit. A command input module is used to control the SCR turn-on operation by clamping the SCR gate circuit to the SCR cathode until turn-on is required, at which time the clamp is interrupted and a ground applied to the gate to bias the SCR into the conducting state. The SCR can be turned off via back-biasing of the gate.

A low-current voltage regulator operated from the P-channel battery furnishes power for the cruise-mode telemetry. The regulator voltage is −27.5 ±0.5 v dc for the current range of 0.140 to 0.360 amp, with a nominal cruise drain of approximately 0.165 amp. The circuit limits at 0.360 amp; thus, a failure in the telemetry will not deplete the battery before terminal-mode P-channel operation is required.

e. Command and control assembly and associated control circuitry. The command and control circuitry for the subsystem operation is designed for minimum dependency upon the spacecraft and to provide complete

separation of the F- and P-channels where feasible, so that a failure in one channel will not affect the other.

Table 14 describes the prime commands applicable to the subsystem operation during the cruise and terminal portions of the mission. Ground-test command functions are not described.

f. TV backup clock. The TV subsystem incorporates a command clock to initiate F-channel operation at a preset time before lunar impact. The clock serves as a backup to the prime commands from the ground or the CC&S; the commands are dependent upon the spacecraft command link being functional at the initiation of the terminal maneuver, as the CC&S command counter is initiated by RTC-6. The count operation is initiated by a microswitch closure upon spacecraft/*Agena* separation approximately 20 min after launch. The clock was preset prior to liftoff for initiation of F-channel operation at I−45 min for *Rangers VIII* and *IX*. This time was based upon prelaunch predictions for arrival-time dispersions as a function of the booster performance, nondependent upon the midcourse-correction capabilities. The 1-σ probability error for predicting normal impact time is 30 min. Considering the tradeoff of impact-time prediction and total safe operating time allowable for the TV subsystem

Table 14. Prime commands for TV operation

Command	Mechanization	Time issued
Cruise-mode telemetry on	Operational support equipment	Prior to launch
	Hydraulic timer	S + 30 min
	Solar-panel microswitch	L + 60 min or S + 46 min
Clock-start	Microswitch	Separation
Ground-enable	Hydraulic timer	S + 30 min
	Solar-panel microswitch	L + 60 min or S + 46 min
TV-subsystem warmup	CC&S TV-2	I − 15 min
	RTC-7	I − 12 min
	Clock—Ch. F only	S + 64 hr (setting varies with mission)
TV-subsystem full power	Sequence counter	Warmup + 80 sec
	CC&S TV-3	I − 10 min
TV-subsystem off and clock-disable	RTC-5	In the event of abnormal turn-on or fast clock count

assemblies, a preset time of I−30 min was chosen for the *Ranger VI* and *VII* missions; however, the trajectory for these missions yielded an earlier arrival time than the predictions. Therefore, the *Ranger VIII* and *IX* clocks were preset for initiation at I−45 min to compensate for the previous earlier arrival times. The *Ranger VIII* and *IX* mission trajectories were such that the arrival time was late; therefore, the midcourse maneuver corrected the trajectory (limited by other spacecraft constraints) to give a clock turn-on operating time within the capability of the TV subsystem. The *Ranger VIII* clock was preset to initiate Channel F at S + 64¼ hr, and the *Ranger IX* clock was preset for S + 63½ hr. If the mission trajectories had been such that the clock would have initiated F-channel operation at a time greater than the allowable operating time for the subsystem, it could have been disabled or deactivated by the transmission of an RTC-5 command. As the RTC-5 command serves multiple functions, an inhibit circuit in the subsystem control circuitry prevents the command from disabling the clock until the interval of S + 32 hr has elapsed.

The assembly is a solid-state timer with an overall accuracy of ±5 min over the total mission time duration. The clock is designed to provide predetermined outputs, in 15-min increments, between 60 and 70 hr; however, the range can accommodate any time between 0 and 128 hr. The exact time is preset by insertion of a shorting plug across the time-decoding gate matrix to give the accumulated time equivalent to the desirable "S+" time needed to satisfy the predicted mission profile.

g. Structure and thermal control

Structure. The basic structure consists of a lower structural assembly, an upper structural assembly, and a thermal-shroud assembly. The external appearance of the structure is that of the frustum of a right-circular cone topped by a cylindrical section. The overall structure height is 59.283 in., with a cone-base diameter of 25 in., tapering down to a diameter of 16.0 in. at the top of the cylindrical section. The primary strength of the lower assembly is provided by two box-spars: an internal box-spar consisting of four longerons attached by means of stiffened panel sections to an external box-spar consisting of eight longerons. The thermal-shroud assembly, fabricated in two sections, is attached to the main structure by screw-type fasteners and, being a load-carrying member, contributes to the stiffness of the assembly and provides torsional support. The upper cylindrical section encloses the camera assembly and provides structural support for the spacecraft omnidirectional antenna, which is mounted on top of the TV subsystem,

with the omni RF cable routed through the subsystem. The panels between the longerons provide mounting and attachment points for the individual TV assemblies. The primary structure is painted black to heat-sink the attached electronic assemblies. The six camera head assemblies are mounted on a solid machined camera-bracket housing within the upper cylindrical section, and the bracket is attached to the primary, or lower, structural assembly. A camera-optics view area is cut out of the external thermal shroud.

The subsystem is mechanically attached to the spacecraft by six mounting legs at the base of the lower structural assembly, and TV subsystem–spacecraft and OSE interface cabling is accomplished by means of connectors located in the base ring of the lower structural assembly. The structure is manufactured from sheet aluminum alloy.

Thermal Control. The thermal control is entirely passive, with minimum thermal exchange between the subsystem and the mating spacecraft. The primary, or lower, structural-assembly thermal mass is utilized as the heat-sink during equipment operation. The thermal shroud assembly (with associated fins), with appropriate surfaces and finishes, is used to control the radiative exchange of thermal energy. The thermal configuration is capable of providing temperature regulation in a space vacuum environment with a solar illumination of one solar constant (0.9 ± 0.03 w/in.^{2}).

During cruise-mode operation, the spacecraft is Sun-oriented, so that the shroud fins' projection shadows the shroud skin, preventing solar energy from striking the shroud. The fins are covered with different paints having varying solar-absorptivity characteristics to control the thermal-energy balance of the subsystem. The interior of the shroud is black to absorb heat generated within the subsystem, while the exterior is highly polished to reflect and radiate the heat energy during terminal-mode operation.

During cruise-mode operation, the temperature of the subsystem is controlled such that the equilibrium temperatures of assemblies mounted on the inert payload are approximately 50 to 86°F. In terminal mode (15 min of operating time), the temperatures of the mounting structures are maintained at less than 95°F for the camera (vidicon) assemblies and less than 140°F for all other equipment assemblies. The subsystem is limited thermally by the camera vidicons and the transmitter ×12 multiplier units. The thermal design maintains adequate temperature margins to permit 60 min of terminal-mode operation on the F-channel and 30 min on the P-channel in nominal ambient temperatures.

2. Design Changes for *Rangers VIII* and *IX*

a. Communications. The major change in the communications subsystem from that used for *Ranger VII* was the incorporation of a new intermediate power amplifier. A Resdel cavity utilizing a 3CX100 triode tube replaced the previously used RCA unit containing a 7870 tetrode tube. The new intermediate power amplifier operated more efficiently, had improved stability, and delivered greater output drive to the final power amplifier. Also, telemetry monitoring was provided for the intermediate power-amplifier cathode current, and the Varactor diodes in the ×4 multiplier unit were changed to an MA-4048 D type.

b. Current-sensor unit. The current-sensor unit was changed to obtain increased sensitivity in current measurement resolution during cruise-mode operation. The *Ranger VII* unit was designed to give greater resolution for high-current drains during terminal mode; as a magnetic amplifier was employed, the high-current resolution was obtained by sacrificing the low-current reading capability. The new design incorporated a nonlinear loop for compensation.

c. Structure, mechanics, and cabling. *Rangers VIII* and *IX* were equipped with new cable harnesses, which incorporated the following changes:

Indirect routing was eliminated.

Splices were removed where feasible.

Cannon Hi-Rel connectors were incorporated where available.

Stainless-steel screws were used on connectors.

Updated JPL specs were used in manufacturing.

New split battery connectors were used.

The camera preamplifiers were reworked to incorporate either multiple-wrap leads on the nuvistor or the new long-lead-type nuvistors. As a result of a proof-test-model (PTM) nuvistor failure prior to the *Ranger VII* mission, it had been determined that the nuvistor leads which had only a single wrap before soldering were susceptible to cold joints and subsequent fracture.

An effective shutter-shock gasket isolator was introduced between the camera shutter and head housing to eliminate shutter-induced microphonics in the camera preamplifier. Castellated gasket isolators (Solithane 113,

formulation 5) were used for the four shutter screws, and a mounting grommet (Solithane 113, formulation 8) was used for the fifth point of the shutter mounting.

d. Camera and associated electronics. On the basis of the *Ranger VII* photographs, it was decided to decrease the sensitivity of cameras P_1, P_2, and F_B, and the gain was lowered from a saturation level of 2700 to 1500 ft-L. Cameras P_3, P_4, and F_A remained at a saturation level of 650 ft-L.

The optical focusing techniques for the cameras were changed to avoid the severe optical defocusing problems noted during the pre-flight thermal-vacuum tests made on *Ranger VIII*. An investigation resulted in a revision of the optical focusing techniques for the f/2 cameras intended to compensate for the air-to-vacuum change in focus. This change is caused by the difference in the refractive index of the two media. The displacement in the image plane for the two media is about 2.5 mils. This displacement is taken into account by inserting a shim behind the camera lens before focusing. The position of the vidicon is adjusted to maximize the video response at 167 TV lines while viewing a collimator focused at infinity in air. The shim is then removed to provide the required displacement.

The displacement of the image plane in the f/1 cameras was about 0.8 mils, and it was considered impractical to implement the same procedure on these cameras. The focusing of the f/1 cameras was accomplished by adjusting the lens position to maximize the video response at 178 TV lines while viewing a collimator focused at infinity in air. No fixed displacement was provided; however, an effort was made to bias the position slightly in the direction of the displacement.

e. Timing. The turn-on time for the F-channel backup clock was changed from I − 30 min to I − 45 min.

3. Performance of *Ranger VIII* TV Subsystem

A pre-launch reduced-power test conducted on the TV subsystem showed both camera and telemetry performance to be as expected, indicating a state of launch readiness. During the launch phase, the tracking station at AFETR was able to maintain lock with the spacecraft until the space vehicle went over the horizon. The data indicated that the subsystem performance was normal throughout this critical boost phase.

At spacecraft/*Agena* separation, the TV backup clock (programmed to start warmup on the F-channel in 64 hr, 15 min) was initiated. Thirty minutes after separation, the spacecraft hydraulic timer commanded ground-enable for the SCR turn-on circuits. These circuits had been disabled during the boost phase to ensure that the subsystem operation would not be initiated inadvertently in the critical pressure region of the atmosphere. A backup ground-enable command at L + 61 min was provided via a microswitch actuated by deployment of the $-x$ solar panel and monitored by a data-encoder B2-4 event.

As the spacecraft turned to acquire the Sun at L + 63 min, the camera lens was turned into the Sun momentarily, causing the sharp temperature rise noted in Fig. 43. After completion of Sun acquisition, the temperature returned to nominal. Two and one-half hours later, at L + 3 hr, 30 min, the top hat (Fig. 43) increased in temperature. This rise was due to the turning of the spacecraft during the Earth-acquisition phase of the flight. After completion of Earth acquisition, the top-hat temperature returned to nominal.

At S + 8 hr and + 16 hr, respectively, confirmation was received that the clock was functioning properly.

In cruise mode, the TV subsystem furnishes 15 commutated points of battery, backup clock, and temperature measurements. During the midcourse maneuver, this telemetry was switched off from the end of pitch turn to the start of Sun reacquisition to allow motor-burn information to be transmitted over Channel 8. Because of problems in the bus transmitter area, the Channel 8 signal was lost from the stop of the roll turn to the start of motor burn. During the maneuver, the temperatures in the TV subsystem fluctuated. The top hat and the lower shroud (Fig. 43) exhibited sharp rises in temperature during the pitch-turn and Sun-reacquisition phases. After about 15 hr, the temperatures stabilized.

Without a midcourse maneuver, the clock would have turned the F-channel into warmup at I − 2 hr, 8 min. With the midcourse correction used, the scheduled time of the clock turn-on of the F-channel was I − 11 min. The nominal time of I − 30 min was not chosen for the time of TV initiation via the clock because of the cone-angle constraints on the omniantenna.

During the remainder of the cruise period, confirmations of proper clock operation were received at S + 24, 32, 48, and 64 hr; and all current voltages and temperatures indicated that the TV was functioning normally. Trading off higher resolution on the final pictures for overall broader coverage and possible stereoscopic effects, it was decided to leave the spacecraft in its cruise-oriented

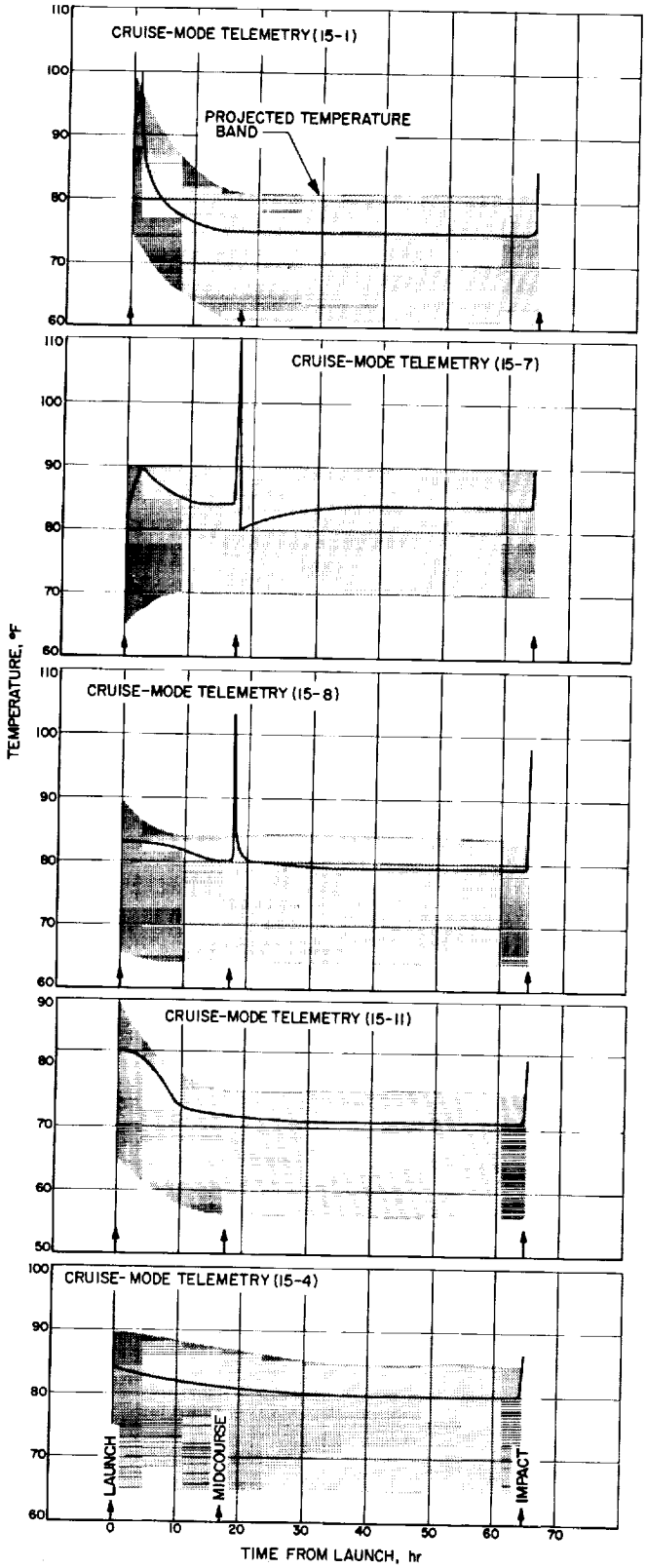

Fig. 43. *Ranger VIII* TV subsystem flight temperatures

position. Therefore, in the terminal maneuver, the RTC-8 command was sent prior to the RTC-6 in order to disconnect the spacecraft attitude-control system from the CC&S. In this manner, timing functions of the CC&S could be used without changing the spacecraft attitude.

In order to obtain a larger area of coverage for the initial pictures, the RTC-6 command was sent 69 min, 26 sec before impact. Forty-five minutes after spacecraft receipt of the RTC-6 command, the TV-2 command was generated, indicating warmup in both the F- and P-channels approximately 24 min, 26 sec before impact. This event was monitored by noting the change from 15- to 90-point telemetry and was confirmed by a change in points 55 and 60 from 0 to 2.4 v and a change in current level from approximately 0 to 8 amp on F and from 0 to 10 amp on P. The rest of the data received during this warmup period indicated that operation was normal for both channels. The current drain, the battery voltage, and the heat-sink temperature (Fig. 44) indicated that both channels would be able to operate for the required 24 min, 26 sec. Since the CC&S performed flawlessly, the need to initiate an RTC-7 command, which had been held in readiness, never arose.

During the terminal period, the temperature on the lens housing increased 10°F as a result of reflected and radiated light energy from the Moon's surface.

The batteries, which had reached a plateau at −34.8 v for the F-channel and −34.7 v for P, fell to −32.5 v for F and −32.4 v for P when high current demands were placed on them during the terminal phase of the mission. These voltage levels indicated that the batteries were operating under proper load and, together with the predicted usage data shown in Fig. 45, further indicated that the batteries would have at least another 30 min of life remaining at the end of the mission.

Both channels turned into full-power operation via the internal 80-sec sequencer as confirmed by a change in points 55 and 60 from 2.4 to 0.6 v, a change in current on the F-channel from 8 to 13 amp, and a change in current on the P-channel from 10 to 15 amps. At this point, Goldstone Station confirmed the receipt of strong video from both F- and P-channels. However, because of the initial high light level, the F_A, P_3, and P_4 pictures exhibited minimum detail.

A warmup command to the F-channel initiated by the backup clock had no effect, since both channels had previously been turned on by the CC&S. It was estimated

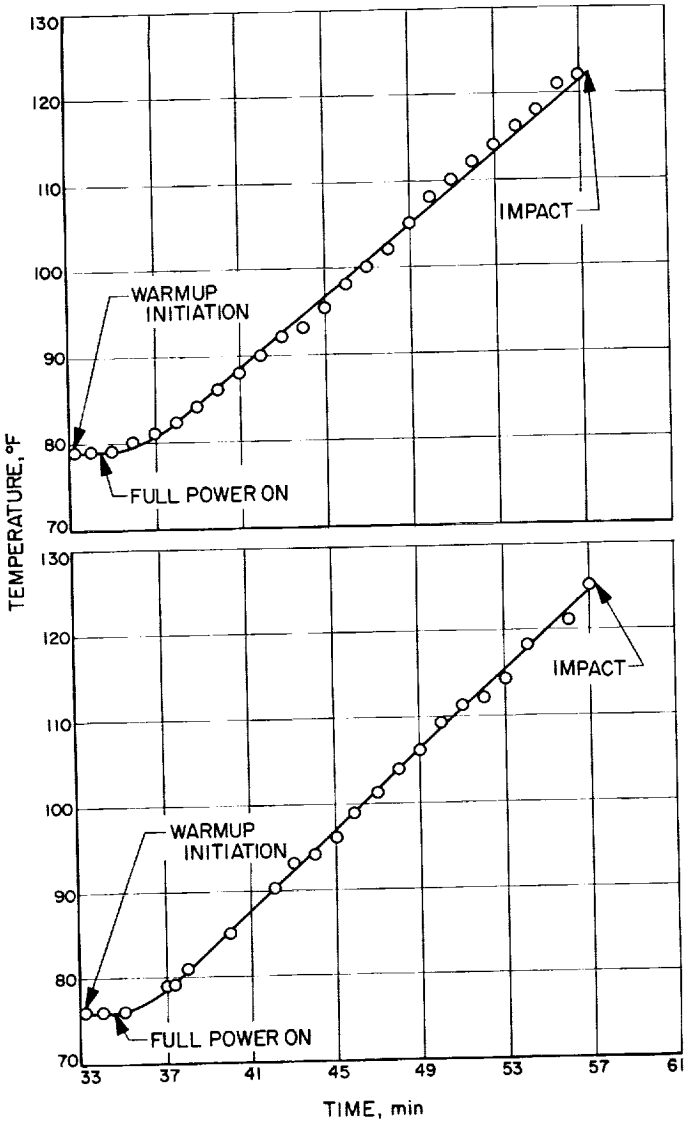

Fig. 44. *Ranger VIII* heat-sink temperatures during terminal phase

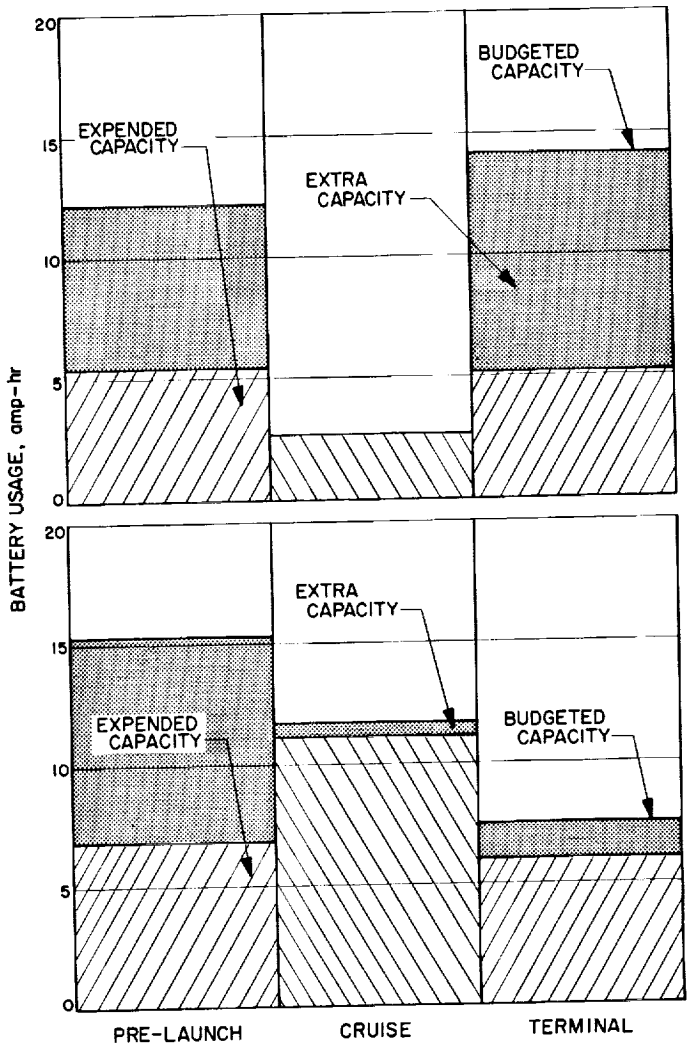

Fig. 45. *Ranger VIII* expended and budgeted battery capacity

that the clock had been 1 min slow for the entire 64-hr, 15-min period; this performance was well within the design tolerance of ±5 min.

The CC&S backup command (TV-3) to initiate full power on both channels was timed to occur 50 min after the spacecraft received the RTC-6 command. This event was noted by monitoring a blip on the B-2-1 channel of the data encoder. Again, since both channels had previously been turned to full power by the TV's internal 80-sec sequencer, the TV-3 command had no effect.

The top-hat, lower-shroud, and camera-electronics temperatures increased sharply at the end of the mission as a result of the heat generated by the TV subsystem in full-power operation. The battery temperature increase was due to the high-current drain in the terminal portion of the mission. The transmitter heat-sink temperatures (Fig. 44) exhibited their expected rise. The readings were sufficiently below the maximum temperatures, however, to permit operation of the TV subsystem for at least another 19 min.

The TV performance during the 64 hr, 52 min, 36 sec of the *Ranger VIII* mission was as predicted. All operating parameters were within design specifications, and all cameras and systems performed perfectly, except for the microphonics on the P_2-camera (see Section 4 below). The 6,597 P pictures and the 538 F pictures gave a broad coverage of the lunar surface, viewing both the highland

areas and the maria. In order to obtain this broad coverage, some resolution had to be sacrificed on the final pictures.

One peculiarity in performance that was noted throughout the flight was that the temperatures of the TV subsystem were about 5°F higher than the predicted nominal. However, all temperatures were still well within the overall stabilized limits.

4. *Ranger VIII* Anomalies

It was anticipated and noted that the Channel 8 VCO exhibited a minor slow drift of 1 or 2 cps over the entire mission. This was within the overall tolerance of ±5 cps for the VCO.

During the terminal phase, the P_2-camera was subjected to high shutter-induced microphonics. These microphonics had been observed during ground testing of *Ranger VIII*, but at about one order of magnitude lower frequency than during the mission. The reason for the increase in microphonics cannot be fully ascertained, but the best estimate of the situation indicates that the increased temperature caused by the 24 min, 26 sec of camera operation was one of the major contributors.

5. Performance of *Ranger IX* TV Subsystem

As in the case of *Ranger VIII*, the pre-launch testing and launch operations were normal. At spacecraft/*Agena* separation, the TV backup clock (programmed to initiate F-channel warmup at S + 63 hr, 30 min) was initiated; 30 min later, the hydraulic timer commanded the ground-enable for the SCR turn-on circuits. At L + 61 min, this command was backed up by a microswitch actuated by the deployment of the $-x$ solar panel and monitored by a data-encoder B-2-4 event.

As the spacecraft passed through the Earth's shadow for approximately 34 min during the early phases of the flight, the temperatures throughout the TV subsystem dropped; this was especially evident in the top-hat, lower-shroud, and camera-electronics temperatures (Fig. 46). A few hours after the spacecraft passed out of the Earth's shadow, the temperatures stabilized at their nominal levels. Telemetry confirmation of proper clock operation was received at S + 8, 16, 24, and 32 hr. The telemetry indicated that the clock was an average of 10 sec slow every 8 hr. This time was within the specification for accumulated clock counting.

As with *Ranger VIII*, the TV telemetry information was switched off during the period from the end of the

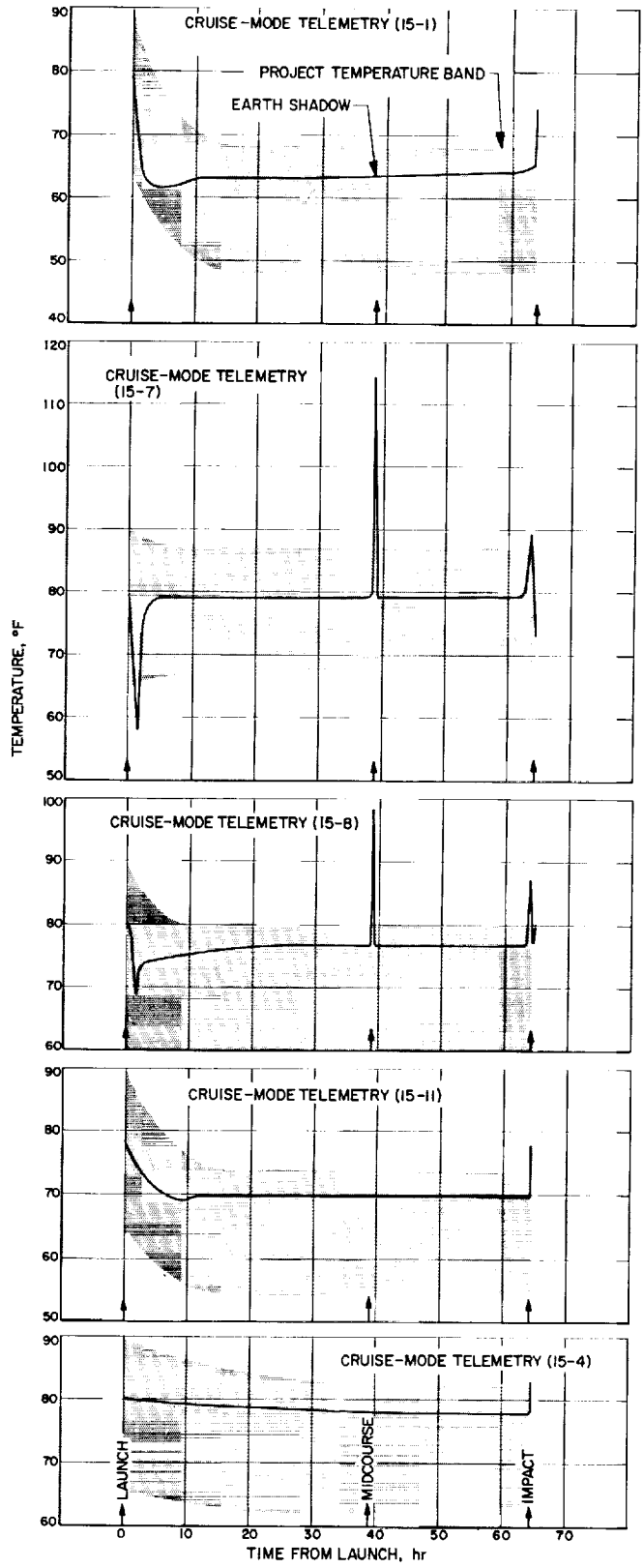

Fig. 46. *Ranger IX* TV subsystem flight temperatures

pitch turn to the start of Sun acquisition to allow motor-burn information to be transmitted from the spacecraft over Channel 8.

During the midcourse maneuver, the spacecraft turned +128 deg in the pitch direction. This increased the solar-heat input to the $-y$ side of the TV tower, causing the top-hat and lower-shroud temperatures to increase 45 and 21°F, respectively. When the spacecraft turned to reacquire the Sun, the temperatures returned to nominal.

During this phase of the *Ranger IX* mission, trajectory studies indicated that the clock would turn on the F-channel at I − 1 hr, 3 min. With the midcourse correction selected, clock turn-on of the F-channel was scheduled for I − 45 rather than the nominal corrected time of I − 30 because of the cone-angle constraints on the omnidirectional antenna and post-midcourse dispersion-ellipse constraints. Another factor in reducing the post-midcourse dispersion ellipse was the initiation of midcourse at L + 39 hr instead of the nominal L + 16 hr, thus having more precise trajectory inputs on which to base the maneuver. By following this approach, the built-in protection against disabling the clock by an RTC-5 was eliminated, since the inhibit on clock turn-off was released at L + 32 hr.

All telemetered voltages and temperatures indicated that the TV subsystem was functioning normally throughout the cruise period, and continued clock operation was confirmed by telemetry at S + 48 hr.

In order to have the TV pictures nest over the crater Alphonsus and to reduce smear to a minimum, it was decided to perform a terminal maneuver. To obtain a larger area of coverage for the initial pictures, the RTC-6 command was to be sent 65 min before impact, initiating TV warmup at I − 20 min. The exact time of the RTC-6 (83:13:03.13) was so adjusted that the last F picture would be taken by the B-camera, capable of three times the magnification of the A-camera. On *Rangers VII* and *VIII*, the final pictures were taken by the A-cameras.

The first pitch turn of the terminal maneuver was +5 deg. This turned the $-y$ side of the TV tower slightly into the Sun, causing the top-hat and lower-shroud temperatures to rise 10°F.

Because of the tradeoff constraints imposed upon the midcourse correction and subsequent trajectory correction, the backup clock would have initiated F-channel operation at approximately I−45 min. As the command link was functional and the terminal maneuver had initiated and verified that the CC&S counter was functional, it was decided to disable the clock by sending an RTC-5 command. The pictures obtained at I−45 would be less in resolution than existing lunar photographs, and thermal limitations might be imposed upon the TV subsystem. Telemetry indicated the clock reset as the clock telemetry indication (point 15-9) returned to zero; the F-channel current decreased to zero, and the F-battery voltage increased by approximately ½ v.

The second pitch turn of the terminal maneuver (−20 deg) caused the $-y$ side of the tower to be placed in shadow, resulting in a drop of the top-hat and lower-shroud temperatures.

Forty-five minutes after the initiation of RTC-6, the CC&S counter, via TV-2, turned both channels into warmup at 20 min, 07 sec before impact. This event was monitored by noting the change from 15 to 90-point telemetry, and was confirmed by a change in points 55 and 60 from 0 to 2.4 v and a change in current level from approximately 0 to 8 amp on Channel F and from 0 to 10 amp on P. The rest of the data received during this warmup period indicated that operation was normal for both channels. The current drain, the battery voltage, and the heat-sink temperature indicated that both channels would be able to operate for the required 20 min, 07 sec. Since the CC&S performed flawlessly, the need to initiate the RTC-7 command, which had been held in readiness, did not arise.

During the terminal period, the temperature on the lens housing increased 10°F as a result of reflected and radiated light energy from the Moon's surface, and was apparently the same as for *Ranger VIII*.

As in *Ranger VIII*, the batteries reached a plateau at −34.8 v for the F- and −34.7 v for the P-channel. The power level dropped to −32.5 v when the high-current demands were placed on the batteries during the terminal phase of the mission. The voltage levels indicated that the batteries were operating under normal load and, together with the predicted usage data (Fig. 47), that they would have at least another 30 min of life remaining at the end of the mission.

Both channels were turned into full-power operation via the internal 80-sec sequencer. This was confirmed by a change in points 55 and 60 from 2.4 to 0.6 v, and a change in current on the F-channel from 8 to 13 amp, and on the P-channel from 10 to 15 amp. At this point, Goldstone Station confirmed the receipt of strong video from both channels. As a result of the terminal maneuver, the

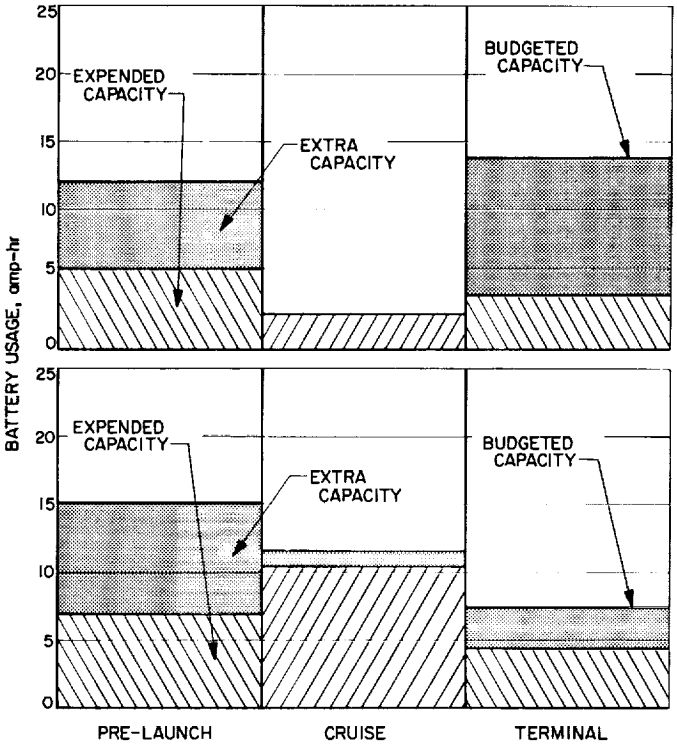

Fig. 47. *Ranger IX* expended and budgeted battery capacity

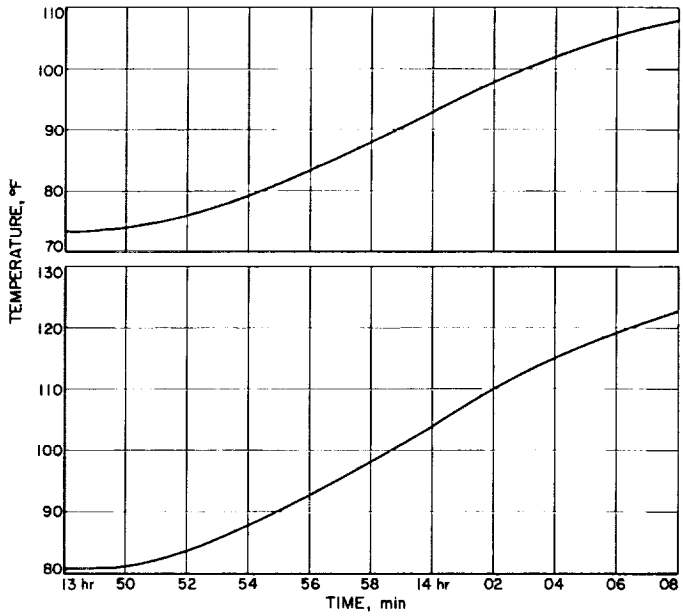

Fig. 48. *Ranger IX* transmitter heat-sink temperatures during terminal phase

pictures nested very well, and all cameras recorded high-quality video photographs.

The CC&S backup command (TV-3) to initiate full power on both channels was timed to occur 50 min after the spacecraft received the RTC-6 command. This event was noted by monitoring a data-encoder blip on the B2-1 channel. Since both TV channels had previously been turned to full power by the internal 80-sec sequencer, the TV-3 command had no effect.

The heat generated by the full-power operation of the TV subsystem caused the drop in temperature on the top hat to be limited to 6°F below nominal. On the lower shroud, the added heat caused the temperature trend to reverse, raising the shroud temperature to 80°, and on the F_B-camera electronics, temperatures rose sharply to 88°F. The battery-temperature increase was due to the high-current drain in the terminal portion of the mission. The transmitter heat-sink temperatures (Fig. 48) exhibited their expected rise. However, the starting temperatures of the F- and P-transmitters differed by 8°. This was caused by uneven heating due to the terminal maneuver's net effect of a change in the orientation of the spacecraft to −15 deg off the Sun-oriented position. This led to a 10° higher final temperature than originally predicted for the F-channel. As a result of the failure of some ground equipment at Goldstone, Channel 8 and the rest of the bus telemetry lost lock for about 1 min, starting at 13:58 GMT. However, since the 90-point information was also transmitted over the 225-kc F-channel, none of the information was lost, and confirmation of proper performance was given by the telemetry during this period.

The TV performance during the *Ranger IX* mission was normal. All operating parameters were within design specification, and all cameras and systems performed perfectly.

The 5,814 pictures gave a nested view of the crater Alphonsus, with good contrast and high shadowing on the final pictures. The resolution on the final F_B, P_1, and P_3 pictures was 0.3 m—the best resolution obtained from any *Ranger* Block III mission.

6. *Ranger IX* Anomalies

One peculiarity that was noted throughout the mission was that the temperatures of the TV subsystem were about 5 to 8°F higher than predicted nominal. However, these temperatures were still well within their overall stabilized limits.

It was noted at Cape Kennedy during spacecraft checkout that the P-battery-case temperature sensor was not in the proper resistance range. Since this point is almost

redundant with point 15-4, the P-battery internal temperature sensor, it was decided to recalibrate rather than change this part. It was anticipated that the higher resistance might be due to a crack in the sensor; therefore, there was a possibility that the launch environment would further change the sensor characteristics and render it useless as a telemetry measure. This became a reality during the actual *Ranger IX* flight, when the sensor gave erroneous readings as compared to the readings on the 15-point telemetry.

V. DEEP SPACE NETWORK SYSTEM

The Deep Space Network consists of the Deep Space Instrumentation Facility, the Space Flight Operations Facility, and the Ground Communications Subsystem.

A. Deep Space Instrumentation Facility

The DSIF is a precision tracking and communications system capable of providing command, control, tracking, and data acquisition for deep-space flight missions. Continuous coverage during missions is provided by locating antennas approximately 120 deg apart in longitude; accordingly, stations are located in Australia and South Africa, as well as in Southern California. The foreign stations are maintained and operated by personnel of cooperating agencies in these countries. A block diagram of the Goldstone Echo Station (DSIF 12), in *Ranger VIII* and *IX* configuration, is presented in Fig. 49.

The DSIF support for *Rangers VIII* and *IX* consisted of permanent stations located at Goldstone, California (DSIF 11 and 12), Woomera, Australia (DSIF 41), and Johannesburg, South Africa (DSIF 51); and a spacecraft monitoring station (DSIF 71) at Cape Kennedy, Florida. Equipment of the five stations is listed in Table 15.

1. Mission Preparation

Prior to the *Ranger VIII* and *IX* missions and their associated operational-readiness testing, a series of calibration and checkout tests were performed at each station. These tests consisted of comprehensive system and subsystem checks to ensure compatibility, reliability, and operator proficiency. Pre-mission tests, designed to exercise the station configuration after modifications partly associated with the *Mariner* Mars mission, were performed at the overseas stations. A series of operational-readiness tests to exercise components of the entire Space Flight System was concluded just prior to launch.

For the *Ranger VIII* and *IX* missions, three DSIF stations — DSIF 11, DSIF 41, and DSIF 51 — converted their RF systems and station configuration to L-band. The conversions for stations 41 and 51 were completed several days prior to the missions, thus allowing tests of the stations prior to launch. However, the conversion at DSIF 11 (employed as a backup reception station in the TV operations) was not scheduled to take place until approximately 6 hr prior to the spacecraft's impact on the Moon. Consequently, no test time was available.

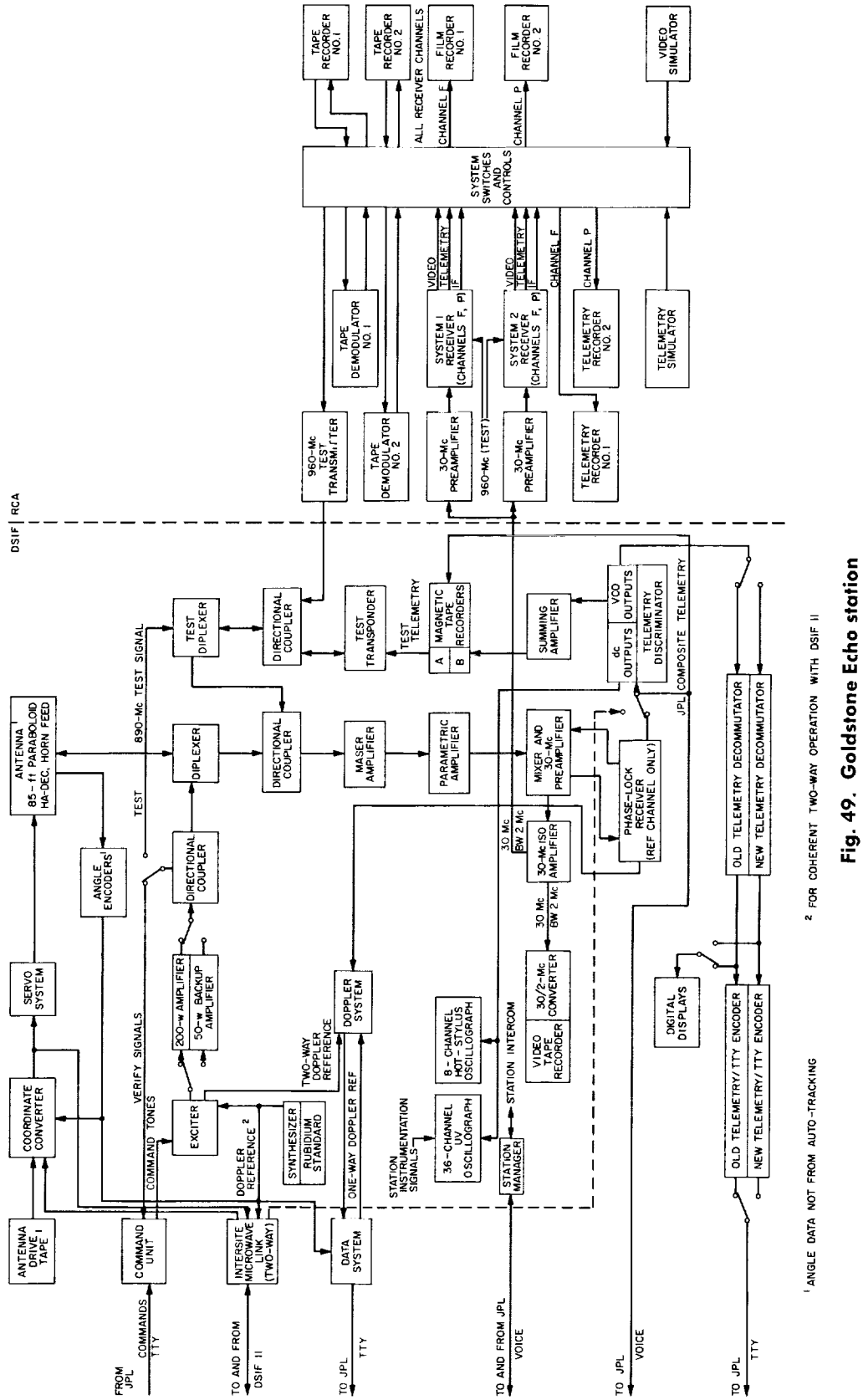

Fig. 49. Goldstone Echo station

Table 15. DSIF L-band master equipment list

Equipment	DSIF stations				
	Goldstone		Australia	South Africa	Cape
	11	12	41	51	71
Antennas					
85-ft paraboloid HA-DEC	O	O	O	O	
10-ft paraboloid Az-El					
6-ft paraboloid Az-El					O
Low-noise amplifiers					
Maser	O	O			
Paramp	O	O	O	O	
Feeds and diplexers					
Tracking feed			O	O	
Horn feed	O	O			
Acquisition aid			O	O	
Dipole					O
Diplexer		O	O	O	O
Receiver					
960-Mc GSDS modified					O
960-Mc GSDS	O	O	O	O	
Transmitter					
50-w backup		O			
10-kw (operated 200 w for Ranger Block III)		O	O	O	
25-w					O[a]
Rubidium standard		O			
Synthesizer		O			
Doppler					
One-way		O	O	O	
Two-way		O	O	O	
Two-way two-station noncoherent		O	O	O	

Equipment	DSIF stations				
	Goldstone		Australia	South Africa	Cape
	11	12	41	51	71
Recording					
Ch. 7 magnetic tape	2	2	2	2	2
Strip chart					
Ch. 36 ultraviolet	O	O	O	O	O
Ch. 8 hot stylus	O	O	O	O	
Acquisition aids					
10-cps modulator		O	O	O	
Mission-oriented equipment					
Command system		O	O	O	
Command interrupt		O			
Telemetry decommutator/ encoder		O	O	O	
Telemetry discriminator		10	10	10	
Prime RCA TV GSE		O			
Secondary RCA TV GSE	O				
JPL TV GSE		O[b]	O	O	
Prime test equipment					
Test transponder	O	O	O	O	O
Closed-loop RF system	O	O	O	O	O
Bit-error checker		O			
Optical star tracker		O			
Miscellaneous					
Intersite microwave	O	O			
Coordinate converter	O	O			

[a]Transmitter used for pre-launch only.
[b]Redundant system backup magnetic-tape converter/FR-800.

During *Ranger VIII* pre-launch countdown, DSIF 51 reported failure of the exciter generator for the prime motor generator, and subtolerance output of the read-write-verify unit. Both were corrected prior to launch. DSIF 41 reported a switch failure in the antenna system during *Ranger IX* pre-launch countdown. The switch was replaced and the system rendered operational prior to launch. There were no such problems experienced during the missions.

2. *Ranger VIII* Tracking

The spacecraft monitoring station (DSIF 71) at Cape Kennedy acquired the spacecraft in two-way lock 42 min before launch for telemetry reception and possible command, at 16:05 GMT on February 17, 1965. RWV modulation was on, and the spacecraft signal level was −90 dbm. At liftoff, the receiver signal level at DSIF 71 was −80 dbm. Except for a momentary dropout at 17:07:21 GMT, DSIF 71 maintained lock until the spacecraft passed over the horizon at 17:12:48. The initial signal level of −80 dbm dropped to −105 dbm by L + 10 sec because of changes in vehicle attitude. As the vehicle rose higher, the level increased to −95 dbm and remained approximately at this point until booster-engine jettison. As in past operations, momentary dropouts were noted at this time. The signal level then decreased gradually to −115 dbm just prior to shroud

separation. An increase to −110 dbm occurred following the normal transients as the shroud moved away from the spacecraft. From this point, the signal decayed gradually to −130 dbm at the horizon.

DSIF 51 at Johannesburg had been instructed to acquire the spacecraft in the two-way mode as early as possible. This was accomplished by turning the transmitter at the station to the 2-w level at 17:27:51, prior to the spacecraft rise above the horizon. The spacecraft transmitter was first acquired at 17:33:30. The signal level at acquisition was reported at −90 dbm. Indications were that it was in two-way lock at that time. The transmitter remained on until 17:51:25, when the decision was made to drop lock momentarily with the spacecraft and reacquire in order to ensure against false lock. The transmitter was turned back on at 17:51:49. Indications were that the spacecraft had been in proper two-way lock throughout the entire period. The tracking data derived from this early period were extremely valuable in generating a high-quality orbit.

At 17:52, DSIF 41 at Woomera acquired the spacecraft transmitter and reported a signal level of −130 dbm. A series of transfers of two-way lock were executed between Woomera and Johannesburg. A momentary drop of lock was experienced in these transfers when the receivers at the stations were switched from the two-way to the three-way mode.

At 21:25, DSIF 51 transmitted the antenna-changeover command (RTC-3). When the spacecraft responded to the receipt of this command, the received signal strength at stations 41 and 51 increased from −115 to −107 dbm.

DSIF 12 at Goldstone acquired the spacecraft in one-way lock at 05:57:29 on January 18 for their first pass. The signal level at acquisition was reported at −140 dbm, but by 06:05:01, it had increased to −109.5 dbm. At 10:00:00, RTC-4 was transmitted to *Ranger VIII*. The stored commands, SC-1, -2, and -3, had been transmitted and verified as correct; both spacecraft and DSIF station operation looked normal. Shortly after the transmission of RTC-4, the signal strength of the spacecraft dropped to a very low level — slightly above threshold. It remained at this level, fluctuating occasionally as high as −155 dbm, until the scheduled time for motor burn, when the signal suddenly jumped to the expected value for the maneuver. This anomaly is discussed elsewhere; analysis of DSIF data indicates that no problems were encountered at the station. The spacecraft continued in a relatively uneventful cruise mode, with acquisitions and transfers at the DSIF stations occurring normally.

As discussed elsewhere in this report, it was decided to send an RTC-6, terminal maneuver, and an RTC-8, attitude-control disconnect, to provide an additional backup turn-on command for the TV subsystem. The RTC-6 was transmitted to the spacecraft at 09:33:09 on February 20, 1965, by DSIF 12.

DSIF 12 was prepared to transmit RTC-7 backup turn-on commands in the event of failure in the spacecraft timing systems. Both F- and P-channel video came on with full power as scheduled, but the RTC-7 was retained in the command system until impact in the event that the television should turn off for some reason. Reception of video at both DSIF 12 (Echo) and DSIF 11 (Pioneer) was of excellent quality, with all systems functioning properly.

3. *Ranger VIII* Tracking Performance

On the whole, the performance of the DSIF stations was excellent. The maintenance of two-way lock to the horizon by DSIF 71 and the early acquisition of the spacecraft by DSIF 51 added considerably to the coverage of the mission. There were, however, the following problem areas.

In the midcourse phase, DSIF 12 experienced drop-locks during the roll and pitch maneuvers. During the maneuvers, the signal level fell drastically and appeared erratic. When this condition occurred, DSIF 12's receiver dropped lock. Throughout the midcourse, the receiver operator made only minor tuning adjustments to follow the predictions in an attempt to reacquire the signal. The records show that the maximum adjustment made of the VCO frequency was 7 cps (or ×30 = 210 cps at 960 Mc).

Each time the spacecraft signal became strong enough for DSIF 12 to acquire, the receiver was relocked — significantly, always on the carrier and not on a sideband. When the spacecraft signal surged back as ignition occurred, the carrier, as well as the telemetry channels, went into lock.

During the mission, signal-level shifts and discrepancies from nominal predictions in downlink occurred. The degrees of variance between the ground-received signal level and predictions were roughly as indicated in Table 16.

The Echo and Johannesburg stations experienced shifts during the third pass. Echo shifted from −117 to −112 dbm, while Pioneer, which was viewing simultaneously,

Table 16. *Ranger VIII*, variance between ground-received signal level and predictions

Station	First pass	Second pass	Third pass
DSIF 51	3 db high at end of pass	4 to 6 db high	4 to 6 db high
DSIF 12	3 db high at start; 2 db high toward end	1 db high	4 db high
DSIF 41	2 to 3 db high	1 to 2 db high	1 to 2 db high

did not experience this shift. Johannesburg had two dropouts. In uplink, at Echo, a shift occurred during cruise after midcourse.

Momentary dropouts were recorded at Johannesburg and Woomera, the L/S-band stations, immediately after changeover from two-way to three-way mode. There were no dropout problems with the L-band stations (Goldstone, Pioneer, and Echo).

4. *Ranger IX* Tracking

Liftoff of the *Ranger IX* space vehicle occurred at 21:37:02 on March 21, 1965. DSIF-71 at Cape Kennedy maintained two-way lock with the spacecraft from prior to liftoff until the vehicle passed below the local horizon at L + 465 sec. The expected momentary dropouts were again noted at booster-engine jettison, followed by a return to normal signal level. The initial signal level at launch of −75 dbm decreased gradually to approximately −130 dbm just prior to loss of signal at the horizon.

DSIF 71 telemetry conditions were very good during the entire launch phase, and no data were lost. Real-time evaluation and subsequent analysis of the spacecraft telemetry indicated proper performance, with no anomalies noted.

DSIF 51 was instructed to acquire while transmitting at the 2-w level in order to provide early two-way tracking data of high quality. Acquisition of the spacecraft in two-way lock was accomplished at 22:01. The signal strength at acquisition was a nominal −93 dbm. DSIF 51 confirmed the acquisition of the Sun and Earth by the spacecraft at their nominal times.

Because of the launch characteristics and the position of injection chosen for this flight, DSIF 41's view of the spacecraft consisted of a relatively short pass low over the horizon. Consequently, the signal strength was quite low (−140 dbm) when the station acquired at 22:52:08. Even though the signal strength was low, two-way transfer was initiated at 00:04 on March 22, and two-way lock was confirmed almost immediately. Because of the low signal level, difficulty was experienced in maintaining lock at both DSIF 41 and DSIF 51, but this was expected.

At 00:25:20, the spacecraft was transferred back to DSIF 51. The RTC-3 antenna-changeover command was transmitted by DSIF 51 at 09:30. A rise in the spacecraft signal level from −122.2 to −109.8 dbm signified a successful antenna changeover.

DSIF 12 acquired the spacecraft for its first pass at 08:24:10. Because of the high accuracy of the launch, it was decided to postpone the midcourse maneuver until Goldstone's second pass. The spacecraft continued in cruise mode, with the only significant occurrence being the transmission of the antenna hinge-angle update command (RTC-2) by DSIF 41 at 22:30.

The midcourse-maneuver sequence was transmitted to the spacecraft during DSIF 12's second pass. The timed RTC-4 procedure was used. This system provides a significant increase in the potential accuracy of the midcourse maneuver. RTC-4 was transmitted by DSIF 12 at 12:03 on March 23. The spacecraft performed the expected maneuver. The DSIF continued tracking *Ranger* in the cruise mode after midcourse until Goldstone's third pass.

Station 12 acquired the spacecraft at 08:51:49 on March 24, and preparations were made both at the SFOF and at Goldstone to transmit the terminal-maneuver commands.

The stored commands, SC-4, -5, and -6, containing the magnitudes of the desired maneuver, were transmitted to the spacecraft. Then RTC-6 was transmitted by DSIF 12 at 13:02:34. The timing of this command to within the nearest second was necessitated by the precision desired in the turn-on of the television subsystem aboard the spacecraft. RTC-5 was transmitted at 13:17 to prevent television turn-on by the TV backup clock.

The television subsystem turned on both channels at the nominal time, and DSIF 12 and 11 began receiving excellent photographs of the lunar surface. However, at approximately −10 min, the DSIF 12 transmitter failed for an unknown reason. This in no way affected the

reception of television pictures, but it did cause a momentary loss in downlink lock from the spacecraft on the telemetry channels. The transmitter was operational 2 min after the failure, but the decision was made not to turn it back on again. As a result, the last 10 min of the flight data was received in one-way lock. Shortly before impact, the spacecraft rose over the DSIF 41 horizon, and that station successfully recorded video tape of the final sequence of the flight.

5. *Ranger IX* Tracking Performance

There were no failures or problems which jeopardized the mission, and few operational difficulties were noted during the mission. System noise-temperature and receiver-calibration thresholds are summarized in Table 17. The following is a station summary of the problem areas encountered during the *Ranger IX* mission.

DSIF 51. At pre-launch, the receiver was reported showing transients on the dynamic phase error. These transients reportedly appeared occasionally but were not of such magnitude as to cause receiver lock drop.

The first portion of the DSIF 51 first pass was marked by doppler data on the order of 4 to 5 times more noisy than nominally acceptable. The cause seems to be fairly well established at this date as being the intermittent noise on the rubidium standard, possibly caused by an overload. When the VCO, the standby rubidium standard, or the synthesizer was used, the doppler data were not marred by excessive noise.

During the first pass, the jitter on the doppler was on the order of 15 to 20 deg, occurring randomly, often at intervals of 30 min or more and lasting about 2 or 3 min. The receiver did not drop lock.

The DSIF 51 receiver anomalies remained a chronic condition in all passes during the mission. Drop of lock began to occur and became increasingly frequent as the mission progressed, particularly during the third pass.

The spacecraft AGC indicated that Johannesburg's uplink power level was on the average 3.5 db in excess of the nominal predictions during the first pass. This was after solar acquisition and when the spacecraft was no longer tumbling. Periodically during the first pass, the uplink power level at the spacecraft was 4 to 5 db above nominal predictions. During the remaining passes, DSIF 51 exceeded nominals on the order of 1.5 to 2.0 db.

In general the received signal level at DSIF 51 during the mission was high relative to nominal predictions, being on the order of +2 to +3.5 db.

DSIF 12. As was the case at DSIF 51, Echo's uplink power to the spacecraft exceeded predicted nominals, particularly during the first pass, when levels of +5 to slightly higher than +6 db above nominal were detected by the spacecraft AGC.

Ten minutes before impact, the transmitter failed. The main power was off, the beam-voltage ready indicator was out, and the 2-min-time-delay light was on. A check of the klystron-filament undercurrent-interlock circuitry was made, and an unsoldered wire was discovered.

When the transmitter failed, a lock drop occurred; however, the downlink was quickly re-established, and no video data were lost. No attempt was made to regain two-way lock so as not to impair video reception in any manner.

Table 17. Station calibration figures

Station	Pass	Calibration system noise temperature, °K		Specification system noise temperature, °K	Calibration receiver threshold, dbm		Specification receiver threshold, dbm
		Pre-track	Post-track		Pre-track	Post-track	
12	1	117	115	110±30	−166	−165	−165±1.5
	2	113	117		−165	−164	
	3	108	110		−166	−166	
41	1	220	230	240^{+25}_{-65}	−162.5	−163.5	−162±1.5
	2	225	230		−162.5	−162.5	
	3	225	220		−162.5	−162.5	
51	1	190	185	240^{+25}_{-65}	−161	−161	−162±1.5
	2	190	185		−161	−161.5	
	3	190	185		−162	−162	

DSIF 41. Woomera experienced receiver VCO difficulties on two occasions. On the first, the receiver was out of lock for approximately 4 min while the VCO module was changed. In the case of the second failure, the receiver was intermittently out of lock over a 4-hr period because of a faulty 30.455-Mc VCO. Changing the VCO module cured the situation.

Uplink power discrepancy. Between passes during the mission, DSIF 12 was instructed to recalibrate output power level. These checks indicated that the station was putting out 200 w, as specified. Further calibration checks after the mission substantiated that calibrations made during the mission had been correct.

DSIF 51 and DSIF 41 were also instructed during the mission to recalibrate their power output. The DSIF 51 measurement indicated 200-w output. In addition to the standard calibration check, Woomera conducted a calorimeter test which indicated that the output power level was actually 148 w.

The spacecraft AGC indicated that the DSIF 41 uplink level was in fairly close agreement with the nominal prediction, running on the average about 0.5 to 1.0 db higher than nominal.

In view of the above conditions, the predicted values are subject to conjecture.

B. Space Flight Operations Facility

The SFOF is located at JPL, in Pasadena, California. It utilizes operations control consoles, status and operations displays, computers, and data-processing equipment as tools in the analysis of spacecraft performance and space science experiments, and communication facilities to control space-flight operations.

1. Facility

The SFOF included a display system, a gallery for observers, television output of certain cameras with an audio status line for an internal/external laboratory information system, access control and facility security, standby maintenance personnel support, standby room for operations personnel, bunkroom, and technical-area assistants and support for the Spacecraft Data Analysis Team (SDAT) and the Flight Path Analysis and Command (FPAC) group.

One facility failure occurred two hours before the *Ranger VIII* launch. This was the failure of the No. 2 diesel generator, which was repaired in 1½ hr. Several minor display-equipment failures were corrected in near-real time during the mission.

In an effort to improve electrical system reliability, the SFOF performed a complete facility checkout between the *Ranger VIII* and *IX* missions. The checkout was accomplished on March 8, 9, and 10, during DSIF 51's *Mariner IV* view period, while the station was converting from the S- to L-band configuration and hence was not tracking. The system had not been thoroughly checked out previously because of the heavy operation schedule. Numerous small problems experienced in the past, some of which could cause considerable trouble during the critical periods of a mission, motivated this action.

The performance of the SFOF in support of the *Ranger IX* mission was effective, with all requirements being met. During this mission, the Television Ground Data-Handling System was used for the first time for display of real-time spacecraft television in the SFOF and on commercial television. Figure 50 shows the mission-status board with real-time video displayed.

The SFOF provided a secure area for the analysis of the lunar television pictures by the Space Science Analysis and Command (SSAC) group and the *Ranger* experimenters for two weeks after the conclusion of each flight.

2. Central Computing Complex

The central computing complex consisted of two IBM 7094 computers, three IBM 1401 computers, an SC-4020 plotter, a PDP-1 computer, the Telemetry Processing Station, and the personnel required to operate and maintain the equipment.

During the days prior to the *Ranger VIII* and *IX* launches, the complex executed a launch-checkout sequence of events which included testing and shakedown of both software and hardware. The completion of the checkout indicated a state of mission readiness for the complex.

In general, all computer programs performed well during the missions. The orbit-determination and trajectory-computation effort was very satisfactory, and all scheduled tasks were completed. The computation of the midcourse- and terminal-maneuver commands proved to be excellent. Real-time display of raw and converted engineering telemetry data, including television subsystem data, was supplied to the Spacecraft Performance

Fig. 50. *Ranger IX* video displayed in real time in SFOF

Analysis Area by the PDP-1 computer and the Telemetry Processing Station. Bulk processing, in the form of printed listings and plots, of engineering telemetry data on the IBM 7094's was satisfactory, although more computer time was consumed than had been anticipated.

The few problems which occurred with the computers and associated equipment were minor and caused little or no delay to the operations because quick repair and/or duplicate or backup hardware capabilities were kept available.

Post-flight processing of tracking and telemetry data began immediately after completion of the missions.

3. Communications Center

The performance of the Communications Center during the flights was quite effective. The communications failures experienced within the SFOF were due to terminating apparatus only, and were of a type and quantity well within normal expectations. Mechanical failures of teletype equipment, tubes, and semiconductors and minor technical adjustment problems constituted all of these malfunctions.

C. Ground Communications Subsystem

The DSN Ground Communications Subsystem consisted of voice, normal and high data-rate teletype circuits provided by the NASA world-wide communications network between each overseas DSIF station and the SFOF; teletype and voice circuits between the SFOF, Goldstone stations, and Cape Kennedy; and a microwave link between the SFOF and Goldstone. The ground-communications-net configuration for the *Ranger VIII* and *IX* missions is shown in Fig. 51.

During the *Ranger VIII* mission, a major failure occurred 5 hr after launch, when nine of the 14 circuits to JPL were lost. This disrupted all but the analog circuit to the Cape, and all but the voice circuit to Johannesburg. The problem, caused by a dug-up coax cable in the Los Angeles area, fortunately occurred during a noncritical phase of the mission. The lost circuits apparently were in the same cable, reflecting a lack of the diversity which the common carriers were to provide.

Prior to *Ranger VIII* launch, the circuits had been interrupted by carrier testing. This could have been a

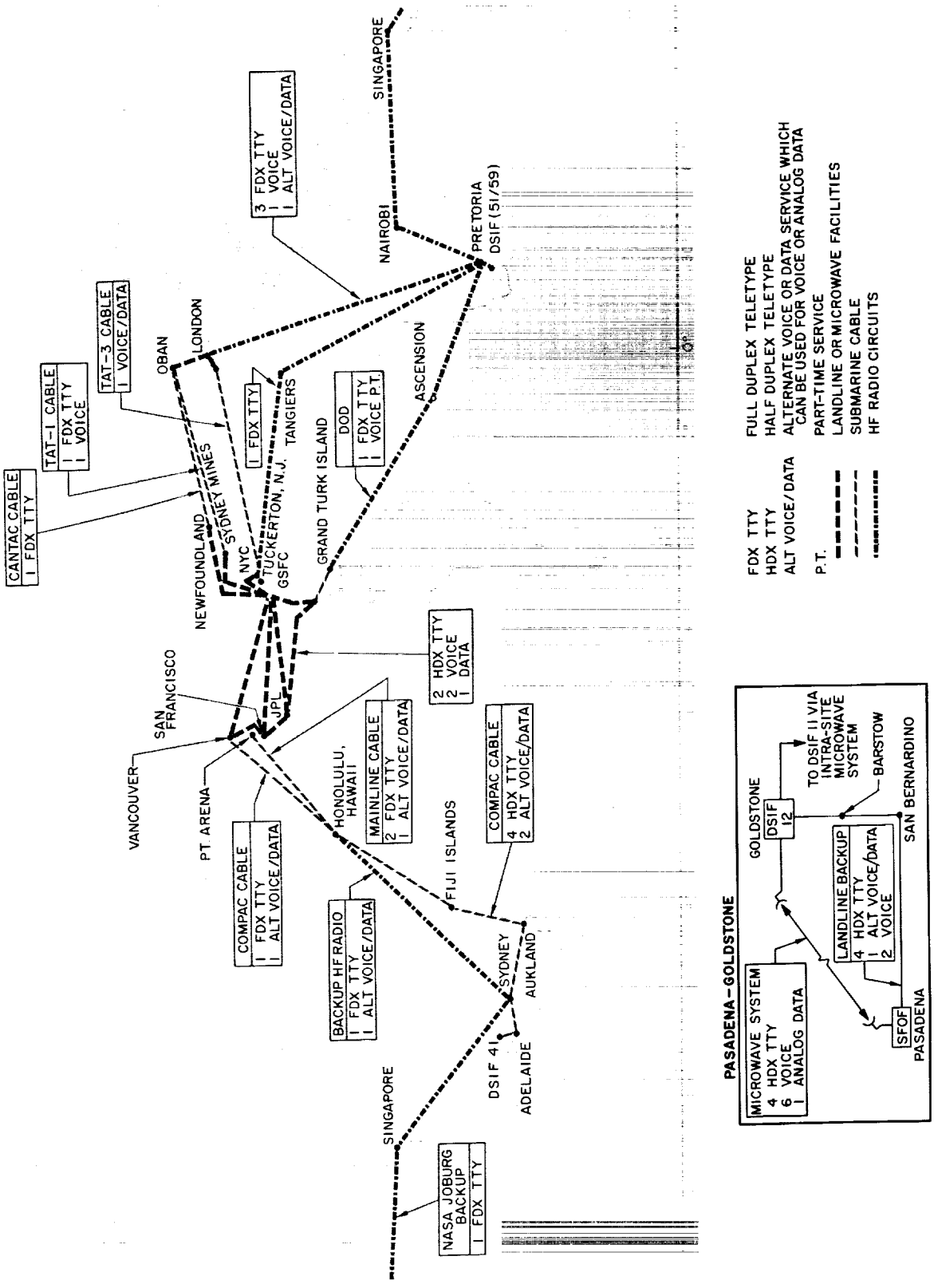

Fig. 51. DSN ground communications

serious problem during the mission, reducing the time available in establishing system contact, and consequent operational status.

Teletype circuits to Johannesburg performed fairly well, with poor radio propagation comprising the major cause of circuit outage. The poor conditions had been expected, as radio-propagation quality is normally inferior during the first quarter of the year.

There were a few nonpropagation failures of lengthy duration — primarily the result of equipment failures at the London Radio Terminal and at RCA, New York. Equipment failures and land-line carrier failures in the Pretoria, South Africa, area, although small in number, caused an appreciable loss of operational time on the teletype circuits.

The teletype circuits to Woomera, Australia, operated exceedingly well despite the fact that they were relatively new and unproven circuits. The small number of outages that did occur on these circuits were caused by equipment failures at the Honolulu and Sydney Radio Terminals.

Voice and analog circuits to DSIF 41 were 100% reliable; there were no outages attributable to circuit problems during the entirety of the Woomera view periods.

Failures of hardware used for communication with the SFOF were limited to vacuum tubes, fuses, semiconductors, diodes, and mechanical maladjustments. All failures were within normal expectations, and loss of circuit times was held to a minimum.

VI. SPACE FLIGHT OPERATIONS SYSTEM

The function of the Space Flight Operations System is to perform those operations on the ground during the flight that are required to achieve the mission objectives. These operations include determining the trajectory of the spacecraft, defining and performing corrections to the trajectory, obtaining and evaluating telemetry from the spacecraft, transmitting required command functions to the spacecraft, and receiving and recording the spacecraft video signals. To fulfill these functions, the Space Flight Operations System makes use of the operational groups required to direct the mission, the tracking nets (AFETR and DSIF) required to obtain tracking and telemetry data from the spacecraft and to transmit commands to the spacecraft, the Earth-based communications between all groups, and the data-processing and computing facilities required to support the operation.

A. Spacecraft Data Analysis Team

It is the responsibility of the SDAT to monitor and analyze the operation of the spacecraft, and to recommend corrective action to be taken in the event of nonstandard spacecraft performance. Fortunately, the near-nominal spacecraft performance of both *Ranger VIII* and *Ranger IX* precluded the necessity for a full exercise of SDAT capabilities. Section IV includes portions of the report of this group.

B. Flight Path Analysis and Command Group

It is the responsibility of the FPAC group to determine the trajectory of the spacecraft and the required midcourse and terminal maneuvers. The functions required of this group were all executed satisfactorily. Section VII presents portions of the FPAC report.

C. Space Science Analysis and Command Group

It is the responsibility of the SSAC group to recommend the aiming points and evaluate the picture quality expected under the mission conditions. No problems were encountered in executing this function. Section VIII presents portions of the SSAC report.

VII. FLIGHT PATH

A. Ranger VIII

The *Ranger VIII* flight commenced with liftoff at 17:05:00.795 GMT, February 17, 1965, from Cape Kennedy, Florida, and culminated in impact at 09:57:36.756, February 20, in the southern portion of Mare Tranquillitatis, some 24 km from the aiming point. A midcourse maneuver was employed to refine trajectory accuracy, but a terminal maneuver to adjust camera angles was judged unnecessary.

1. Launch Phase

After liftoff, the booster rolled to an azimuth of 95.4 deg and pitched as programmed until booster cutoff. During the *Atlas* sustainer and vernier phases, ground guidance was used to adjust cutoff altitude and velocity. Completion of *Agena* first burn left the *Agena*/spacecraft combination in a near-circular southeasterly parking orbit at an altitude of 188 km and an inertial speed of 7.80 km/sec. After a 12.83-min orbital coast, *Agena* second burn was initiated, lasting 87 sec.

2. Cruise Phase

Injection occurred at 17:27:37, over the western coast of South Africa, at geocentric coordinates of 2.35° N, 9.11° W. The *Agena* and spacecraft were at an altitude of 205 km and traveling at an inertial speed of 10.941 km/sec. The *Agena*/spacecraft combination never entered the Earth's shadow. The *Agena* separated from the spacecraft 2 min, 37 sec after injection, then performed a programmed yaw maneuver and ignited its retrorocket. The retrorocket impulse was designed to eliminate interference with the spacecraft operation and reduce the chance of the *Agena* impacting the Moon. Tracking data indicated that the *Agena* passed the upper trailing edge of the Moon at an altitude of 15,825 km about 6 hr after *Ranger VIII* impact.

Sun acquisition had been initiated at injection. After 12 min, 33 sec the Sun was acquired. Within an hour after injection, the spacecraft was receding from the Earth in almost a radial direction with decreasing speed. This reduced the geocentric angular rate of the spacecraft (in inertial coordinates) until, at 1.5 hr after injection, the angular rate of the Earth's rotation exceeded that of the spacecraft. This caused the Earth track of the spacecraft (Fig. 52) to reverse its direction from increasing to decreasing Earth longitude.

3. Midcourse Maneuver

Three gross factors bound a midcourse maneuver: target location, time of flight, and spacecraft capability.

Prior to the flight, *Ranger VIII*'s selected impact site had been designated as the "most desirable" target for the launch day of February 17. Several of the factors leading to this choice are presented in Fig. 53, which shows the portion of the Moon available to impact in terms of the initial flight conditions.*

The criterion of solar illumination of the impact site led to the choice of the zone between 50 and 80 deg from the subsolar point. In order to avoid loss of Earth lock by the Earth sensor, the Earth/probe/near-limb angle was limited to a minimum of 15 deg, which resulted in selection of a region within 75 deg of the sub-Earth point. The intersection of these two regions, for the February 20, 1965, encounter, determined the general desirable impact area for that date.

Within that general area, a number of specific sites were identified as being of particular combined interest to the *Ranger* experimenters and the *Apollo* Project, and one site—that eventually chosen—as best. Similar selections were made for the other days of the period.

Orbit determinations early in the course of the mission identified the uncorrected trajectory to be well within the midcourse-correction capability to reach the desired area. In addition, analysis of the probable dispersion resulting from orbit-determination and midcourse-execution errors indicated a low risk in reaching the near vicinity of the best site.

Transit time from injection to encounter on the uncorrected trajectory was 66.456 hr. The TV-camera backup clock had been set prior to launch to turn on the

*For convenience, these parameters are presented in a plane defined by the miss parameter **B**. This parameter is nearly a linear function of changes at injection conditions, and is defined as the vector from the target's center of mass normal to the incoming asymptote of the osculating conic at closest approach to the target body. $\mathbf{S}_i$ is defined as a unit vector in the direction of the incoming asymptote. In the plane normal to $\mathbf{S}_i$, referred to as the **B**-plane, the unit vector **T** is parallel to the plane of the true lunar equator, and **R** completes a right-hand orthogonal system to describe **B**. This technique is rigorously described in JPL External Publication No. 674 (August, 1957), by W. Kizner.

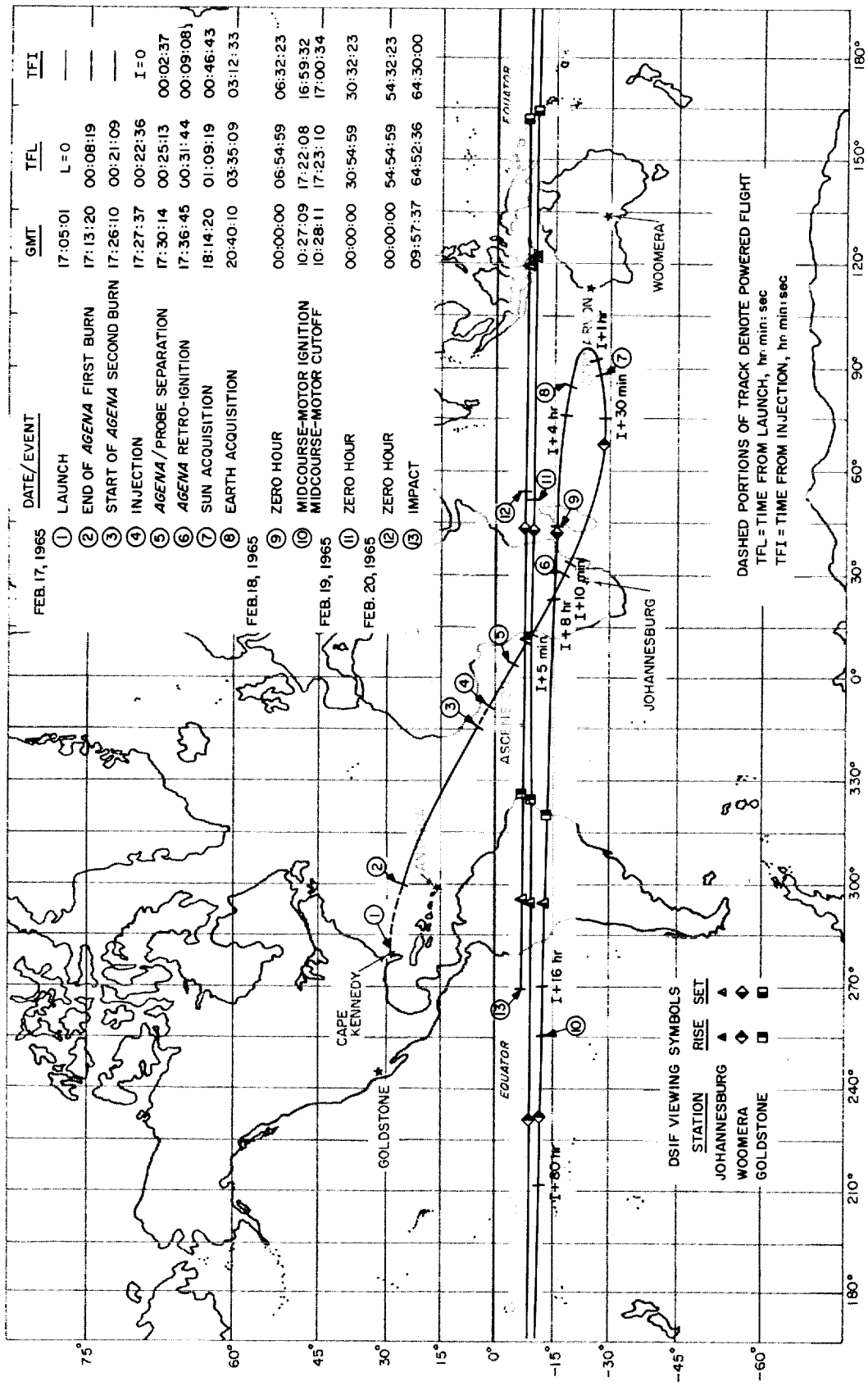

Fig. 52. *Ranger VIII* trajectory Earth track

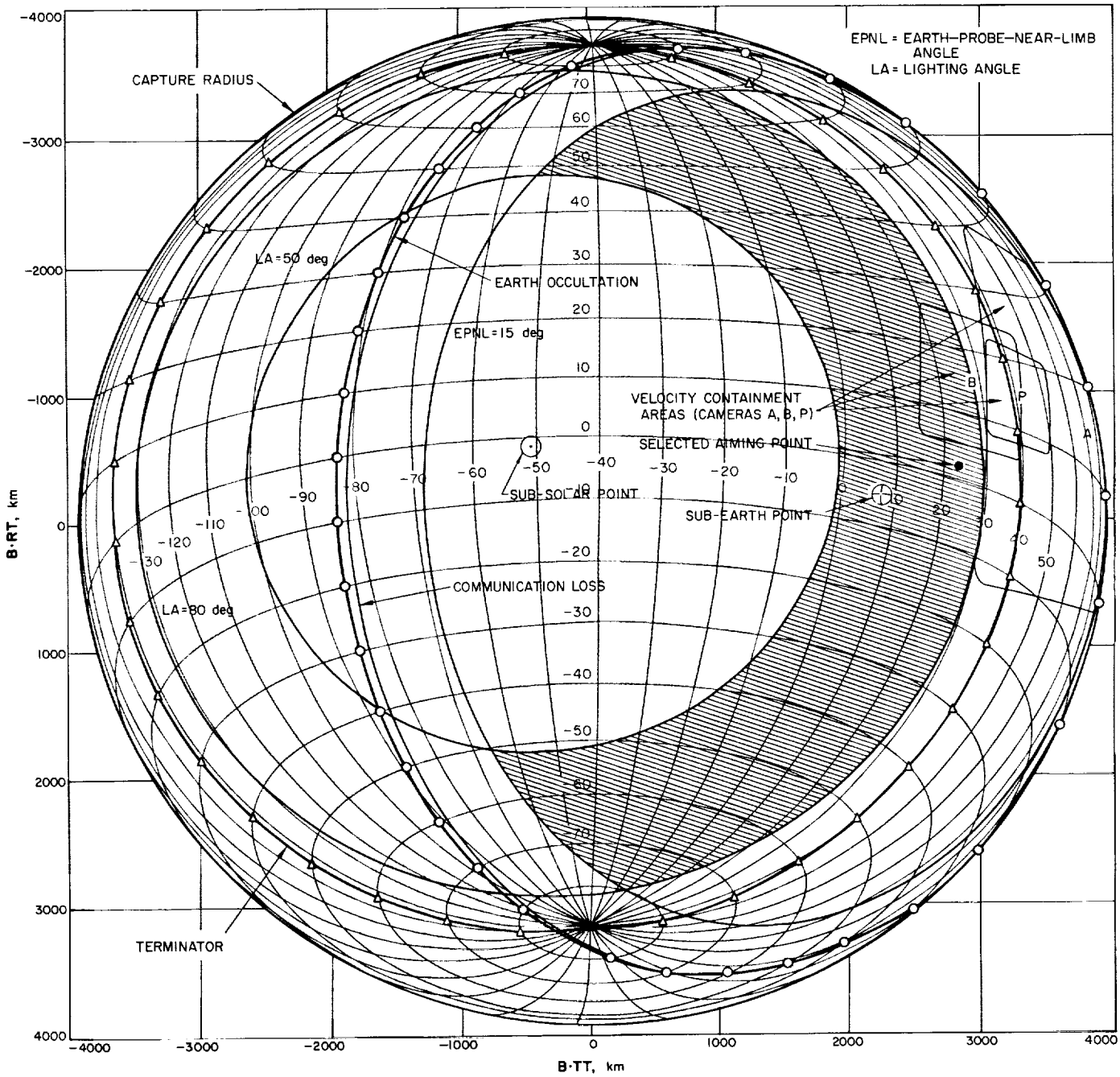

Fig. 53. *Ranger VIII* midcourse-maneuver and site-selection factors

F-cameras 64.313 hr after injection, and the use of this mechanism was considered desirable to enhance mission reliability.

The preferred clock turn-on time was to be between 10 and 30 min prior to impact. Flight-time corrections to realize these turn-on times required midcourse-maneuver roll and pitch sequences which would cause loss of some telemetry channels due to the tracking stations passing through or near the nulls in the omnidirectional-antenna radiation pattern. Further analysis determined that the loss in telemetry would be less serious for the maneuvers resulting in turn-on times less than 30 min prior to impact. However, early turn-on times yield a larger picture coverage because of the greater distance between the spacecraft and the lunar surface. A compromise was made between loss in telemetry and overall picture coverage: the flight time was to be reduced by 1.962 hr in order that the F-camera backup turn-on time be 12 min prior to impact.

The selected midcourse maneuver required the spacecraft to roll 11.60 deg, pitch 151.75 deg, and then burn its motor to slow down the spacecraft by 36.44 m/sec. (The maximum velocity-change capability of the motor was 60.9 m/sec.)

The pre- and post-midcourse trajectories near the Moon and the impact sites are shown in Fig. 54.

The midcourse motor was ignited at 10:27:09 GMT on February 18, 1965, at which time the spacecraft was at a geocentric distance of 169,039 km and traveling with an inertial speed of 1.811 km/sec relative to Earth. At the end of a 59-sec burn duration of the midcourse motor, the geocentric distance had increased to 169,148 km and the inertial speed relative to Earth to 1.840 km/sec. Telemetry data received at the Goldstone tracking station gave positive indication that the midcourse maneuver and motor burn had been executed precisely. This was further verified by the observed doppler data being essentially the same as predicted.

4. Post-Midcourse Cruise

Following the midcourse maneuver, the spacecraft reacquired the Sun and Earth, thus returning to the cruise mode. At about 59 hr from injection and at a geocentric distance of 359,000 km, the spacecraft inertial speed relative to the Earth reached a minimum value of 1.012 km/sec. At this point, the spacecraft was about 31,800 km from the lunar surface, with an inertial speed of 1.31 km/sec relative to the Moon. Because of the lunar gravitational field, the spacecraft velocity then began to increase.

Post-midcourse tracking data reduced within 1 hr after impact were analyzed, and resolved the lunar encounter conditions to a high degree of accuracy, with impact to occur at 2.71° N latitude and 24.81° E longitude, after a flight time from injection of 64.500 hr. The encounter conditions along with the corresponding post-midcourse initial conditions are presented in Table 18.

5. Encounter

During the encounter, the spacecraft was subjected to increasing acceleration due to the pull of the lunar gravity field.

At 1 hr before impact, the speed relative to the Moon had increased to 1.621 km/sec, and the spacecraft was at a lunar altitude of 6154 km.

The spacecraft approached the Moon in direct motion along a hyperbolic trajectory, with the incoming asymptote direction at an angle of 13.59 deg to the lunar equator and the orbit plane inclined 16.06 deg to the equator. About 3 min before impact, the spacecraft crossed the lunar equator at an altitude of 2037 km. At 09:33:08.5 GMT, F- and P-channel warmup was verified. At 09:34:30, at an altitude of 4250 km above the lunar surface, full power on both channels was verified. At 09:57:36.756 on February 20, 1965, *Ranger VIII* crashed onto the southern portion of Mare Tranquillitatis at an impact speed of 2.651 km/sec and at a path angle of −41.7 deg.

B. Ranger IX

The *Ranger IX* flight path began with liftoff at Cape Kennedy at 21:37:02.456 GMT, March 21, 1965, and ended with impact at 14:08:19.999, March 24, in the crater Alphonsus, 4.4 km from the aiming point. To achieve this accuracy, the midcourse trajectory-refining maneuver was delayed until the second Goldstone pass. For the first time, a terminal maneuver was used to align the central camera axis along the impact velocity vector.

1. Launch Phase

After liftoff, the booster rolled to an azimuth of 94.3 deg and performed a programmed pitch maneuver until booster cutoff. During sustainer and vernier stages, adjustments in vehicle attitude and engine-cutoff times were commanded as required by the ground guidance computer to adjust the altitude and velocity at *Atlas* vernier-engine

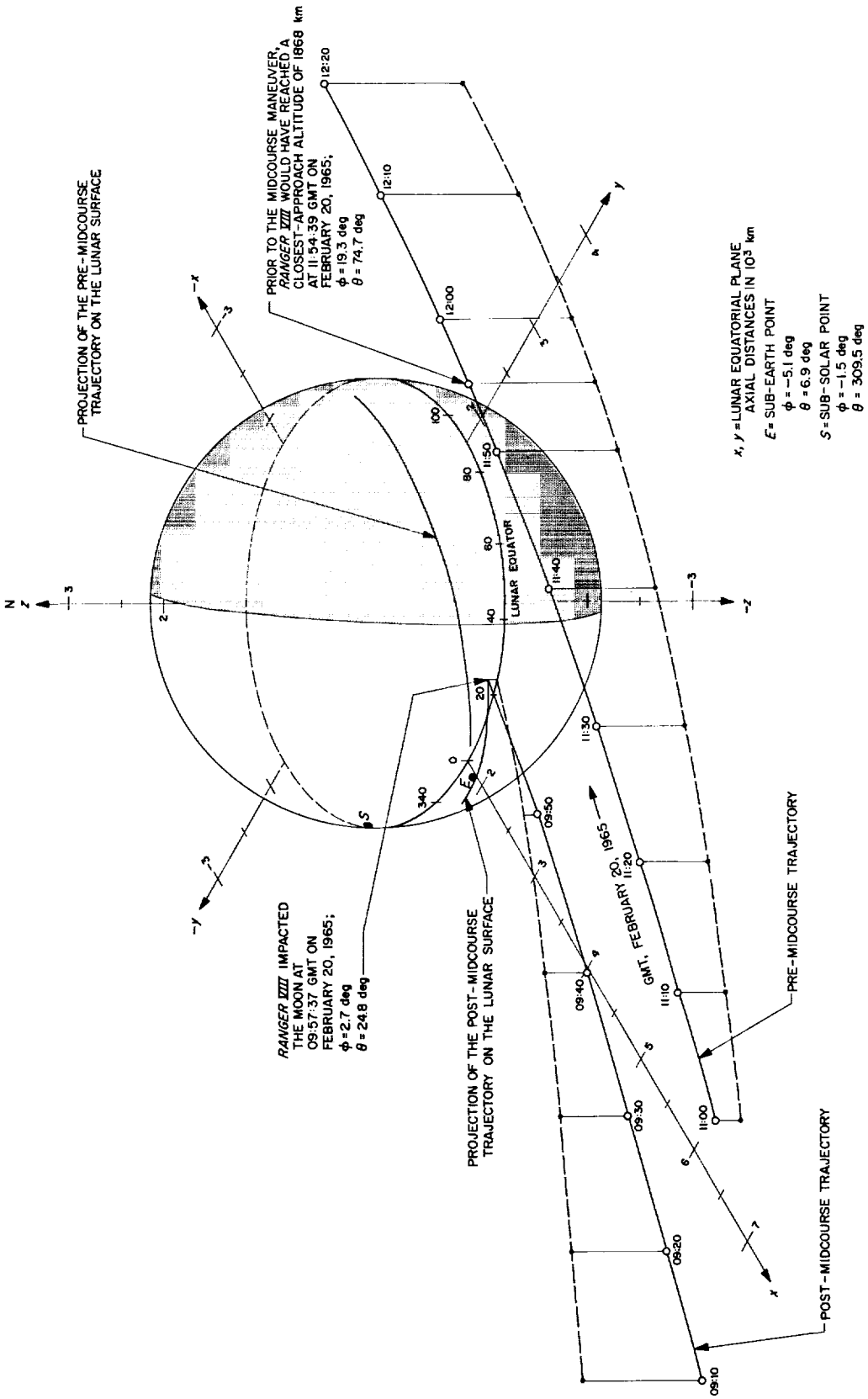

Fig. 54. *Ranger VIII* pre-midcourse and actual lunar encounters

Table 18. *Ranger VIII* pre- and post-midcourse orbits

Parameter[a]	Injection	Post-midcourse
Epoch	17:27:37, February 17, 1965	10:28:08, February 18, 1965
Earth-fixed sphericals		
R	6583.1948 km	169142.90 km
ϕ	2.3530941 deg	−12.683817 deg
θ	350.89155 deg	255.09762 deg
V	10.523490 km/sec	11.803385 km/sec
γ	1.7277902 deg	8.7308957 deg
σ	119.97585 deg	270.97074 deg
Inertial cartesians		
x	5018.6690 km	−154760.64 km
y	4251.8658 km	−57264.116 km
z	270.29093 km	−37138.819 km
$\dot{x}$	−5.7934230 km/sec	−1.5522736 km/sec
$\dot{y}$	7.6624908 km/sec	−0.96692909 km/sec
$\dot{z}$	−5.2380550 km/sec	−0.20057075 km/sec

[a]See *Definition of terms*.
[b]For pre-midcourse or injection conditions, encounter was flyby at altitude shown; after midcourse, encounter was impact at location indicated.
[c]1-σ uncertainty, 5.1 sec.
[d]1-σ uncertainty, 0.1 sec.

Parameter[a]	Injection	Post-midcourse
Orbital elements		
a	288489.38 km	300051.42 km
e	0.97719987	0.97889288
i	28.808329 deg	30.732920 deg
Ω	224.55678 deg	222.54946 deg
ω	171.74995 deg	173.49243 deg
ν	3.3623356 deg	161.06173 deg
Encounter conditions[b]		
Closest-approach epoch	11:54:38.397, February 20	9:57:37.18, February 20
Selenocentric altitude	1867.9459 km	
Selenocentric latitude	19.326950 deg	2.7129144 deg
Selenocentric longitude	74.723510 deg	24.806900 deg
Time of flight from injection	66.456 hr[c]	64.500 hr[d]
$\lvert\mathbf{B}\rvert$	6335.8717[e] km	2909.4591[f] km
$\mathbf{B}\cdot\mathbf{T}$[g]	6137.6450 km	2876.3865 km
$\mathbf{B}\cdot\mathbf{R}$[g]	−1572.4450 km	−437.43943 km

[e]1-σ uncertainty, 12.3 km.
[f]1-σ uncertainty, 8.6 km.
[g]$\mathbf{B}\cdot\mathbf{T}$ and $\mathbf{B}\cdot\mathbf{R}$ are referenced to the true lunar equator (Fig. 53). (For *Ranger VIII* work, the true lunar equator is used as the reference plane. If $\mathbf{N}$ is a unit vector in the lunar north direction, then $\mathbf{T}=\mathbf{S}_i\times\mathbf{N}$ and $\mathbf{R}=\mathbf{S}_i\times\mathbf{T}$.)

Definition of terms

R Spacecraft radius distance, km
ϕ Spacecraft geocentric latitude, deg
θ Spacecraft east longitude, deg
V Spacecraft Earth-fixed velocity, km/sec
γ Path angle of probe Earth-fixed velocity vector with respect to local horizontal, deg
σ Azimuth angle of probe Earth-fixed velocity vector measured east of true north, deg
x, y, z Vernal equinox cartesian coordinates in a geocentric equatorial system, km (The origin is the center of the central body. The principal direction (x) is the vernal equinox direction of date, and the principal plane (x, y) is the Earth equatorial plane of date; z is along the direction of the Earth's spin axis of date.)
$\dot{x}, \dot{y}, \dot{z}$ First time derivatives of x, y, and z, respectively (i.e., cartesian components of the probe space-fixed velocity vector), km/sec
a Semimajor axis, km
e Eccentricity
i Inclination, deg
Ω Longitude of ascending mode, deg
ω Argument of pericenter, deg
ν True anomaly, deg

cutoff. After first burn of the *Agena* engine, the *Agena*/spacecraft combination was placed in a nearly circular parking orbit in a southeasterly direction, at an altitude of 188 km and an inertial speed of 7.80 km/sec. After an orbit coast time of 2.97 min, determined by the ground guidance computer and transmitted to the *Agena* during the *Atlas* vernier stage, a second ignition of the *Agena* engine occurred. Eighty-six seconds later, the *Agena* was cut off, with the *Agena*/spacecraft combination in a nominal Earth–Moon transfer orbit.

2. Cruise Phase

Injection took place at 21:49:48 over the Atlantic Ocean, at a geocentric latitude and longitude of 20.53°N and 42.32°W, respectively. The *Agena* and spacecraft were at an altitude of 197 km and traveling at an inertial speed of 10.967 km/sec. Thirty-four seconds after injection, the *Agena*/spacecraft combination entered the Earth's shadow. The *Agena* separated from the spacecraft 2 min, 38 sec after injection, then performed a programmed yaw maneu-

ver and ignited its retrorocket. Tracking data indicated that the *Agena* passed the upper trailing edge of the Moon at an altitude of 5353 km about 5 hr after *Ranger IX* impact.

The spacecraft left the Earth's shadow 34 min, 19 sec after injection, after a total shadow duration of 33 min, 45 sec. Sun acquisition had been initiated prior to that time and was accomplished 57 min, 42 sec after the spacecraft left the Earth's shadow. Within an hour after injection, *Ranger IX* was receding from the Earth in an almost radial direction with decreasing speed. This reduced the geocentric angular rate of the spacecraft (in inertial coordinates) until, at 1.5 hr after injection, the angular rate of the Earth's rotation exceeded that of the spacecraft. As a result, the Earth track of the spacecraft (Fig. 55) reversed its direction from increasing to decreasing Earth longitude.

3. Midcourse Maneuver

Prior to the flight, *Ranger IX*'s selected impact site had been designated as the "most desirable" target for the launch day of March 21. Several of the factors leading to this choice are presented in Fig. 56, which presents the portion of the Moon available to impact in terms of the initial flight conditions* for the March 24, 1965, encounter.

Within that general area, a number of specific sites were identified as being of particular interest to the *Ranger* experimenters, and one site was eventually chosen as best. Similar selections were made for the other days of the period.

Orbit determinations indicated an extremely accurate injection, with a flight path which would have resulted in a lunar impact 1693 km from the target specified to the

*For convenience, these parameters are presented in a plane defined by the miss parameter **B**. This parameter is nearly a linear function of changes at injection conditions and is defined as the vector from the target's center of mass normal to the incoming asymptote of the osculating conic at closest approach to the target body. $\mathbf{S}_t$ is defined as a unit vector in the direction of the incoming asymptote. In the plane normal to $\mathbf{S}_t$, referred to as the **B**-plane, the unit vector **T** is parallel to the plane of the true lunar equator, and **R** completes a right-hand orthogonal system to describe **B**. This technique is rigorously described in JPL External Publication No. 674 (August, 1957), by W. Kizner.

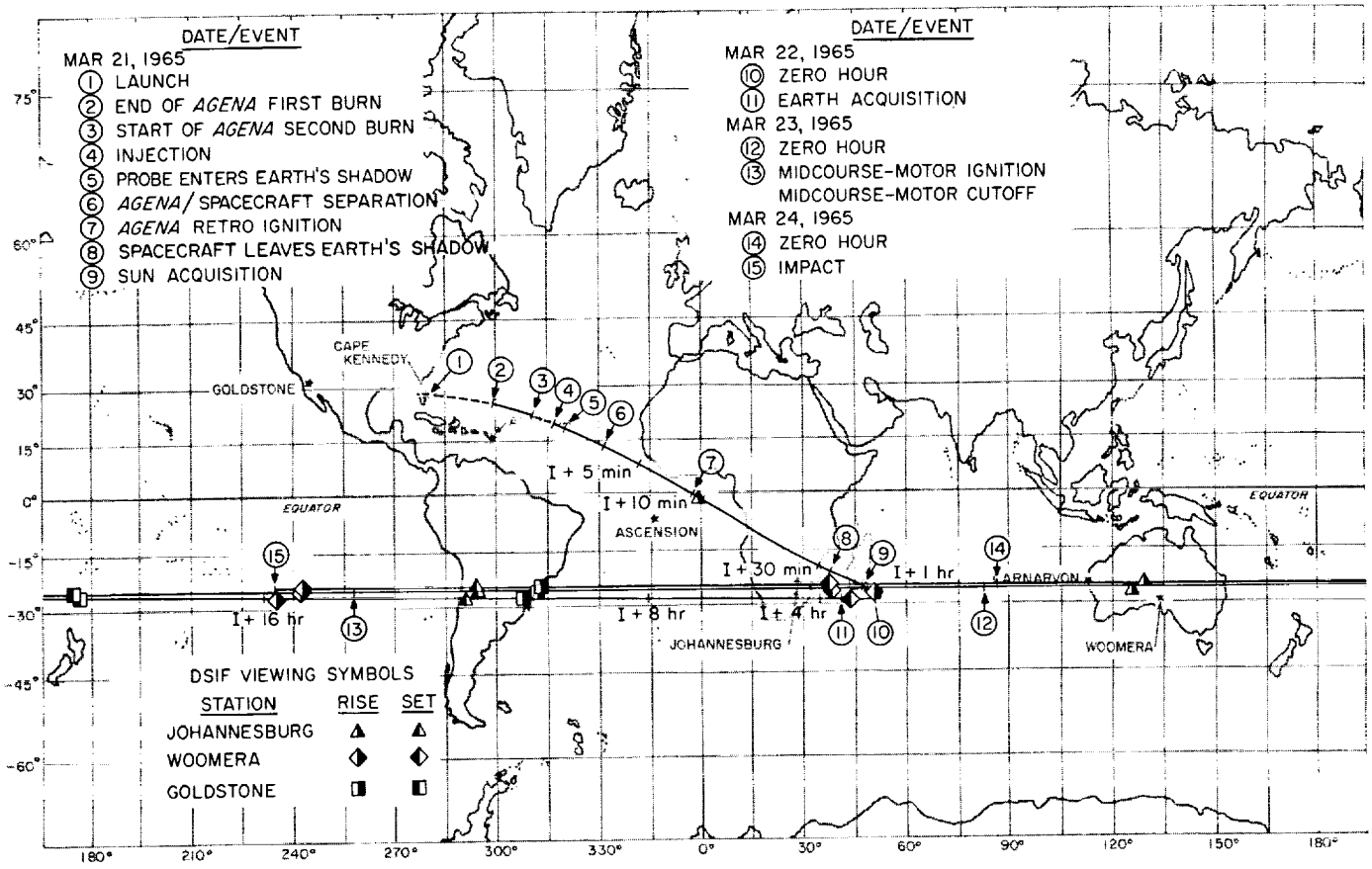

Fig. 55. *Ranger IX* trajectory Earth track

launch vehicle and only 520 km north of the primary aiming point of the crater Alphonsus. The particular location within Alphonsus of 13.0°S latitude and 2.5°W longitude was chosen to provide camera coverage of the crater rim and the central peak while maintaining a low probability of impacting in the shadow of the central peak.

Maneuver analyses determined that the midcourse maneuver could have been performed on either the first (L + 17 hr) or second (L + 39 hr) Goldstone pass, with little difference in the dispersions at the aiming point due to midcourse-execution errors. On the other hand, the additional multistation tracking data available for a second

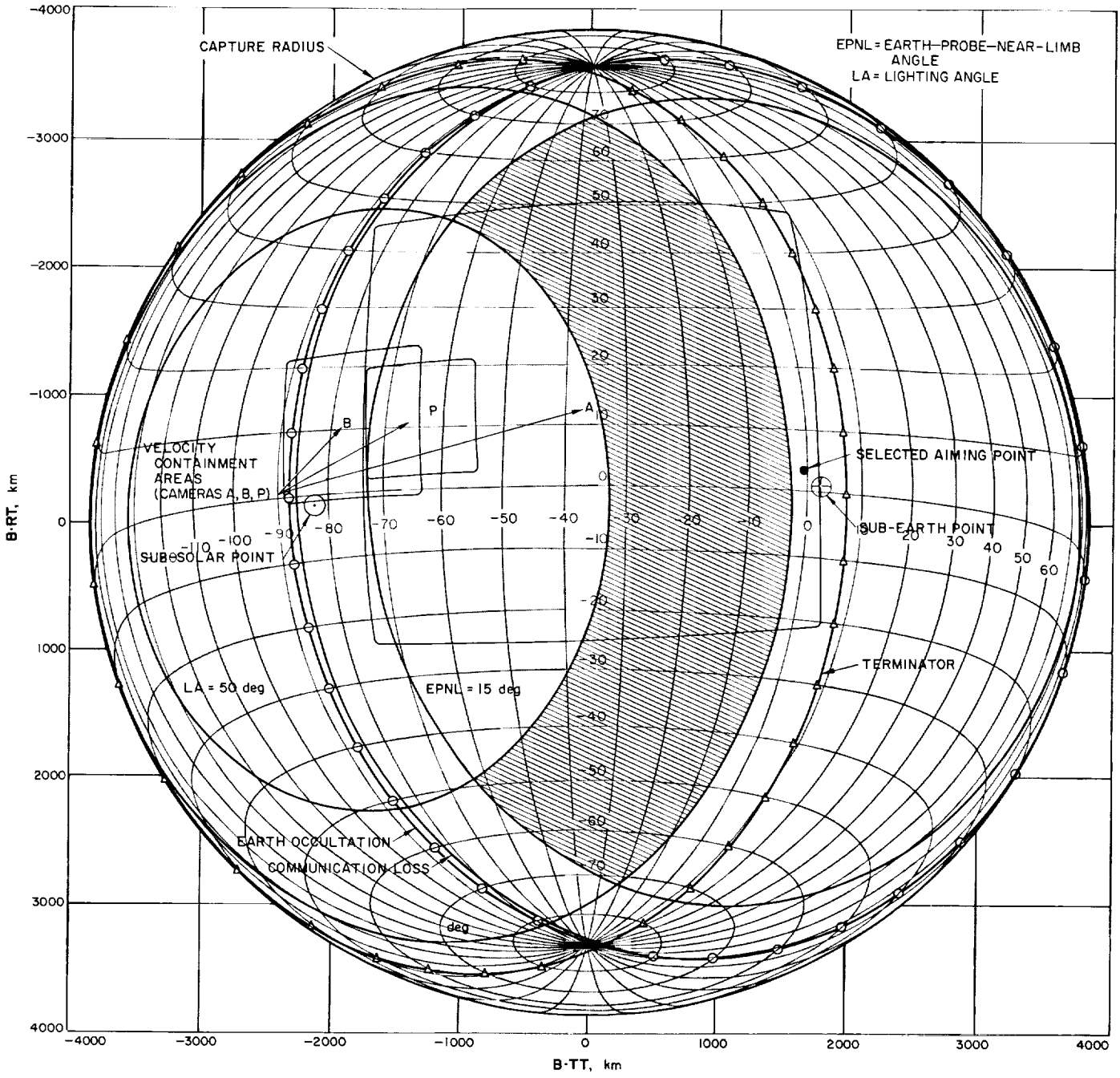

Fig. 56. *Ranger IX* midcourse-maneuver and site-selection factors

Goldstone pass maneuver would provide a decrease in the orbit uncertainty and might uncover any obscure tracking-data discrepancies. Because of the accuracy required for the selected target and the fact that no other factors considered indicated a degradation in final results, the second Goldstone pass maneuver was selected.

The flight time of *Ranger IX* was to have been adjusted so that impact would occur 30 min after the backup clock turned on the F-channel cameras. The maneuver required to achieve the impact point and the desired flight time, however, would have violated the nominal antenna constraint angle of 40 deg. Because of the particular antenna radiation patterns and the rotations to be performed by the spacecraft, the number of channels and the time spent by each in the antenna nulls could be reduced by modifying the maneuver to yield different flight times. Several maneuvers for varying arrival times were computed; each was examined in detail for expected telemetry loss.

The overall analysis determined that longer flight times would result in less serious loss of telemetry, smaller dispersions at the target due to maneuver-execution errors, and longer TV running times. In order to realize the smaller dispersions at the target and improve the telemetry recovery, a longer flight time was selected, for which the backup clock would turn on the F-channel 45 min prior to impact. This TV running time was taken as a reasonable upper limit. Once the terminal maneuver had been initiated, the backup clock could be inhibited from turning on the TV at I − 45 min. This would leave two means of TV turn-on at the more desirable I − 17 to 20 min: the clock in the CC&S (started at initiation of the terminal maneuver) and an RTC-7. The desired flight time from injection was to be reduced from 64.618 to 64.309 hr.

The selected midcourse maneuver required the spacecraft to roll −27.41 deg, pitch +127.96 deg, and then burn its motor to increase the speed of the spacecraft by 18.15 m/sec. (The maximum velocity-change capability of the motor was 60.09 m/sec.)

The pre- and post-midcourse trajectories near the Moon and the impact sites are shown in Fig. 57.

The midcourse motor was ignited at 12:30:09 on March 23, 1965, at which time the spacecraft was at a geocentric distance of 291,014 km and traveling with an inertial speed of 1.308 km/sec relative to Earth. At the end of a 31-sec burn of the midcourse motor, the geocentric distance had increased to 291,054 km and the inertial speed relative to Earth to 1.319 km/sec. Telemetry data received at the Goldstone tracking station gave positive indication that the midcourse maneuver and motor burn had been executed precisely. This was further verified by the observed doppler data being essentially as predicted.

4. Post-Midcourse Cruise

Following the midcourse maneuver, the spacecraft reacquired the Sun and Earth, thus returning to the cruise mode. At about 58 hr from injection and at a geocentric distance of 373,336 km, the spacecraft inertial speed relative to the Earth reached a minimum value of 1.120 km/sec. At this point, the spacecraft was about 33,625 km from the lunar surface, with an inertial speed of 1.336 km/sec relative to the Moon. Because of the lunar gravitational field, the spacecraft velocity then began to increase.

Post-midcourse tracking data were analyzed and resolved the lunar-encounter conditions to a high degree of accuracy, with impact to occur at 12.91°S latitude and 2.38°W longitude after a flight time from injection of 64.524 hr. The encounter conditions, along with the corresponding post-midcourse initial conditions, are presented in Table 19.

5. Terminal Maneuver

For the first time in *Ranger* Block III, an active terminal maneuver was performed to change the spacecraft orientation. The nominal maneuver, which aligned the central camera axis along the impact velocity vector, was chosen from among a number of alternatives.

The predicted impact point was so close to the aiming point that the pre-launch maneuver analysis was generally valid. Conditions prior to the terminal maneuver are given in Fig. 58. The **A**- and **B**-vectors represent the axes of cameras F_A and F_B; the **C**-vector represents the central axis of the four P-cameras. The impact velocity vector is represented by **V**. In this geometry, the impact velocity of 2.669 km/sec and 2-msec shutter speed of the P-cameras would result in motion blurring of 2.2 m, considerably greater than the desired final resolution.

The nominal terminal maneuver would align the **C**-vector parallel to the **V**-vector, and the motion blurring would be essentially eliminated. With the resulting spacecraft orientation, the central peak of Alphonsus would remain in the field of view of the A-camera until the last few frames, and the east wall and the dark-haloed craters nearby would be viewed by the B-camera at relatively close range.

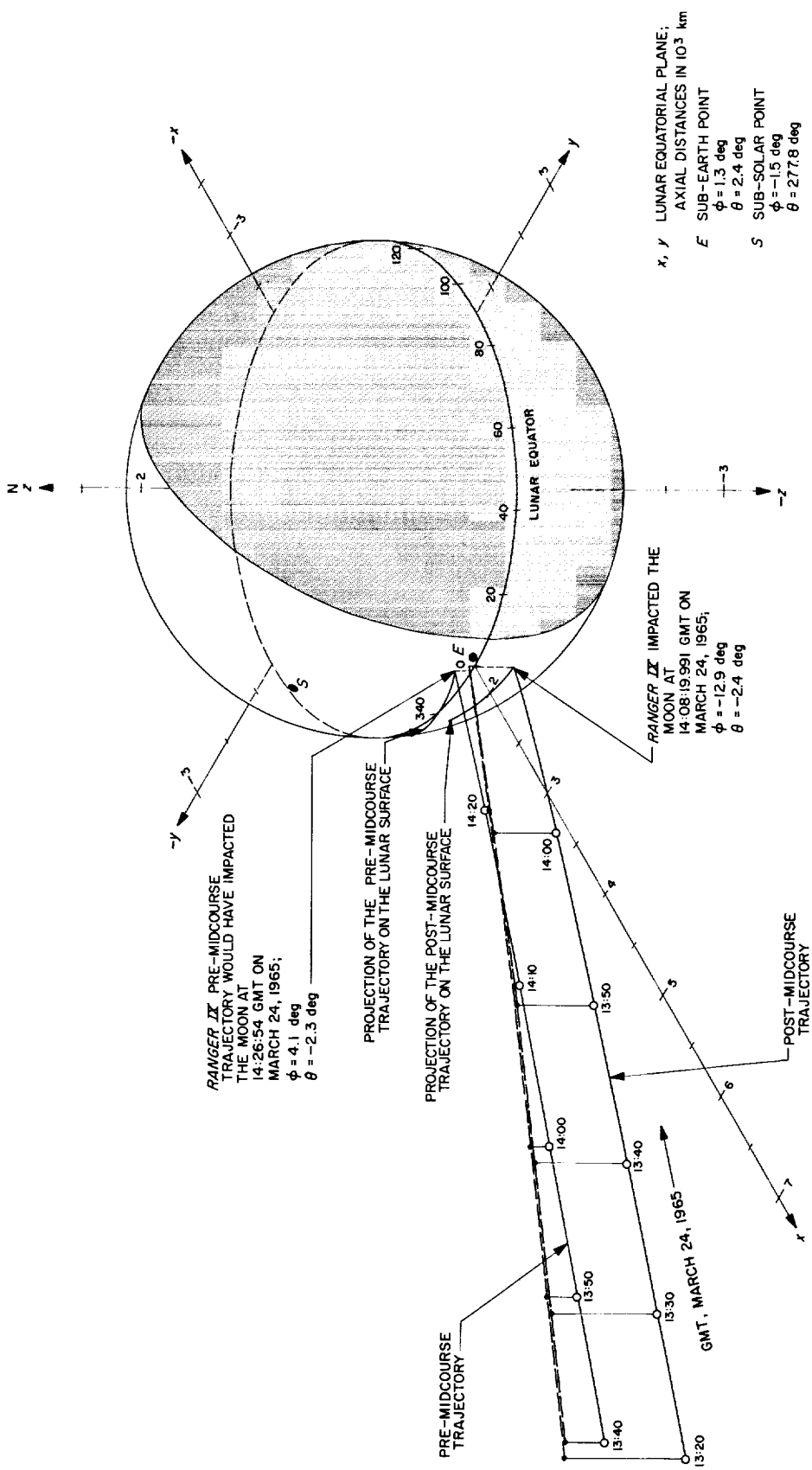

Fig. 57. *Ranger IX* pre-midcourse and actual lunar encounters

Table 19. *Ranger IX* pre- and post-midcourse orbits

Parameter[a]	Injection	Post-midcourse
Epoch	21:49:48, March 21, 1965	12:30:38, March 23, 1965
Earth-fixed sphericals		
R	6578.4000 km	291051.08 km
ϕ	20.525267 deg	−28.382973 deg
θ	316.68299 deg	257.32602 deg
V	10.547199 km/sec	18.994623 deg
γ	1.6968853 deg	3.9208555 deg
σ	111.00130 deg	270.15758 deg
Inertial cartesians		
x	−1418.9946 km	−19401.815 km
y	5989.3706 km	−262237.06 km
z	2304.4179 km	−124763.90 km
$\dot{x}$	−10.386731 km/sec	0.13595686 km/sec
$\dot{y}$	−0.79848218 km/sec	−1.2091069 km/sec
$\dot{z}$	−3.4289787 km/sec	−0.50967493 km/sec
Orbital elements		
a	392638.81 km	399059.45 km
e	0.98327464	0.98571852
i	28.461476 deg	28.343391 deg
Ω	327.00969 deg	327.36181 deg
ω	129.34037 deg	128.28277 deg
ν	3.2915287 deg	167.17228 deg
Impact parameters		
Impact epoch	14:26:53.735, March 24, 1965	14:08:19.652, March 24, 1965
Selenocentric latitude	4.1388701 deg	−12.914655 deg
Selenocentric longitude	357.72987 deg	357.61885 deg
Time of flight from injection	64.618 hr[b]	64.524 hr[c]
$\mathbf{B}$	1689.8286 km[d]	1613.6942 km[e]
$\mathbf{B}\cdot\mathbf{T}^{r}$	1628.5745 km	1561.0405 km
$\mathbf{B}\cdot\mathbf{R}^{r}$	−450.84979 km	408.85372 km

[a]See Table 17 for definition of terms.

[b]1-σ uncertainty of 3.087 sec.

[c]1-σ uncertainty of 0.668 sec.

[d]1-σ uncertainty of 10.271 km.

[e]1-σ uncertainty of 9.988 km.

[f]$\mathbf{B}\cdot\mathbf{T}$ and $\mathbf{B}\cdot\mathbf{R}$ are referenced to the true lunar equator (Fig. 53). (For *Ranger IX* work, the true lunar equator is used as the reference plane. If $\mathbf{N}$ is a unit vector in the lunar north direction, then $\mathbf{T}=\mathbf{S}_1\times\mathbf{N}$ and $\mathbf{R}=\mathbf{S}_1\times\mathbf{T}$.)

6. Encounter

During the encounter, the spacecraft was subjected to increasing acceleration due to the pull of the lunar gravity field.

The spacecraft approached the Moon in direct motion along a hyperbolic trajectory, with the incoming asymptote direction at an angle of −5.59 deg to the lunar equator and the orbit plane inclined 15.67 deg to the equator.

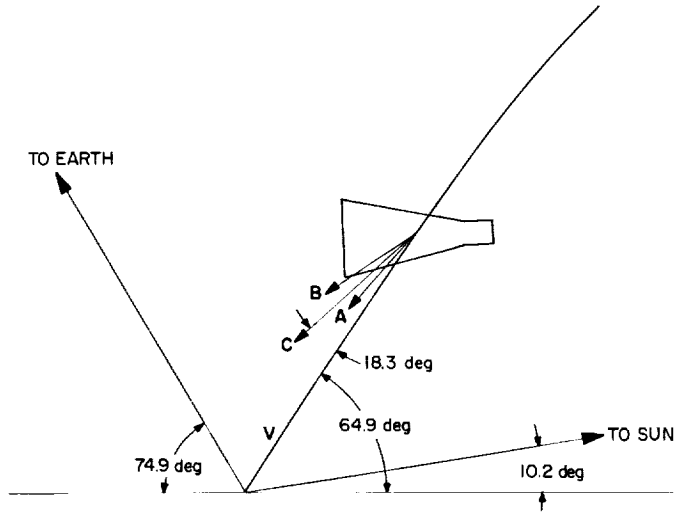

Fig. 58. *Ranger IX* terminal-maneuver approach geometry

The standard terminal maneuver in which the camera reference direction is aligned along the impact velocity vector was selected as the best camera viewing orientation. This maneuver not only minimized the image motion in the pictures but resulted in very desirable coverage of the points of scientific interest within Alphonsus.

At 65 min, 46 sec before impact the terminal-maneuver sequence was initiated. The speed relative to the Moon had increased to 1.606 km/sec, and the spacecraft was at a lunar altitude of 7211 km.

To align the camera reference direction along the impact velocity vector, the spacecraft was commanded to pitch +5.20 deg, yaw −16.30 deg, and pitch back again −20.50 deg, all the while keeping the high-gain antenna pointed toward the Earth. At the completion of the second pitch turn 37 min, 3 sec prior to impact, the speed had increased to 1,758 km/sec, and the spacecraft had dropped to an altitude of 4360 km.

F and P full power was verified at an altitude of 2376 km, 18 min, 27 sec prior to impact. At 14:08:19.999 on March 24, 1965, *Ranger IX* crashed into the center of the crater Alphonsus at a speed of 2.671 km/sec and a path angle of −64.9 deg.

VIII. SPACE SCIENCE ANALYSIS

A. Target Selection and Terminal Maneuver

1. *Ranger VIII*

In selecting an aiming point for *Ranger VIII*, it was necessary to consider the results of *Ranger VII* and the number of remaining launches in the *Ranger* series, as well as the interests of the *Apollo* and *Surveyor* programs. The *Ranger VII* impact yielded high-resolution data of a mare with slightly reddish coloring (subsequently named Mare Cognitum). In several meetings prior to the launch of *Ranger VIII*, the following objectives for the mission were decided upon:

1. Obtain pictures of a "blue" mare, preferably in Mare Tranquillitatis.
2. Impact near the equator so as to be of maximum benefit to the *Apollo* Project.
3. Impact nearer the terminator than did *Ranger VII* so as to increase the scene contrast.

The first day of the launch period, February 17, 1965, could fulfill all the desired objectives and therefore was chosen as the prime launch day. On the basis of the expected light levels, and recalling the very successful midcourse maneuvers of *Rangers VI* and *VII*, it was further decided that the impact point should be about 15 deg from the terminator. Thus, the impact point of 3° N latitude and 24° E longitude was chosen as the primary target point for the February 17 launch date, and a midcourse maneuver was performed to correct the injection trajectory achieved by the *Atlas/Agena* so that the spacecraft would impact this target.

Two terminal maneuvers and the no-maneuver case were investigated to determine the best orientation of the cameras for their picture-taking sequence. Even though the image motion would be rather large (approximately 1.2 m) and would be the predominant degrading factor in the last two to three P-camera pictures, the experimenters gave a scientific recommendation not to perform a terminal orientation of the cameras. Their recommendation was based upon four considerations:

1. The no-maneuver choice provided a large picture trace across the lunar surface prior to impact. This coverage would allow grouping of pictures from different cameras of the same lunar area into stereo pairs and thus provide high-resolution stereo mapping of the lunar surface.
2. Without a terminal maneuver, higher-resolution photographs of the highland region bounding the edge of Mare Tranquillitatis could be obtained than with either maneuver.
3. The no-maneuver case provided a larger photometric phase angle and less oblique views of the surface.
4. The greater area coverage just prior to impact possible without the maneuver would increase the likelihood of viewing some interesting phenomena of the lunar surface.

2. *Ranger IX*

With the success of *Rangers VII* and *VIII*, it was decided that the last *Ranger* mission, *Ranger IX*, should be utilized to investigate an area of special scientific interest. No sites suitable for this purpose could be chosen for the original first two launch days, so the first launch day was rescheduled for March 21, 1965. The target area was the crater Alphonsus, long considered one of the most interesting lunar features because of gaseous emissions observed near the central peak and the dark-haloed craters near the northeast, southeast, and west wall areas. Even though this target was only 10 deg from the terminator, the highland material of which it appears to be composed has a reflectance of nearly twice that of the mare surfaces and thus sufficient scene brightness to allow excellent photography.

Because of the precise injection, only a small trajectory correction was needed to impact in Alphonsus. So as to specify the pre-midcourse trajectory more accurately, the midcourse maneuver was delayed until the second Goldstone pass. The small trajectory correction, in turn, enabled a more specific selection of the impact area. As a result, the pre-launch aiming point was shifted northeast of the central peak of Alphonsus. This new aiming point potentially would yield high-resolution photography of the east wall, and dark-haloed craters in the northeast and the central peak, while avoiding the possibility of landing in the shadow cast by the peak which had existed with the original aiming point.

Two terminal maneuvers plus the no-maneuver case were examined to decide the best orientation of the cameras for their picture-taking sequence. The nominal maneuver, in which the central axis of the camera system is aligned along the velocity vector at impact, was found

to be far superior to the other maneuvers. It would not only reduce image motion to a minimum but would yield photographs of the central peak down to the fourth-from-the-last A-camera frame. In addition, the dark-haloed craters near the northeast wall and the wall itself would be recorded in the last 10 to 15 B-camera frames. The coverage of these last 20 A- and B-camera pictures is shown in Fig. 59.

B. Camera Performance

The camera performance was excellent for both the *Ranger VIII* and *IX* missions. Only one significant change had been introduced following the *Ranger VII* mission. The video gain was adjusted on the f/2 cameras so that the peak signal acceptable was reduced from 2700 to 1500 ft-L. This change was made because of luminance information received from *Ranger VII* and a desire to aim closer to the terminator for increased contrast. The peak signal level of the f/1 cameras remained 650 ft-L.

The terminal resolution on *Ranger VIII* was limited by image motion to about 1.5 m. On *Ranger IX*, the terminal resolution was determined by the altitude of the final exposure. The P_3- and B-cameras were exposed at nearly the same altitude and yielded resolutions of approximately 0.4 m.

1. *Ranger VIII*

At the time of camera turn-on, the A-camera was pointing nearly 60 deg from the terminator, while the B-camera was pointing 41 deg from the terminator. The high Sun angle reduced contrast and increased the average brightness to such a degree that the f/1 cameras were saturated in the highland regions. These effects had been anticipated, however, and there was no expectation that the early pictures from the f/1 cameras would be of any value. The early f/2 camera photographs, while providing some information, were also of little value because of the low surface contrast. As the picture-taking sequence progressed, the illumination decreased while contrast was increasing, and progressively better photographs were yielded. During the last several minutes, the picture quality was very good.

There were a number of internally generated noise sources which disturbed the photographs. The most serious were the 15-kc interference on the F-cameras and microphonics on the P_2-camera. The microphonics increased in amplitude as the system temperature increased and became severe near the end of the mission. These effects had been present during the pre-flight testing and can be nearly eliminated by computer processing.

Camera focus appeared somewhat improved over that of *Ranger VII* as a result of the techniques developed subsequent to that flight. Cameras P_1 and P_2 appeared to have soft focus, but this effect was caused by the lower sensitivity of the cameras. Cameras P_3 and P_4 were four times more sensitive than P_1 and P_2, while A and B were, respectively, eight and two times more sensitive.

2. *Ranger IX*

The *Ranger IX* cameras had been improved somewhat over those of *Rangers VII* and *VIII*, mainly in the reduction of vidicon shading and electrical interference. These improvements, in conjunction with the high scene contrast obtained from the near-terminator impact and highland-type terrain, resulted in very high-quality pictures throughout the sequence. The performance of the *Ranger IX* cameras in some instances exceeded the design goals and no anomalies were noted. As was the case with *Ranger VIII*, the improved focusing techniques proved effective, and image quality was improved over that of *Ranger VII*.

C. Preliminary Photometric Results

Approximately 2 weeks prior to launch, each of the *Ranger VIII* and *IX* cameras was calibrated at Cape Kennedy. This calibration included an extended field light-source test series in which several scenes of constant luminance were imaged through the camera system and recorded on magnetic tape. The magnetic tapes are used to convert the camera-system output voltages during the mission to lunar scene luminances. This process is performed most accurately by use of digital-computer techniques; however, preliminary evaluations can be obtained by use of the mission 35-mm film and the calibration tapes, which were replayed onto the mission film at Goldstone immediately after impact. In the preliminary results presented here, a densitometer was used for the film data reduction.

1. *Ranger VIII* Photometric Results

The A-camera on *Ranger VIII* made an extensive survey across the surface of the Moon. Included in the first photographs was Mare Cognitum; later, Mare Nubium to the right of Guericke and, finally, Mare Tranquillitatis were photographed.

Figure 60 shows the predicted mare luminance values that would be observed by the A-camera on *Ranger VIII*

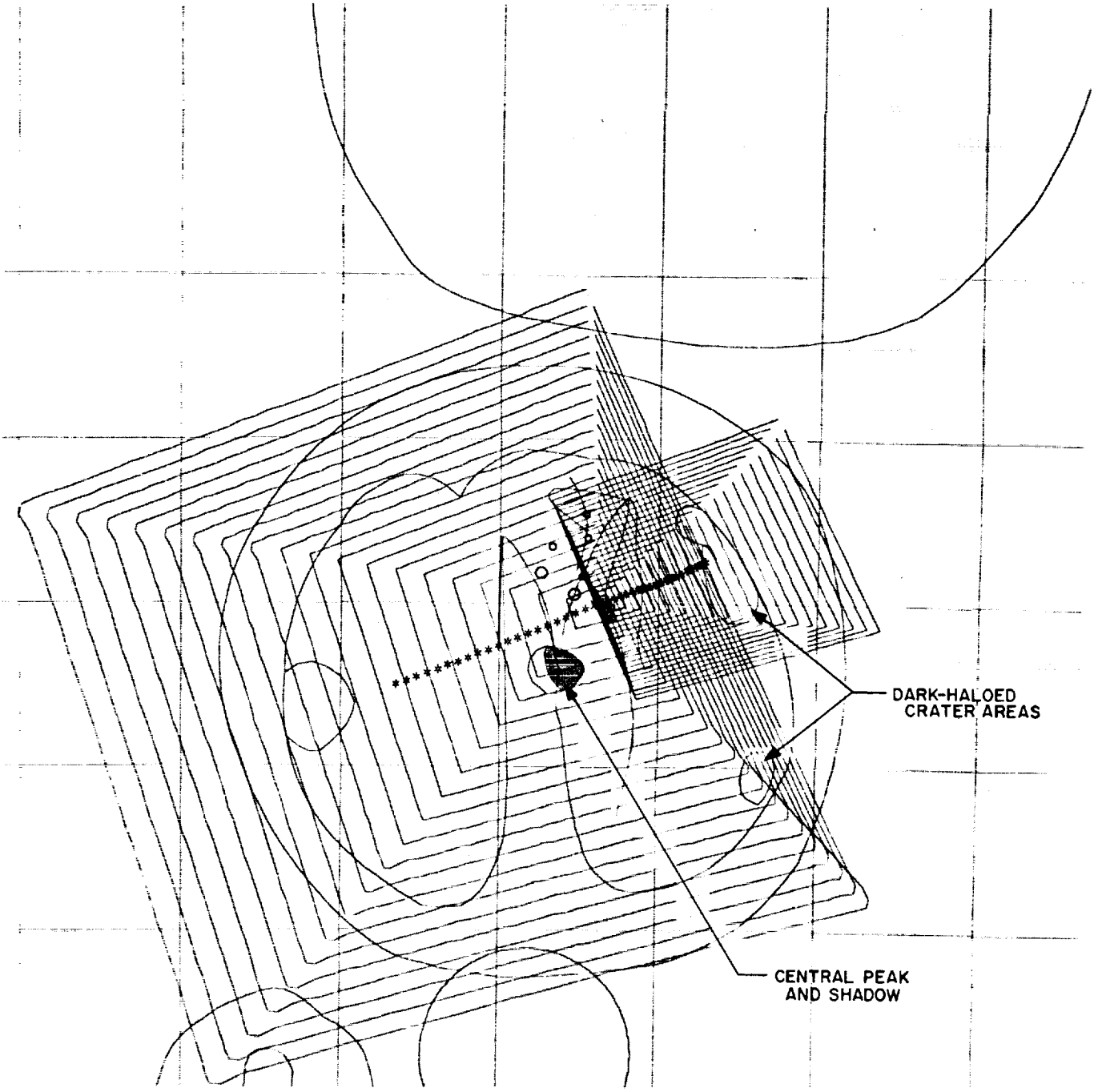

Fig. 59. *Ranger IX* A- and B-camera coverage, last 20 frames

during its descent. The angle α is the luminance longitude. These predicted values were obtained from a lunar reflectance function, which is a single function applied as an average for all mare areas. The camera transfer function is given in Fig. 61. Superimposed on Fig. 60 are data points obtained from the mission 35-mm film in the areas of Cognitum, Nubium, and Tranquillitatis.

Assuming that the theoretical function is correct, except for an amplitude adjustment, one would conclude from Fig. 60 that Mare Cognitum and Mare Nubium have a greater full-Moon albedo than Tranquillitatis. Both Cognitum and Nubium are classified as "red" maria, while Tranquillitatis is a "blue" or dark mare. Thus, Tranquillitatis is generally assumed darker than the other two maria, and the A-camera data appear consistent with this assumption. A shift in amplitude of the theoretical curve certainly appears to fit the Tranquillitatis data for one scale value, and the Cognitum and Nubium data for another value.

Results from cameras P_3 and P_4 for the Tranquillitatis region, however, give luminance values closer to those predicted, so that a more thorough investigation using the digital techniques is indicated.

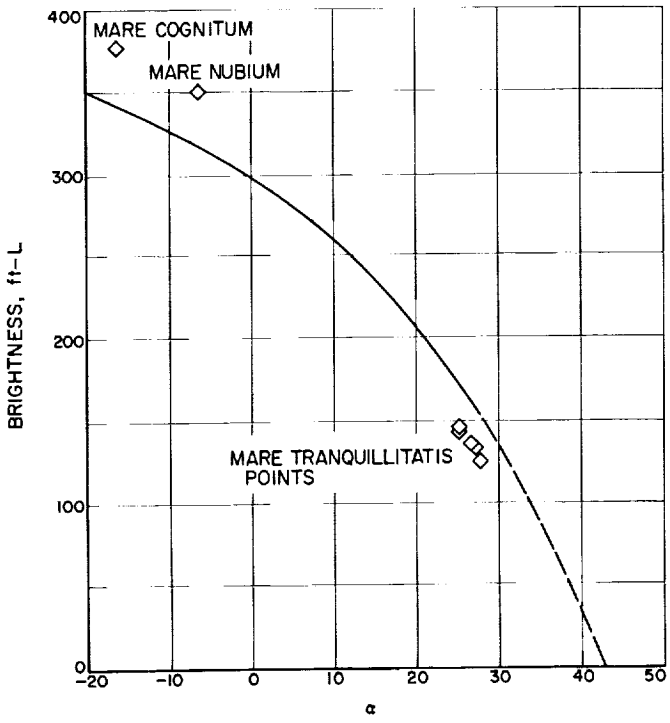

Fig. 60. *Ranger VIII* A-camera predicted vs observed brightness values

2. *Ranger IX* Photometric Results

Because of the nesting characteristic of the *Ranger IX* photographs, many areas are viewed in common by three or more of the cameras. The luminance values registered by cameras B, P_3, and P_4 for the area of Alphonsus shown in Fig. 62 by (x) were reduced by use of the calibration data. The observed values are as follows:

Camera	*Luminance, ft-L*
B	133–150
P_3	160–162
P_4	142–162

The transfer characteristics of the three cameras are given in Fig. 63. Note that the area marked in Fig. 62 appears to be darker than most of the other floor areas of Alphonsus. The predicted value for this region, assuming that highland material has twice the reflectance of the average mare material, was approximately 200 ft-L. The spread in brightness values for camera B was due to apparent variations in exposure on alternate shutter strokes, even though almost no shutter variation was noted for this camera in pre-flight calibration. Both cameras P_3 and P_4 had significant shutter variations prior to launch, which caused most of the variations that were noted in consecutive photographs of the area in question.

The luminances observed by cameras P_1 and P_2 in areas more representative of the average reflectance of

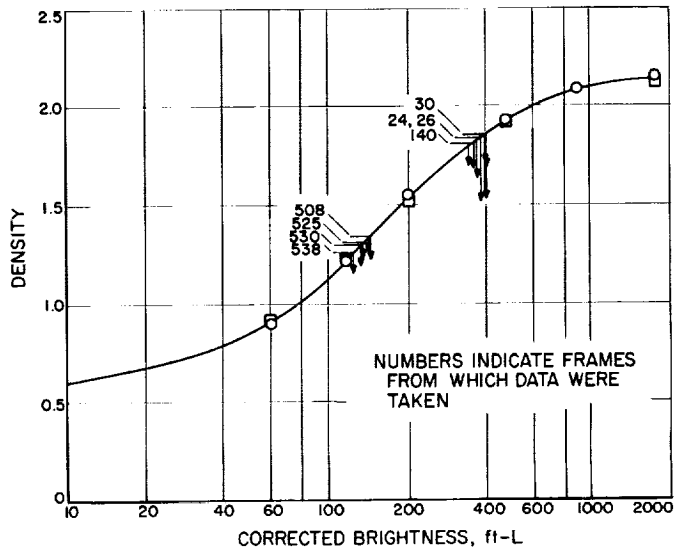

Fig. 61. *Ranger VIII* A-camera transfer characteristic

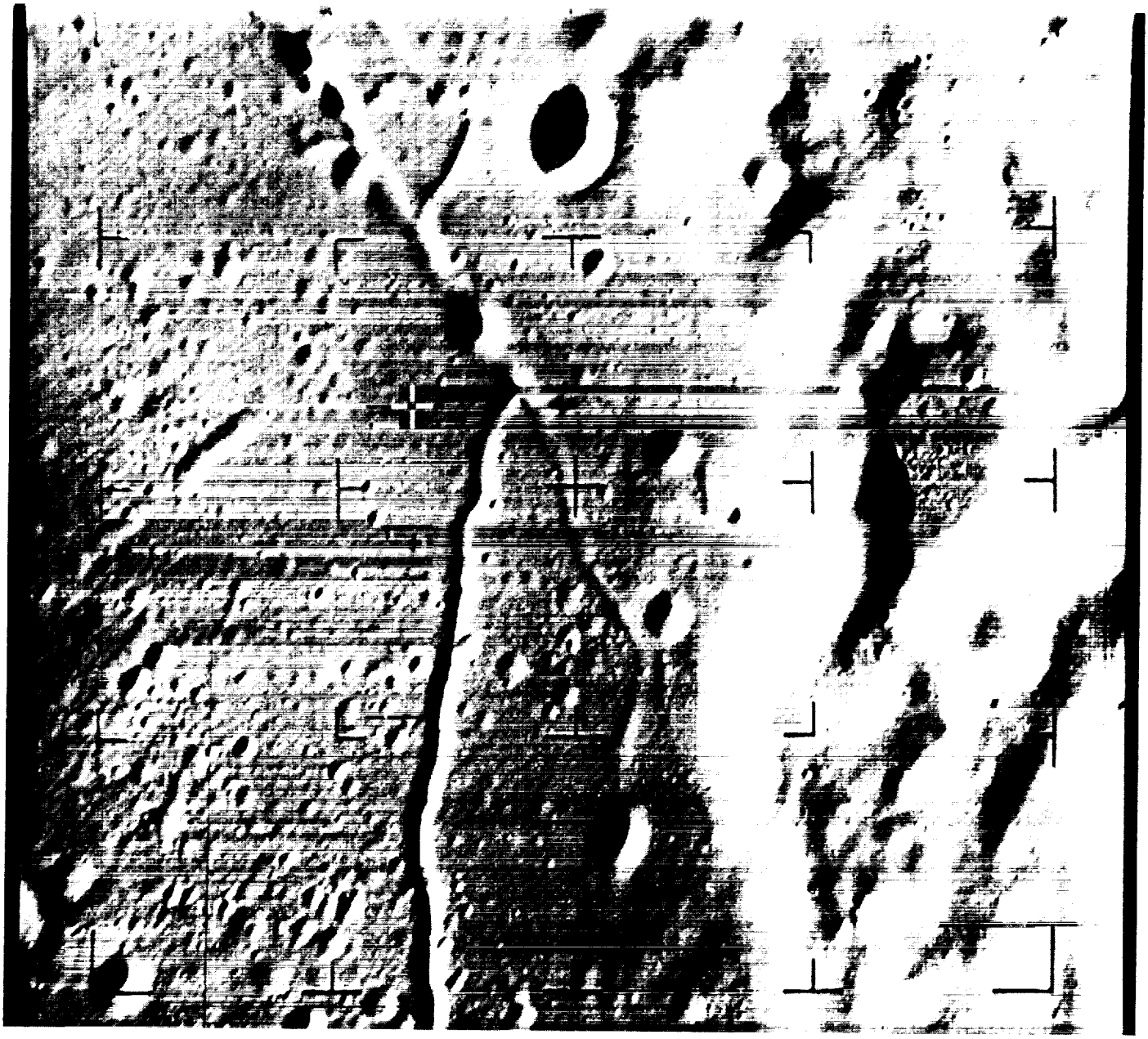

Fig. 62. Alphonsus area used for brightness comparison, B-, P_3-, and P_4-cameras

the Alphonsus floor were found to range from 182 to 200 ft-L. The predicted value for these areas was also about 200 ft-L.

3. Conclusion

Based upon these preliminary results, the photometric behavior of the Moon for resolutions down to that obtained on the last few A- and B-camera frames is not radically different from the behavior observed from Earth. The reflectance function presently in use predicts luminance values within the bounds of accuracy claimed for it, and with proper magnitude normalization to the observed data, it appears to be a good model with which to obtain brightness-to-slope conversions.

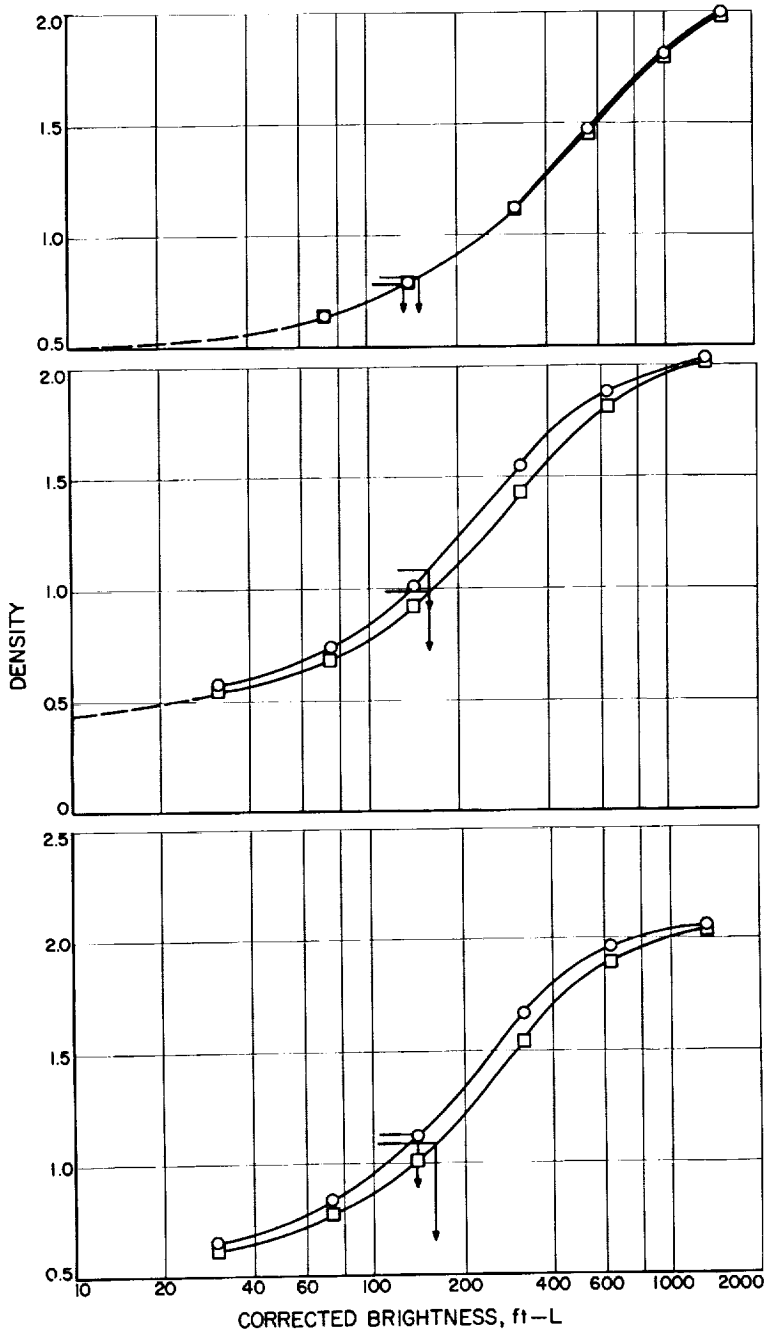

Fig. 63. *Ranger IX* B-, P_3-, and P_4-camera transfer characteristics

APPENDIX A

Spacecraft Flight Events

I. *RANGER VIII*, FEBRUARY 17–20, 1965

Spacecraft flight events	Nominal mission time[a]	Predicted time (GMT)	Actual time (GMT)
			February 17
Spacecraft power on	T − 210 min	–	12:25:00
Transmission of one RTC-2 command	T − 126 min	–	13:51:00
Antenna preset hinge angle, 135 deg	–	–	–
Television low-power mode checks started	T − 115 min	–	13:59:00
Television low-power mode checks completed	T − 106 min	–	14:04:00
15-min hold	–	–	14:15:00
Countdown resumed	–	–	14:25:00
Programmed hold	T − 60 min	–	15:05:00
Countdown resumed	T − 60 min	–	15:55:00
Television cruise-mode telemetry on	T − 15 min	–	16:40:00
H9 sync end reported by AFETR		–	16:44:00
Programmed hold	T − 07 min	–	16:48:00
Countdown resumed (launch plan 17E)	T − 07 min	–	16:58:00
Spacecraft internal power on	T − 05 min	17:00:00	17:00:00
CC&S inhibit release	T − 02 min	17:03:00	17:03:00
CC&S clear relays event (B-2-1)	T − 01 min	17:04:00	17:04:00.5
Liftoff	T = L	17:05:00	17:05:00.795
Spacecraft squib-firing assemblies armed	L + 10 sec	17:05:10	–
Mark 1	–	–	17:07:17.63
Mark 2	–	–	17:07:20.5
Mark 3	–	–	17:09:47.73
Mark 4	–	–	17:10:04.3
Mark 5 – shroud ejection	–	–	17:10:05.5
Mark 6	–	–	17:10:08.55
Mark 7	–	–	17:10:49.23
DSIF 71 lock lost; spacecraft over horizon	–	–	17:12:48
Mark 8	–	–	17:13:20.37
Mark 9	–		17:26:10.4
Mark 10 – second *Agena* cutoff	–		17:27:36.8
Transmitter power up commanded by CC&S (B-2-1)	L + 23 min	17:28:00.5	17:28:00.5

Spacecraft flight events	Nominal mission time[a]	Predicted time (GMT)	Actual time (GMT)
Mark 11 – payload interface connectors fired	S − 5 sec	–	17:30:09.4
Mark 12 – spacecraft/*Agena* separation	S + 0 sec	–	17:30:14.4
a. TV backup clock (F-channel) started	–	–	–
b. BUCT started	–	–	–
c. CC&S relay clamp removed	–	–	–
Spacecraft acquired by DSIF 51	–	–	17:33:20
Two-way lock established	–	–	17:34:00
Mark 13 – *Agena* retro-maneuver	–	–	17:36:45.0
Spacecraft acquired by DSIF 41 (one-way lock)	–	–	17:52:17
Solar-panel extension commanded by CC&S	L + 60 min	–	–
a. B-2-1 event commanded by CC&S	–	18:05:00.5	18:05:00.5
b. B-2-2 event (SFA "A")	–	18:05:04.5	18:05:04.5
c. B-2-3 event (SFA "B")	–	18:05:08.5	18:05:08.5
d. B-2-4 event (panels extended, TV subsystem armed)	–	18:05:40	18:05:39.5
Sun-acquisition sequence commanded by CC&S (B-2-1)	L + 63 min	18:08:00.5	18:08:00.5
Antenna at preset angle	–	–	18:13:21
Sun acquisition	≤L+100 min	–	18:14:20
Earth-acquisition sequence commanded by CC&S (B-2-1)	L + 211 min	20:36:00.5	20:36:00.5
Earth-sensor threshold signal	–	–	20:37:43
Earth acquisition	≤L+241 min	–	20:40:23
Spacecraft antenna transfer command transmitted by DSIF 51	L + 265 min	–	–
a. First RTC-0 initiated	–	21:21:00	21:21:00
b. First RTC-0 verified	–	21:21:38	21:21:38
c. Second RTC-0 initiated	–	21:23:00	21:23:00
d. Second RTC-0 verified	–	21:23:38	21:23:38
e. RTC-3 initiated	–	21:25:00	21:25:00
f. RTC-3 verified	–	21:25:38	21:25:39

[a]T = anticipated liftoff; L = actual liftoff; S = separation; M = midcourse-maneuver counter start; C = terminal-maneuver counter start.

APPENDIX A (Cont'd)

Spacecraft flight events	Nominal mission time[a]	Predicted time (GMT)	Actual time (GMT)
g. B-20 event	—	21:25:39	21:25:39
h. Spacecraft high-gain antenna on		—	21:27:33
			February 18
TV backup clock 8-hr pulse reported by DSIF 51	S + 08 hr	01:30:14	01:30:12
Midcourse stored commands transmitted by DSIF 12	M − 70 min	—	—
a. First RTC-0 initiated	—	08:50:00	08:50:00
b. First RTC-0 verified	—	08:50:38	08:50:38
c. Second RTC-0 initiated	—	08:52:00	08:52:00
d. Second RTC-0 verified	—	08:52:38	08:52:38
e. SC-1 initiated (25-1121-1; +11.60 deg)	—	08:54:00	08:54:00
f. SC-1 received (53-sec positive roll)	—	08:54:39	08:54:39
g. B-2-1 event (capacitor cycling pulse)	—	—	08:54:41.6
h. SC-2 initiated (35-2741-1; +151.75 deg)	—	08:56:00	08:56:00
i. SC-2 received (681-sec positive pitch)	—	08:56:39	08:56:39
j. SC-3 initiated (03-2564-1; 36.44 m/sec)	—	08:58:00	08:58:00
k. SC-3 received (59-sec burn)	—	08:58:42	08:58:41
TV backup clock 16-hr pulse	S + 16 hr	09:30:10	09:30:35
Spacecraft antenna transfer command transmitted by DSIF 12	M − 20 min	—	—
a. First RTC-0 initiated	—	09:36:00	09:36:00
b. First RTC-0 verified	—	09:36:38	09:36:38
c. Second RTC-0 initiated	—	09:38:00	09:38:00
d. Second RTC-0 verified	—	09:38:38	09:38:38
e. RTC-3 initiated	—	09:40:00	09:40:00
f. RTC-3 verified	—	09:40:38	09:40:38
g. B-20 event	—	09:40:39	09:40:39
h. Spacecraft low-gain antenna on	—	—	09:43:17
Midcourse-maneuver sequence initiated by DSIF 12	—	—	10:00:00
a. RTC-4 initiated	—	10:00:00	10:00:00
b. RTC-4 verified	—	10:00:38	10:00:38

Spacecraft flight events	Nominal mission time[a]	Predicted time (GMT)	Actual time (GMT)
B-20 event (B-counter counting)	M − 0	10:00:39	10:00:39.1
a. Roll-maneuver start commanded by CC&S (B-2-1)	M + 05 sec	10:00:44	10:00:44.5
b. Roll-maneuver stop commanded by CC&S (B-2-1)	Item a + 53 sec	10:01:37.5	10:01:37.5
c. Transmitter power drop; loss of lock on all telemetry channels	—	—	10:01:40.8
d. Pitch-maneuver start commanded by CC&S (B-2-1)	M + 9.5 min	10:10:08.5	Not known
e. Pitch-maneuver stop commanded by CC&S (B-2-1)	Item d + 681 sec	10:21:29.5	Not known
f. Telemetry Mode II; accelerometer data on Channel 8	—	10:21:29.5	Not known
g. Midcourse-motor ignition commanded by CC&S	M + 26.5 min	—	—
(1) All telemetry channels back in lock	—	—	10:27:07.5
(2) Start of accelerometer pulses	—	10:27:08	10:27:07.6
(3) Squib-firing event (B-2-1)	—	10:27:08.5	10:27:08.5
(4) B-2-2 event	—	10:27:12.5	10:27:12.5
(5) B-2-3 event	—	10:27:16.5	10:27:16.5
h. Midcourse-motor shutoff commanded by CC&S	Item g + 59 sec	—	—
(1) End of accelerometer pulses	—	10:28:08	10:28:08.8
(2) Squib-firing event (B-2-1)	—	10:28:09.5	10:28:09.5
(3) B-2-2 event	—	10:28:13.5	10:28:13.5
(4) B-2-3 event	—	10:28:17.5	10:28:17.5
Sun-reacquisition sequence commanded by CC&S (B-2-1)	M + 30 min	10:30:38.5	10:30:38.5
Telemetry Mode III	—	10:30:38.5	10:30:38.7
Sun reacquisition	≤M + 60 min	—	10:40:13
Earth-reacquisition sequence commanded by CC&S (B-2-1)	M + 58 min	10:58:38.5	10:58:38.5
Earth reacquisition	≤M + 88 min	—	11:00:43

[a]T = anticipated liftoff; L = actual liftoff; C = separation; M = midcourse-maneuver counter start; C = terminal-maneuver counter start.

APPENDIX A (Cont'd)

Spacecraft flight events	Nominal mission time*	Predicted time (GMT)	Actual time (GMT)
Spacecraft antenna transfer command transmitted by DSIF 12	M + 88 min	–	–
a. First RTC-0 initiated	–	11:30:00	11:30:00
b. First RTC-0 verified	–	11:30:38	11:30:38
c. Second RTC-0 initiated	–	11:32:00	11:32:00
d. Second RTC-0 verified	–	11:32:38	11:32:38
e. RTC-3 initiated	–	11:34:00	11:34:00
f. RTC-3 verified	–	11:34:38	11:34:38
g. B-20 event	–	11:34:39	11:34:39
h. Spacecraft high-gain antenna on	–	–	11:37:36
TV backup clock 24-hr pulse	S + 24 hr	17:30:46	17:30:48 *February 19*
TV backup clock 32-hr pulse	S + 32 hr	01:30:55	01:30:51
TV backup clock 48-hr pulse	S + 48 hr	17:31:09	17:31:07 *February 20*
Terminal stored commands transmitted by DSIF 12	C − 70 min	–	–
a. First RTC-0 initiated	–	07:37:00	07:37:00
b. First RTC-0 verified	–	07:37:38	07:37:38
c. Second RTC-0 initiated	–	07:39:00	07:39:00
d. Second RTC-0 verified	–	07:39:38	07:39:38
e. SC-4 initiated (23-1777-1)	–	07:41:00	07:41:00
f. SC-4 received (1-sec positive pitch; B-20)	–	07:41:30	07:41:39
g. B-2-1 event (capacitor cycling pulse)	–	–	07:41:42
h. SC-5 initiated (13-1777-1)	–	07:43:00	07:43:00
i. SC-5 received (1-sec positive yaw; B-20)	–	07:43:39	07:43:40
j. SC-6 initiated (33-1777-1)	–	07:45:00	07:45:00
k. SC-6 received (1-sec positive pitch; B-20)	–	07:45:39	07:45:40
Maneuver override command transmitted by DSIF 12	C − 25 min	–	–
a. First RTC-0 initiated	–	08:23:00	08:23:00
b. First RTC-0 verified	–	08:23:38	08:23:38
c. Second RTC-0 initiated	–	08:25:00	08:25:00
d. Second RTC-0 verified	–	08:25:38	08:25:38
e. RTC-8 initiated	–	08:27:00	08:27:00
f. RTC-8 verified	–	08:27:38	08:27:38
g. B-20 event (CC&S disconnected from A/C)	–	08:27:39	08:27:39
Terminal-maneuver sequence initiated by DSIF 12	C − 40 sec	–	–
a. RTC-6 initiated	–	08:47:30	08:47:30
b. RTC-6 verified	–	08:48:10	08:48:10
B-20 event (C-counter counting)	C	08:48:10	08:48:09
a. Start first pitch maneuver commanded by CC&S (B-2-1)	C + 05 sec	08:48:15	08:48:15.0
b. Stop first pitch maneuver commanded by CC&S (B-2-1)	Item 58a + 1 sec	08:48:16.0	(See Note)
c. Start yaw maneuver commanded by CC&S (B-2-1)	C + 9.5 min	08:57:39.0	08:57:39.0
d. Stop yaw maneuver commanded by CC&S (B-2-1)	Item 58c + 1 sec	08:57:40.0	(See Note)
e. Start second pitch maneuver commanded by CC&S (B-2-1)	C + 26.5 min	09:14:39.0	09:14:39.0
f. Stop second pitch maneuver commanded by CC&S (B-2-1)	Item 58e + 1 sec	09:14:40.0	(See Note)
g. Telemetry Mode IV	Item 58e + 1 sec	09:14:40	09:15:52
TV backup clock 64-hr pulse	S + 64 hr	09:31:24	09:31:28
TV on (warmup) commanded by CC&S	C + 45 min	–	–
a. TV in warmup	–	09:33:08	09:33:08.5
b. B-2-1	–	09:33:09.0	09:33:09.0
TV in full power	Item 60 + 80 sec	09:34:28	09:34:30
TV full power (backup) commanded by CC&S (B-2-1)	C + 50 min –	– 09:38:09.0	– 09:38:09.0
Impact	–	09:57:36.8	09:57:36.756

*T = anticipated liftoff; L = actual liftoff; C = separation; M = midcourse-maneuver counter start; C = terminal-maneuver counter start.
Note: Mechanization of event coder does not permit the readout of a B-2-1 event occurring within 2 sec of a previous B-2-1 event.

APPENDIX A (Cont'd)

II. *RANGER IX*, MARCH 21–24, 1965

Spacecraft flight events	Nominal mission time[a]	Predicted time (GMT)	Actual time (GMT)
			March 21
Spacecraft power on	T − 210 min	–	16:21:00
Transmission of two RTC-2 commands	T − 126 min	–	17:48:00 17:49:00
Antenna preset hinge angle, 122 deg	–	–	–
H-9 sync end	–	–	17:50:11.6
Television low-power mode checks started	T − 115 min	–	17:55:00
Television low-power mode checks completed	T − 106 min	–	18:01:00
Programmed hold	T − 60 min	–	18:51:00
Countdown resumed	T − 60 min	–	19:56:00
Television cruise-mode telemetry on	T − 15 min	–	20:41:00
Programmed hold	T − 07 min	–	20:49:00
Countdown resumed (launch plan 21A)	T − 07 min	–	21:04:00
Spacecraft internal power on	T − 05 min	–	21:06:00
Recycled to T − 7 and holding	–	–	21:08:30
Countdown resumed (launch plan 21D)	T − 07 min	–	21:30:00
Spacecraft internal power on	T − 05 min	–	21:32:00
CC&S inhibit release	T − 02 min	–	21:35:00
CC&S clear relays event (B-2-1)	T − 01 min	21:36:00	21:36:00.8
Liftoff (launch azimuth, 93.6 deg)	T = L	21:37:01	21:37:02.456
Spacecraft squib-firing assemblies armed	L + 10 sec	21:37:11	–
Mark 1	–	–	21:38:08.0
Mark 2	–	–	21:39:20.97
Mark 3	–	–	21:41:48.3
Mark 4	–	–	21:42:06.54
Mark 5 – shroud ejection	–	–	21:42:08.0
Mark 6	–	–	21:42:11.51
Mark 7	–	–	21:42:52.5
DSIF 71 lock lost; spacecraft over horizon	–	–	21:44:43
Mark 8	–	–	21:45:24.2
Mark 9	–	–	21:48:21.7
Mark 10 – second *Agena* cutoff	–	–	21:49:48.3
Spacecraft entered Earth shadow	–	–	21:50:22
Mark 11 – payload interface connectors fired	S − 5 sec	–	21:52:20.60
Mark 12 – spacecraft/*Agena* separation	S + 0 sec	–	21:52:25.70
a. TV backup clock (F-channel) started	–	–	–
b. BUCT started	–	–	–
c. CC&S relay clamp removed	–	–	–
Mark 13 – *Agena* retro-maneuver	–	–	21:58:58.66
Transmitter power up commanded by CC&S (B-2-1)	L + 23 min	22:00:00	Not known
Spacecraft left Earth shadow	–	–	22:24:07
Solar-panel extension commanded by CC&S	L + 60 min	–	–
a. B-2-1 event commanded by CC&S	–	22:37:00.8	22:37:01
b. B-2-2 event (SFA "A")	–	22:37:04.8	22:37:06
c. B-2-3 event (SFA "B")	–	22:37:08.8	22:37:10
d. B-2-4 event (panels extended, television subsystem armed)	–	22:37:47	22:37:51
Sun-acquisition sequence commanded by CC&S (B-2-1)	L + 63 min	22:40:00.8	22:40:01
Sun acquisition	≤ L + 100 min	–	22:47:30
			March 22
Earth-acquisition sequence commanded by CC&S (B-2-1)	L + 211 min	01:08:00.8	01:08:02
Earth acquisition	≤ L + 241 min	–	01:11:50
TV backup clock 8-hr pulse reported by DSIF 51	S + 08 hr	05:52:26	05:52:36
Spacecraft antenna transfer command transmitted by DSIF 12	L + 265 min	–	–
a. First RTC-0 initiated	–	–	09:26:00
b. First RTC-0 verified	–	–	09:26:38
c. Second RTC-0 initiated	–	–	09:28:00
d. Second RTC-0 verified	–	–	09:28:38

[a]T = anticipated liftoff; L = actual liftoff; S = separation; M = midcourse-maneuver counter start; C = terminal-maneuver counter start.

APPENDIX A (Cont'd)

Spacecraft flight events	Nominal mission time[a]	Predicted time (GMT)	Actual time (GMT)
e. RTC-3 initiated	—	—	09:30:00
f. RTC-3 verified	—	—	09:30:38
g. B-20 event	—	09:30:39	09:30:39
h. Spacecraft high-gain antenna on	—	—	09:33:00
TV backup clock 16-hr pulse	S + 16 hr	13:52:36	13:52:47
TV backup clock 24-hr pulse	S + 24 hr	21:52:58	21:52:54
Hinge update command transmitted by DSIF 41	—	—	—
a. First RTC-0 initiated	—	—	22:26:00
b. First RTC-0 verified	—	—	22:26:38
c. Second RTC-0 initiated	—	—	22:28:00
d. Second RTC-0 verified	—	—	22:28:38
e. RTC-2 initiated	—	—	22:30:00
f. RTC-2 verified	—	—	22:30:38
g. B-20 event	—	22:30:39	22:30:39
			March 23
TV backup clock 32-hr pulse	S + 32 hr	05:53:01	05:53:01
Midcourse stored commands transmitted by DSIF 12	M − 70 min	—	—
a. First RTC-0 initiated	—	—	10:50:00
b. First RTC-0 verified	—	—	10:50:38
c. Second RTC-0 initiated	—	—	10:52:00
d. Second RTC-0 verified	—	—	10:52:38
e. SC-1 initiated (25-1007-0; −27.41 deg)	—	—	10:54:00
f. SC-1 received (126-sec negative roll)	—	10:54:40	10:54:40
g. B-2-1 event (capacitor cycling pulse)	—	—	10:54:43
h. SC-2 initiated (35-1646-1; +127.96 deg)	—	—	10:56:00
i. SC-2 received (587-sec positive pitch)	—	10:56:40	10:56:40
j. SC-3 initiated (03-2672-1; 18.15 m/sec)	—	—	10:58:00
k. SC-3 received (30-sec burn)	—	10:58:43	10:58:42
Spacecraft antenna transfer command transmitted by DSIF 12	M − 20 min	—	—
a. First RTC-0 initiated	—	—	11:31:00
b. First RTC-0 verified	—	—	11:31:38
c. Second RTC-0 initiated	—	—	11:33:00
d. Second RTC-0 verified	—	—	11:33:38
e. RTC-3 initiated	—	—	11:35:00
f. RTC-3 verified	—	—	11:35:38
g. B-20 event	—	11:35:40	11:35:40
h. Spacecraft low-gain antenna on	—	—	11:38:40
Midcourse-maneuver sequence initiated by DSIF 12	—	—	—
a. RTC-4 initiated	—	—	12:03:00
b. RTC-4 verified	—	—	12:03:38
B-20 event (B-counter counting)	M = 0	12:03:39	12:03:39.5
a. Roll-maneuver start commanded by CC&S (B-2-1)	M + 05 sec	12:03:44	12:03:44.5
b. Roll-maneuver stop commanded by CC&S (B-2-1)	Item a + 126 sec	12:05:50.5	12:05:50.5
c. Pitch-maneuver start commanded by CC&S (B-2-1)	M + 9.5 min	12:13:08.5	12:13:08.5
d. Pitch-maneuver stop commanded by CC&S (B-2-1); telemetry Mode II; accelerometer data on Channel 8	Item c + 587 sec	12:22:55.5	12:22:55.5
e. Midcourse-motor ignition commanded by CC&S	M + 26.5 min	—	—
(1) Start of accelerometer pulses	—	12:30:08	12:30:08.3
(2) Squib-firing event (B-2-1)	—	12:30:08.5	12:30:08.6
(3) B-2-2 event	—	12:30:12.5	12:30:12.6
(4) B-2-3 event	—	12:30:16.5	12:30:16.6
f. Midcourse-motor shutoff commanded by CC&S	Item e + 30 sec	—	—
(1) End of accelerometer pulses	—	12:30:38	12:30:38.7
(2) Squib-firing event (B-2-1)	—	12:30:38.5	12:30:38.6
(3) B-2-2 event	—	12:30:42.5	12:30:42.6
(4) B-2-3 event	—	12:30:46.5	12:30:46.6

[a]T = anticipated liftoff; L = actual liftoff; C = separation; M = midcourse-maneuver counter start; C = terminal-maneuver counter start.

APPENDIX A (Cont'd)

Spacecraft flight events	Nominal mission time[a]	Predicted time (GMT)	Actual time (GMT)
Sun-reacquisition sequence commanded by CC&S (B-2-1)	M + 30 min	12:33:38	12:33:38.2
Telemetry Mode III	–	12:33:38.5	12:33:38.6
Sun reacquisition	≤ M + 60 min	–	12:42:20
Earth-reacquisition sequence commanded by CC&S (B-2-1)	M + 58 min	13:01:38.5	13:01:38.5
Earth reacquisition	M + 88 min	–	13:02:40
Spacecraft antenna transfer command transmitted by DSIF 12	M + 88 min	–	–
a. First RTC-0 initiated	–	–	13:26:00
b. First RTC-0 verified	–	–	13:26:38
c. Second RTC-0 initiated	–	–	13:28:00
d. Second RTC-0 verified	–	–	13:28:38
e. RTC-3 initiated	–	–	13:30:00
f. RTC-3 verified	–	–	13:30:38
g. B-20 event	–	13:30:39	13:30:39.4
h. Spacecraft high-gain antenna on	–	–	13:33:00
TV backup clock 48-hr pulse	S + 48 hr	21:53:15	21:53:28 *March 24*
Terminal stored commands transmitted by DSIF 12	C − 70 min	–	–
a. First RTC-0 initiated	–	–	11:54:00
b. First RTC-0 verified	–	–	11:54:38
c. Second RTC-0 initiated	–	–	11:56:00
d. Second RTC-0 verified	–	–	11:56:38
e. SC-4 initiated (23-1645-1)	–	–	11:58:00
f. SC-4 received (24-sec positive pitch; B-20)	–	11:58:40	11:58:40
g. B-2-1 event (capacitor cycling pulse)	–	–	11:58:42.5
h. SC-5 initiated (13-1005-0)	–	–	12:00:00
i. SC-5 received (75-sec negative yaw; B-20)	–	12:00:40	12:00:40
j. SC-6 initiated (33-2737-0)	–	–	12:02:00
k. SC-6 received (94-sec negative pitch; B-20)	–	12:02:39	12:02:39
Terminal-maneuver sequence initiated by DSIF 12	C − 40 sec	–	–
a. RTC-6 initiated	–	–	13:02:34
b. RTC-6 verified	–	–	13:03:12
B-20 event (C-counter counting)	C	13:03:13.3	13:03:13.5
a. Start first pitch maneuver commanded by CC&S (B-2-1)	C + 05 sec	13:03:18	13:03:18.4
b. Stop first pitch maneuver commanded by CC&S (B-2-1)	Item a + 24 sec	13:03:42.4	13:03:42.4
c. Start yaw maneuver commanded by CC&S (B-2-1)	C + 9.5 min	13:12:42.4	13:12:42.4
d. Stop yaw maneuver commanded by CC&S (B-2-1)	Item c + 75 sec	13:13:57.4	13:13:57.4
TV clock inhibit command transmitted by DSIF 12	–	–	–
a. RTC-5 initiated	–	–	13:17:00
b. RTC-5 verified	–	–	13:17:38
c. B-20 event; TV clock off; telemetry Mode IV	–	13:17:39	13:17:39.5
Terminal-maneuver sequence (combined)			
a. Start second pitch maneuver commanded by CC&S (B-2-1)	C + 26.5 min	13:29:42.4	13:29:42.4
b. Stop second pitch maneuver commanded by CC&S (B-2-1), telemetry Mode I	Item e + 94 sec	13:31:16.4	13:31:16.4
TV on (warmup) commanded by CC&S	C + 45 min	–	–
a. TV in warmup	–	13:48:12	13:48:12.0
b. B-2-1	–	13:48:12.4	13:48:12.5
TV in full power	Item 60 + 80 sec	13:49:32	13:49:33
TV full power (backup) commanded by CC&S (B-2-1)	C + 50 min –	– 13:53:12.4	– 13:53:12.5
Impact	–	14:08:20	14:08:19.999

[a]T = anticipated liftoff; L = actual liftoff; C = separation; M = midcourse-maneuver counter start; C = terminal-maneuver counter start.

APPENDIX B

Spacecraft Configuration and Interfaces

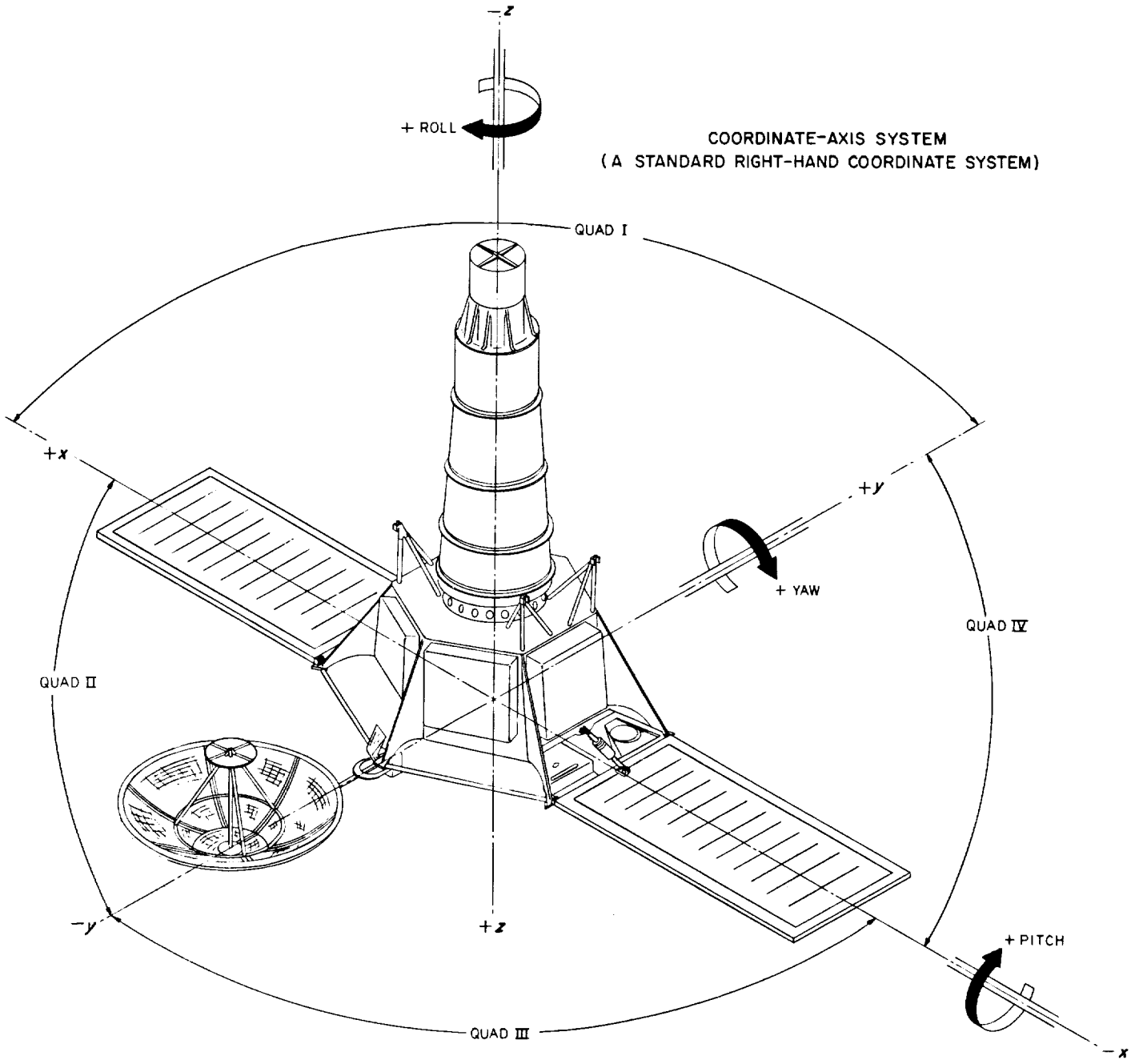

Fig. B-1. Coordinate-axis system

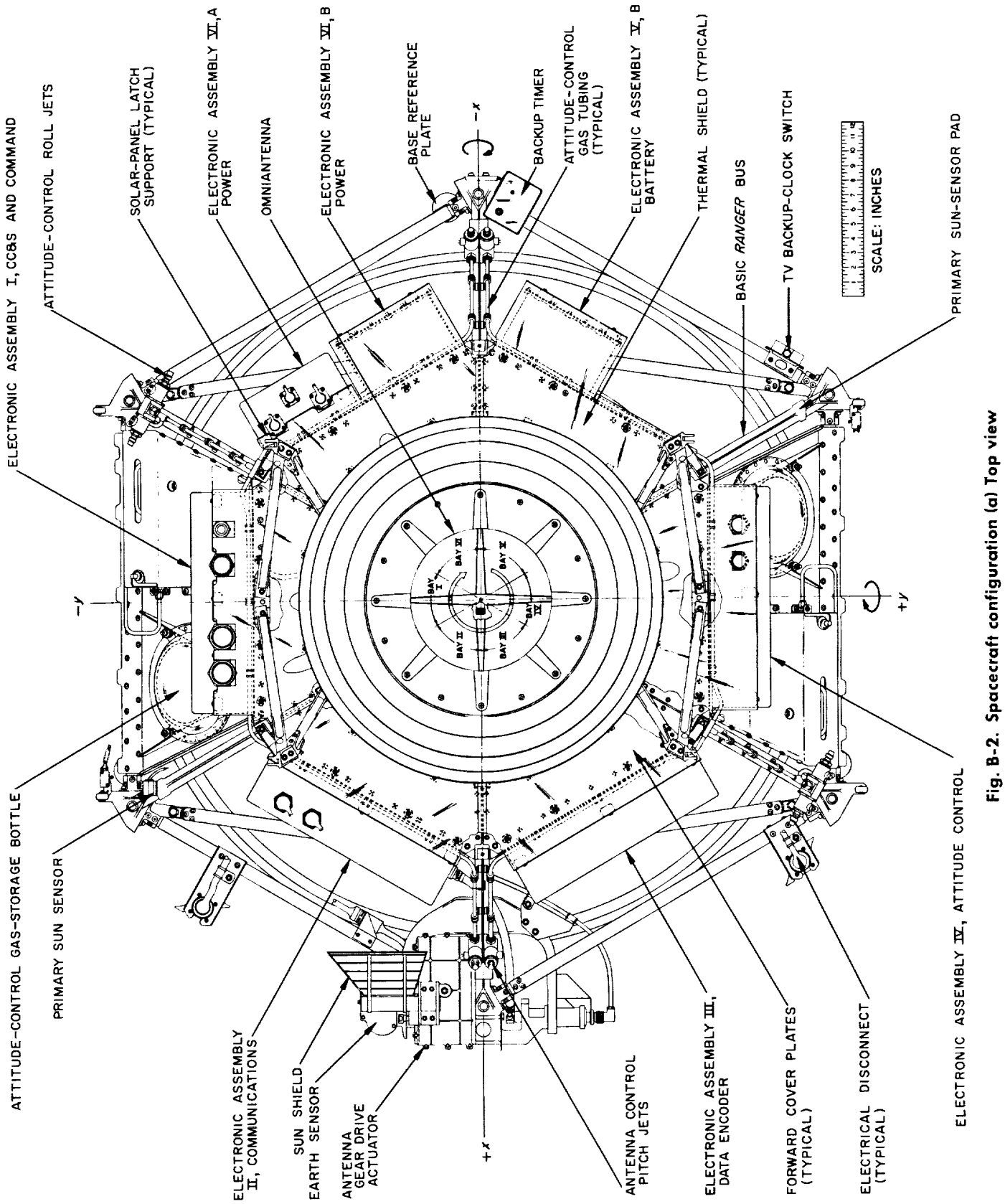

Fig. B-2. Spacecraft configuration (a) Top view

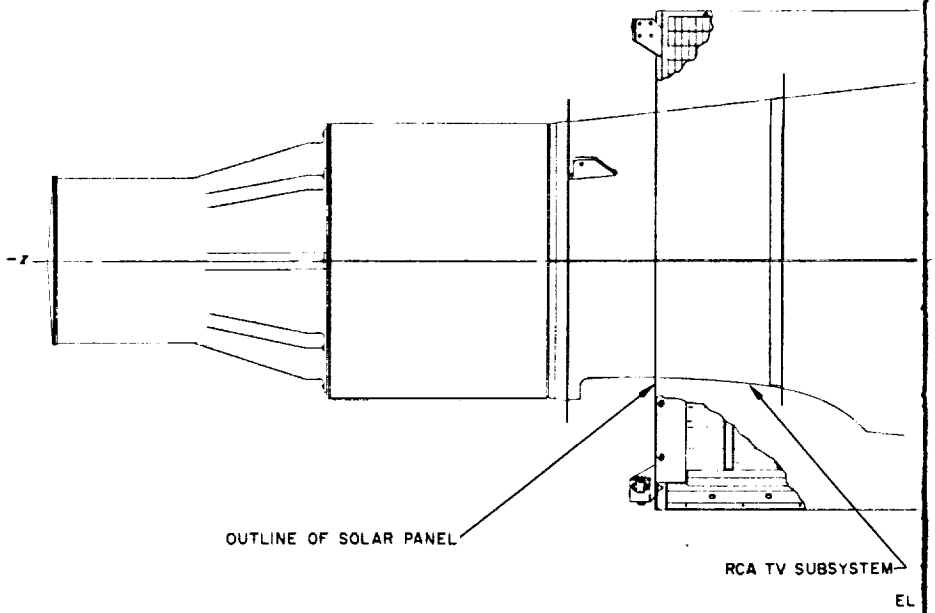
ATTITUDE-
ELECTRO
SOLAR-PANEL
OUTLINE OF SOLAR PANEL
RCA TV SUBSYSTEM
EL
EL

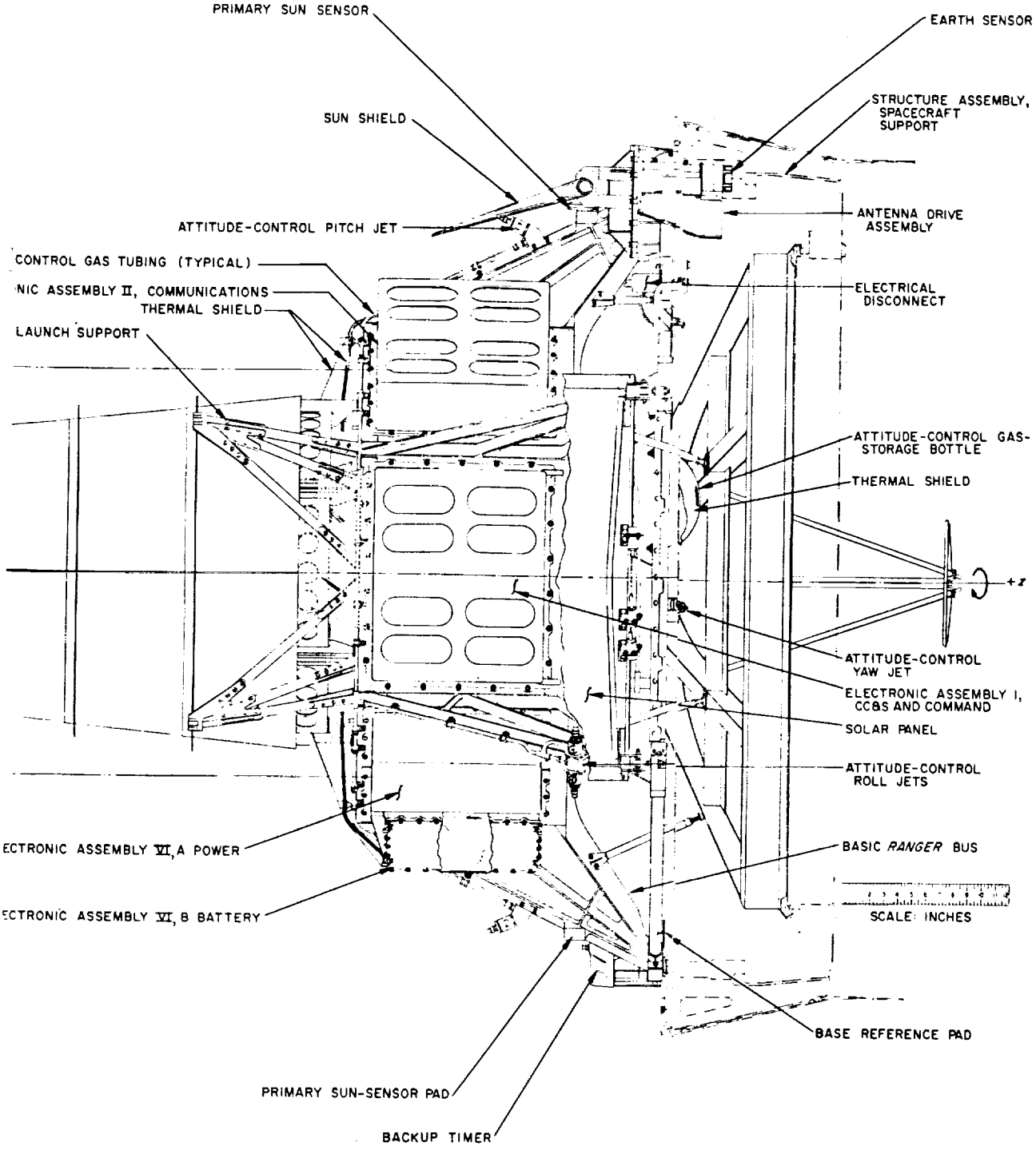

Fig. B-2. Spacecraft configuration (b) Pitch axis

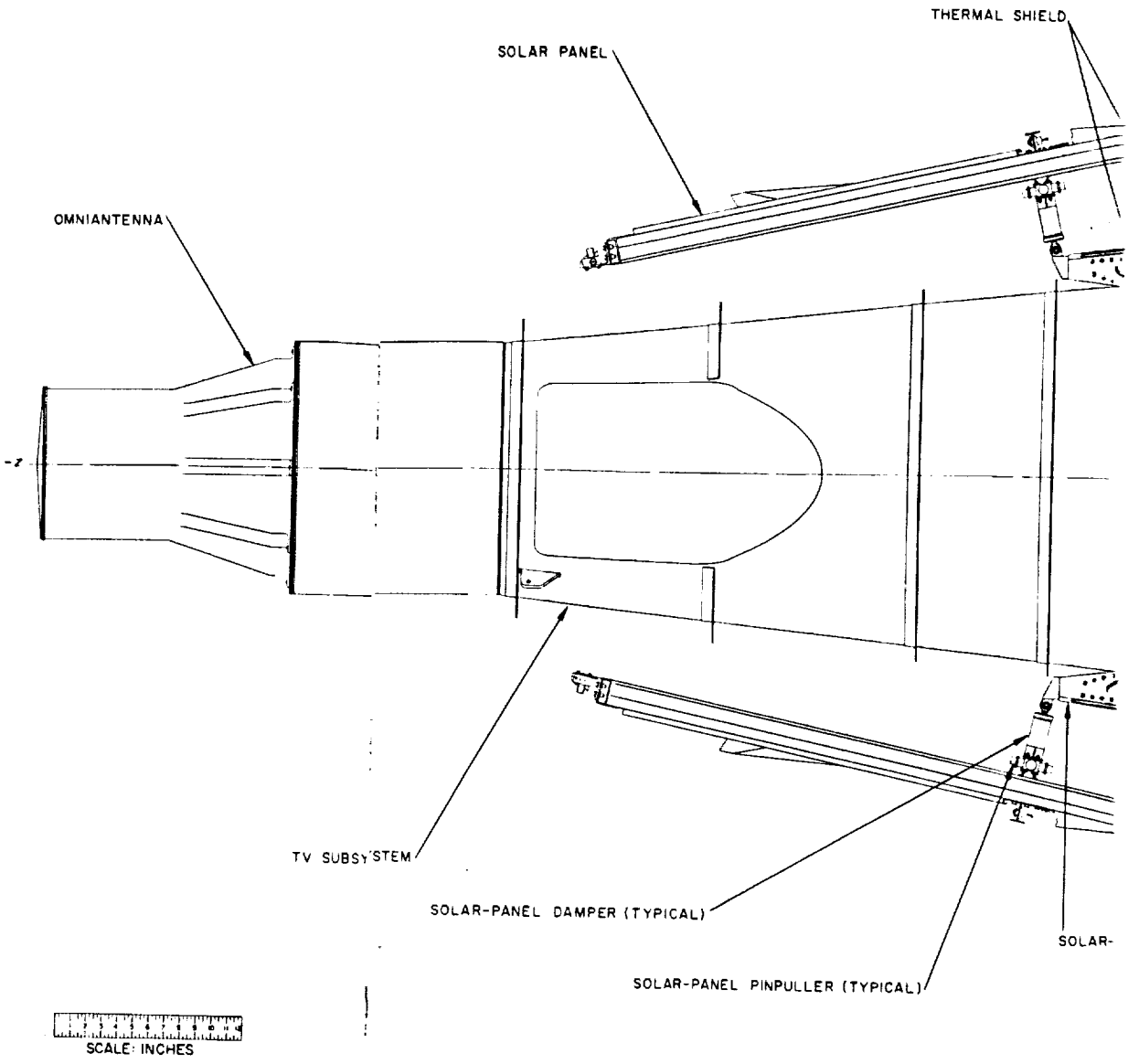

Fig. B-2. Spacecraft configuration (c) Yaw axis

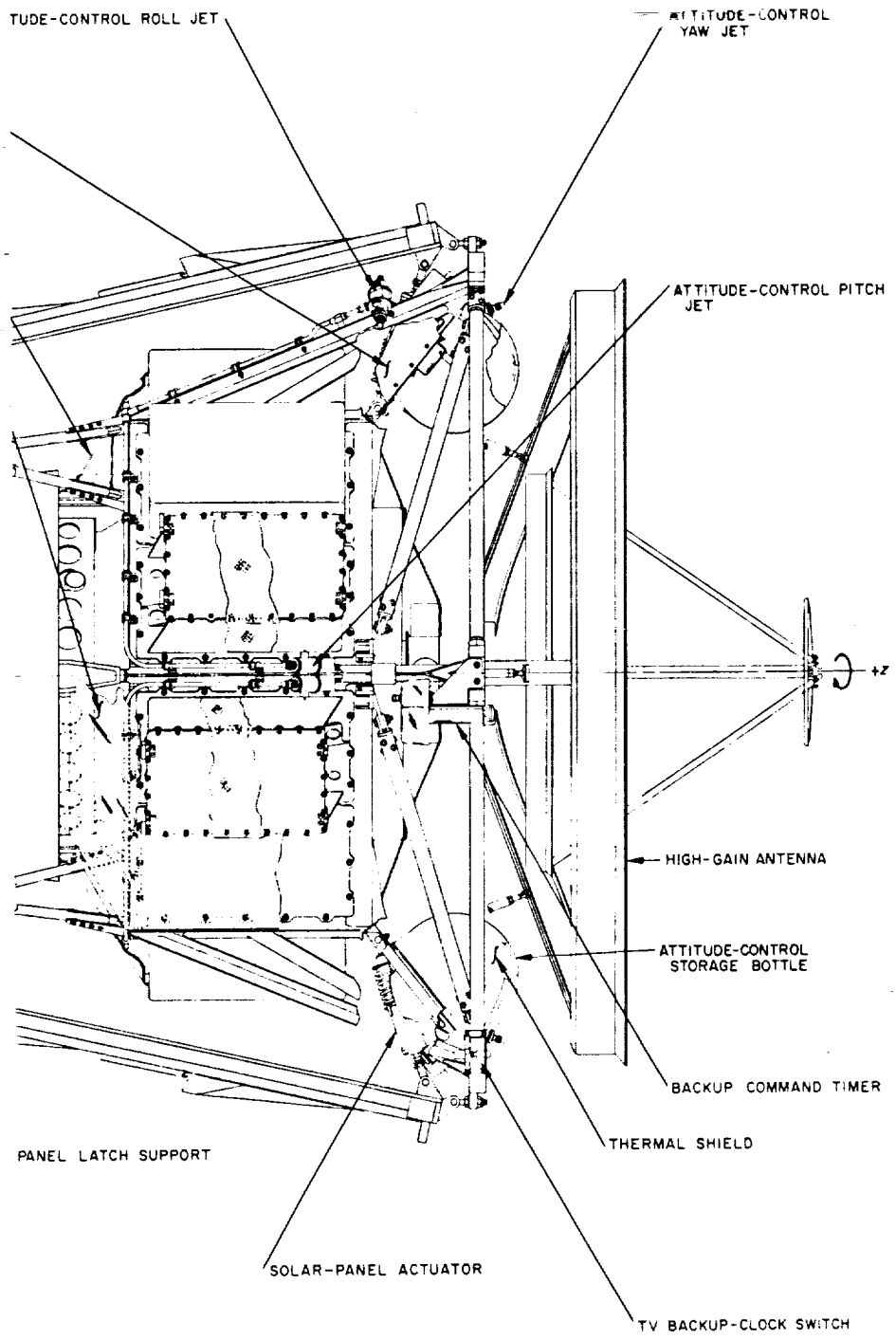
TUDE-CONTROL ROLL JET
ATTITUDE-CONTROL YAW JET
ATTITUDE-CONTROL PITCH JET
+Z
HIGH-GAIN ANTENNA
ATTITUDE-CONTROL STORAGE BOTTLE
BACKUP COMMAND TIMER
THERMAL SHIELD
PANEL LATCH SUPPORT
SOLAR-PANEL ACTUATOR
TV BACKUP-CLOCK SWITCH

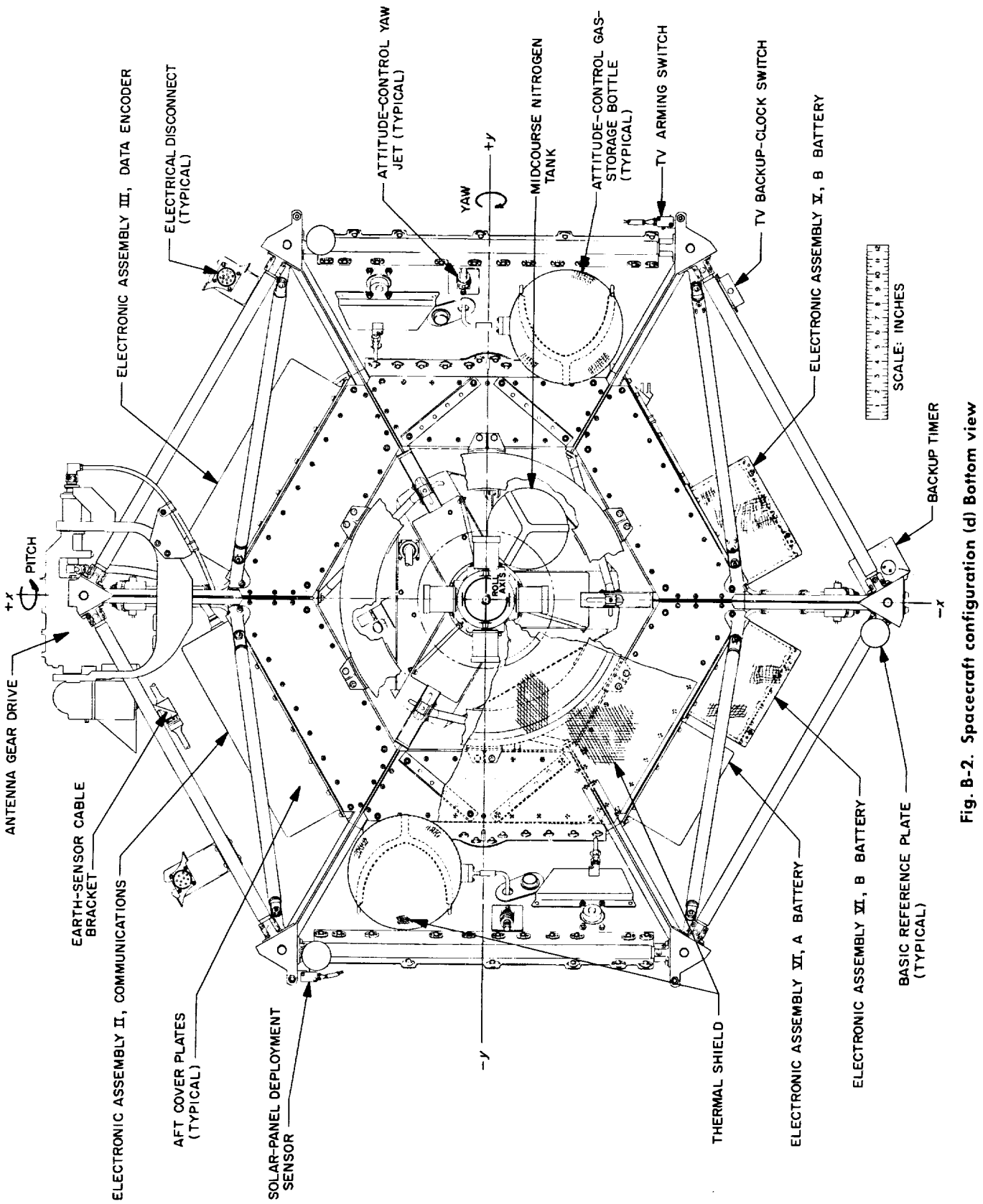

Fig. B-2. Spacecraft configuration (d) Bottom view

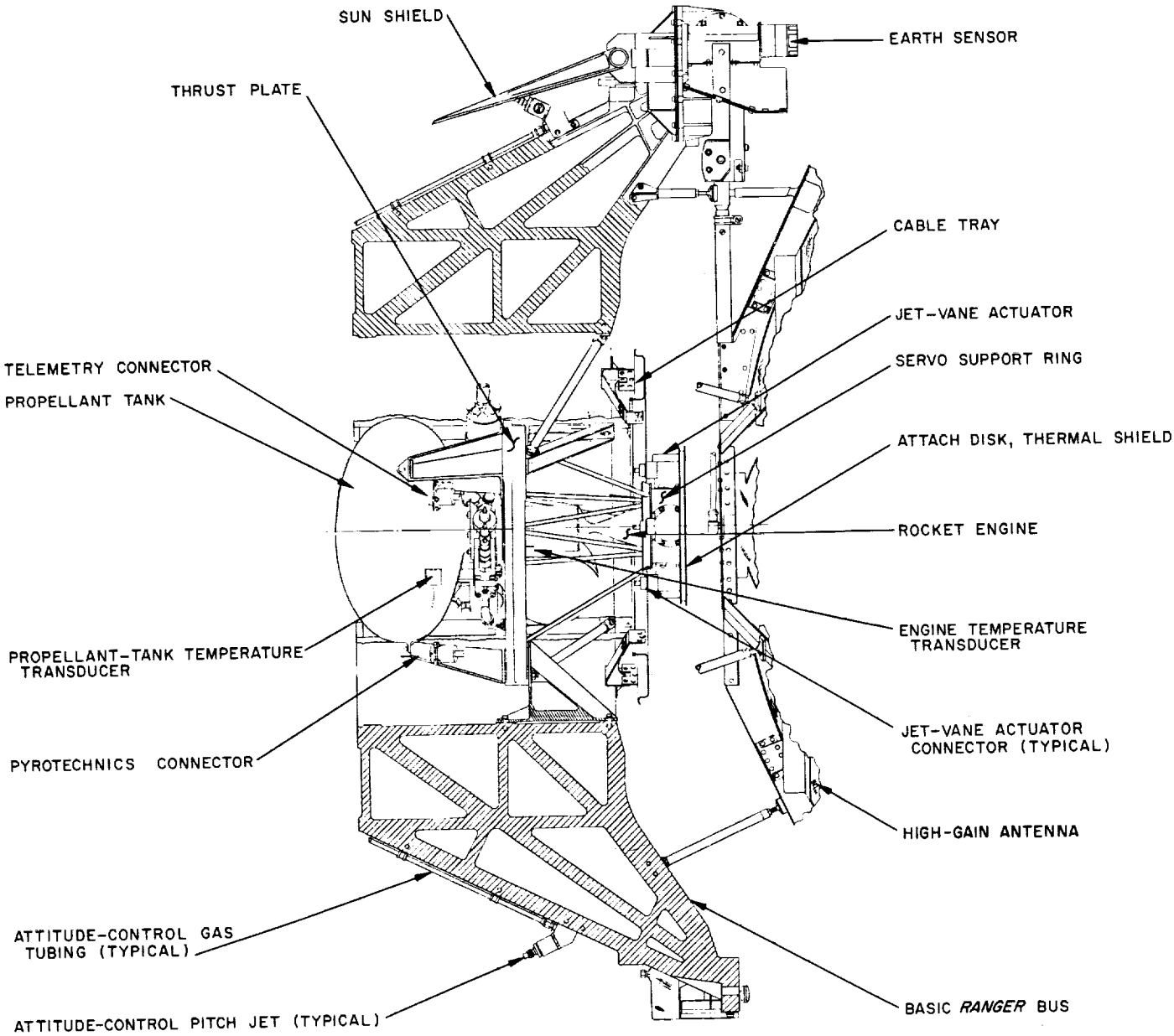

Fig. B-3. Spacecraft bus interior and spaceframe section

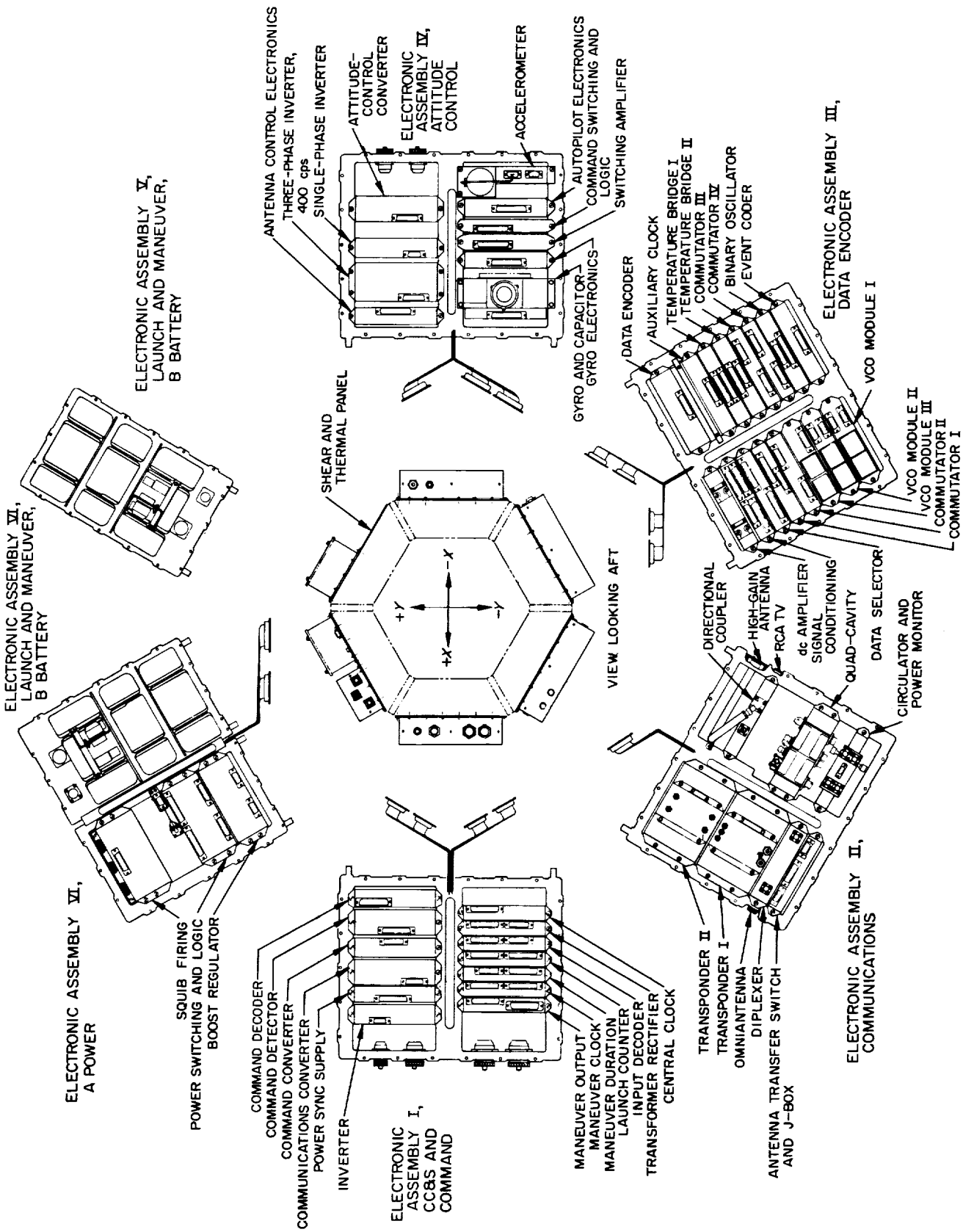

Fig. B-4. Electronics assembly locations

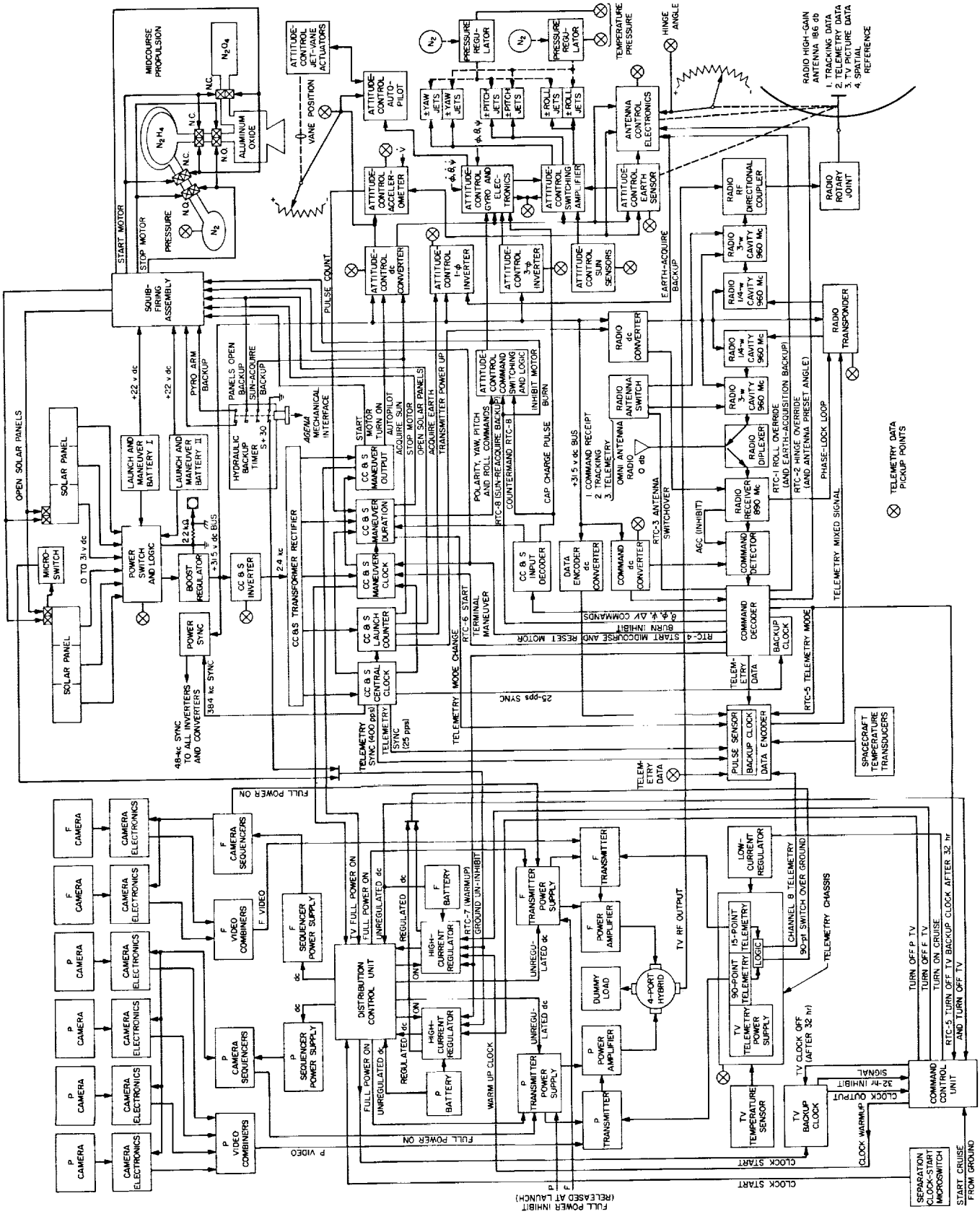

Fig. B-5. Spacecraft block diagram

BIBLIOGRAPHY

Project and Mission

Ranger Block III Project Development Plan, JPL Project Document No. 8, October 31, 1963.

Ranger Block III Mission Operations Plan (Launch Operations Phase), Ranger C, JPL Project Document No. 33, February 5, 1965.

Ranger Block III Mission Operations Plan (Launch Operations Phase), Ranger D, JPL Project Document No. 40, March 19, 1965.

Ranger Block 3 Project Policy and Requirements, Revision 1 with Addendum 1, JPL internal communication, March 8, 1963, and July 22, 1963.

Travers, E. S., *Ranger Block III Launch Constraints Planning Document*, JPL Project Document No. 18, June 26, 1964.

Winneberger, R. A., *Post Injection Standard Trajectory, Ranger Block III, for February, March, April 1965 Launch Periods*, JPL Project Document No. 28, January 15, 1965.

Ranger VII Mission Description and Performance, JPL Technical Report No. 32-700, Part I, December 15, 1964.

Heacock, R. L., Kuiper, G. P., Shoemaker, E. M., Urey, H. C., and Whitaker, E. A., *Ranger VII Experimenters' Analyses and Interpretations*, JPL Technical Report No. 32-700, Part II, February 10, 1965.

Ranger VII Photographs of the Moon: Part I, Camera "A" Series, NASA SP-61, U.S. Government Printing Office, September 1964.

Ranger VII Photographs of the Moon: Part II, Camera "B" Series, NASA SP-62, U.S. Government Printing Office, February 1965.

Ranger VII Photographs of the Moon: Part III, Camera "P" Series, NASA SP-63, U.S. Government Printing Office (in press).

Heacock, R. L., Kuiper, G. P., Shoemaker, E. M., Urey, H. C., and Whitaker, E. A., *Ranger VIII and IX Experimenters' Analysis and Interpretations*, JPL Technical Report No. 32-800, Part II (in preparation).

Ranger VIII and IX Photographs of the Moon, NASA, U.S. Government Printing Office (in preparation).

Wollenhaupt, W. R., Trask, D. W., Winneberger, R. A., Kirhofer, W. F., Piaggi, E. G., Liu, A., and Borncamp, F., *The Ranger VIII Flight Path and Its Determination from Tracking Data*, JPL Technical Report No. 32-766 (in preparation).

Vegos, C. J., Trask, D. W., Winneberger, R. A., Kirhofer, W. E., Piaggi, E. G., Liu, A., and Borncamp, F., *The Ranger IX Flight Path and Its Determination from Tracking Data*, JPL Technical Report No. 32-767 (in preparation).

Spacecraft System

Spacecraft Design Specifications, Ranger Block III (FR 3), JPL, September 3, 1963. (Includes 29 specifications, revised various dates.)

Ranger TV Subsystem (Block III) Final Report, Astro-Electronics Division, Defense Electronics Products, Radio Corporation of America, AED R-2620, July 22, 1965.

BIBLIOGRAPHY (Cont'd)

Test and Operations Plan, Ranger Block III, JPL 3R 001.03, March 8, 1965.

System Test and Operations Report, Ranger Block III, RA-C (VIII) Spacecraft, JPL internal communication, May 12, 1965.

System Test and Operations Report, Ranger Block III, RA-D (IX) Spacecraft, JPL internal communication, May 28, 1965.

Ranger 8 Flight Acceptance Environmental Test Results Summary, JPL internal communication, April 13, 1965.

Ranger 9 Flight Acceptance Environmental Test Results Summary, JPL internal communication, April 13, 1965.

Ranger Spacecraft Dynamic Environment — Final Report, JPL internal communication (in preparation).

Turk, W., *Ranger Block III Attitude Control System*, JPL Technical Report No. 32-663, November 15, 1964.

Launch-Vehicle System

See: *MSVP Satellites and Probe Programs* (Revised), Lockheed Missiles and Space Co., LMSC-A602037-A, January 30, 1965.

Atlas/Agena Ranger-C Flash Flight Report, NASA Goddard Launch Operations, Eastern Test Range, GLOR-159, February 17, 1965.

Atlas/Agena Ranger-D Flash Flight Report, NASA Goddard Launch Operations, Eastern Test Range, GLOR-167, March 21, 1965.

Preliminary Flight Test Report, Mod III Guidance System with Launch 196-D Range Test No. 235 Ranger Space Project RA-8, G.E./Burroughs ET 65-56752, February 17, 1965 (SECRET).

Preliminary Flight Test Report, Mod III Guidance System with Launch 204-D Range Test No. 0300 Ranger Space Project RA-9, G.E./Burroughs ET 65-56755, March 21, 1965 (SECRET).

Ranger 8 Launch Report, Lockheed Missiles and Space Co., Space Systems Div., AFETR Test Operations, LMSC-B040697, March 4, 1965 (SECRET).

Ranger 9 Launch Report, Lockheed Missiles and Space Co., Space Systems Div., AFETR Test Operations, LMSC-B040724, April 8, 1965 (SECRET).

Atlas Launch Vehicle Flight Evaluation Report 196D, General Dynamics/Convair, GDC/BKF 65-008, March 31, 1965 (SECRET).

Atlas Launch Vehicle Flight Evaluation Report 204D, General Dynamics/Convair GDC/BKF 65-019, March 21, 1965 (SECRET).

Ranger 8 (Atlas 196-D) Thirty-Day Post-Flight Report, TRW/Space Technology Laboratories, 8679-6069-TC-000, March 17, 1965 (CONFIDENTIAL).

Ranger 9 (Atlas 204-D) Thirty-Day Post-Flight Report, TRW/Space Technology Laboratories, 8679-6073-TC-000, April 16, 1965 (CONFIDENTIAL).

BIBLIOGRAPHY (Cont'd)

Evaluation Report of Mod III Radio Guidance and Instrumentation System with Launch Vehicle 196-D, Ranger 8, General Electric 65D200, March 22, 1965 (SECRET).

Evaluation Report of Mod III Radio Guidance and Instrumentation System with Launch Vehicle 204-D, Ranger 9, General Electric Co., 65D200, April 21, 1965 (SECRET).

Ranger Agena Vehicle 6006 Flight Evaluation and Performance Analysis Report, Lockheed Missiles and Space Co., LMSC-A731742, April 3, 1965 (CONFIDENTIAL).

Ranger Agena Vehicle 6007 Flight Evaluation and Performance Analysis Report, Lockheed Missiles and Space Co., LMSC-A744185, May 14, 1965 (CONFIDENTIAL).

Deep Space Network

Tracking Instruction Manual, Ranger 8 and 9, JPL internal communication, December 15, 1964.

Tracking Operations Memorandum, Ranger 8, JPL internal communication, April 19, 1965.

Tracking Operations Memorandum, Ranger 9, JPL internal communication (in preparation).

Operations Analysis Report, Ranger 8, JPL internal communication (in preparation).

Operations Analysis Report, Ranger 9, JPL internal communication (in preparation).

Space Flight Operations

Space Flight Operations Plan, Ranger 8 and 9, JPL internal communication, December 21, 1964.

Space Flight Operations Memorandum, Rangers VIII and IX, JPL internal communication, August 9, 1965.

Capabilities and Procedures, Space Flight Operations Facility, Ranger Block III (Rev. 3), JPL internal communication, July 20, 1964.